

44811.

National Library
of CanadaBibliothèque nationale
du Canada

Canadian Theses Division / Division des thèses canadiennes

Ottawa, Canada
K1A 0N4**PERMISSION TO MICROFILM — AUTORISATION DE MICROFILMER**

• Please print or type — Écrire en lettres moulées ou dactylographier

Full Name of Author — Nom complet de l'auteur

LALMOHAN SAMANTARAYA

Date of Birth — Date de naissance

18th Aug. 1944

Country of Birth — Lieu de naissance

Permanent Address — Résidence fixe

4506-52st CAMPORE ALBERTA

Title of Thesis — Titre de la thèse

DEFLECTION OF COMPOSITE BEAM AT SERVICE LOAD

University — Université

UNIVERSITY OF ALBERTA

Degree for which thesis was presented — Grade pour lequel cette thèse fut présentée

M.Sc

Year this degree conferred — Année d'obtention de ce grade

1980

Name of Supervisor — Nom du directeur de thèse

Prof J. Longworth

Permission is hereby granted to the NATIONAL LIBRARY OF CANADA to microfilm this thesis and to lend or sell copies of the film.

The author reserves other publication rights, and neither the thesis nor extensive extracts from it may be printed or otherwise reproduced without the author's written permission.

L'autorisation est, par la présente, accordée à la BIBLIOTHÈQUE NATIONALE DU CANADA de microfilmer cette thèse et de prêter ou de vendre des exemplaires du film.

L'auteur se réserve les autres droits de publication; ni la thèse ni de longs extraits de celle-ci ne doivent être imprimés ou autrement reproduits sans l'autorisation écrite de l'auteur.

Date

10/11/1980

Signature

Prof J. Longworth



National Library of Canada
Collections Development Branch

Canadian Theses on
Microfiche Service

Bibliothèque nationale du Canada
Direction du développement des collections

Service des thèses canadiennes
sur microfiche

NOTICE

The quality of this microfiche is heavily dependent upon the quality of the original thesis submitted for microfilming. Every effort has been made to ensure the highest quality of reproduction possible.

If pages are missing, contact the university which granted the degree.

Some pages may have indistinct print especially if the original pages were typed with a poor typewriter ribbon or if the university sent us a poor photocopy.

Previously copyrighted materials (journal articles, published tests, etc.) are not filmed.

Reproduction in full or in part of this film is governed by the Canadian Copyright Act, R.S.C. 1970, c. C-30. Please read the authorization forms which accompany this thesis.

**THIS DISSERTATION
HAS BEEN MICROFILMED
EXACTLY AS RECEIVED**

AVIS

La qualité de cette microfiche dépend grandement de la qualité de la thèse soumise au microfilmage. Nous avons tout fait pour assurer une qualité supérieure de reproduction.

S'il manque des pages, veuillez communiquer avec l'université qui a conféré le grade.

La qualité d'impression de certaines pages peut laisser à désirer, surtout si les pages originales ont été dactylographiées à l'aide d'un ruban usé ou si l'université nous a fait parvenir une photocopie de mauvaise qualité.

Les documents qui font déjà l'objet d'un droit d'auteur (articles de revue, examens publiés, etc.) ne sont pas microfilmés.

La reproduction, même partielle, de ce microfilm est soumise à la Loi canadienne sur le droit d'auteur, SRC 1970, c. C-30. Veuillez prendre connaissance des formules d'autorisation qui accompagnent cette thèse.

**LA THÈSE A ÉTÉ
MICROFILMÉE TELLE QUE
NOUS L'AVONS REÇUE**

THE UNIVERSITY OF ALBERTA

DEFLECTION OF COMPOSITE BEAMS

AT SERVICE LOAD

by



LALMOHAN SAMANTARAYA

A THESIS

SUBMITTED TO THE FACULTY OF GRADUATE STUDIES

IN PARTIAL FULFILMENT OF THE REQUIREMENTS FOR THE DEGREE OF

MASTER OF SCIENCE

DEPARTMENT OF CIVIL ENGINEERING

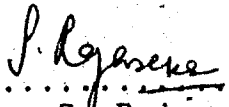
EDMONTON, ALBERTA

SPRING, 1980

THE UNIVERSITY OF ALBERTA
FACULTY OF GRADUATE STUDIES

The undersigned certify that they have read,
and recommend to the Faculty of Graduate Studies for
acceptance, a thesis entitled DEFLECTION OF COMPOSITE
BEAMS AT SERVICE LOAD submitted by LALMOHAN SAMANTARAYA
in partial fulfilment of the requirements for the degree
of Master of Science.


.....
J. Longworth (Supervisor)


.....
S. Rajasekaran


.....
S. Kennedy

ABSTRACT

The deflection behavior of composite beams under service load conditions is investigated. The effects of load-slip behavior of stud shear connectors, shear deformation, and degrees of shear connection are considered.

Basic equilibrium equations in terms of displacement and slip are formulated for composite beams with partial shear connection and the classical solutions are obtained for simply supported beams subjected to concentrated and uniformly distributed load. A numerical technique, based on numerical integration of slip strain, is developed for continuous or simply supported beams with a linear or nonlinear load-slip relationship. This technique involves a corrective iterative procedure for slip applied to an assumed initial slip, and the numerical integration technique using a fourth order Runge-Kutta method.

Solutions obtained from the numerical analysis are compared with theoretical and experimental results of other investigators. The numerical technique satisfactorily predicts the deflection and slip up to service load conditions. The effects of partial and full shear connection, linear and nonlinear load-slip characteristics of the shear connectors, cracking of concrete, and the type of construction method are significant in the evaluation of deflection of composite beams.

ACKNOWLEDGEMENTS

The author expresses sincere thanks to everyone involved in the preparation of this thesis. The author is particularly indebted to Dr. D. W. Murray and Professor J. Longworth, his supervisor, without whose guidance and encouragement this work would not have been completed. The time and advise given by other members of the Department of Civil Engineering are sincerely appreciated. Sincere acknowledgement is also made to fellow graduate student, in particular Mr. T. Sexton. Special acknowledgement is due to his family for their moral support and patience, and to his wife for typing the manuscript.

This investigation was made possible through financial assistance provided by the National Science and Engineering Research Council of Canada.

TABLE OF CONTENTS

	PAGE
* RELEASE FORM	i
TITLE PAGE	ii
APPROVAL SHEET	iii
ABSTRACT	iv
ACKNOWLEDGEMENTS	v
TABLE OF CONTENTS	vi
LIST OF TABLES	xi
LIST OF FIGURES	xii
LIST OF SYMBOLS	xvii
CHAPTER I INTRODUCTION	1
1.1 Introductory Remarks	1
1.2 Composite Action	1
1.2.1 Full Interaction	2
1.2.2 Partial Interaction	3
1.3 Deformation of Composite Beams	3
1.4 Scope	4
CHAPTER II REVIEW OF PREVIOUS RESEARCH	8
2.1 Load-Slip Relationship for Shear Connectors	8
2.1.1 Push-Out Test	8
2.1.2 Linear Load-Slip Behavior	9
2.1.3 Non-Linear Load-Slip Behavior	9
2.2 Section Properties	11
2.2.1 Positive Moment Region	11
2.2.2 Negative Moment Region	12
2.3 Analytical Studies of Simply Supported Composite Beams	15
2.3.1 Elastic Analysis	15
2.3.2 Inelastic Analysis	17

CHAPTER II (Cont'd.)	PAGE
2.4 Analytical Studies of Continuous Composite Beams	18
2.4.1 Elastic Analysis	18
2.4.2 Inelastic Analysis	19
2.5 Effect of Slip	20
 CHAPTER III FORMULATION AND CLASSICAL SOLUTION OF BASIC EQUATIONS FOR COMPOSITE BEAMS	 29
3.1 Formulation of Basic Equations	29
3.1.1 Assumptions for Displacements and Stresses	29
3.1.2 Equilibrium Equations in Terms of Displacements	32
3.1.3 Governing Equation for Slip	35
3.1.4 Governing Equation for Deflection	36
3.2 Slip Strain at Inflection Point	38
3.3 Boundary Conditions	40
3.4 Linear Closed Form Solutions	41
3.5 Formulation for Nonlinear Load-Slip Relationships	44
 CHAPTER IV A NUMERICAL SOLUTION TECHNIQUE FOR COMPOSITE BEAMS	 52
4.1 Introduction	52
4.2 Numerical Integration of Slip Equation	53
4.3 Correction and Iteration for Slip	56
4.4 Evaluation of Slip Strain	58
4.5 Evaluation of Deflection	60
4.6 Solution Procedure for Continuous Beams	62
4.7 Special Problems in Solving Continuous Beams	66
4.8 Computer Program	67

	PAGE
CHAPTER V VERIFICATION OF NUMERICAL TECHNIQUE . . .	74
5.1 Introduction	74
5.2 Program Verification for Linear Behavior	75
5.2.1 Simply Supported Beams	75
5.2.2 Continuous Beams	76
5.3 Program Verification for Nonlinear Behavior	78
5.4 Comparisons with Test Results	80
5.4.1 Comparison with Hamada and Longworth	80
5.4.2 Comparison with Chapman and Balakrishnan	81
5.5 Conclusion	82
CHAPTER VI APPLICATIONS	99
6.1 Introduction	99
6.2 Deflection of a Linear Elastic Simply Supported Composite Beam Subjected to Uniform Load	100
6.3 Evaluation of Shear Deflection for a Simply Supported Composite Beam Subjected to Uniform Load	102
6.4 Influence of Type of Loading, Shear Connection and Load-Slip Characteristics of the Shear Connectors and Shear Deformation on Deflection	104
6.4.1 Simply Supported Beam Subjected to Uniformly Distributed Load and a Concentrated Load	104
6.5 Deflection of a Continuous Beam Subjected to Uniform Load	106
6.6 Deflection of a Two-Span Continuous Beam Subjected to Concentrated Loads	108
6.7 Influence of Negative Moment Cracking in Continuous Beams	108
6.8 Analyses of a Three-Span Beam for Shored and Unshored Construction	109
6.9 Conclusions	110

	PAGE
CHAPTER VII SUMMARY AND CONCLUSIONS	136
7.1 Summary	136
7.2 Conclusions	138
BIBLIOGRAPHY	142
APPENDICES	
APPENDIX A CLOSED FORM SOLUTION (TWO-SPAN CONTINUOUS BEAM)	146
A.1 Classical Solution	146
A.2 Summary of Equations	151
A.3 Equations Used in Solution of Constants of Integration and Redundant Moment	155
A.4 Constants Used in Closed Form Solution	158
APPENDIX B LINEAR CLOSED FORM SOLUTION FOR A SIMPLY SUPPORTED BEAM WITH CONCENTRATED LOAD AT CENTER	160
B.1 Classical Solution	160
B.2 Evaluation of Shear Deflections for a Simply Supported Composite Beam Subjected to a Concentrated Load at the Center	164
APPENDIX C EVALUATION OF SERVICE LOADS OF COMPOSITE BEAMS FOR TEST PROBLEMS	169
C.1 Introduction	169
C.2 Simply-Supported Beam with Concentrated Load at Center (Chapman and Bala- krishnan)	170
C.3 Two-Span Continuous Composite Beam Subjected to Equal Concentrated Load at the Center of Each Span (Hamada and Longworth)	174
APPENDIX D EVALUATION OF SHEAR CONNECTOR STIFFNESS FOR VARIOUS TYPES OF SHEAR CONNECTOR	186
D.1 Evaluation of Shear Connector Stiffness	186

APPENDIX E SHEAR STRESS DISTRIBUTION IN COMPOSITE

BEAM SECTIONS 197

E.1 Evaluation of Shear Stress 197

APPENDIX F COMPUTER PROGRAM 206

F.1 Introduction 206

F.2 Description of Program 208

F.3 List of Computer Programs 213

F.4 List of Data and Outputs 234

LIST OF TABLES

		PAGE
TABLE 5.1	PROPERTIES OF COMPOSITE BEAMS FOR TEST PROBLEMS	83
TABLE 5.2	TEST PROBLEMS COMPUTED VALUES	84
TABLE 6.1	SHEAR FORM FACTORS (K_{sh}) FOR COMPOSITE BEAMS	111
TABLE 6.2	DEFLECTION COMPARISON OF SIMPLY SUPPORTED BEAMS AT SERVICE LOAD	112
TABLE 6.3	SLIP COMPARISON OF SIMPLY SUPPORTED BEAMS AT SERVICE LOAD	113
TABLE 6.4	DEFLECTION COMPARISON OF CONTINUOUS COMPOSITE BEAM AT SERVICE LOAD	114
TABLE 6.5	PROPERTIES OF COMPOSITE BEAMS USED FOR APPLICATION	115
TABLE D.1	STIFFNESS OF HEADED SHEAR STUD CONNECTORS	190

LIST OF FIGURES

		PAGE
1.1	COMPOSITE BEAM WITH SHEAR CONNECTORS	6
1.2	STRAIN DISTRIBUTION FOR DIFFERENT DEGREES OF INTERACTION	7
2.1	PUSH-OUT TEST SPECIMEN	22
2.2	LOAD-SLIP RELATIONSHIP FROM PUSH-OUT TEST (CHAPMAN AND BALAKRISHNAN)	23
2.3	LOAD-SLIP RELATIONSHIP (VAN DALEN)	24
2.4	LOAD-SLIP RELATIONSHIP (YAM AND CHAPMAN)	25
2.5	SECTION THROUGH A COMPOSITE BEAM	26
2.6	ELASTIC STRAIN AND STRESS DISTRIBUTION FOR COMPOSITE BEAM	27
2.7	CONDITIONS IN AN ELEMENT OF A COMPOSITE BEAM	28
3.1	COMPOSITE SYSTEM	46
3.2	DEFORMATION AND DISPLACEMENT OF COMPOSITE BEAM	47
3.3	STEP FUNCTION	48
3.4	STRAIN DISTRIBUTION IN COMPOSITE BEAM SECTION	49
3.5	CONDITIONS AT INFLECTION POINT	50
3.6	BOUNDARY CONDITIONS	51
4.1	BASIS FOR NUMERICAL PROCEDURE	69
4.2	AXIAL FORCE AT THE END OF THE BEAM	70
4.3	DISTRIBUTION OF SLIP STRAIN ACROSS THE POINT OF INFLECTION	71
4.4	DEFLECTION AND ITS CORRECTION	72
4.5	ILLUSTRATION OF FLEXIBILITY METHOD	73
5.1	COMPARISON OF CLASSICAL AND NUMERICAL VALUES FOR SLIP	85
5.2	COMPARISON OF CLASSICAL AND NUMERICAL VALUES FOR SLIP STRAIN	86
5.3	COMPARISON OF CLASSICAL AND NUMERICAL VALUES FOR DEFLECTION	87

	PAGE
5.4 PLUM AND HORNE'S TEST BEAM	88
5.5 COMPARISON OF SLIP VALUES (PLUM AND HORNE AND NUMERICAL SOLUTION)	89
5.6 COMPARISON OF SLIPSTRAIN VALUES (PLUM AND HORNE AND NUMERICAL SOLUTION)	90
5.7 COMPARISON OF AXIAL FORCE VALUES (PLUM AND HORNE AND NUMERICAL SOLUTION)	91
5.8 COMPARISON OF DEFLECTION VALUES (PLUM AND HORNE AND NUMERICAL SOLUTION)	92
5.9 YAM AND CHAPMAN'S TEST BEAM	93
5.10 COMPARISON OF SLIP VALUES (YAM AND CHAPMAN AND NUMERICAL SOLUTION)	94
5.11 COMPARISON OF DEFLECTION VALUES (YAM AND CHAPMAN AND NUMERICAL SOLUTION)	95
5.12 SHEAR FLOW AND SLIP RELATIONSHIP (YAM AND CHAPMAN)	96
5.13 COMPARISON OF DEFLECTION VALUES (HAMADA AND LONGWORTH AND NUMERICAL SOLUTION)	97
5.14 COMPARISON OF DEFLECTION VALUES (CHAPMAN AND BALAKRISHNAN AND NUMERICAL SOLUTION)	98
6.1 DEFLECTION RATIO (δ_f/δ_0) VS ξ FOR A SIMPLY SUPPORTED BEAM WITH UNIFORMLY DISTRIBUTED LOAD	116
6.2 SHEAR FORM FACTOR (K_{sh}) VS SLAB WIDTH (bc) FOR COMPOSITE BEAMS	117
6.3 LOAD-DEFLECTION RELATIONSHIP (SIMPLY SUPPORTED BEAM, FULL AND PARTIAL SHEAR CONNECTION, UNIFORMLY DISTRIBUTED LOAD)	118
6.4 LOAD SLIP RELATIONSHIP (SIMPLY SUPPORTED BEAM, UNIFORMLY DISTRIBUTED LOAD)	119
6.5 LOAD DEFLECTION RELATIONSHIP (SIMPLY SUPPORTED BEAM, FULL AND PARTIAL SHEAR CONNECTION, CONCENTRATED LOAD AT CENTER)	120

6.6	LOAD SLIP RELATIONSHIP (SIMPLY SUPPORTED BEAM, CONCENTRATED LOAD AT CENTER)	121
6.7	DEFLECTION RATIO (δ_f/δ_o) VS ξ FOR A TWO-SPAN CONTINUOUS BEAM WITH UNIFORMLY DISTRIBUTED LOAD	122
6.8	DEFLECTION RATIO (δ_t/δ_o) VS ξ FOR A TWO-SPAN CONTINUOUS BEAM WITH UNIFORMLY DISTRIBUTED LOAD	123
6.9	LOAD DEFLECTION RELATIONSHIP (CONTINUOUS BEAM, CONSTANT 'I', FULL AND PARTIAL SHEAR CONNECTION)	124
6.10	LOAD SLIP RELATIONSHIP (CONTINUOUS BEAM, CONSTANT 'I', FULL AND PARTIAL SHEAR CONNECTION)	125
6.11	LOAD DEFLECTION RELATIONSHIP (CONTINUOUS BEAM, VARIABLE 'I', FULL AND PARTIAL SHEAR CONNECTION)	126
6.12	LOAD SLIP RELATIONSHIP (CONTINUOUS BEAM, VARIABLE 'I', FULL AND PARTIAL SHEAR CONNECTION)	127
6.13	COMPARISON OF DEFLECTION VALUES (CONSTANT AND VARIABLE 'I')	128
6.14	COMPARISON OF SLIP VALUES (CONSTANT AND VARIABLE 'I')	129
6.15	COMPARISON OF SLIP STRAIN VALUES (CONSTANT AND VARIABLE 'I')	130
6.16	COMPARISON OF FORCE VALUES (CONSTANT AND VARIABLE 'I')	131
6.17	COMPARISON OF DEFLECTION VALUES (SHORED AND UNSHORED CONSTRUCTION)	132
6.18	COMPARISON OF SLIP VALUES (SHORED AND UNSHORED CONSTRUCTION)	133
6.19	COMPARISON OF SLIP STRAIN VALUES (SHORED AND UNSHORED CONSTRUCTION)	134
6.20	COMPARISON OF FORCE VALUES (SHORED AND UNSHORED CONSTRUCTION)	135

	PAGE
A.1	TWO-SPAN CONTINUOUS COMPOSITE BEAM 147
A.2	BOUNDARY CONDITIONS FOR CONTINUOUS COMPOSITE BEAM 150
B.1	BEAM GEOMETRY AND BOUNDARY CONDITION 166
B.2	DEFLECTION RATIO (δ_f/δ_0) VS ξ FOR A SIMPLY SUPPORTED BEAM WITH A CONCENTRATED LOAD AT CENTER 167
C.1	SIMPLY SUPPORTED COMPOSITE BEAM SUBJECTED TO CONCENTRATED LOAD AT MIDSPAN (CHAPMAN AND BALAKRISHNAN) 179
C.2	DETAILS OF TEST SPECIMEN (HAMADA AND LONGWORTH) 180
C.3	SECTION THROUGH TEST BEAM (HAMADA AND LONGWORTH) 181
C.4	IDEALIZED STRESS CONDITIONS AT ULTIMATE MOMENT IN POSITIVE BENDING 182
C.5	STRESS DISTRIBUTION IN A NEGATIVE MOMENT REGION 183
C.6	IDEALIZED STRESS DISTRIBUTION AT ULTIMATE MOMENT IN NEGATIVE BENDING 184
D.1	LOAD-SLIP RELATIONSHIP FOR PUSH-OUT SPECIMEN . 191
D.2	LOAD-SLIP RELATIONSHIP FOR PUSH-OUT SPECIMEN . 192
D.3	LOAD-SLIP RELATIONSHIP FOR PUSH-OUT SPECIMEN . 193
D.4	LOAD-SLIP RELATIONSHIP FOR PUSH-OUT SPECIMEN . 194
D.5	LOAD-SLIP RELATIONSHIP FOR PUSH-OUT SPECIMEN . 195
E.1	STATICAL MOMENT AND SHEAR STRESS DISTRIBUTION IN COMPOSITE SECTION (NEUTRAL AXIS IN SLAB). 199
E.2	STATICAL MOMENT AND SHEAR STRESS DISTRIBUTION IN COMPOSITE SECTION (NEUTRAL AXIS IN WEB) . 200
E.3	STATICAL MOMENT AND SHEAR STRESS DISTRIBUTION IN COMPOSITE SECTION (NEUTRAL AXIS IN TOP FLANGE) 201
E.4	SHEAR FORM FACTOR (K_{sh}) VS SLAB WIDTH FOR COMPOSITE BEAMS 202

	PAGE
E.5 SHEAR FORM FACTOR (K_{sh}) VS SLAB WIDTH FOR COMPOSITE BEAMS	203
E.6 SHEAR FORM FACTOR (K_{sh}) VS SLAB WIDTH FOR COMPOSITE BEAMS	204
F.1 FLOW CHART FOR COMPUTER PROGRAM	211
F.2 INPUT DATA	212

LIST OF SYMBOLS

a = Depth of stress block in concrete slab

a = Constant defined in Eq. 2.5

A_c = Transformed area of concrete slab

A_s = Area of steel beam

A_t = Area of composite section

A_{sf} = Area of flange of steel beam

A_{sr} = Area of reinforcing steel

A_{sw} = Area of web of steel beam

b = Constant defined in Eq. 2.5

bc = Width of concrete slab

b_f = Width of flange of steel beam

C = Compressive force in concrete slab

d = Depth of steel beam

d = Diameter of shear connectors in Eq. 2.3

ds = Depth of steel beam

d_w = Depth of web of steel beam

E_c = Modulus of elasticity of concrete

E_s = Modulus of elasticity of steel

f_1, f_2, f_3 = Values of function at points 1, 2, and 3

f'_c = 28 days concrete cylinder strength

f_y = Yield stress of steel

f_{yf} = Yield stress of flange of steel section

f_{yr} = Yield stress of reinforcement
 f_{yw} = Yield stress of web of steel section
 F = Compressive force in concrete slab
 F = Flexibility matrix
F.S.C. = Full shear connection
 G = Shear or rigidity modulus of steel
 h = Step size
 I_c = Moment of inertia of concrete slab
 I_t = Moment of inertia of concrete beam
 k = Constant in Eq. A1
 K = Shear connector modulus or stiffness
 ℓ = Spacing of shear connector
 L = Length of the beam
 M = Bending moment
 M_p = Plastic moment
 M_u = Ultimate moment capacity
 n = Inverse of modular ratio
 n_a = Number of shear connectors between zero and maximum
moment
 n_b = Number of shear connectors between maximum moment
and inflection point
 n_c = Number of shear connectors between inflection point
and first interior support
 N = Number of shear connectors
 P = Concentrated load
 P_u = Ultimate load
 P_w = Service load

P.S.C. = Partial shear connection

q = Shear flow

Q = Statical moment

Q_1 = Load per connector

Q_u = Ultimate load capacity for connectors in Appendix C

Q_u = Ultimate capacity per connector

R = Foundation modulus of concrete in Eq. 2.4

R = Redundants

s = Slip

s' = Slip strain

s'_L, s'_R = Strain at the centroid of steel section, at the
left and right of inflection point

t = Thickness of concrete slab

t_c = Thickness of concrete slab

t_f = Thickness of flange of steel beam

T = Ultimate strength of steel section

T_r = Ultimate strength of reinforcement

u = Horizontal displacement in steel beam

u_0 = Horizontal displacement at origin

U_{cyl} = 28 days concrete cylinder strength

v = Deflection

v'' = Curvature

V = Shear

w = Uniform load

w_w = Width of web of steel beam

W = Concentrated load

x = Distance along the length of the beam

X = Any quantity (moment, shear, deflection)

y = Centroidal distance between centroid of concrete slab and steel beam

Y_c = Centroidal distance between composite section and concrete slab centroids

Y_s = Centroidal distance between composite section and steel section centroids

z = Centroidal distance between the centroids of concrete slab and steel beam

α^2 = Constant defined in Eq. 3.21

β = Constant defined in Eq. 3.22

γ = Slip

γ = Shear strain in Eq. 6.6 and B30

δ_0 = Midspan deflection due to bending only assuming full interaction

δ_f = Midspan deflection due to bending and slip

δ_s = Shear deflection

δ_t = Midspan deflection due to bending, slip and shear

δ_{BB} = Deformation at B due to unit load at B

δ_{BC} = Deformation at B due to unit load at C

δ_{CC} = Deformation at C due to unit load at C

δ_{CB} = Deformation at C due to unit load at B

Δ_i = Deformation at support i

Δ_B, Δ_C = Deformations due to external loading at redundants B and C

ϵ_b = Strain in steel beam at interface
 ϵ_0 = Strain difference at interface
 ϵ_s = Strain in concrete slab at interface
 ϵ_x = Strain in horizontal direction
 ϵ_0 = Strain in horizontal direction at origin
 ξ = Constant defined in Eq. 6.4
 η = Constant defined in Eq. 6.5
 θ = Angle
 λ = Constant defined Eq. 4.24
 ρ = Constant defined in Eq. 3.49
 σ = Stress
 ψ = Constant defined in Eq. 3.29
 χ_L = Constant defined in Eq. 3.34
 χ_R = Constant defined in Eq. 3.35
 ϕ = Curvature
 μ = Shear connector modulus

CHAPTER I

INTRODUCTION

1.1 Introductory Remarks

One significant advantage of composite construction is that beam deflections are considerably reduced as a result of increased stiffness. Composite behavior is dependent on the shear connection between the component parts.

1.2 Composite Action

Shear connectors attached to the steel section and embedded in the concrete slab resist shear at the interface of the slab and steel section, thus creating an interaction between two components. The degree of interaction may be complete or partial. A typical composite beam is illustrated in Fig. 1.1. If there is no shear connection or friction at the interface between the concrete and steel, the compatibility requirement reduces to equal vertical deflection of two components. Therefore the applied load is divided between two components in proportion to their stiffnesses and each component acts as if it were an isolated member. Assuming the materials can resist tensile stress, equal and opposite strains develop

at the top and bottom fibers of each component, as illustrated in Fig. 1.2(a). However, tensile cracks may occur in the concrete slab as concrete is relatively weak in tension. The difference in strain between the adjacent fibers of concrete and steel at the interface is known as slip strain, since it results from a horizontal slip that occurs between the two components.

1.2.1 Full Interaction

If the concrete slab and steel section are joined together by infinitely stiff shear connectors, the two members behave as a unit with no slip occurring at the interface. The vertical deflections of the components are equal at any point along the length of the beam. Slip and slip strains are zero everywhere along the interface and it can be assumed that plane sections remain plane during bending. This condition is known as full interaction, and is illustrated in Fig. 1.2(c). Bending stresses and deflections due to service loads for the condition of complete interaction are usually determined by employing simple elastic beam theory using section properties associated with the transformed cross section.

In practice the majority of design methods for composite beams are based on the assumption of full interaction. However, CSA S16.1-1974, "Steel Structures for Buildings - Limit State Design", (3) also specifies

methods for composite design based on partial interaction.

1.2.2 Partial Interaction

The assumption of full interaction is only valid if there is no relative movement or slip at the steel-concrete interface. It is generally assumed that the horizontal shear force at the interface is transmitted only by shear connectors and not by bond. Due to the compressibility of the concrete slab and the flexibility of the connectors, the shear force cannot be transmitted without some slip occurring, and therefore the interaction must be partial, or incomplete. The strain distribution relating to this type of behavior is shown in Fig. 1.2(b). In every composite structure, interaction is less than complete, irrespective of the relative strength of the component parts. It is therefore important to understand how the behavior of a composite beam is modified by the presence of slip.

1.3 Deformation of Composite Beams

Beam deformation is caused by bending and shear. Composite beam deformation is also influenced by the slip along the interface of the two components. Stiffness rather than strength is the governing criteria for deflection at service loads. Stiffness is influenced

by the geometry of the cross section and the material properties of the components involved.

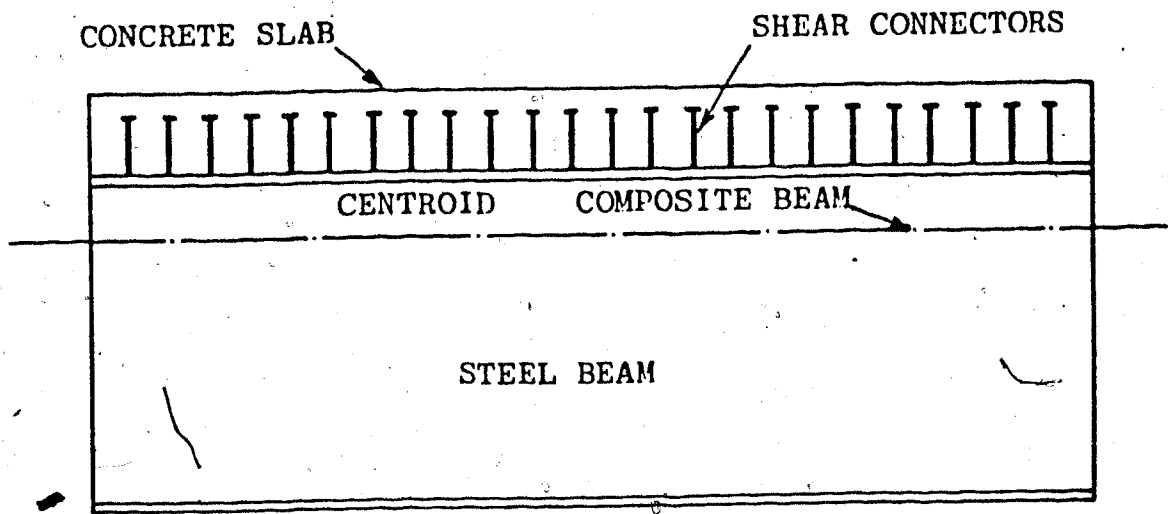
Bending deflections are dependent on the moment-curvature relationship. Shear deformation can be evaluated independently of bending deformation by applying the principle of virtual work. Deflection due to slip depends on the stiffness of the shear connection which is defined by load-slip relationship for the type of shear connector.

In continuous beams, the flexural stiffness in the negative moment region is different from that in the positive moment region. In the negative moment region, due to tensile cracking of concrete, the moment of inertia of the cross-section is reduced considerably resulting in a reduction in stiffness which influences the deflection. Improper distribution of shear connectors or faulty connection may increase slip at the interface. Premature yielding of shear connectors produces a non-linear load-slip relationship at working loads which influences the magnitude of slip and hence the deflection.

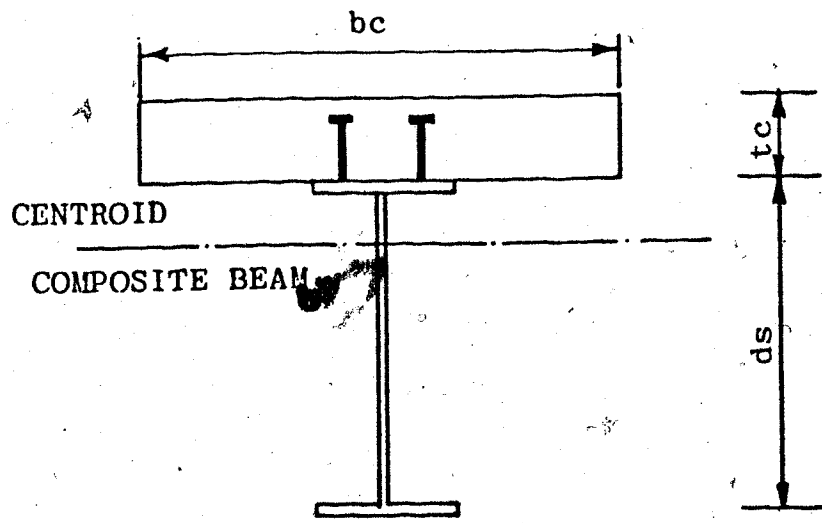
1.4 Scope

The present study investigates the deflection behavior of composite beams under service load conditions. The effect of the load-slip behavior of stud shear connectors on deflection is considered. The effects of partial and full shear connection and shear deformation are examined. A

numerical analysis technique is developed for the analysis of single span and continuous composite beams. A further objective is to compare deflections produced in shored and unshored construction.



(a) SIDE VIEW



(b) SECTION

FIGURE 1.1 COMPOSITE BEAM WITH SHEAR CONNECTORS

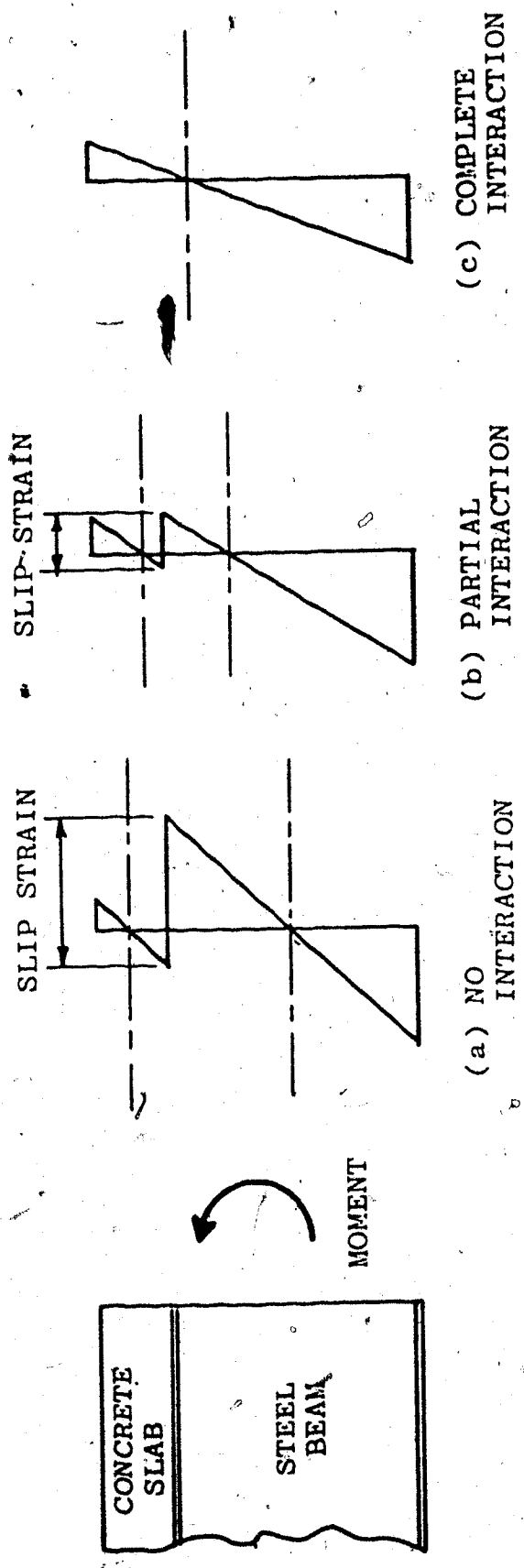


FIGURE 1.2 STRAIN DISTRIBUTION FOR DIFFERENT DEGREES OF INTERACTION

CHAPTER II

REVIEW OF PREVIOUS RESEARCH

2.1 Load-Slip Relationship for Shear Connectors

2.1.1 Push-Out Test

The push-out test has been used at least since 1930 (26) as a means of evaluating the load carrying capacity of shear connectors and the load-slip relationship for shear connectors is normally determined from such a test. Fig. 2.1 shows a typical push-out test specimen and Fig. 2.2 illustrates typical results obtained from such a test.

In push-out tests, one approach considers that the function of shear connectors is to control the magnitude of slip between the concrete slab and the steel section. The load carried by the connectors at some limiting slip is defined as the "useful load capacity" (25). A second approach considers that the function of shear connectors between sections of zero and maximum moment is to transfer across the concrete-steel interface the maximum compressive force that can be developed in the concrete slab, or the maximum tension force in the steel section without consideration of the magnitude of slip which has occurred.

2.1.2 Linear Load-Slip Behavior

Newmark et al (17), in interpreting their push-out test results, concluded that the amount of slip is directly proportional to the applied load. They observed that slip depends upon the stiffness and spacing of the shear connectors and defined the shear connector modulus, K , as

$$K = \frac{Q}{\gamma} \quad (2.1)$$

$$K = \frac{q\ell}{\gamma} \quad (2.2)$$

where Q is load per connector, q is horizontal shear force transmitted per unit length of beam at the interface of steel and concrete (shear flow), γ is the slip in inches and ℓ is the spacing of connectors in inches.

2.1.3 Non-Linear Load-Slip Behavior

On the basis of a study of numerous push-out tests, Slutter and Driscoll (22) defined the ultimate load capacity of a stud connector as

$$Q_u = 930d^2 \sqrt{U_{cyl}} \quad (2.3)$$

where Q_u is the ultimate load capacity of a shear connector, d is the diameter of the connector in inches, and U_{cyl} is the 28-day concrete cylinder strength in psi.

Van Dalen (24) proposed the following relationship between slip, applied shear force and foundation modulus:

$$\gamma = 3.7 \times 10^{-2} QR^{-0.75} \quad (2.4)$$

where Q is the applied shear force in pounds, and R is foundation modulus in psi. The foundation modulus was defined as the modulus of elasticity of concrete. Fig. 2.3 illustrates the relationship proposed by Van Dalen. From his tests he concluded that:

1. The ultimate load carrying capacity of a stud connector embedded in a concrete slab is primarily dependent upon the tension in the connector resulting from a separation of concrete and steel at the interface.
2. The ultimate load of a connector in a push-out test should not be adopted as the ultimate load for a connector in a beam unless the expected separation at the concrete-steel interface in the beam is less than that at failure in a push-out test.

Yam and Chapman (30) proposed an exponential relationship between load and slip for a stud shear connector:

$$Q_u = a(1 - e^{-b\gamma}) \quad (2.5)$$

where a and b are constants. The exponential relationship was obtained by establishing the best fit curve for experimental results. By selecting two slip values in an experimental load-slip plot such that one slip value is two times the other, the constants a and b can be evaluated as

$$a = \frac{Q_1^2}{2Q_1 - Q_2} \quad (2.6)$$

$$b = \frac{1}{\gamma_1} \ln \frac{Q_1}{Q_2 - Q_1} \quad (2.7)$$

Fig. 2.4 illustrates this exponential load-slip relationship and defines values of γ_1 , γ_2 , Q_1 and Q_2 . The ultimate capacity of a shear connector was defined by Yam and Chapman as the load at which the slip attains a limiting value of 0.055 inches.

2.2 Section Properties

2.2.1 Positive Moment Region

Properties of composite beams are different in positive and negative moment regions. In a positive moment region as shown in Fig. 2.5(a), the concrete slab, or a portion thereof, depending upon the location of neutral axis, is in compression and contributes significantly to moment resistance. In evaluating the elastic stiffness of a composite section, it is customary

to transform the concrete slab area into an equivalent area of steel by applying the modular ratio (E_c/E_s), as a multiplier of the effective slab width.

Slutter and Driscoll (22) proposed that the load capacity of a connector in a positive moment region should be the ultimate load as obtained in a push-out test, whereas Chapman and Balkrishnan (5) propose 80% of ultimate capacity.

2.2.2 Negative Moment Region

In the vicinity of an interior support, a continuous composite beam is subjected to negative bending moment which produces tension in the slab. If the concrete cracks, the composite section consists of the longitudinal slab reinforcement and the steel section as shown in Fig. 2.5(b). The cracked concrete acts as a medium for transferring horizontal shear forces required to develop tension stress in the longitudinal steel. Thus the stiffness is significantly lower than that in a positive moment region. This decreased stiffness may result in an increase of as much as 25% in the value of the positive moment based on uniform stiffness. The elastic stress and strain distribution for composite beams in positive and negative moment region is illustrated in Fig. 2.6.

Siess (21) reported results of tests on two-span continuous bridge beams, one with shear connectors provided along the total length of the beam, and the other with shear connectors only in the region of positive moment. Longitudinal slab reinforcement was provided in the negative moment region of both beams. Siess concluded that, at ultimate moment, complete interaction existed in the positive moment region of the beam with shear connectors throughout the length, whereas partial interaction was present in the other beam. The tests thus showed that shear connectors are effective in the negative moment region and they are necessary to achieve effective composite action.

Van Dalen (24) concluded that stud shear connectors form a satisfactory shear connection in a negative bending moment region. However, he concluded, their capacity is somewhat less than that attained in a positive moment region.

Wastlund and Ostlund (29) tested composite beams loaded so that the concrete slab was on the tension side. One beam had only two bow-shaped shear connectors, while a second beam contained no shear connectors but contained slab reinforcement bent down and welded to the steel beam at the ends. The third beam had a prestressed concrete slab with three bow-shaped connectors at each end. The authors concluded that:

1. In a composite beam subjected to negative bending moment, the concrete cannot be assumed to act compositely with the steel section, as the concrete cracks at very small tensile stresses.
2. If the connection between the steel section and slab is sufficient (there is no indication of what might be a sufficient connection) the longitudinal reinforcement acts jointly with the steel section.
3. The ultimate load capacity of shear connectors in a negative moment region is considerably smaller than that found for similar shear connectors in positive moment regions.

The amount of longitudinal reinforcement affects the behavior of composite beams in the negative moment region. Piepgrass (20) observed that the ratio of experimental to theoretical ultimate moment decreases with an increase of amount of longitudinal reinforcement in negative moment regions. Davison (6) concluded that the amount of longitudinal reinforcement increases the negative moment capacity but reduces the rotation capacity of plastic hinges in the negative moment region. In his study the amount of longitudinal reinforcement was 0.111 to 0.232 times the area of the steel section.

2.3 Analytical Studies of Simply Supported Composite Beams

2.3.1 Elastic Analysis

Newmark et al (17) developed a closed form solution for a simply supported composite beam. They assumed a linear stress-strain relationship for steel and concrete and a linear load-slip relationship for shear connectors. Their analysis is based on the following assumptions:

1. The shear connection between slab and the beam is assumed to be continuous along the length of the beam.
2. The amount of slip occurring in the shear connector is assumed to be directly proportional to the load transmitted.
3. The distribution of strain throughout the depth of slab and steel section is assumed linear.
4. The steel section and the concrete slab are assumed to deflect equal amounts at all points along the span length.

They defined slip, or the relative movement between the concrete slab and steel section interface, as

$$\gamma = \frac{Q}{K} = \frac{q\ell}{K} = \frac{\ell}{K} \cdot \frac{dF}{dx} \quad (2.8)$$

where F is the compressive force in the concrete slab. The rate of change of slip is equal to the difference between strain in the concrete slab and the steel section at the interface.

$$\frac{d\gamma}{dx} = \epsilon_b - \epsilon_s \quad (2.9)$$

where ϵ_b is the strain in the steel and ϵ_s is the strain in the concrete.

Using a linear stress relationship they developed the following second order differential equation for force in terms of moment, shear connector modulus and section properties:

$$F'' + \frac{K}{l} (f_1 M - f_2 F) = 0 \quad (2.10)$$

where M is bending moment, and

$$f_1 = \frac{y}{E_s I_s + E_b I_b} \quad (2.11a)$$

$$f_2 = \frac{1}{E_s A_s} + \frac{1}{E_b A_b} + f_1 y \quad (2.11b)$$

E_s , E_b are the values of modulus of elasticity of concrete and steel, respectively, I_s and I_b are moment of inertia of slab and beam, respectively, and y is the distance between centroid of the concrete slab and the centroid of the steel section.

Newmark et al (17) also presented a solution for Equation 2.10 for a simply supported beam subjected to a single concentrated load only. They found close

agreement between theoretical results and experimental results obtained from a series of tests.

2.3.2 Inelastic Analysis

Yam and Chapman (30) studied ultimate load behavior of simply supported composite beam using a non-linear stress-strain relationship and inelastic load-slip behavior for the shear connectors. Based on the equilibrium of a segment of the slab, the shear flow, q , at the interface of the concrete slab and steel section may be defined as

$$q = \frac{dC}{dx} \quad (2.12)$$

where C is the compressive force as shown in Fig. 2.7.

Strain difference at the interface due to the relative horizontal movement of two components may be expressed as

$$\epsilon_d = \frac{dy}{dx} \quad (2.13)$$

Using an exponential load-slip relationship as described in Section 2.13, they derived the following two first order simultaneous equations with the dependent variables C and γ as

$$C' = \frac{dC}{dx} = \frac{a}{s} (1 - e^{-b\gamma}) \quad (2.14)$$

$$\gamma' = \frac{d\gamma}{dx} = f(M, C) \quad (2.15)$$

where $f(M, C)$ is an implicit function of moment and compressive force.

By eliminating γ , the following second order differential equation, with C as a dependent variable, results:

$$C'' + C' \left[\frac{1}{l} \frac{dl}{dx} - bf(M,C) \right] + \frac{ab}{l} f(M,C) = 0 \quad (2.16)$$

This equation may be solved by the predictor-corrector method of numerical integration. For a simply supported beam a value of slip is assumed at one end and force is computed at the other end. If the computed force is zero, then the assumed slip value is correct, otherwise successive corrections are applied. Yam and Chapman found good correlation between theoretical and experimental results up to 98% of the failure load, but there was significant difference at connector failure.

2.4 Analytical Studies of Continuous Composite Beams

2.4.1 Elastic Analysis

Plum and Horne (19) developed a closed form solution for a continuous composite beam of two unequal spans with equal concentrated loads on each span. They used a linear load-slip relationship for the shear connectors, elastic properties for the concrete slab and steel section, and partial interaction between the concrete slab and steel section. They derived the following governing fourth order differential equation, in terms of deflection as the dependent variable:

$$v^{IV} - kv'' = - \frac{w}{(\Sigma EI)} - \frac{\mu M}{\overline{EA}(\Sigma EI)} \quad (2.17)$$

$$k = \frac{\mu(\Sigma EI + \overline{EA}z^2)}{\overline{EA}(\Sigma EI)} \quad (2.18)$$

where μ is the interface stiffness (shear connector modulus), v is the deflection, M is the bending moment, w is the uniformly distributed load, (ΣEI) and \overline{EA} are composite section properties, and z is the distance between the centroids of the concrete slab and steel section.

Beams with constant and variable flexural stiffness were studied. For constant flexural stiffness, the cracking of the concrete slab in the negative bending moment region was ignored and the composite beam was assumed to be of uniform cross section over the entire length. Variable stiffness was treated by means of an equivalent haunched beam in which depth of the beam along the length varied in accordance with the moment of inertia of the actual beam section. In other words, the variable stiffness did not arise from cracking of concrete in the negative moment region. A comparison of theoretical and experimental deflection values indicated good agreement.

2.4.2 Inelastic Analysis

Yam and Chapman (31) extended their analysis of a simply supported beam to a two-span symmetric continuous beam which could be modeled as a single span

propped cantilever. Equal concentrated loads were applied to each span and the same composite section was used as for the simple span case. The effect of shear connector spacing and types of loading on deflection and slip were studied. They used the governing equation 2.16 and the same integration procedure as for the simply supported beam. In the solution for a continuous beam, values of both slip at the exterior support and bending moment at the interior support must be initially assumed. Therefore, more iterations requiring considerable computational time must be performed to obtain correct values.

Hamada and Longworth (9) suggested the computational time required in Yam and Chapman's procedure can be significantly reduced by assuming that the slip strain is constant along the shear span. This assumption is based on linear slip distribution and is satisfactory for a simply supported beam but is not valid for a continuous beam.

2.5 Effect of Slip

The slip at the interface of the slab and the steel section affects stress, strain and deflection at all sections along the beam. According to Siess (21) the effect of slip on strain is a maximum at the interface and minimum at the bottom of the steel section where the strain is maximum. His tests indicated that the effect of slip on the distribution of strain was a relatively localized

effect confined to the region of the applied concentrated load.

Johnson (11) reported that within the elastic range, slip may change the stress distribution by as much as 5% and may increase deflection by as much as 13%. Newmark et al (17) obtained similar results in full scale beam tests.

Plum and Horne (19) stated that incomplete interaction may increase the deflection as much as 40%. Their test results indicate that slip may increase deflection as much as 50% and decrease the compressive force in the slab up to 20%.

Hamada and Longworth (9) proposed an analysis for computing deflections of continuous composite beams which included the effect of shear and slip. They found that shear deformations were significant and their analytical results were in close agreement with actual deflections determined in tests.

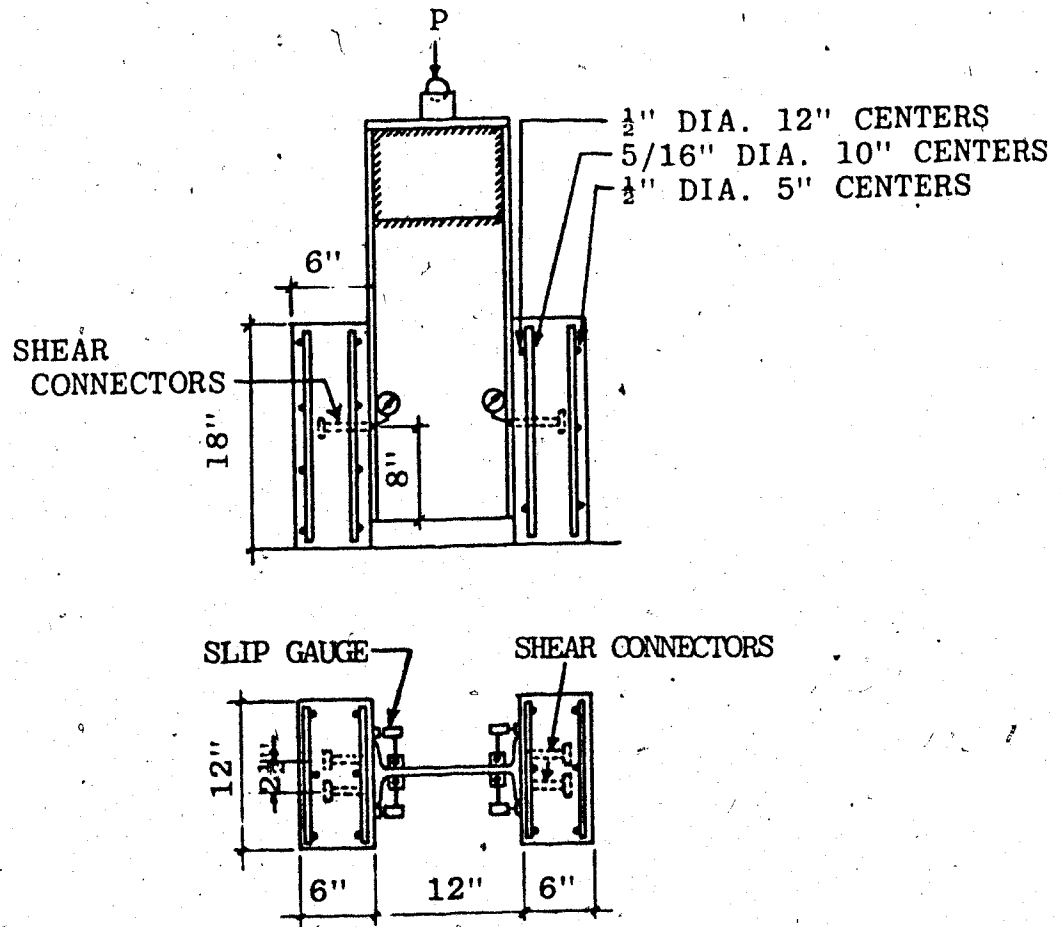


FIGURE 2.1 PUSH-OUT TEST SPECIMEN

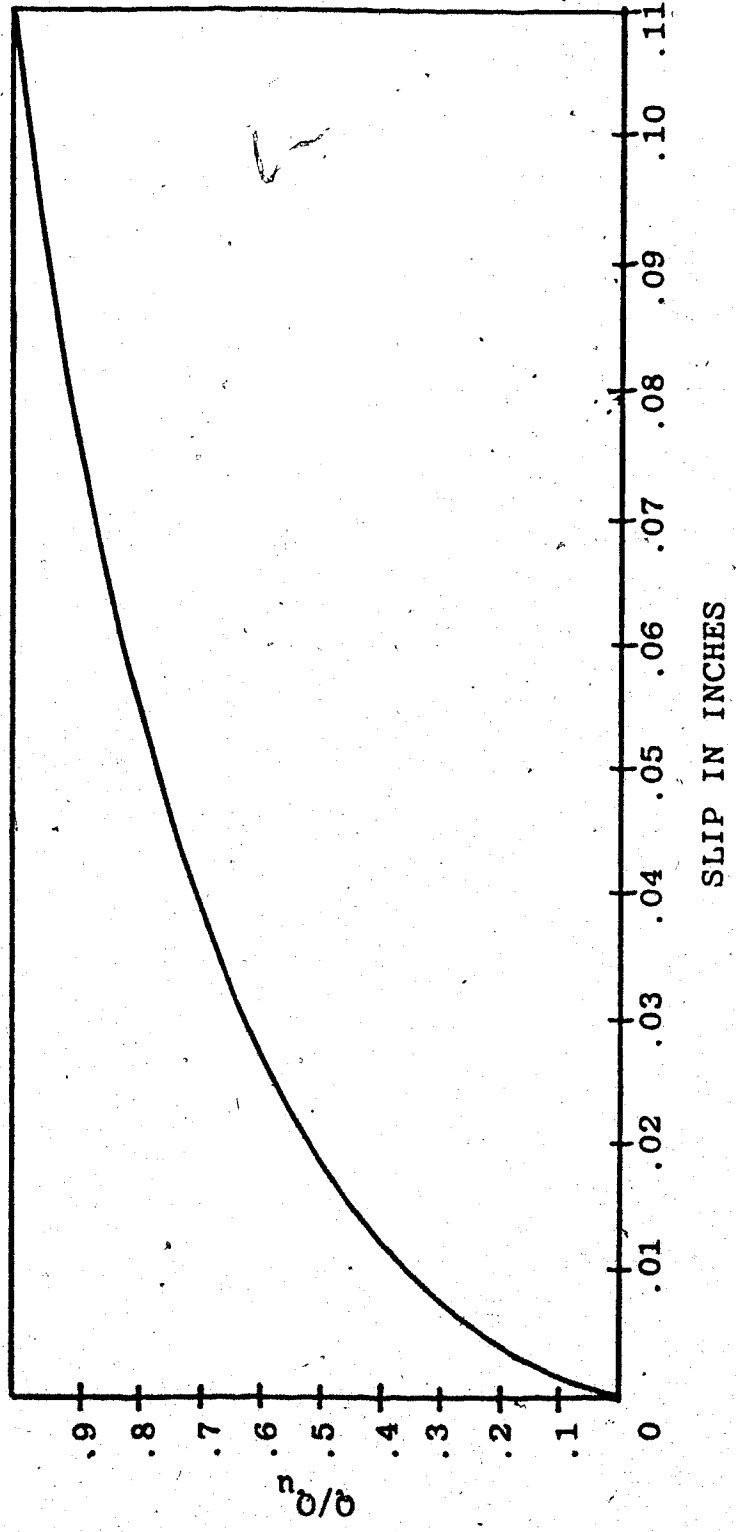


FIGURE 2.2 LOAD-SLIP RELATIONSHIP FROM PUSH-OUT TEST
(CHAPMAN AND BALAKRISHNAN)

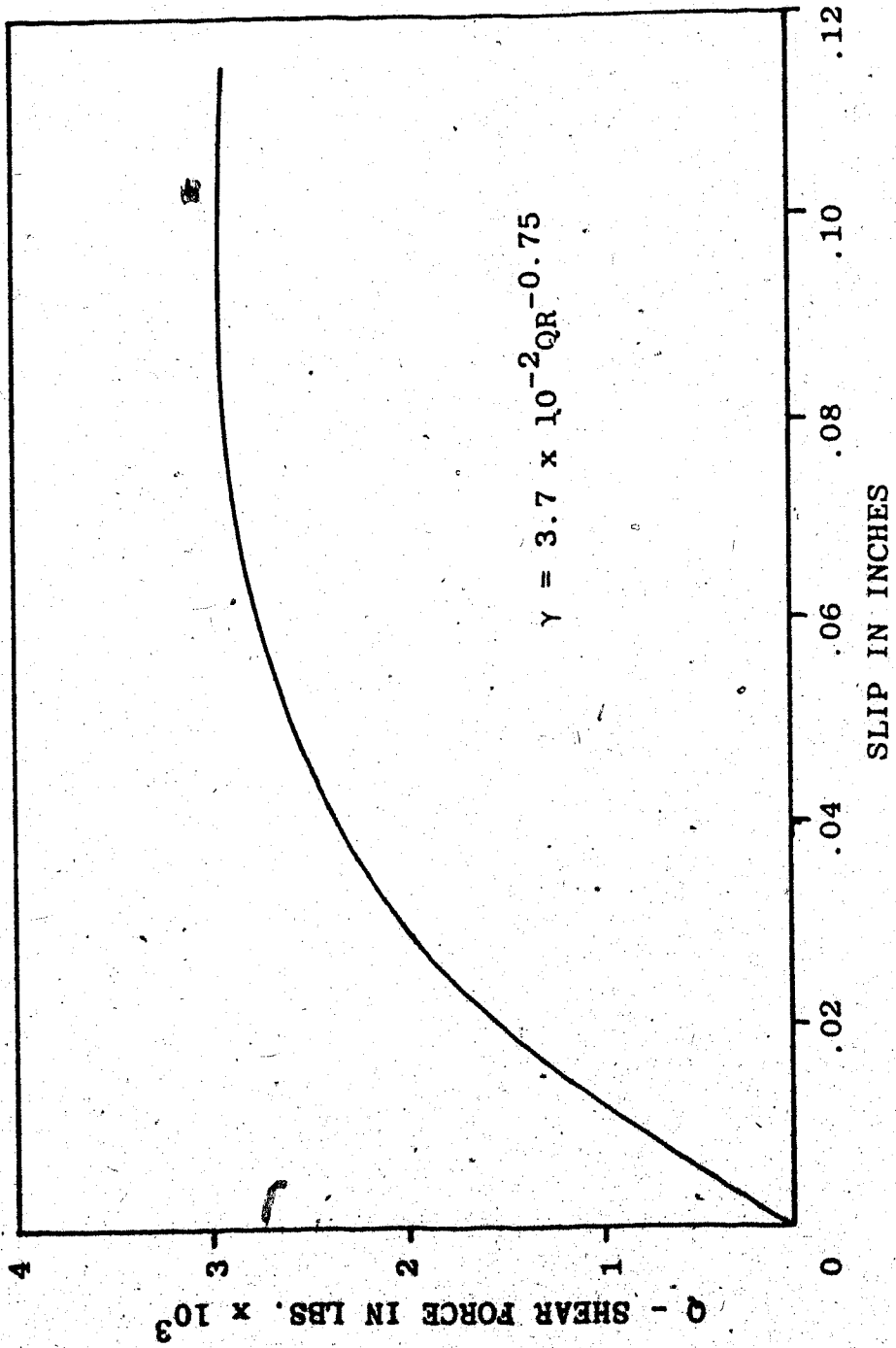


FIGURE 2.3 LOAD-SLIP RELATIONSHIP (VAN DALEN)

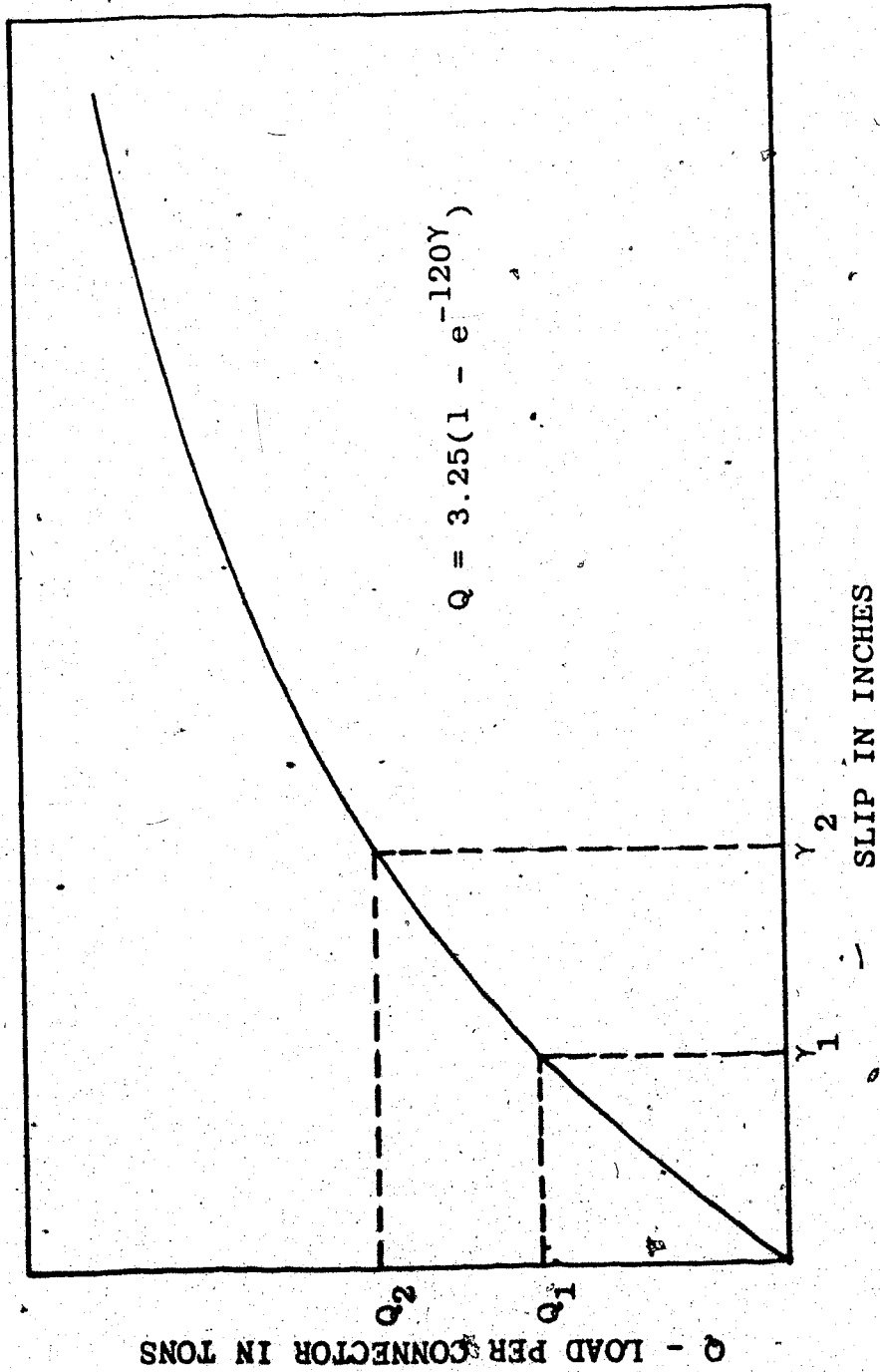
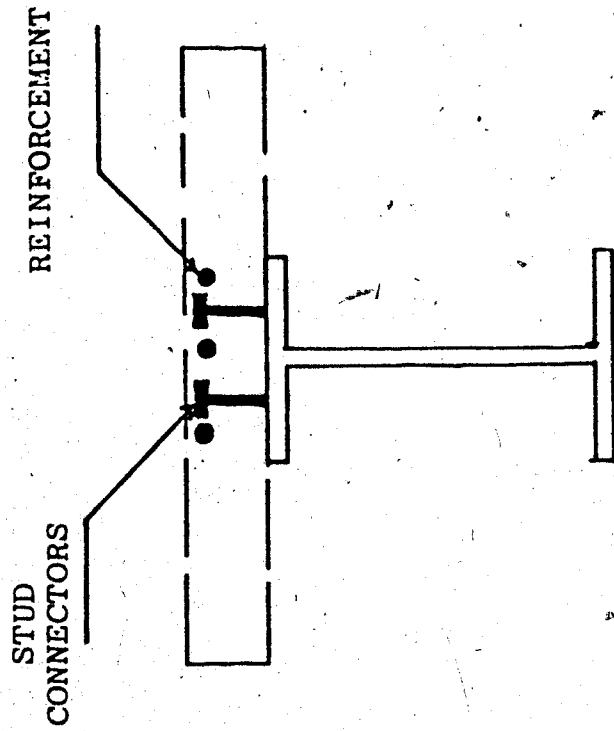
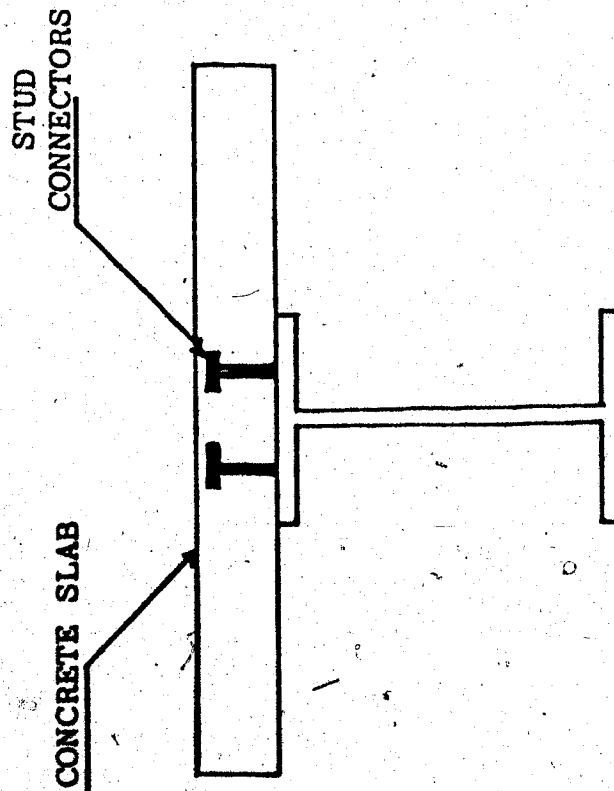


FIGURE 2.4 LOAD-SLIP RELATIONSHIP (YAM AND CHAPMAN)

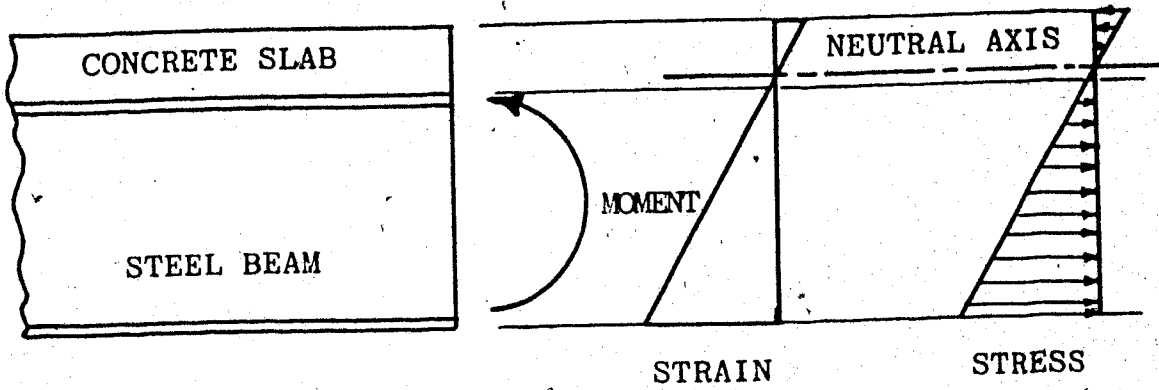


(a) POSITIVE MOMENT REGION

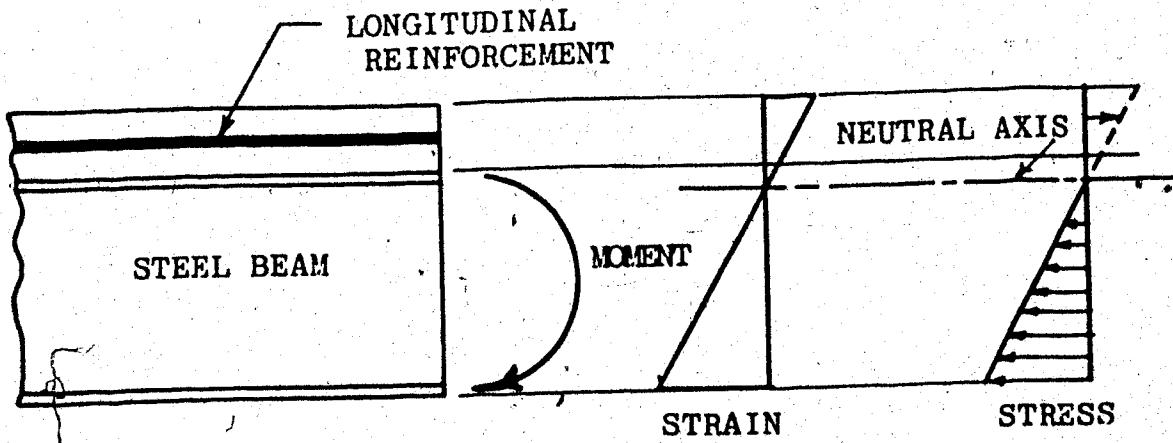


(b) NEGATIVE MOMENT REGION

FIGURE 2.5 SECTION THROUGH A COMPOSITE BEAM

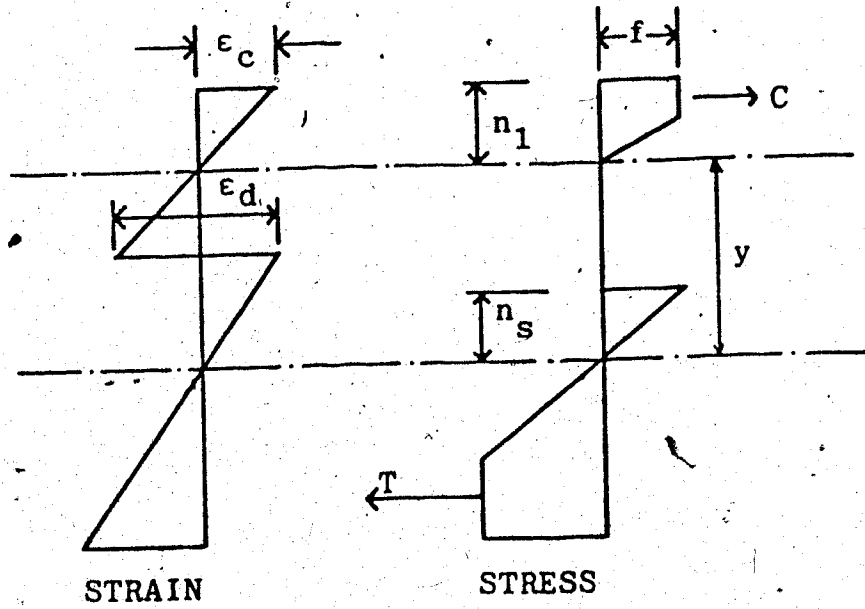


(a) POSITIVE MOMENT REGION

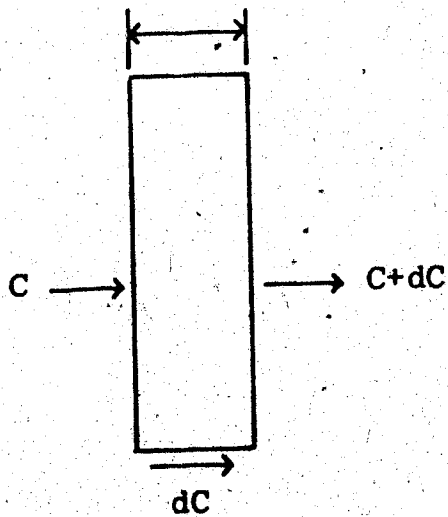


(b) NEGATIVE MOMENT REGION

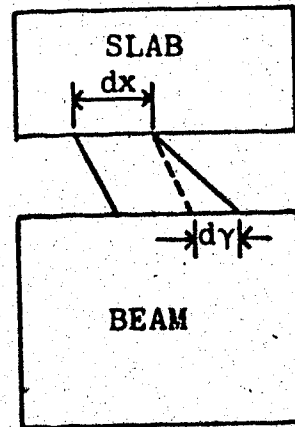
FIGURE 2.6 ELASTIC STRAIN AND STRESS DISTRIBUTION FOR COMPOSITE BEAM



(a) STRESS & STRAIN ACROSS A SECTION



(b) ELEMENT OF SLAB



(c) ELEMENT OF COMPOSITE BEAM

FIGURE 2.7 CONDITIONS IN AN ELEMENT OF A COMPOSITE BEAM

CHAPTER III

FORMULATION AND CLASSICAL SOLUTION OF BASIC EQUATIONS FOR COMPOSITE BEAMS

3.1 Formulation of Basic Equations

3.1.1 Assumptions for Displacements and Stresses

In the analysis, the following assumptions are made:

1. The distribution of strain is linear over the depth of slab and the depth of steel beam, respectively.
2. The shear connection between the slab and steel beam acts as a continuous medium along the length of the beam.
3. Concrete has no tensile strength.
4. It is assumed that the reinforcement bars are placed at one depth in the concrete slab.
5. The stress/strain curves for steel are the same in tension and in compression.
6. Within service load range the stress/strain for concrete and steel are linear.
7. The concrete slab and steel beam deflect equally at all points along the beam so that at any

cross section they have equal curvature and that uplift forces are resisted by the shear connectors without separation and do not affect the behavior of composite beams.

Fig. 3.1 shows a portion of a composite system with the slab spanning over several equally spaced beams. In the transverse direction the slab is considered to act as a continuous one-way slab supported by the beams. A portion of the slab, of width b_c , acts compositely with each steel section. The coordinate system and reference dimensions for a typical composite beam are shown in Fig. 3.2(a) and the assumed deformation and displacements are shown in Fig. 3.2(b).

As a result of partial interaction, cross section ABCD which is plane before deformation will not remain plane after deformation. The slip, s , creates a discontinuity at the interface of the concrete and steel as shown in Fig. 3.2(b).

The strains at any point in the beam may be determined directly from the horizontal displacement u and the vertical displacement v through the use of standard beam assumptions and strain displacement equations.

Assuming plane sections remain plane, the horizontal displacements in the steel may be expressed as

$$u = u_0 + v'y \quad 0 < y < d \quad (3.1)$$

the horizontal displacements in the concrete may be expressed as

$$u = u_0 + v'y + s \quad d < y < (d + t) \quad (3.2)$$

Combining Equations 3.1 and 3.2, and using a step function (7) so that the last term of Equation 3.2 is zero in the range $0 < y < d$, the displacement across the entire section can be expressed as

$$u = u_0 + v'y + \langle y - d \rangle^0 s \quad 0 < y < (d + t) \quad (3.3)$$

where $\langle y - d \rangle^0$ has a value of 0 for a negative argument and 1 for a positive argument. The strain in the horizontal direction can now be determined from the strain displacement equation as

$$\epsilon_x = u' \quad (3.4)$$

Differentiating Equation 3.3, yields

$$\epsilon_x = u'_0 + v''y + \langle y - d \rangle^0 s' \quad (3.5)$$

Defining the reference axis strain,

$$u'_0 = \epsilon_0 \quad (3.5a)$$

the curvature as

$$v'' = -\phi \quad (3.5b)$$

and slip strain as

$$\frac{ds}{dx} = s' \quad (3.5c)$$

Equation 3.5 may be written as

$$\epsilon_x = \epsilon_0 - \phi y + \langle y - d \rangle^0 s' \quad (3.6)$$

For a linear elastic stress-strain relationship, stress is expressed as

$$\sigma = E \epsilon_x \quad (3.7)$$

Substituting Equation 3.6 into Equation 3.7 gives stress in the terms of displacement derivatives as

$$\sigma = E(\epsilon_0 - \phi y + \langle y - d \rangle^0 s') \quad (3.8)$$

3.1.2 Equilibrium Equations in Terms of Displacements

Three basic equilibrium equations may be written for the composite beam shown in Fig. 3.4. These are

$$\int_A \sigma dA = 0 \quad (3.9)$$

$$\int_A \sigma y dA = -M \quad (3.10)$$

$$\frac{d}{dx} \left[\int_0^d \sigma dA \right] = \frac{dP}{dx} = -Ks = -q \quad (3.11)$$

where q is the shear flow on the interface between steel and concrete. Equation 3.11 is valid only if there is a relationship between shear flow and slip. Substituting Equation 3.8 into Equations 3.9 to 3.11, and carrying out the integration, we obtain

$$E(A_S + A_C) \epsilon_0 - E(A_C Y_C + A_S Y_S) \phi + EA_C s' = 0 \quad (3.12)$$

$$E(A_C Y_C + A_S Y_S) \epsilon_0 - E(I_C + A_C Y_C^2 + I_S + A_S Y_S^2) \phi + EA_C Y_C s' = -M \quad (3.13)$$

$$EA_S \epsilon_0' - EA_S Y_S \phi' = -Ks \quad (3.14)$$

in which Y_S and Y_C indicate the distances from neutral axis of the composite section to the centroids of the area of steel, A_S , and the transformed area of concrete, A_C (neglecting concrete area in tension), respectively, E is the modulus of elasticity of the steel, and n ($= E_C/E_S$) is the inverse modular ratio. Equations 3.12 to 3.14 may be simplified by shifting the x -axis to the centroid of the transformed section, in which case the following definitions apply:

$$(A_S Y_S + A_C Y_C) = 0 \quad (3.14a)$$

$$\text{and} \quad (I_C + A_C Y_C^2 + I_S + A_S Y_S^2) = I_t \quad (3.14b)$$

where I_S is the moment of inertia of the steel about the steel section centroidal axis, I_C is the moment of

inertia of the transformed area of the concrete slab about its centroidal axis in compression and I_t is the moment of inertia of the transformed composite section about the centroidal axis of the composite section. Thus ϵ_0 becomes the strain at the composite section centroid level, and

$$A_s + A_c = A_t \quad (3.14c)$$

is the total area of transformed section. The simplified forms of Equations 3.12 to 3.14 are

$$EA_t \epsilon_0 + EA_c s' = 0 \quad (3.15)$$

$$-EI_t \phi + EA_c Y_c s' = -M \quad (3.16)$$

$$EA_s \epsilon'_0 - EA_s Y_s \phi' = -Ks \quad (3.17)$$

Equations 3.15 to 3.17 express the basic equilibrium conditions, i.e., Equations 3.9 to 3.11, in terms of the three displacement gradients $\epsilon_0 = \frac{du_0}{dx}$, $\phi = -\frac{d^2 v}{dx^2}$, and $s' = \frac{ds}{dx}$; the section properties of the transformed area and the stiffness of the shear connectors, K . However, in order to obtain a solution, it is desirable to eliminate all but one of the displacements from the equations and derive governing equations to enable the solution of one displacement independently from the others.

3.1.3 Governing Equation for Slip

By differentiating Equations 3.15 and 3.16, ϵ'_0 and ϕ' may be expressed in terms of derivatives of s . Thus,

$$\epsilon_0 = -\frac{A_c}{A_t} s' \quad (3.18a)$$

$$\epsilon'_0 = -\frac{A_c}{A_t} s'' \quad (3.18b)$$

$$\phi = \frac{A_c Y_c s'}{I_t} + \frac{M}{EI_t} \quad (3.19a)$$

$$\phi' = \frac{A_c Y_c s''}{I_t} + \frac{V}{EI_t} \quad (3.19b)$$

Substituting these expressions for ϵ'_0 and ϕ' into Equation 3.17 and grouping the terms with a common order of derivative of slip, s , yields

$$s'' - \left[\frac{K}{EA_c \frac{A_s}{A_t} + \frac{A_s Y_s Y_c}{I_t}} \right] s = -\frac{V}{E} \frac{A_s Y_s}{I_t A_c} \left[\frac{1}{\frac{A_s}{A_t} + \frac{A_s Y_s Y_c}{I_t}} \right] \quad (3.20)$$

Letting
$$\left[\frac{K}{EA_c \frac{A_s}{A_t} + \frac{A_s Y_s Y_c}{I_t}} \right] = \alpha^2 \quad (3.21)$$

and
$$\left[\frac{A_s Y_s}{EI_t A_c} \frac{1}{\frac{A_s}{A_t} + \frac{A_s Y_s Y_c}{I_t}} \right] = \beta \quad (3.22)$$

Equation 3.20 becomes

$$s'' - \alpha^2 s = -\beta V \quad (3.23)$$

This is a second order differential equation and is the governing equation for slip. When the beam is statically determinate, V is a known function of x , and s can be determined by solving the differential equation. With the slip known, the curvature can be obtained directly from Equation 3.15. Integrating Equation 3.16 twice yields the value of transverse deflection v , and integrating Equation 3.15 once yields the value of u_0 . Thus the complete solution may be obtained from Equations 3.23, 3.15, and 3.16.

3.1.4 Governing Equation for Deflection

An alternative solution technique consists of deriving a governing fourth order equation in terms of the transverse displacement v . Differentiating Equation 3.17 and expressing terms as displacement gradients yields

$$EA_s u_0'' + EA_s Y_s v^{iv} + Ks' = 0 \quad (3.24)$$

From Equation 3.16,

$$s' = \frac{-M}{EA_c Y_c} - \frac{I_t}{A_c Y_c} v'' \quad (3.25)$$

By substituting Equation 3.25 in Equation 3.18a and differentiating twice, u_0'' may be obtained in terms of v . Thus

$$u_0'' = \frac{A_c}{A_t} \left(\frac{M}{EA_c Y_c} + \frac{I_t v''}{A_c Y_c} \right) \quad (3.26)$$

$$u''''_0 = \frac{-w}{EY_c A_t} + \frac{I_t v^{iv}}{A_t Y_c} \quad (3.27)$$

Substituting Equations 3.25 and 3.27 into Equation 3.24 results in

$$-v^{iv} EA_s A_c \left(\frac{I_t + A_t Y_s Y_c}{A_t} \right) + KI_t v'' = \frac{KM}{E} + \frac{A_c A_s}{A_t} w \quad (3.28)$$

Letting

$$EA_s A_c \left(\frac{I_t + A_t Y_s Y_c}{A_t} \right) = \psi \quad (3.29)$$

Equation 3.28 becomes

$$v^{iv} - \frac{KI_t}{\psi} v'' = \frac{-KM}{E\psi} - \frac{A_s A_c}{A_t \psi} w \quad (3.30)$$

This is a fourth order differential equation in terms of deflection. If the beam is statically determinate, M is a known function of x and w (the uniform loading) and v can be determined as the solution to the differential equation. With deflection known, the curvature may be determined by differentiation and the slip strain determined from Equation 3.25 by substitution. The slip may be evaluated by integrating Equation 3.25 and u_0 is determined from Equation 3.26. The complete solution is therefore available from Equations 3.30, 3.25, and 3.26.

3.2 Slip Strain at Inflection Point

Figure 3.5 illustrates the neutral axis positions in a continuous composite section under positive and negative bending for uniform and discontinuous section properties. In the negative bending moment region, assuming the concrete has no tension strength, the concrete slab is not effective. Theoretically there is an abrupt change in the position of neutral axis at the point of inflection as shown in Fig. 3.5(b). The slip strain is affected by this abrupt change in the neutral axis position and the abrupt change in effective area of concrete slab.

In order to maintain continuity of the force F between positive and negative moment regions, the strain at the centroid of steel section must be equal on both sides of the point of inflection.

$$\epsilon_{sL} = \epsilon_{sR} \quad (3.31)$$

where subscripts L and R refer to locations to the left and right of inflection point. In the positive moment region the strain at the centroid of the steel section can be expressed in terms of the curvature and the strain at the neutral axis of the transformed section. From Equation 3.6,

$$\epsilon_{sL} = \epsilon_{oL} - \phi_L Y_{sL} \quad (3.32a)$$

Similarly for the negative moment region,

$$\epsilon_{sR} = \epsilon_{oR} - \phi_R Y_{sR} \quad (3.32b)$$

Now substituting values of ϵ_{oL} , ϵ_{oR} , ϕ_L and ϕ_R from Equations 3.18(a), and 3.19(a) into Equations 3.32(a) and 3.32(b), and equating the results as indicated by Equation 3.31, the following relationship is obtained:

$$\begin{aligned} & - \left(\frac{A_{cL}}{A_{tL}} + \frac{Y_{sL} A_{cL} Y_{cL}}{I_{tL}} \right) s'_L + \frac{MY_{sL}}{EI_{tL}} \\ & = - \left(\frac{A_{cR}}{A_{tR}} + \frac{Y_{sL} A_{cR} Y_{cR}}{I_{tR}} \right) s'_R + \frac{MY_{sR}}{EI_{tR}} \end{aligned} \quad (3.33)$$

If uniform or constant section properties are assumed over the entire length of beam; there will be no change in the concrete area at the inflection point and the neutral axis will not shift its position. Hence the section properties to the left of the inflection point will be the same as section properties to the right. From Equation 3.33 it is evident that with uniform section properties the slip strain to the left of the inflection point is equal to that to the right. Thus it can be proved that continuity of slip strain exists with constant section properties.

If there is a change in section properties the slip strain to the right of the inflection point will be related to slip strain to the left but there will be discontinuity at the inflection point. Let

$$-\frac{A_{cL}}{A_{tL}} + \frac{Y_{sL} A_{cL} Y_{cL}}{I_{tL}} = \chi_L \quad (3.34)$$

and

$$-\frac{A_{cR}}{A_{tR}} + \frac{Y_{sR} A_{cR} Y_{cR}}{I_{tR}} = \chi_R \quad (3.35)$$

By substituting Equations 3.34 and 3.35 into Equation 3.33 and eliminating moment terms (moment is zero at the inflection point), the slip strain to the right of the inflection point may be written as

$$s'_R = \frac{\chi_L}{\chi_R} s'_L \quad (3.36)$$

3.3 Boundary Conditions

In order to evaluate the constants of integration involved in the solution, boundary conditions must be established for any particular problem. For example, for a simple span beam the bending moment, stresses and strains are zero, i.e., $M = 0$, $\sigma = 0$, $\epsilon_0 = 0$ at $x = 0$ and at $x = L$. Hence, from Equation 3.15, s' must be zero and, from Equation 3.16, it may be concluded that ϕ is also zero at $x = 0$ and at $x = L$.

From compatibility requirements, it is obvious that slip is continuous. Also, as explained in Section 3.2, the strain at the centroid of the steel section is continuous since the force P in the slab must be continuous and therefore s' is continuous wherever section properties are continuous. For equilibrium, the

summation of the axial force over the entire section must be zero. The boundary conditions for a simply supported beam and a continuous beam are shown in Fig. 3.6.

3.4 Linear Closed Form Solutions

The governing equation for slip, Equation 3.23, is

$$s'' - \alpha^2 s = -\beta V \quad (3.37)$$

The particular solution of this equation for a uniformly distributed load, w , is

$$s_p = -\frac{\beta}{\alpha^2} \left(\frac{wL}{2} - wx \right) \quad (3.38)$$

The homogeneous solution is

$$s_h = A \sinh \alpha x + B \cosh \alpha x \quad (3.39)$$

Hence the general solution is

$$s = A \sinh \alpha x + B \cosh \alpha x + \frac{\beta}{\alpha^2} \left(\frac{wL}{2} - wx \right) \quad (3.40)$$

The boundary conditions relating to slip strain are

$$\text{at } x = 0, \quad \frac{ds}{dx} = 0 \quad (3.41a)$$

$$\text{at } x = L, \quad \frac{ds}{dx} = 0 \quad (3.41b)$$

Differentiating Equation 3.40 results in a slip strain equal to

$$\frac{ds}{dx} = A\alpha \cosh \alpha x + B\alpha \sinh \alpha x + \frac{\beta}{\alpha^2} (-w) \quad (3.42)$$

By introducing the boundary condition Equation 3.41a, Equation 3.42 becomes

$$0 = A\alpha - \frac{\beta}{\alpha^2} w \quad (3.43a)$$

from which

$$A = \frac{\beta}{\alpha^3} w \quad (3.43b)$$

Substituting the second boundary condition, Equation 3.41b, into Equation 3.42 gives

$$0 = \frac{\beta w}{\alpha^2} \cosh \alpha L + B\alpha \sinh \alpha L - \frac{\beta}{\alpha^2} w \quad (3.44a)$$

from which

$$B = \frac{w\beta}{\alpha^3} \left[\frac{1 - \cosh \alpha L}{\sinh \alpha L} \right] \quad (3.44b)$$

Substituting Equations 3.43b and 3.44b into Equations 3.40 and 3.42 yields

$$s = \frac{w\beta}{\alpha^3} \left[\sinh \alpha x + (1 - \cosh \alpha L) \frac{\cosh \alpha x}{\sinh \alpha L} \right] + \frac{\beta}{\alpha^2} \left(\frac{wL}{2} - wx \right) \quad (3.45)$$

and

$$s' = \frac{w\beta}{\alpha^2} \left[\cosh \alpha x + (1 - \cosh \alpha L) \frac{\sinh \alpha x}{\sinh \alpha L} \right] - \frac{w\beta}{\alpha^2} \quad (3.46)$$

The deflection may now be determined by integration of Equation 3.46 using Equation 3.19(a).

Combining these two equations yields

$$-v'' = \frac{w}{2EI_t} (Lx - x^2) + \frac{A_c Y_c}{I_t} \frac{w\beta}{\alpha^2} \left[\cosh \alpha x + (1 - \cosh \alpha L) \frac{\sinh \alpha x}{\sinh \alpha L} - 1 \right] \quad (3.47)$$

Integrating twice yields

$$-v = \frac{w}{2EI_t} \left(\frac{Lx^3}{6} - \frac{x^4}{12} \right) + \frac{A_c Y_c \beta w}{I_t \alpha^4} \left[\cosh \alpha x + \rho \sinh \alpha x - \frac{\alpha^2 x^2}{2} + D + Cx \right] \quad (3.48)$$

in which

$$\rho = (1 - \cosh \alpha L) / \sinh \alpha L \quad (3.49)$$

Subjecting Equation 3.48 to the boundary condition, $v(0) = 0$, yields $D = -1$. Imposing the boundary condition $v(L) = 0$ yields

$$0 = \frac{wL^4}{24EI_t} + \frac{A_c Y_c \beta w}{I_t \alpha^4} \left(-\frac{\alpha^2 L^2}{2} + CL \right) \quad (3.50a)$$

from which

$$C = -\frac{\alpha^4 L^3}{24EA_c Y_c \beta} + \frac{\alpha^2 L}{2} \quad (3.50b)$$

Substituting into Equation 3.48 and rearranging yields

$$-v = \frac{w}{2EI_t} \left(\frac{Lx^3}{6} - \frac{x^4}{12} \right) - \frac{wL^3 x}{24EI_t} + \frac{A_c Y_c \beta w}{I_t \alpha^4} \left[\cosh \alpha x + \rho \sinh \alpha x + \frac{\alpha^2}{2} (Lx - x^2) - 1 \right] \quad (3.51)$$

Equations 3.45, 3.46 and 3.51 give the solution for slip, slip-strain and deflection of a simply supported uniformly loaded beam. A solution of the

differential equations for a continuous beam with two unequal spans subjected to two equal midspan concentrated loads is derived in Appendix A. The evaluation of the constants of integration for this case is so complex that they can only be obtained by solving a matrix equation in the computer. Therefore solutions can only be obtained once numerical values are assigned to all variables.

3.5 Formulation for Nonlinear Load-Slip Relationships

The solutions in Section 3.4 and Appendix A assume a linear relationship between shear flow and slip. This assumption was introduced in Equation 3.11, where it was assumed that

$$q = Ks \quad (3.52)$$

When the slip is nonlinear, Equation 3.52 may be replaced by the general expression

$$q = f(s) \quad (3.53)$$

in which $f(s)$ is any nonlinear function of s .

Yam and Chapman (31) introduced an exponential relationship in the form

$$Q = a (1 - e^{-bs}) \quad (3.54)$$

to represent a nonlinear load-slip relationship between the total shear connector force, Q , and the slip, s :

This may be reduced to a shear flow relationship by dividing by the connector spacing, ℓ . Then Equation 3.52 becomes

$$q = \frac{Q}{\ell} = \frac{a}{\ell} (1 - e^{-bs}) \quad (3.55)$$

which is a particular form of the more general relationship represented by Equation 3.54.

If the relationship of Equation 3.53 is used in place of Equation 3.52, Equation 3.11 becomes

$$\frac{dP}{dx} = -f(s) = -q \quad (3.56)$$

Equation 3.17 becomes

$$EA_S \epsilon_0' - EA_S Y_S \phi' = -f(s) \quad (3.57)$$

and the governing equation for slip, Equation 3.23, becomes

$$s'' - \alpha^2 f(s) = -\beta V \quad (3.58)$$

in which, from Equation 3.21,

$$\alpha^2 = \left[\frac{K}{EA_c \frac{A_s}{A_t} + \frac{A_s Y_s Y_c}{I_t}} \right] \quad (3.59)$$

and

$$\beta = \left[\frac{A_s Y_s}{EI_t A_c} \frac{1}{\frac{A_s}{A_t} + \frac{A_s Y_s Y_c}{I_t}} \right] \quad (3.60)$$

Since Equation 3.58 is nonlinear, there are no closed form solutions. Therefore, numerical solution techniques be applied as discussed in Chapter IV.

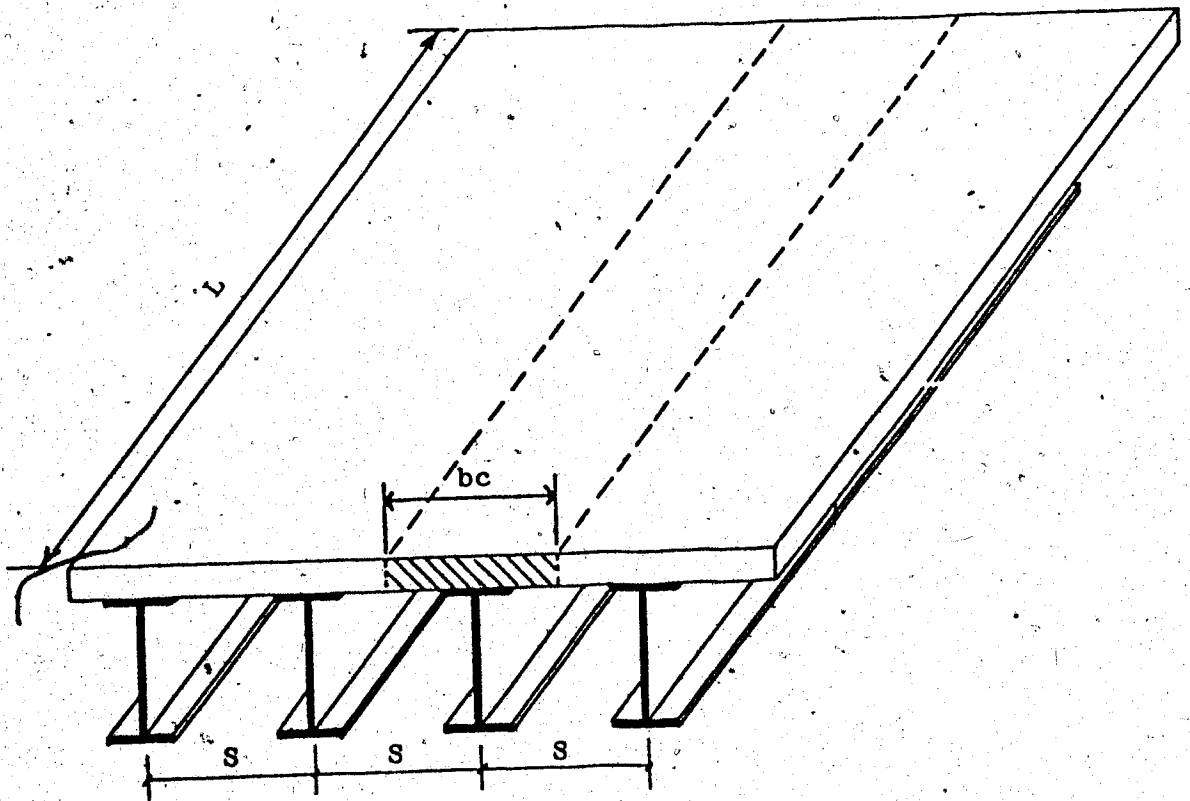
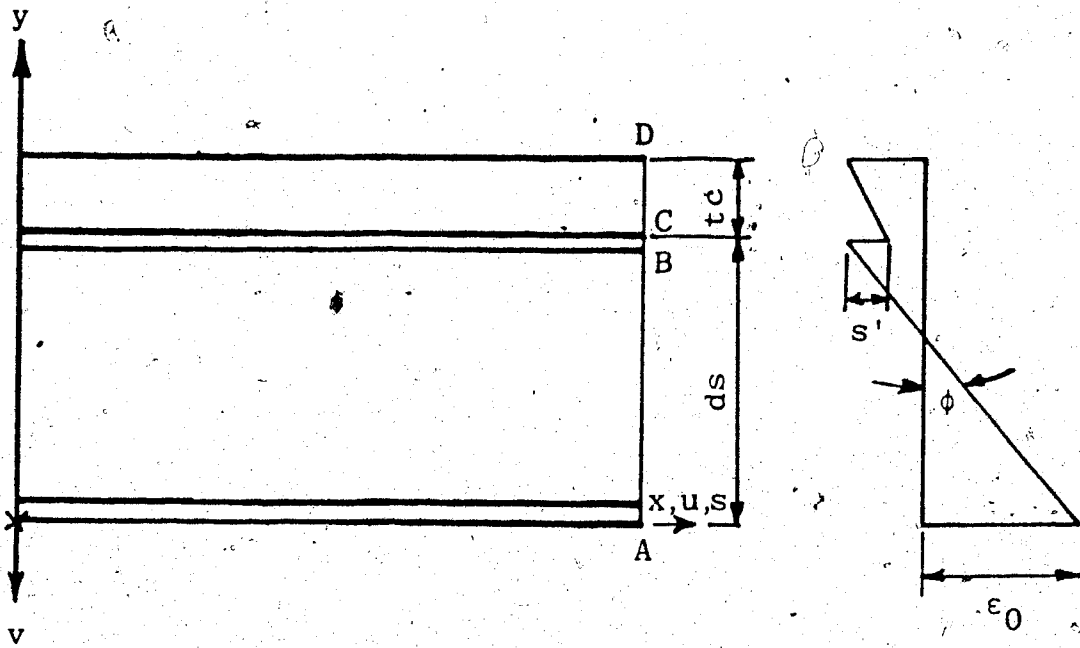
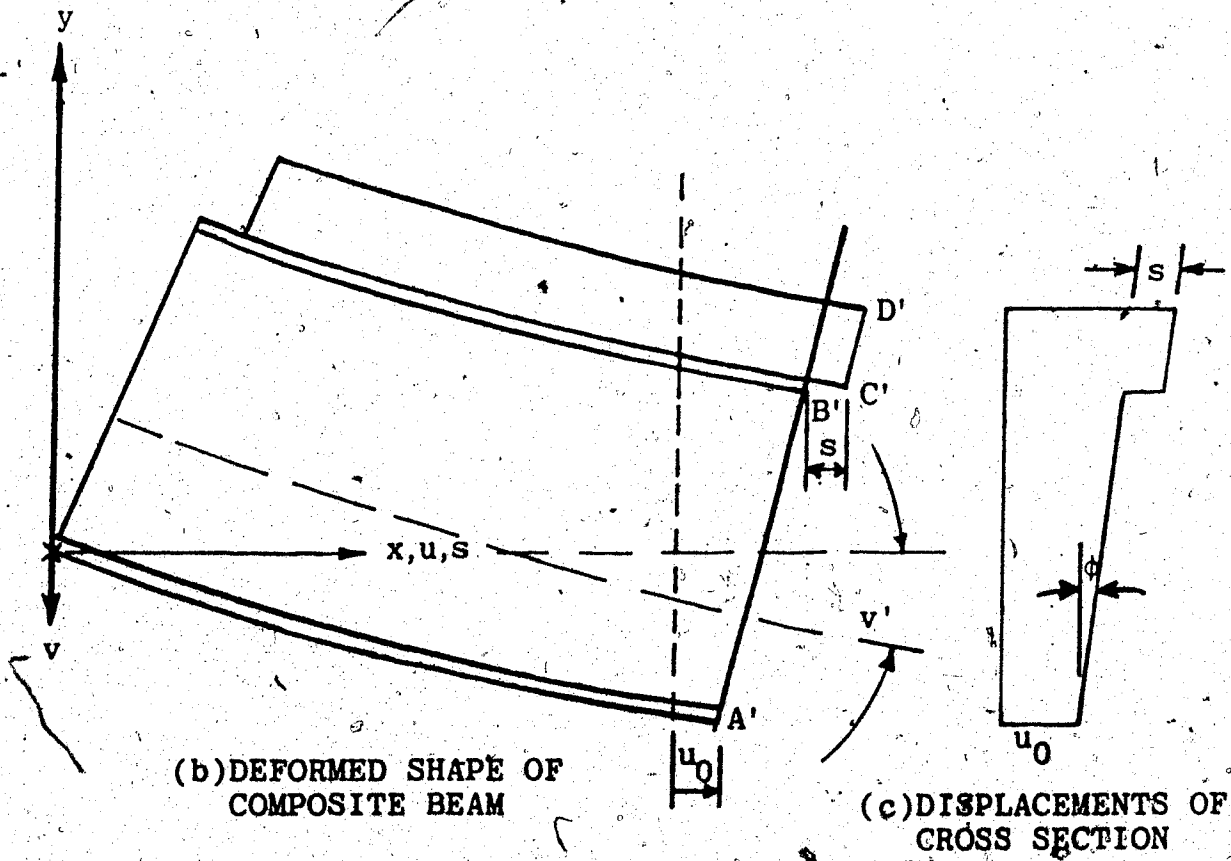


FIGURE 3.1 COMPOSITE SYSTEM



(a) COÖRDINATE SYSTEM & STRAIN DISTRIBUTION



(b) DEFORMED SHAPE OF COMPOSITE BEAM

(c) DISPLACEMENTS OF CROSS SECTION

FIGURE 3.2 DEFORMATION AND DISPLACEMENT OF COMPOSITE BEAM

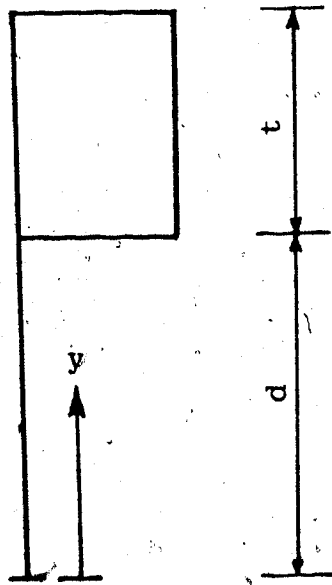


FIGURE 3.3 STEP FUNCTION

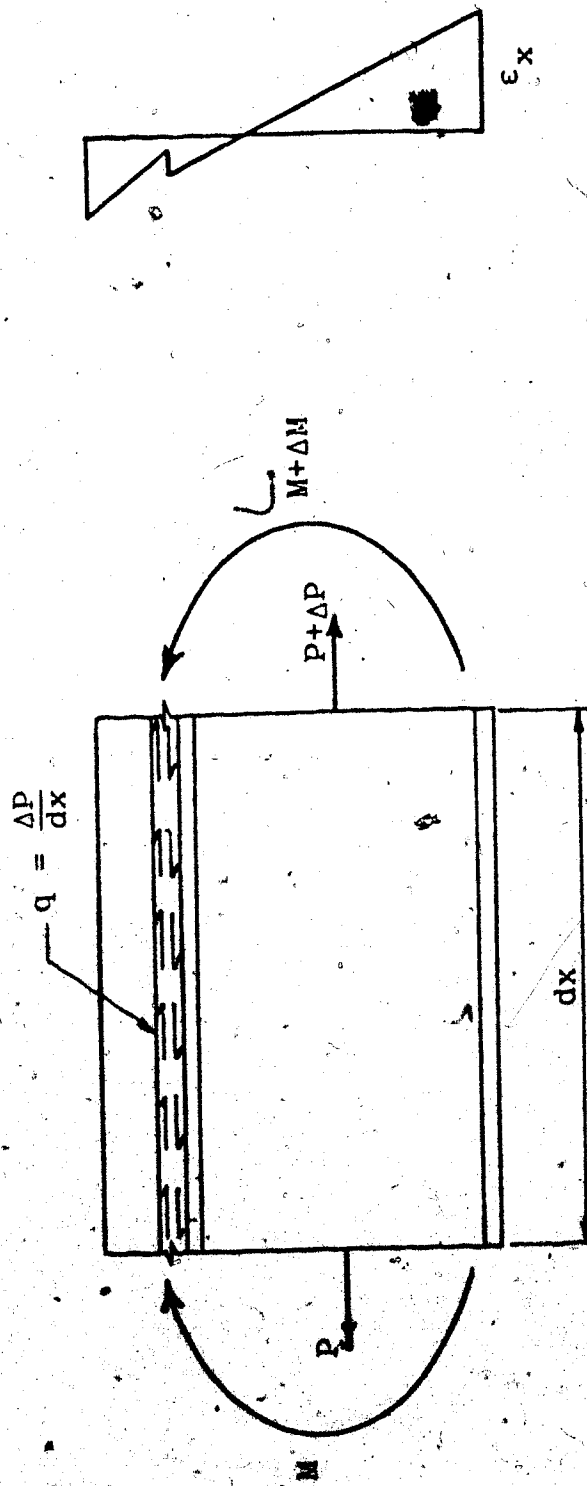
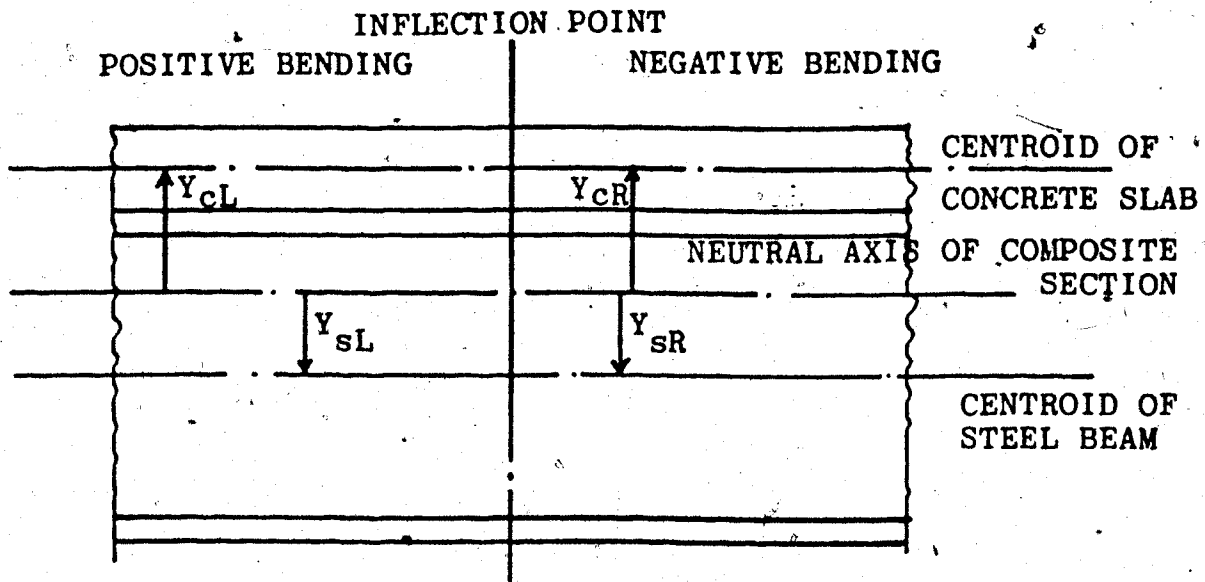
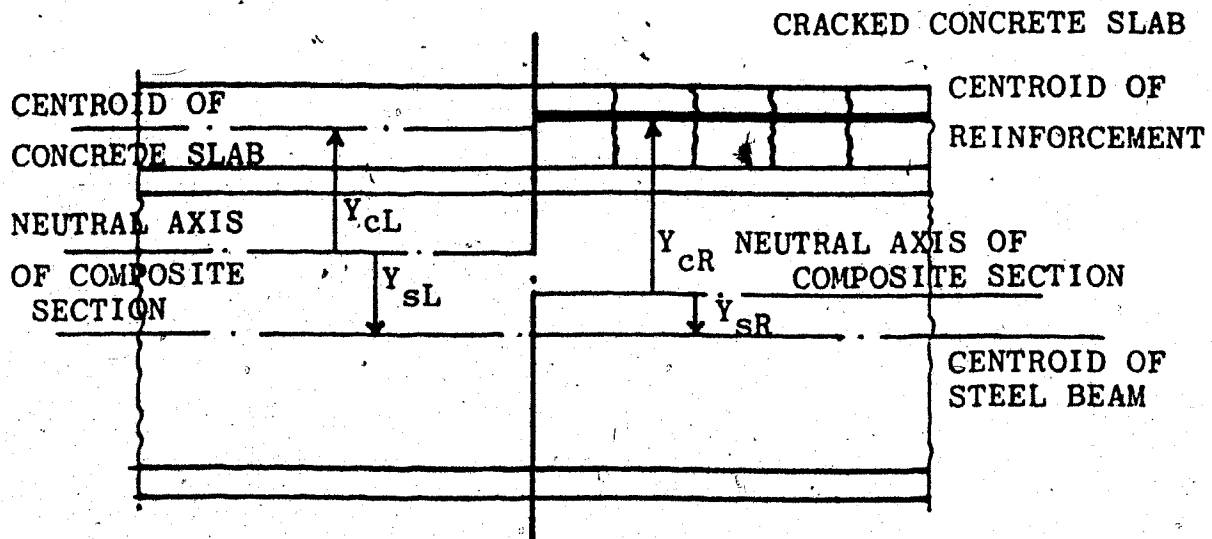


FIGURE 3.4 . STRAIN DISTRIBUTION IN COMPOSITE BEAM SECTION

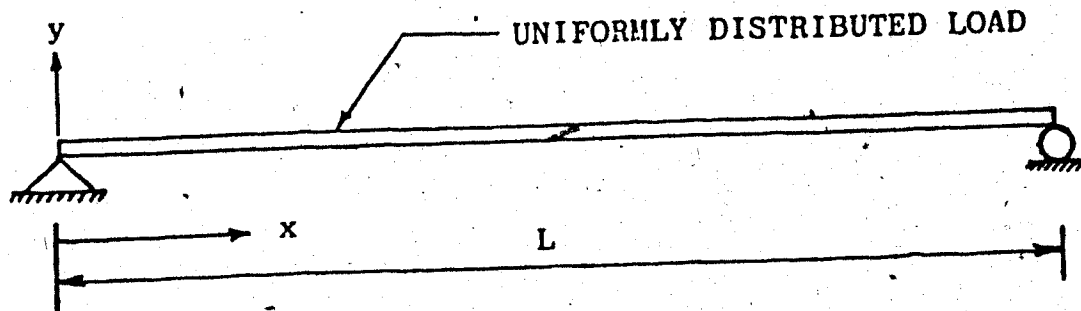


(a) UNIFORM STIFFNESS



(b) VARIABLE STIFFNESS

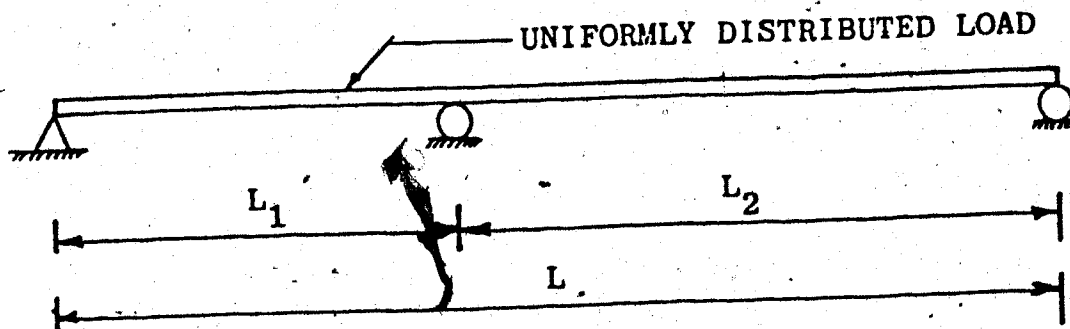
FIGURE 3.5 CONDITIONS AT INFLECTION POINT



Boundary Conditions

a) Slip	$s' = 0$		$s' = 0$
Strain			$\phi = 0$
b) Curvature	$\phi = 0$		$P = 0$
c) Force	$P = 0$		
d) Σ Force		$\int_0^L k s dx = 0$	

(a) SIMPLY SUPPORTED BEAM



Boundary Conditions

a) Slip	$s_1 = s_2$	$s_2 = s_3$	$s_3 = s_4$		
b) Slip Strain	$s'_1 = 0$	$s'_1 = s'_2$	$s'_2 = s'_3$	$s'_3 = s'_4$	$s'_4 = 0$
c) Curvature	$\phi_1 = 0$	$\phi_1 = \phi_2$	$\phi_2 = \phi_3$	$\phi_3 = \phi_4$	$\phi_4 = 0$
d) Force	$P_1 = 0$	$P_1 = P_2$	$P_2 = P_3$	$P_3 = P_4$	$P_4 = 0$
e) Σ Force	$\int_0^{L_1/2} k s_1 dx$	$\int_{L_1/2}^{L_1} k s_2 dx$	$\int_{L_1}^{L_1+L_2/2} ds_3 dx$	$\int_{L_1+L_2/2}^L k s_4 dx = 0$	

(b) CONTINUOUS BEAM

FIGURE 3.6 BOUNDARY CONDITIONS

CHAPTER IV

A NUMERICAL SOLUTION TECHNIQUE FOR COMPOSITE BEAMS

4.1 Introduction

Classical solutions for deflections of composite beams are limited to simple sections with no material nonlinearities. Furthermore, as may be seen in Appendix A, the evaluation of constants of integration becomes tedious for continuous beams. Numerical techniques offer an alternative in these cases.

A technique for obtaining numerical solutions for continuous composite beams with a nonlinear load-slip relationship is developed in this Chapter. The governing equation for slip, Equation 3.23, is the basis of the numerical solution technique. Beginning with an initial assumed slip, the numerical technique involves a process of iteration which is continued until the slip has an acceptable degree of accuracy.

4.2 Numerical Integration of Slip Equation

A three-span continuous composite beam, shown in Fig. 4.1, is divided into a number of segments of length h . Each end of a segment length is defined by a nodal point, as illustrated in Fig. 4.1(b). The continuous beam is changed into a simple beam primary structure subjected to two sets of loadings. The first loading consists of the external loading while the second consists of the redundant reactions. This scheme is illustrated in Figs. 4.1(c) and 4.1(d), respectively.

As derived in Section 3.5, the governing second order equation for slip is

$$s'' - \alpha^2 f(s) = -\beta V \quad (4.1)$$

Setting $s' = v$ (which is not to be confused with v of Chapter III), the second order Equation 4.1 may be expressed as the following two first order simultaneous equations:

$$s' = v \quad (4.2)$$

$$v' = \alpha^2 f(s) - \beta V \quad (4.3)$$

Equations 4.2 and 4.3 may be solved by using a Runge-Kutta method of integration, and iterating each equation in turn. In applying the Runge-Kutta method (7)

Equations 4.2 and 4.3 are expressed as

$$s' = H(s, x, v) \quad (4.4)$$

$$v' = G(s, x, v) \quad (4.5)$$

in which H and G represent the functional forms in Equations 4.2 and 4.3. The recursive equations for the fourth order Runge-Kutta solution of Equations 4.4 and 4.5 are

$$s_{i+1} = s_i + \frac{h}{6} (k_{1s} + 2k_{2s} + 2k_{3s} + k_{4s}) \quad (4.6)$$

$$v_{i+1} = v_i + \frac{h}{6} (k_{1v} + 2k_{2v} + 2k_{3v} + k_{4v}) \quad (4.7)$$

Equations 4.6 and 4.7 are used alternately and the k_{is} and k_{iv} values are determined as follows:

$$k_{1s} = H(x_i, s_i, v_i) \quad (4.8)$$

$$k_{1v} = G(x_i, s_i, v_i) \quad (4.9)$$

$$k_{2s} = H(x_i + \frac{h}{2}, s_i + \frac{hk_{1s}}{2}, v_i + \frac{hk_{1v}}{2}) \quad (4.10)$$

$$k_{2v} = G(x_i + \frac{h}{2}, s_i + \frac{hk_{1s}}{2}, v_i + \frac{hk_{1v}}{2}) \quad (4.11)$$

$$k_{3s} = H(x_i + \frac{h}{2}, s_i + \frac{hk_{2s}}{2}, v_i + \frac{hk_{2v}}{2}) \quad (4.12)$$

$$k_{3v} = G(x_i + \frac{h}{2}, s_i + \frac{hk_{2s}}{2}, v_i + \frac{hk_{2v}}{2}) \quad (4.13)$$

$$k_{4s} = H(x_i + h, s_i + hk_{3s}, v_i + hk_{3v}) \quad (4.14)$$

$$k_{4v} = G(x_i + h, s_i + hk_{3s}, v_i + hk_{3v}) \quad (4.15)$$

The initial values of x_i , s_i , v_i determine k_{1s} and k_{1v} from Equations 4.8 and 4.9 respectively. The remaining values, k_{js} and k_{jv} , where $j = 2, 3, 4$, are determined from Equations 4.10 through 4.15 successively.

Equations 4.6 and 4.7 determine values of slip and slip strain, respectively. The computation of slip starts from the left end of the beam at $x_i = 0$ and progresses through all nodal points to the right end of the beam as shown in Fig. 4.1(b). The shear flow at any nodal point in the beam may be computed by using either a linear or a nonlinear relation for slip in which, from Equation 3.52,

$$q = Ks \quad (4.16a)$$

or, from Equation 3.55,

$$q = \frac{a}{l}(1 - e^{-bs}) \quad (4.16b)$$

The axial force in the concrete at the right end of the beam is computed by using the relationship

$$F = \int_0^L q dx \quad (4.17)$$

If the axial force computed at the right end is zero, the assumed initial slip value is correct and hence the total solution is correct. If the axial force is not zero at the right end, a correction is applied to satisfy the boundary condition

$$F(L) = 0 \quad (4.18)$$

4.3 Correction and Iteration for Slip

An unbalanced axial force in the slab at the right end of the beam, as shown in Fig. 4.2a, creates an unbalanced moment. An equal and opposite balancing moment produces a correction to the initial assumed slip value. The general solution to Equation 3.37 for this loading case is

$$s = A \sinh \alpha x + B \cosh \alpha x + \frac{\beta}{\alpha^2} \frac{F(Y_c - Y_s)}{L} \quad (4.19)$$

Evaluating s' , and equating it to zero for $x = 0$ requires that A is zero. Fig. 4.2(b) illustrates the moment correction to remove the unbalanced force. Using Equation 3.6, the strains at the centroids of the slab and steel section at the end of the span are

$$\epsilon_c = \epsilon_0 - \phi Y_c + s'_L = \frac{-F}{EA_c} \quad (4.20)$$

$$\epsilon_s = \epsilon_0 - \phi Y_s = \frac{F}{EA_s} \quad (4.21)$$

Eliminating ϵ_0 from Equations 4.20 and 4.21, the slip strain, in terms of unbalanced force and curvature, is

$$s'_L = \frac{-F}{E} \left(\frac{1}{A_s} + \frac{1}{A_c} \right) + \phi (Y_c - Y_s) \quad (4.22)$$

From Equation 3.16 the slip strain can also be expressed in terms of curvature and the applied forces required to balance the unbalanced moment as

$$s'_L A_c Y_c = \frac{F}{E} (Y_c - Y_s) + \phi I_t \quad (4.23)$$

by eliminating curvature from Equations 4.22 and 4.23

$$s'_L = -\frac{F}{E} \left[\frac{A_t I_t + A_s A_c (Y_c - Y_s)^2}{A_s A_c \left\{ I_t - A_c Y_c (Y_c - Y_s) \right\}} \right] = \lambda \quad (4.24)$$

Equation 4.24 defines the slip strain boundary condition at the right end of the beam for the balancing moment.

By differentiating Equation 4.19 the slip strain at the right end of the beam, where $x = L$, is

$$s'_R = \alpha B \sinh \alpha L \quad (4.25)$$

By equating Equations 4.24 and 4.25, the constant B is evaluated as

$$B = \frac{\lambda}{\alpha \sinh \alpha L} \quad (4.26)$$

As the A and B values are now known, the slip at the left end, from Equation 4.17, is

$$s = B + \frac{\beta}{\alpha^2} F (Y_q - Y_s) \quad (4.27)$$

Equation 4.27 represents the correction to be applied to the initial assumed slip at the left end of the beam.

The procedure is repeated with the corrected slip value until the force boundary condition at the right end, Equation 4.20, is satisfied. Values of slip and slip strain are then directly available from Equations 4.6 and 4.7; shear flow may be computed from Equations 4.16a or 4.16b, and axial force may be computed from a numerical integration of Equation 4.17.

4.4 Evaluation of Slip Strain

Although the slip strain may be obtained from the Runge-Kutta solution as the variable v_1 , evaluated in Equation 4.7, the slip strain used to determine the shear flow in the program developed herein was obtained as the derivative of a quadratic polynomial passing through three consecutive points on the slip curve. For equally spaced points this reduces to the standard second order finite difference approximation.

The Lagrangian interpolating polynomial, $f(x)$, passing through the values f_1 , f_2 and f_3 at three unequally spaced points as illustrated in Fig. 4.3(a), may be expressed in terms of the local x coordinate, measured from point 1, as

$$f(x) = \frac{(x-l_1)(x-l)}{l_1 l} f_1 + \frac{x(l-x)}{l_1 l_2} f_2 + \frac{x(x-l_1)}{l l_2} f_3 \quad (4.28)$$

Differentiating this expression yields

$$\frac{df}{dx} = \frac{2(x-l_1) - l_2}{l_1 l} f_1 + \frac{-2x}{l_1 l_2} f_2 + \frac{2x - l_1}{l l_2} f_3 \quad (4.29)$$

Evaluating this derivative at the three nodal points

gives

$$\left. \frac{df}{dx} \right|_{x=0} = \frac{-(2l_1+l_2)}{l_1(l_1+l_2)} f_1 + \frac{l_1+l_2}{l_1 l_2} f_2 - \frac{l_1}{2(l_1+l_2)} f_3 \quad (4.30a)$$

$$\left. \frac{df}{dx} \right|_{x=l_1} = \frac{-l_2}{l_1(l_1+l_2)} f_1 - \frac{(l_2-l_1)}{l_1 l_2} f_2 + \frac{l_1}{l_2(l_1+l_2)} f_3 \quad (4.30b)$$

$$\frac{df}{dx} = \frac{\ell_2}{\ell_1(\ell_1 + \ell_2)} f_1 - \frac{(\ell_1 + \ell_2)}{\ell_1 \ell_2} f_2 + \frac{\ell_1 + 2\ell_2}{\ell_2(\ell_1 + \ell_2)} f_3 \quad (4.30c)$$

$x = \ell$

These equations are used to evaluate s'_i . In evaluating s'_i at node i , and letting $\ell_1 = \ell_2 = h$, Equation 4.30 becomes

$$s'_i = \frac{\ell}{2h} (s_{i+1} - s_{i-1}) \quad (4.31)$$

which is the finite difference form.

At an inflection point the section properties may be considered to be discontinuous, as discussed in Section 3.2. Let us consider that the bending moment diagram is as shown in Figure 4.3b and the discontinuity in section properties occurs at point O which is located at a distance 'a' from a node j and at a distance 'b' from node i . In terms of the slip values at nodes $j-1$, j and $j+1$ shown in Figure 4.3c, the slip strain at points j and $j+1$ may be computed by evaluating Equations 4.30b and 4.30c, which become

$$s'_j = \frac{-a}{h(a+h)} s_{j-1} + \frac{a-h}{ah} s_j + \frac{h}{a(a+h)} s_{j+1} \quad (4.32)$$

and

$$s'_{j+1} = \frac{a}{h(a+h)} s_{j-1} - \frac{(a+h)}{ah} s_j + \frac{h+2a}{a(a+h)} s_{j+1} \quad (4.33)$$

Based on the value of s'_{j+1} , the value of s_{i-1} (Figure 4.3c) may be evaluated from Equation 3.36. The standard Runge-Kutta formulae, Equations 4.6 and 4.7, may then be used to evaluate s_i and s_{i+1} . The particular values of

s'_{i-1} and s'_i , obtained from Equations 4.30a and 4.30b, are

$$s'_{i-1} = \frac{-(2b+h)}{b(b+h)} s_{i-1} + \frac{b+h}{bh} s_i - \frac{b}{h(b+h)} s_{i+1} \quad (4.34)$$

and

$$s'_i = \frac{-h}{b(b+h)} s_{i-1} + \frac{h-b}{hb} s_i - \frac{b}{h(b+h)} s_{i+1} \quad (4.35)$$

Therefore, the slip strain can be obtained at nodes adjacent to an inflection point by interpolating through the values of slip at these points.

4.5 Evaluation of Deflections

Once the slip has been determined, the curvature at any point along the length of the beam may be determined by using Equation 3.16, since all the terms are known. The curvature is expressed by Equation 3.16 as

$$v'' = \frac{M}{EI_t} + \frac{A_c Y_c}{I_t} s' \quad (4.36)$$

Defining $v' = z$ the above second order equation may be expressed as two first order simultaneous equations. Note that v is the displacement defined in Chapter III.

$$v' = z \quad (4.37)$$

$$z' = \frac{M}{EI_t} + \frac{A_c Y_c}{I_t} s' \quad (4.38)$$

By employing a second order Runge-Kutta method of integration to each equation in turn, Equations 4.37

and 4.38 may be written symbolically as

$$v' = G(z, v) \quad (4.39)$$

$$z' = H(z, v) \quad (4.40)$$

from which

$$v_{i+1} = \frac{h}{2} (k_{1v} + k_{2v}) + v_i \quad (4.41)$$

$$z_{i+1} = \frac{h}{2} (k_{1z} + k_{2z}) + z_i \quad (4.42)$$

Values of k_{1v} , k_{2v} and k_{2z} are evaluated as

$$k_{1v} = z_i$$

$$k_{1z} = \frac{M_i}{EI_t} + \frac{A Y_c}{I_t} s'_i \quad (4.43)$$

$$k_{2v} = z_i + k_{1z} \times h \quad (4.45)$$

$$k_{2z} = \frac{M_{i+1}}{EI_t} + \frac{A Y_c}{I_t} s'_{i+1} \quad (4.46)$$

By substituting values from Equation 4.43 through 4.46 in Equations 4.41 and 4.42, the deflection at every nodal point is computed. Since the value of $v'(0)$ is unknown 'a priori', a value of zero is first assumed before the integration is carried out. The deflections so obtained are shown in Figure 4.4. To obtain the true deflection at every nodal point, a linear correction must be applied.

As illustrated in Figure 4.4 the slope of the line joining A and N is

$$\theta = \frac{\delta_N - \delta_A}{L} \quad (4.47)$$

Therefore, the corrected deflection at any point is

$$\Delta_i = \theta x_i - \delta_i \quad (4.48)$$

Thus a complete set of deflections is obtained.

The procedure described above is valid for a simply supported or continuous beam. However, to obtain values for a continuous beam, it is necessary to solve for the indeterminate reactions, as described in Section 4.6.

4.6 Solution Procedure for Continuous Beams

The redundancy of a continuous beam may be solved by using the flexibility method. A three span continuous beam with a uniform load w , shown in Figure 4.5a, is statically indeterminate to the second degree. The primary system has been selected as a simple beam which deflects under applied loads as shown in Figs. 4.5b, c and d. With the redundants and deformations as defined in these figures, the continuity equations can be expressed as

$$\delta_{BB} R_B + \delta_{BC} R_C = \Delta_B \quad (4.49)$$

$$\delta_{CB} R_B + \delta_{CC} R_C = \Delta_C \quad (4.50)$$

where Δ_B and Δ_C are deformations due to external loading; δ_{BB} , δ_{CB} are deformations due to unit load at B and δ_{CB} , δ_{CC} are deformations due to unit load at C. R_B and R_C are the reactions.

Equations 4.49 and 4.50 are expressed in the matrix form as

$$\begin{bmatrix} \delta_{BE} & \delta_{EC} \\ \delta_{BC} & \delta_{CC} \end{bmatrix} \begin{Bmatrix} R_B \\ R_C \end{Bmatrix} = \begin{Bmatrix} \Delta_B \\ \Delta_C \end{Bmatrix} \quad (4.51)$$

or

$$[F] \{R\} = \{\Delta\} \quad (4.52)$$

where F is the flexibility matrix, $\{R\}$ is the redundant vector and $\{\Delta\}$ deformation vector. The reactions, determined by inversion of the flexibility matrix, are

$$\{R\} = [F]^{-1} \{\Delta\} \quad (4.53)$$

The total stress resultants are obtained by superimposing the stress resultants due to external loading and those due to interior support reactions.

The continuous beam of Fig. 4.5 may now be solved by the following procedure. Assuming constant section properties, the deflections $\{\Delta\}$ for the uniform load acting on the primary structure are computed by the procedure described in Sections 4.2, 4.3 and 4.5.

Similarly the deflections δ_{BB} and δ_{CB} are computed for a unit redundant applied at B, and the deflections δ_{BC} and δ_{CC} are computed for a unit redundant applied at C.

The matrix $\{F\}$ of Equation 4.52 is then formed, and the redundants determined from equation 4.53.

If the problem were linear a superposition obtained from

$$X = X_0 + X_B R_B + X_C R_C \quad (4.54)$$

in which X represents any quantity (moment, shear, deflection, slip, slip strain, shear flow, etc.), and X_0 , X_B and X_C represent the values obtained for that quantity from the three basic solutions described in the preceding paragraphs. The solution is then complete for classical solutions, such as that of Plum and Horne (19), described in Appendix A.

Two types of nonlinearity have, however, been included herein. The first is that arising from the cracking of the concrete in the negative moment region, and the second is a nonlinear slip/shear/flow relationship. In the following paragraphs, the continuous beam technique will be considered, for the example problem of Fig. 4.5, treating each of the cracking effects separately and then combining them with the nonlinear load-slip relationship.

For the nonlinearities arising from the cracking of the slab, the following technique may be used. Superposition of moment according to Equation 4.54 will produce regions of negative moment. The locations of the points of inflection can be determined from a linear interpolation of the superimposed moments between nodal points, resulting in a number of points along the beam (for the present example, four points) at which a condition similar to that in Fig. 4.3 arises. For the negative moment regions the centroid and section properties of the transformed section are those of the steel section and reinforcing bars only. Hence the discontinuities indicated in Fig. 3.4 arise.

The deflections $\{\Delta\}_1$ required to set up Equation 4.52 are now computed with these nonuniform section properties and by considering the stress resultants obtained from Equation 4.54 with the current values of R_B and R_C . The lack of compatibility in deflection at the redundants are now obtained as

$$\{\delta\Delta\}_1 = \{\Delta\}_1 - \{\Delta\}_1 \quad (4.55)$$

Now the change in redundants to eliminate this lack of compatibility is computed as

$$[F] \{\Delta R\}_2 = \{\delta\Delta\}_1 \quad (4.56a)$$

The improved estimate of reaction is then

$$\{R\}_2 = \{R\}_1 + \{\Delta R\}_2 \quad (4.56b)$$

The total superposition, expressed by Equation 4.54, is now repeated for the new reactions until, for the i th iteration

$$\{\Delta R\}_i = \{0\} \quad (4.57a)$$

or

$$\{\delta\Delta\}_i = \{0\} \quad (4.57b)$$

When conditions 4.57a or 4.57b are satisfied the process is considered to have converged and the 'correct' solution has been obtained.

Since the above iterative process depends only on the consistency of the final beam displacements with the interior support conditions, it may be applied to

beams with a nonlinear load-slip relationship. The primary difference is that the iteration required to determine the proper shear flow, described in Sect. 4.3, which must be carried for each of the separate loading conditions, may take longer to converge because the estimated slip correction described by Equation 4.27 is not as good an estimate as for the linear case.

4.7 Special Problems in Solving Continuous Beams

The general technique developed herein for the solution of continuous beams has been described in Sect. 4.6. In that section it was pointed out that at an inflection point, there is an abrupt change in section properties, if it is assumed that concrete cannot resist tension. This gives rise to the discontinuities illustrated in Fig. 3.4. There is, therefore, a discontinuity in slip strain as derived in Sect. 3.2 and expressed by Equation 3.36. It is necessary to consider this discontinuity in the integration of Equations 4.4 and 4.5, described in Sect. 4.2, when solving continuous beam problems. This results in the following modification of the procedure for the computation of all of the deflections required for Equation 4.55.

The inflection points are located as described in Sect. 4.6. Equation 4.1 is integrated by the application of Equations 4.2 to 4.15 up to node point j of Fig. 4.3.

The value of s and v are then determined for node point $j+1$ by Equation 4.2, s'_L of Equation 3.36 is known and hence s'_R is computed from Equation 3.36. Since slip is continuous, the values of s and s' at node $i-1$ of Fig. 4.3 are now known, and the values at node i are determined by using 'b' of Fig. 4.3 in place of h in Equations 4.6 to 4.15. The integration procedure now proceeds normally to the next inflection point, when the same procedure is used. Thus the discontinuity in slip strain is accounted for in the integration procedure for continuous beams.

4.8 Computer Program.

A number of computer programs was developed during this investigation. The main program, developed on the basis of the numerical solution technique, is included in Appendix F. This appendix includes the flow chart, description and listing for the program, and a test problem.

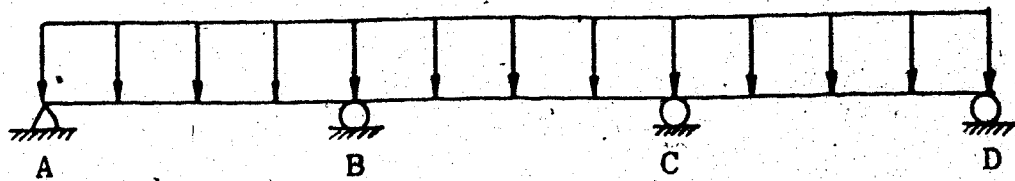
The program is designed to analyse composite beams of up to six spans and can handle any combination of concentrated loads combined with a uniformly distributed loading. Calculations may be performed on the basis of:

- (a) Constant flexural stiffness (EI) for
- (b) Variable flexural stiffness (EI), i.e., different stiffnesses in positive and negative moment

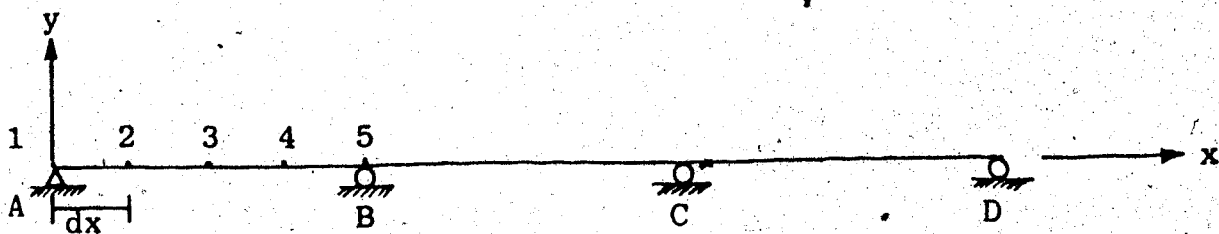
regions, or

(c) Average flexural stiffness (EI_{av}), i.e., the average of positive and negative moment region flexural stiffnesses.

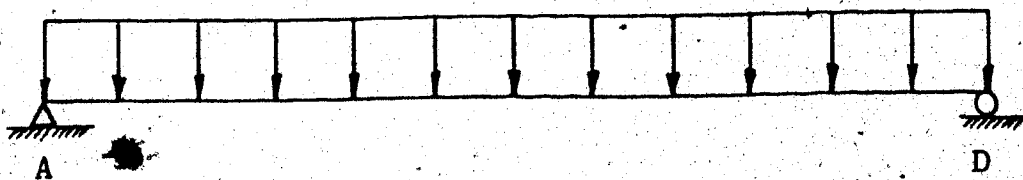
Computations for slip, slip strain, shear flow, force and deflections are based on the procedures described in this Chapter.



(a) BEAM DIVIDED INTO SEGMENTS



(b) NODAL NUMBERING SYSTEM

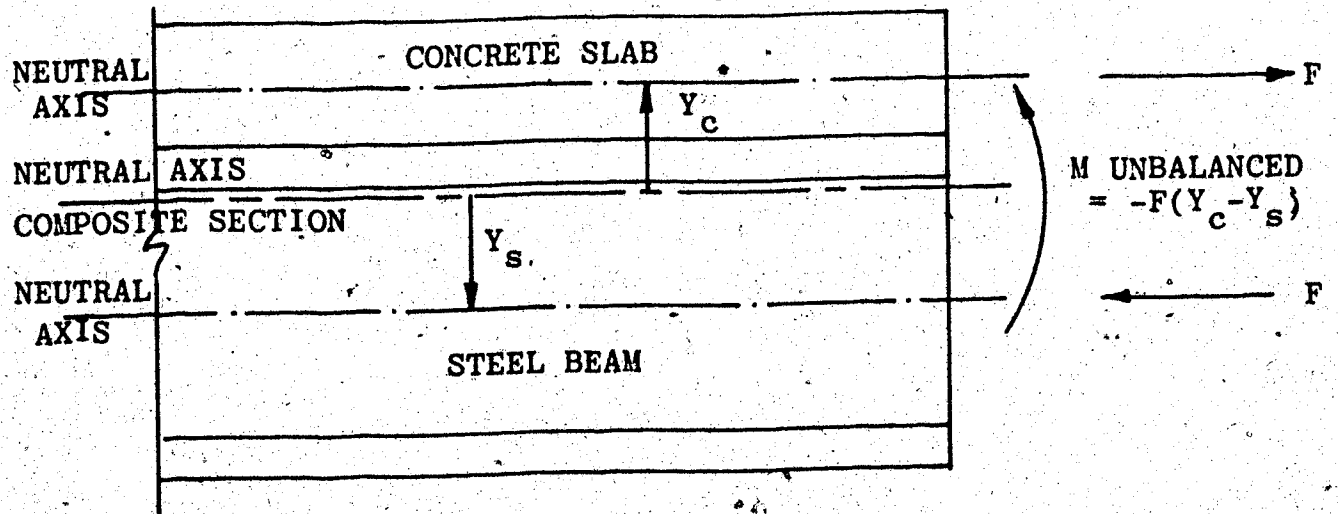


(c) PRIMARY STRUCTURE

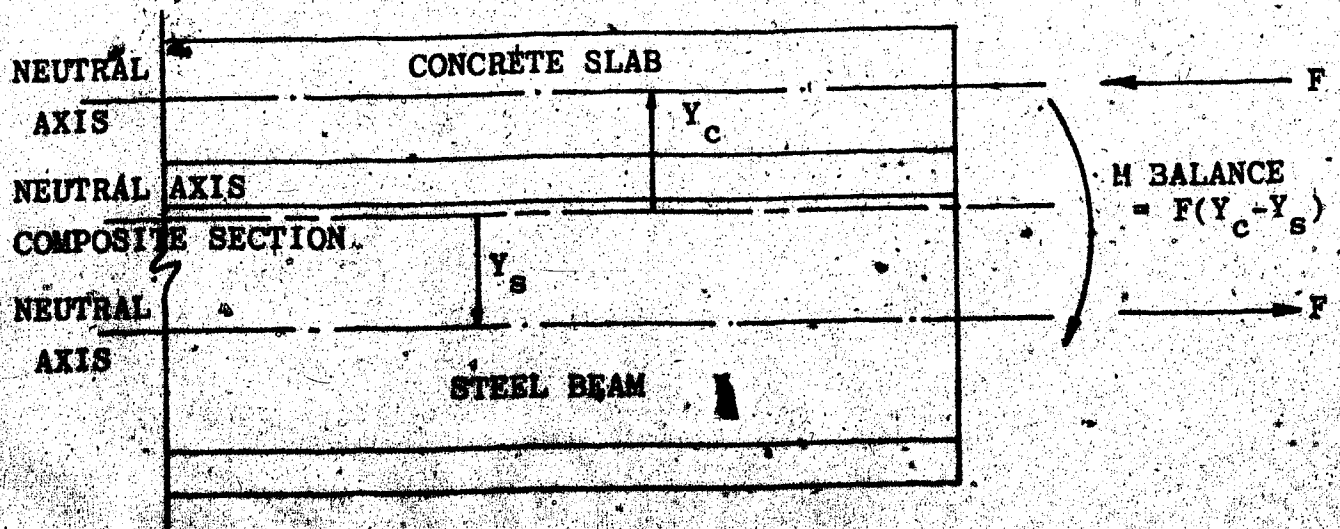


(d) REDUNDANTS

FIGURE 4.1 BASIS FOR NUMERICAL PROCEDURE

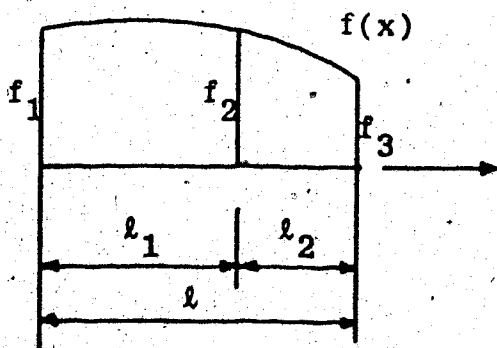


(a) UNBALANCED FORCE F

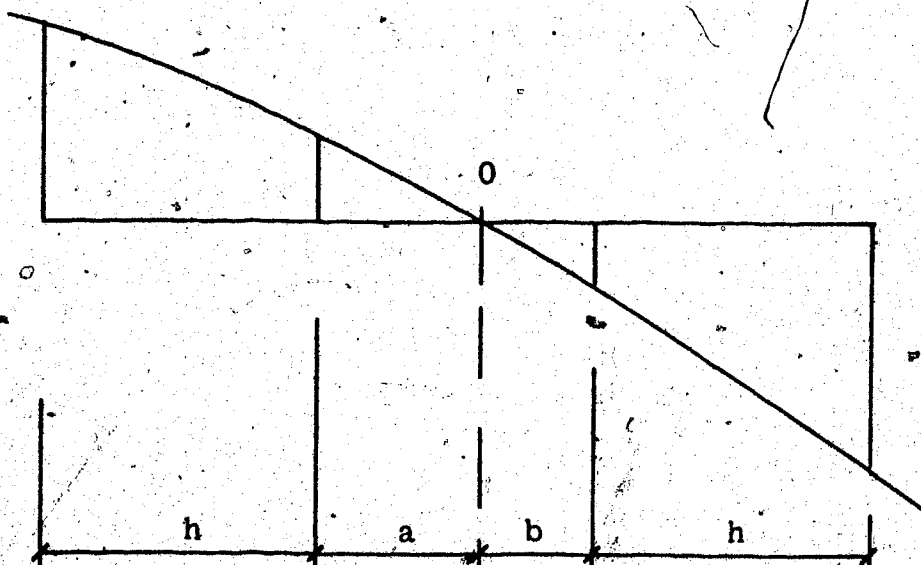


(b) APPLIED BALANCE FORCE F

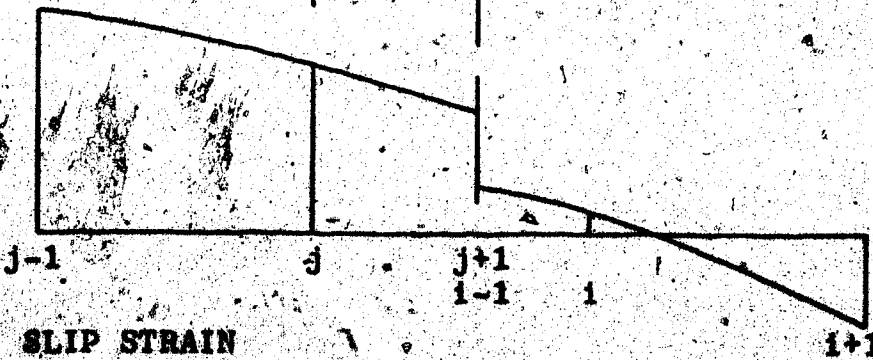
FIGURE 4.2 AXIAL FORCE AT THE END OF THE BEAM



(a) QUADRATIC LAGRANGIAN INTERPOLATION FUNCTION



(b) MOMENT



(c) SLIP STRAIN

FIGURE 4.3 DISTRIBUTION OF SLIP STRAIN ACROSS THE POINT OF INFLECTION

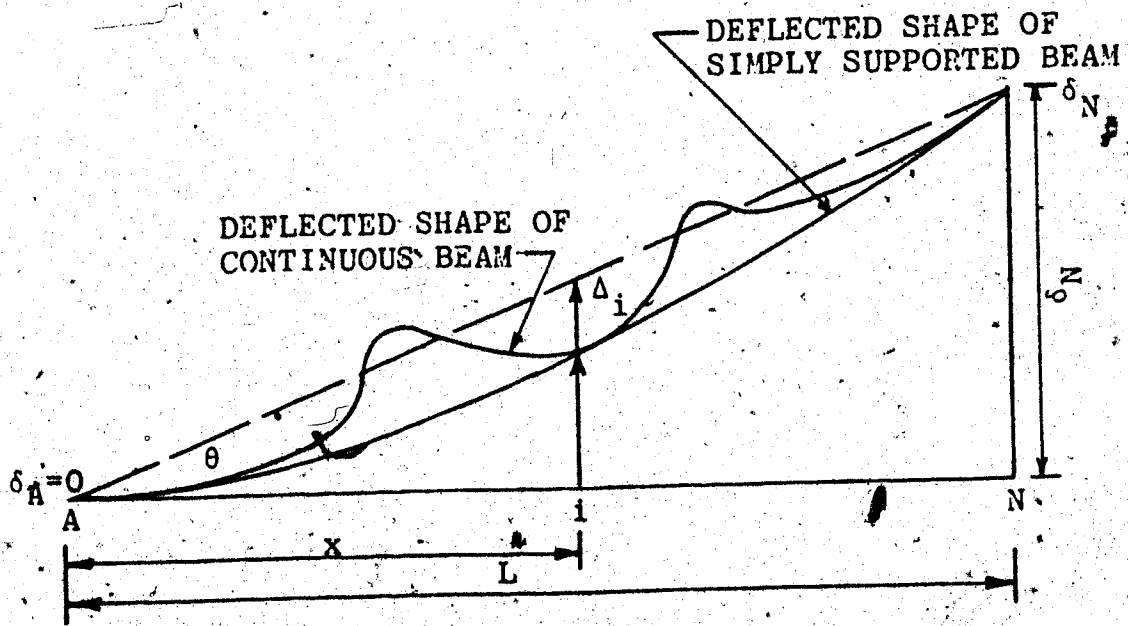
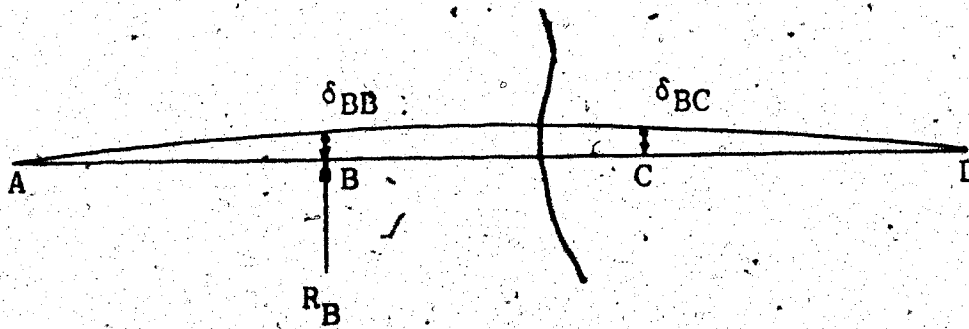
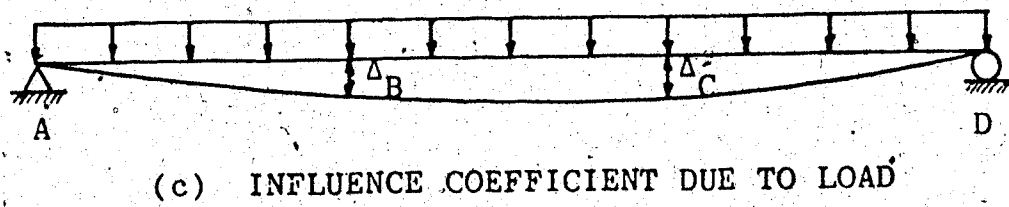
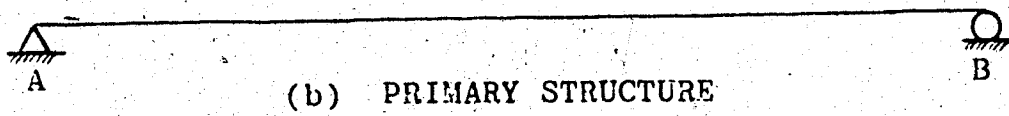
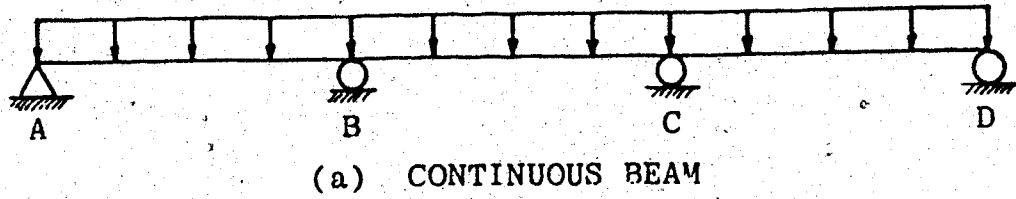
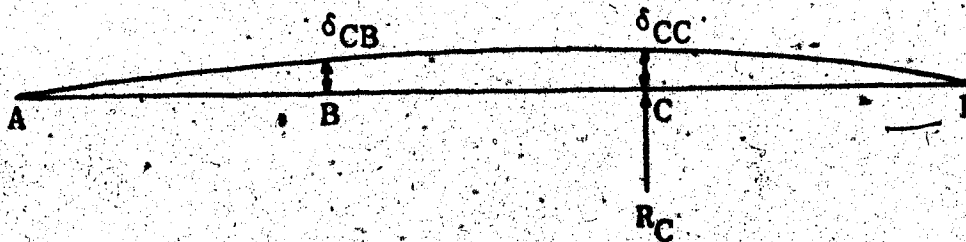


FIGURE 4.4 DEFLECTION AND ITS CORRECTION



(d) FLEXIBILITY COEFFICIENT DUE TO UNIT LOAD AT B



(e) FLEXIBILITY COEFFICIENT DUE TO UNIT LOAD AT C

FIGURE 4.5 ILLUSTRATION OF FLEXIBILITY METHOD

CHAPTER V

VERIFICATION OF NUMERICAL TECHNIQUE

5.1 Introduction

In Chapter IV a numerical technique was established for the solution of continuous composite beam problems under the conditions of: (a) linear response, and (b) nonlinear response in which the nonlinearity is confined to cracking of the concrete in the negative moment region and/or a nonlinear shear connector load-slip relationship. The basis for a computer program to solve such problems was described.

It is the purpose of this Chapter (a) to verify the numerical technique developed in Chapter IV for the problems itemized above and (b) to establish the adequacy of the model for the computation of deflections in simply supported and continuous composite beams.

Since the program does not include the effects of steel yielding or concrete crushing, it cannot be used to compute deflection of composite beams at ultimate load. It also does not include the effect of creep in the concrete. This latter effect, however, may be simulated by using a lower modulus of elasticity for concrete.

5.2 Program Verification for Linear Behavior

5.2.1 Simply Supported Beams

The classical solution for a simply supported uniformly loaded beam with a flexible, but linear elastic, shear connection is derived in Sect. 3.4. A comparison of the numerical results obtained from the program described in Chapter IV with this classical solution is contained in Figs. 5.1 to 5.3. The properties of the chosen cross-section are contained in Column (1) of Table 5.1. The classical solution for a simply supported beam subjected to a concentrated load is included in Appendix B and the results obtained from numerical analysis are compared with the closed form solution.

It can be seen from Figs. 5.1 to 5.3 that, based on linear load-slip behavior of shear connector, the results of the numerical solution for slip, slip strain and deflection (at a load of 30 kips) are indistinguishable from the values obtained in the classical solution.

Nonlinear load-slip behavior for the shear connectors increases the magnitude of slip and deflection throughout the length of the beam.

In addition to the solution for the linear elastic problem, solutions for complete interaction, obtained by setting the shear connector stiffness to a very high value, and for nonlinear load-slip behavior

are also shown on the figures. In Fig. 5.3 deflection, including the effect of shearing deformation, is also shown for comparison purposes.

This example verifies that the results obtained by the numerical technique for simply supported beams are consistent with the linear elastic classical solution.

5.2.2 Continuous Beams

The ability of the computer program (based on numerical technique) to properly analyze a continuous beam with flexible shear connectors but linear elastic response is verified in this Section by solving the problem which was the subject of investigation by Plum and Horne (19). The problem is illustrated in Fig. 5.4. Plum and Horne solved this problem by determining the general solution to the governing equations, derived in Chapter III, and imposing the proper boundary conditions in order to evaluate the constants of integration. For this solution constant section properties throughout the length of the beam, that is, concrete cracking, is ignored in the negative moment region.

Since Plum and Horne did not provide details of their solution, the classical solution for a two-span continuous composite beam has been derived in Appendix A. A computer program to evaluate slip, slip strain and

deflection consistent with the classical solution derived in Appendix A was written, and the problem of Fig. 5.4 was solved in this manner. The properties of the beam are tabulated in Column (2) of Table 5.1. The solution for slip, slip strain, slab force, and deflection obtained by the numerical technique of Chapter IV are compared with the classical solution in Figs. 5.5 to 5.8, respectively.

The only significant discrepancy between the classical solution and the numerical solution is that for slip strain in the region of the concentrated loads and the reactions. This discrepancy appears to arise because the numerical solution technique computes slip strain by averaging values obtained from the two element lengths on each side of the nodal points. This technique does not permit the accurate evaluation of slip strain at the point of application of a concentrated load. Nevertheless, the correspondence between slip curves indicates that the distribution of shear flow (directly proportional to slip in a linear problem) predicts an accurate determination of the distribution of internal forces. The deflections are also reliable.

It is concluded from this problem that the numerical techniques incorporated into the computer program are suitable for the solution of composite beam problems involving linear load-slip response of shear connectors and concentrated loads.

5.3 Program Verification for Nonlinear Behavior

Any solution which includes nonlinearities for composite beams must be based on a numerical technique. Few of these solutions are available. However, Yam and Chapman (31) have published numerical solutions based on predictor corrector technique for continuous composite beams which include the effects of steel yielding, concrete tensile cracking, concrete crushing and a nonlinear exponential relationship between force and slip in the shear connectors.

The primary objective of this thesis is to investigate deflections of composite beams under service loads. Nonlinearities due to yielding of the steel and crushing of the concrete have no effect at this level of load. Therefore, the simpler technique developed herein is appropriate for the present study. In order to demonstrate this, the solution obtained from the present numerical technique is compared, at service load, with the full nonlinear solution of Yam and Chapman.

Yam and Chapman's test beam is shown in Fig. 5.9 and its properties are shown in Column (3) of Table 5.1. Their solution for slip and deflection, at a service load of 7.4 tons, is shown in Figs. 5.10 and 5.11, respectively, where they are compared with the present numerical solution.

The comparison of slip in Fig. 5.10 indicates that, although there are some differences in the vicinity of the concentrated loads, the characteristics of the curves are very similar. In particular, the maximum slip values are essentially the same and occur at approximately the same locations. The comparison of the service load deflections for these two solutions is shown in Fig. 5.7 where the values are seen to be identical for all practical purposes. The increase in deflection produced by the flexible shear connectors and concrete cracking may be seen by comparing values with the complete interaction deflections, shown also in Fig. 5.11 and which are taken from the paper by Yam and Chapman. From Fig. 5.11 it is evident that shear deformation has not been included in Yam and Chapman's analysis. The degree of nonlinearity developed in the load-slip relationship for this problem may be seen by determining the position at which the maximum slip of Fig. 5.6 is located on a load-slip or shear-flow-slip curve. This is shown in Fig. 5.12, from which it may be concluded that there is some nonlinearity associated with the load-slip relationship at service load for this problem.

Figs. 5.10 to 5.12 appear to support the argument that an analysis in which the nonlinearities are confined to cracking of the concrete and the load-slip relationship is capable of producing an adequate simulation of the behavior of composite beams at service loads.

Furthermore, this establish that the program developed herein has incorporated these nonlinearities in such a way that the results are consistent with a more sophisticated treatment of the problem. Thus, it is considered that the reliability of the computational technique is adequate to draw conclusions relative to the effects on service load deflections arising from variations on stiffness parameters.

5.4 Comparisons with Test Results

5.4.1 Comparison with Hamada and Longworth (9)

Hamada and Longworth (9), in an experimental and analytical investigation into the behavior of continuous composite beams, concluded that shear deformation may contribute significantly to the deflection of composite beams. Load deflection computations for one of their beams (CBI) are shown in Fig. 5.13. The properties used in the analysis of this beam are summarized in Column (4) of Table 5.1. The computation of service load for this beam is given in Appendix C and the results are summarized in Column (2) of Table 5.2. Very good agreement is obtained with Hamada and Longworth's results up to 70 kips using nonlinear load-slip behavior of shear connectors and including the shear deformations. It is apparent that, for the shear connector stiffness used in this analysis, it is necessary to include shear deformations to obtain

reasonable agreement with their experimental results. Therefore, shear deflection will be included in many of the parameter studies of Chapter VI.

5.4.2 Comparison with Chapman and Balakrishnan (5)

Chapman and Balakrishnan (5) carried out an extensive testing program of simply supported composite beams with various types of shear connectors. A comparison with one of their tests (Beam A6) is shown in Fig. 5.14. The beam properties are summarized in Column (5) of Table 5.1. The service load is computed in accordance with the procedure of Appendix C and the computation is summarized in Column (3) of Table 5.2.

In contrast to Hamada and Longworth's beam it should be noted that better agreement is obtained with these results when linear load-slip behavior is assumed. This appears to contradict the conclusion obtained from the comparison in Sect. 5.4.1. However, there are uncertainties involved in evaluating shear connector stiffness for Hamada and Longworth's beam. Hence solutions with, and without, shear deformations will be presented in Chapter VI.

5.5 Conclusion

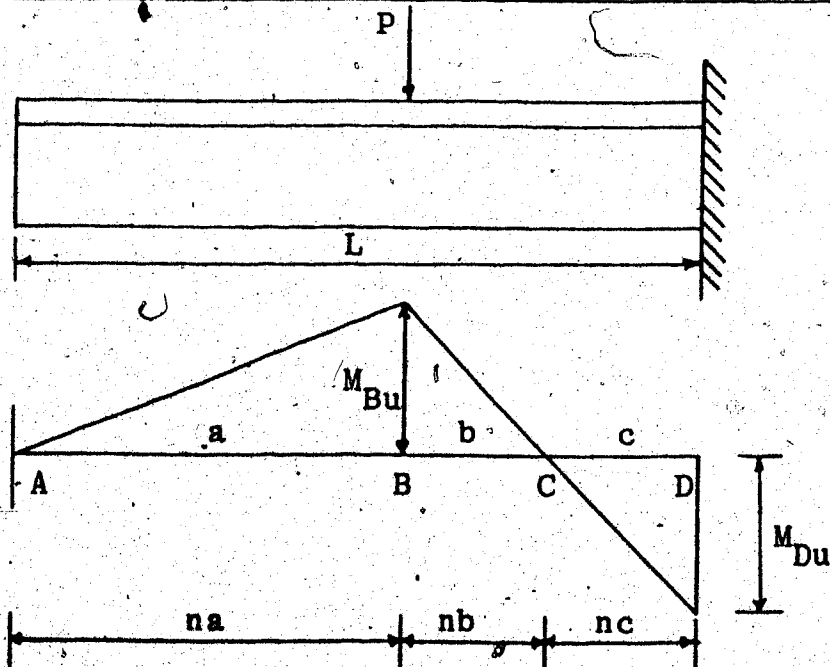
The numerical technique developed in Chapter IV predicts the behavior of composite beams with very good accuracy up to service loads, and hence the validity of the model is established.

TABLE 5.1 PROPERTIES OF COMPOSITE BEAMS
FOR TEST PROBLEMS.

	Simply Supported Beam	Plum and Horne's Beam	Yam and Chapman's Beam	Chapman and Balakrishnan's Beam	Hamada and Longworth's Beam
Beam Designation	BSS12 x 6L	W12 x 31	BSB 108	BSS12 x 6L	W12 x 31
Total Depth d (in.)	18.000	18.090	8.375	18.000	18.090
Concrete Slab					
bc (in.)	48.000	48.000	19.000	48.000	48.000
tc (in.)	6.000	4.000	2.375	6.000	4.000
Ec (ksi)	3.550×10^3	3.750×10^3	4.002×10^3	3.550×10^3	4.527×10^3
f'c (psi)	3440.0	4000.0	6900.0	3440.0	5577.0
Reinforcement					
A _{sr} (sq. in.)	-	1.571	0.890	-	1.600
d _{sr} (in.)	-	3.000	1.750	-	2.000
f _{yr} (ksi)	-	50.000	46.600	-	59.300
E _{sr} (ksi)	-	30.000×10^3	30.000×10^3	-	30.000×10^3
Steel Section					
d _s (in.)	12.000	12.090	8.000	12.000	12.090
A _s (sq. in.)	13.000	9.130	3.530	13.000	9.130
b _f (in.)	8.000	6.530	3.000	6.000	6.530
t _f (in.)	0.717	0.465	0.377	0.717	0.465
t _w (in.)	0.400	0.265	0.230	0.400	0.265
f _{yf} (ksi)	34.832	-	-	34.832	40.500
f _{yw} (ksi)	38.820	44.000	46.600	38.820	46.500
E _s (ksi)	31.140×10^3	30.000×10^3	30.016×10^3	31.140×10^3	30.200×10^3
Shear Connector Type					
Headed Type					
Size	3/4"x4"	3/4"x3"	3/8"x2 1/2"	3/4"x4"	3/4"x3"
K (psi)	150.000×10^4	150.000×10^4	30.440×10^4	14.400×10^4	19.250×10^4
a (psi)	18.200×10^2	-	25.360×10^2	18.200×10^2	21.280×10^2
b	79.160	-	120.000	79.000	90.418
Q _u (kips)	28.000	28.780	7.250	28.716	28.716

TABLE 5.2 TEST PROBLEM COMPUTED VALUES

	Hamada and Longworth's Beam	Chapman and Balakrishnan's Beam
Beam Designation	W12 x 31	BSS12 x 6L
Shear Connectors		
Type	Headed Stud (Paired)	Headed Stud (Paired)
Size	3/4"x3"	3/4"x4"
na	16	16
nb	16	-
nc	8	-
Q_u (kips)	28.716	28.000
$C = .85f'_c bctc$ (kips)	910.170	842.112
$T = A_s f_y$ (kips)	387.456	469.670
na Q_u (kips)	459.456	448.000
nb Q_u (kips)	459.456	-
nc Q_u (kips)	229.728	-
M_{Bu} (ft.-kips)	291.775	393.000
M_{Du} (ft.-kips)	203.147	-
P_u (kips)	129.384	83.463
P_w (kips)	86.250	55.650



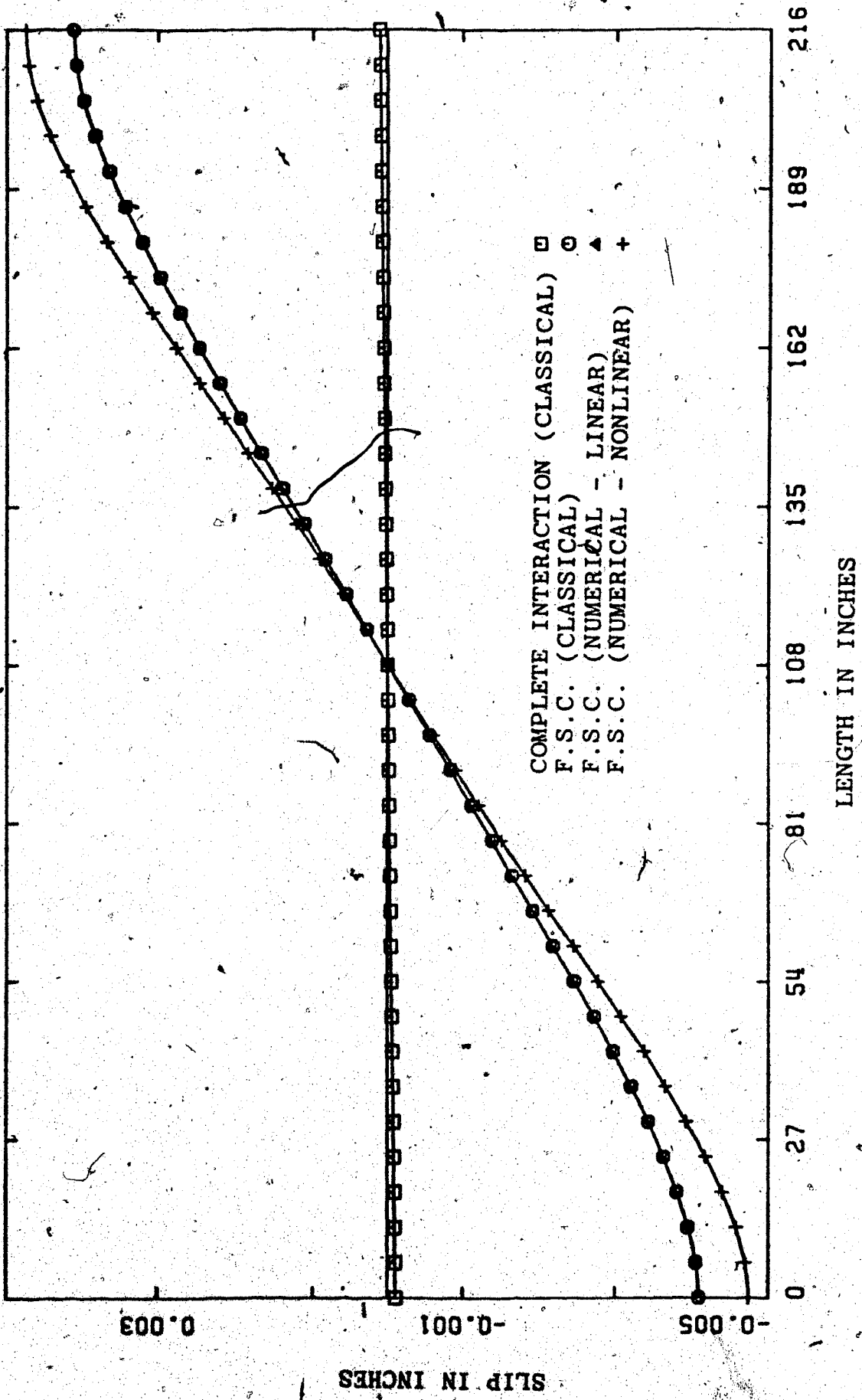


FIGURE 5.1 COMPARISON OF CLASSICAL AND NUMERICAL VALUES FOR SLIP

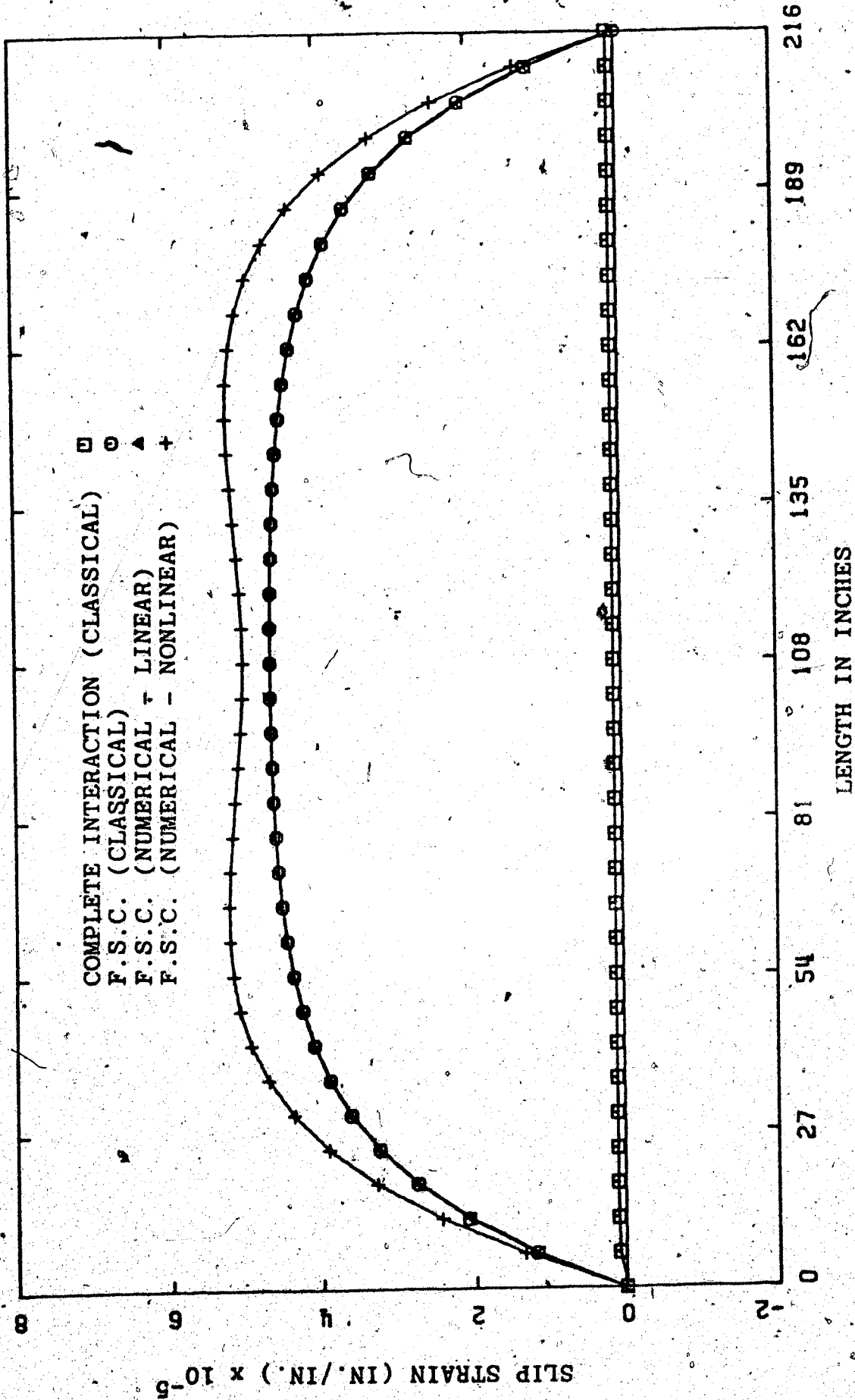


FIGURE 5.2 COMPARISON OF CLASSICAL AND NUMERICAL VALUES FOR SLIP STRAIN

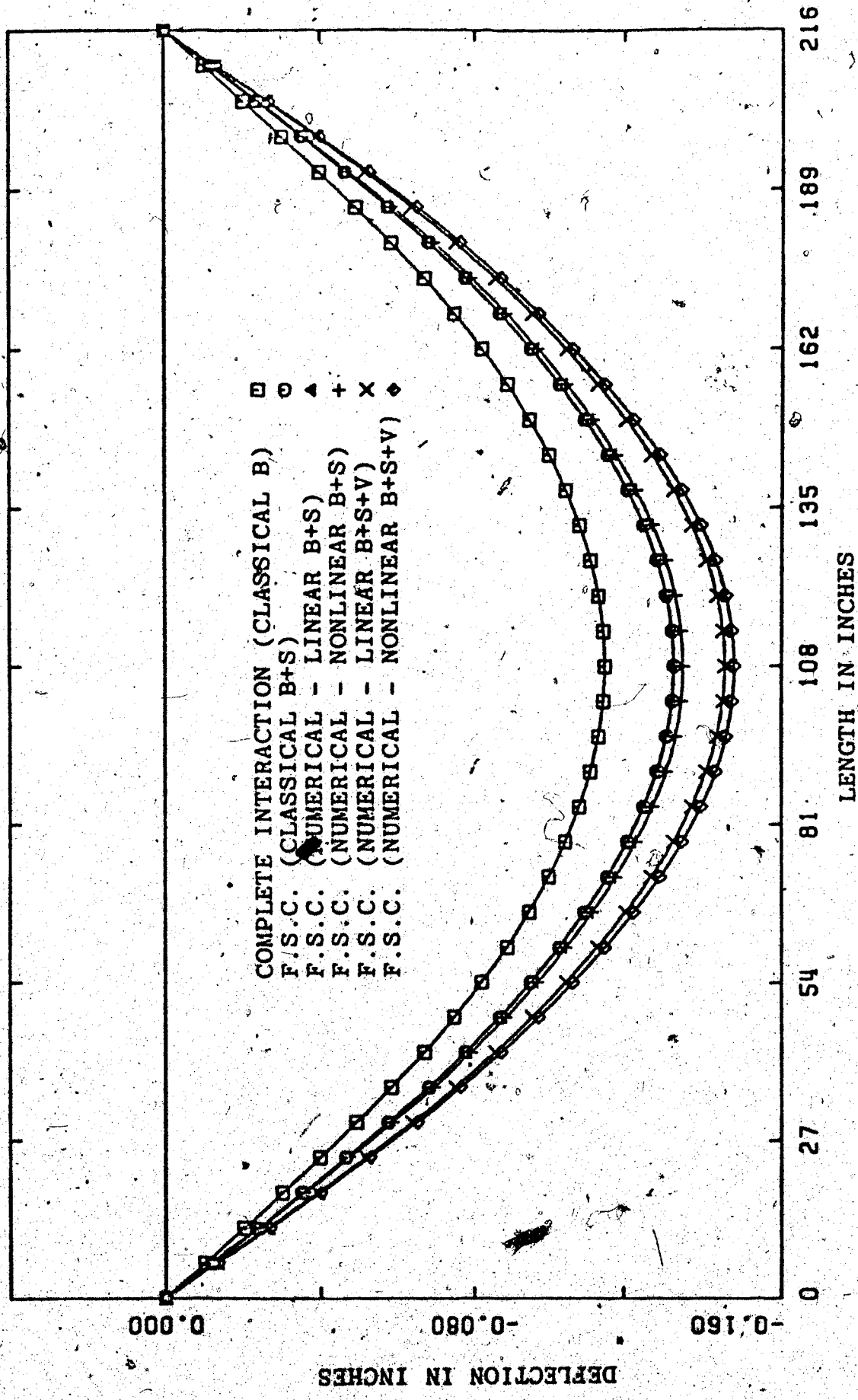


FIGURE 5.3 COMPARISON OF CLASSICAL AND NUMERICAL VALUES FOR DEFLECTION

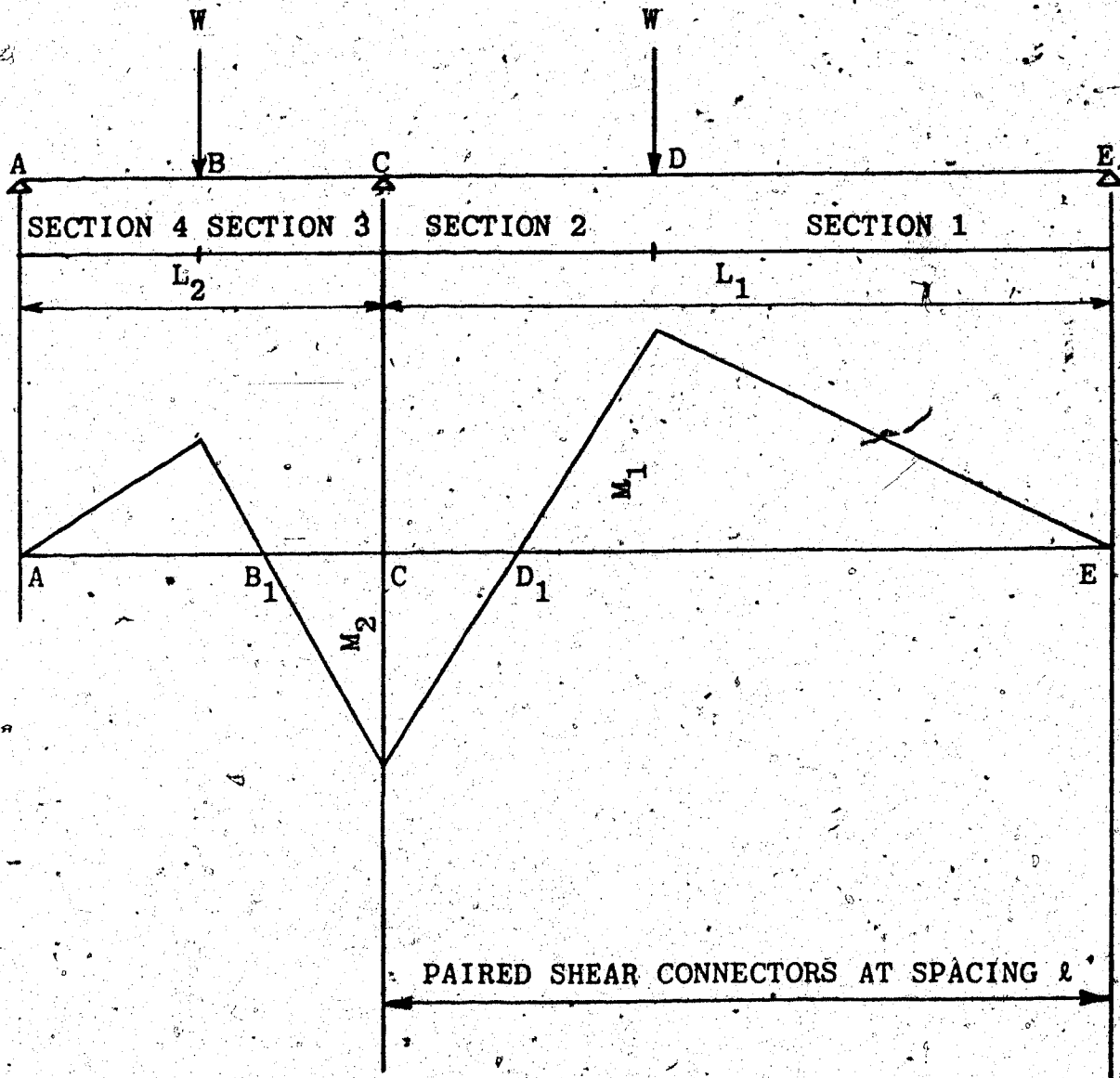


FIGURE 5.4 PLUM AND HORNE'S TEST BEAM

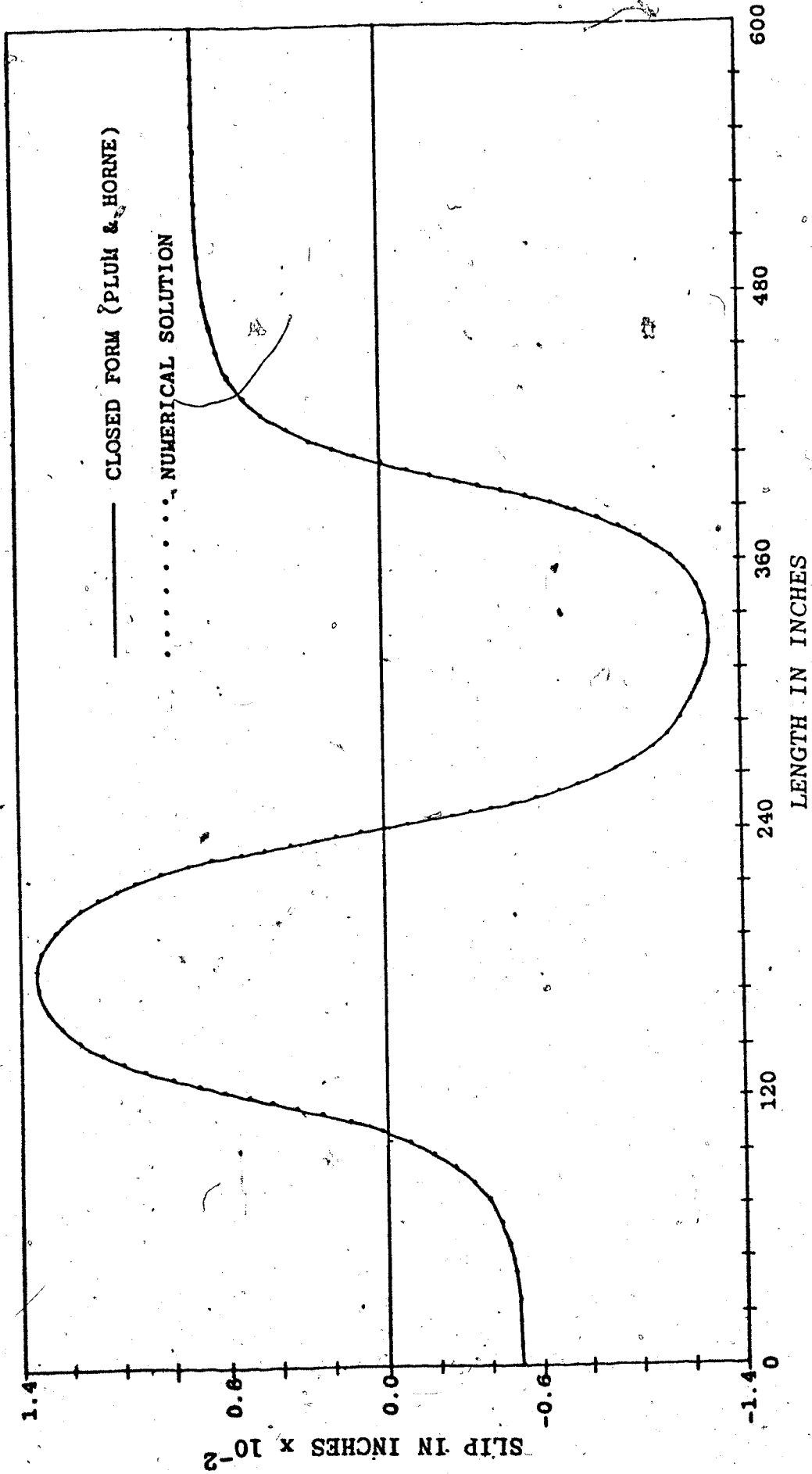


FIGURE 5.5 COMPARISON OF SLIP VALUES (PLUM AND HORNE AND NUMERICAL SOLUTION)

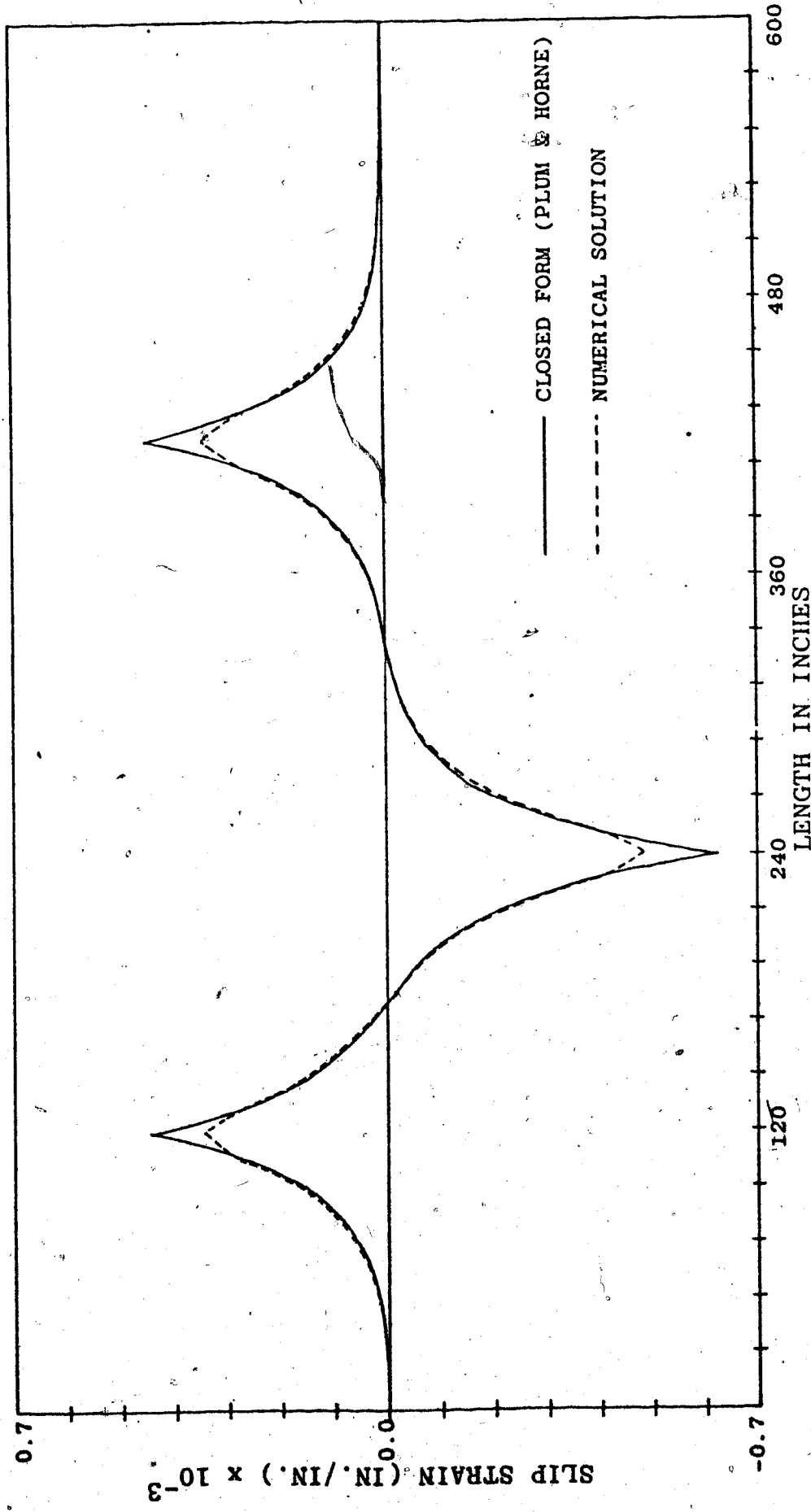


FIGURE 5.6. COMPARISON OF SLIPSTRAIN VALUES (PLUM AND HORNE AND NUMERICAL SOLUTION)

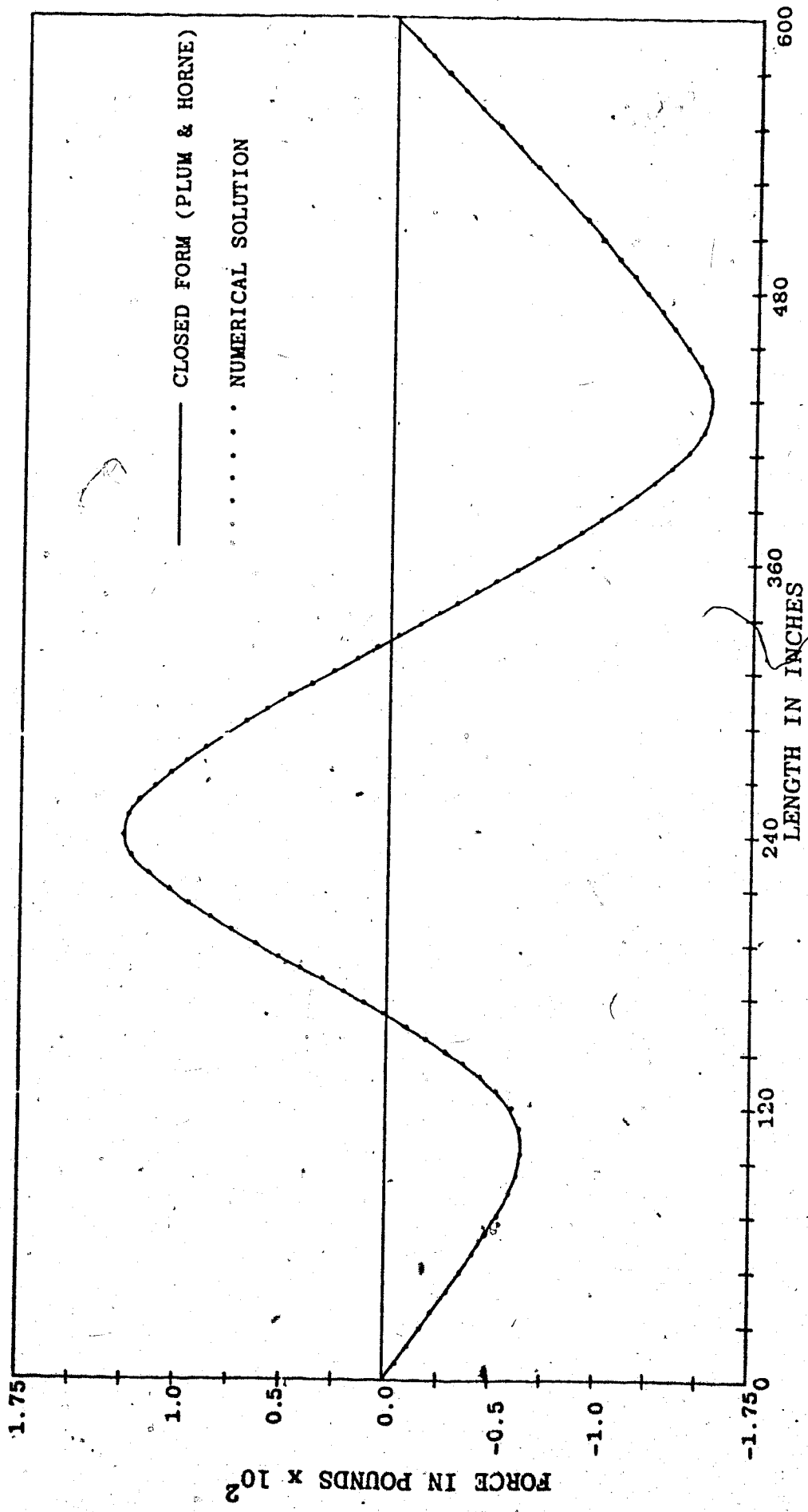


FIGURE 5.7 COMPARISON OF AXIAL FORCE VALUES (PLUM AND HORNE AND NUMERICAL SOLUTION)

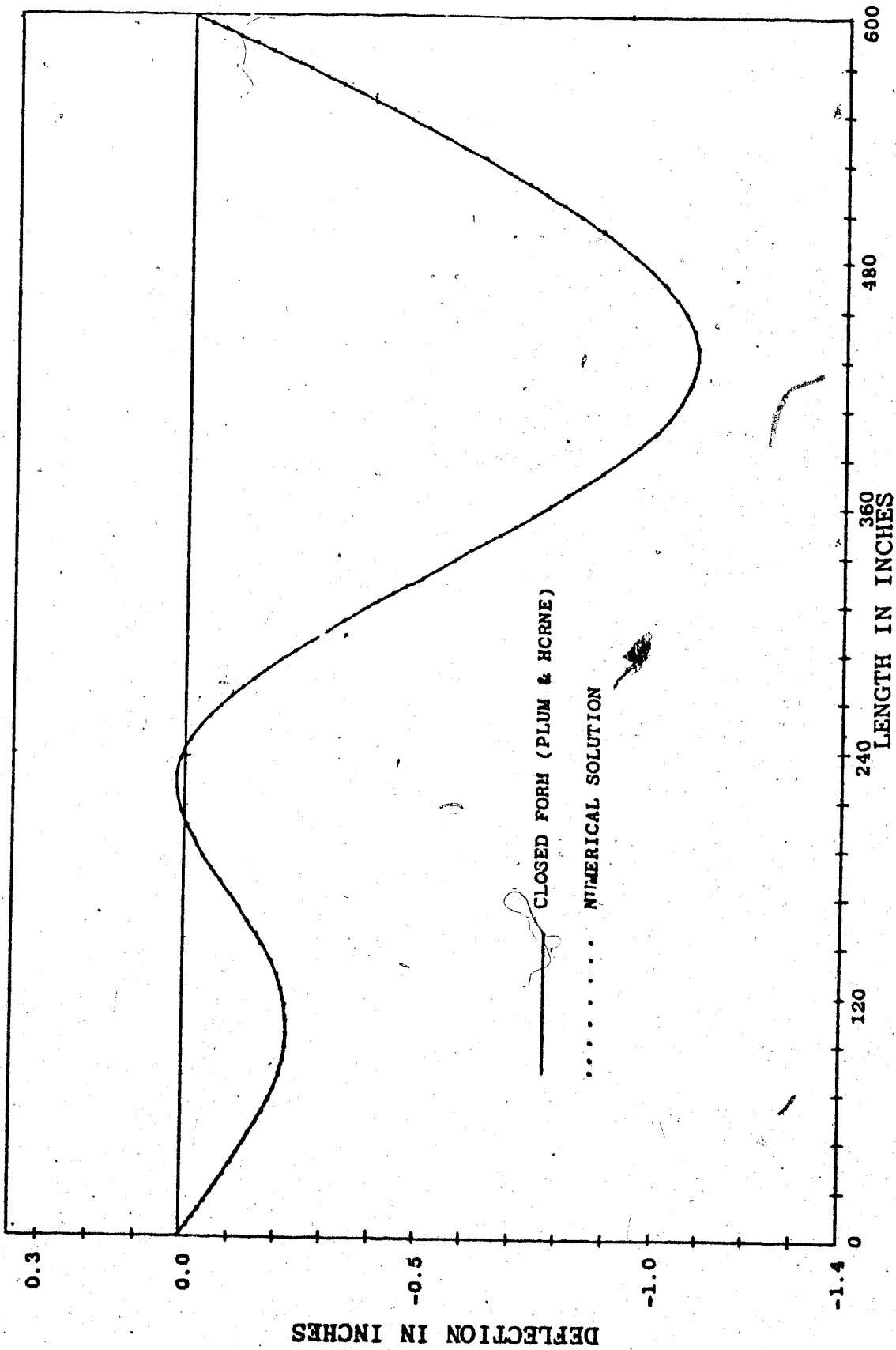
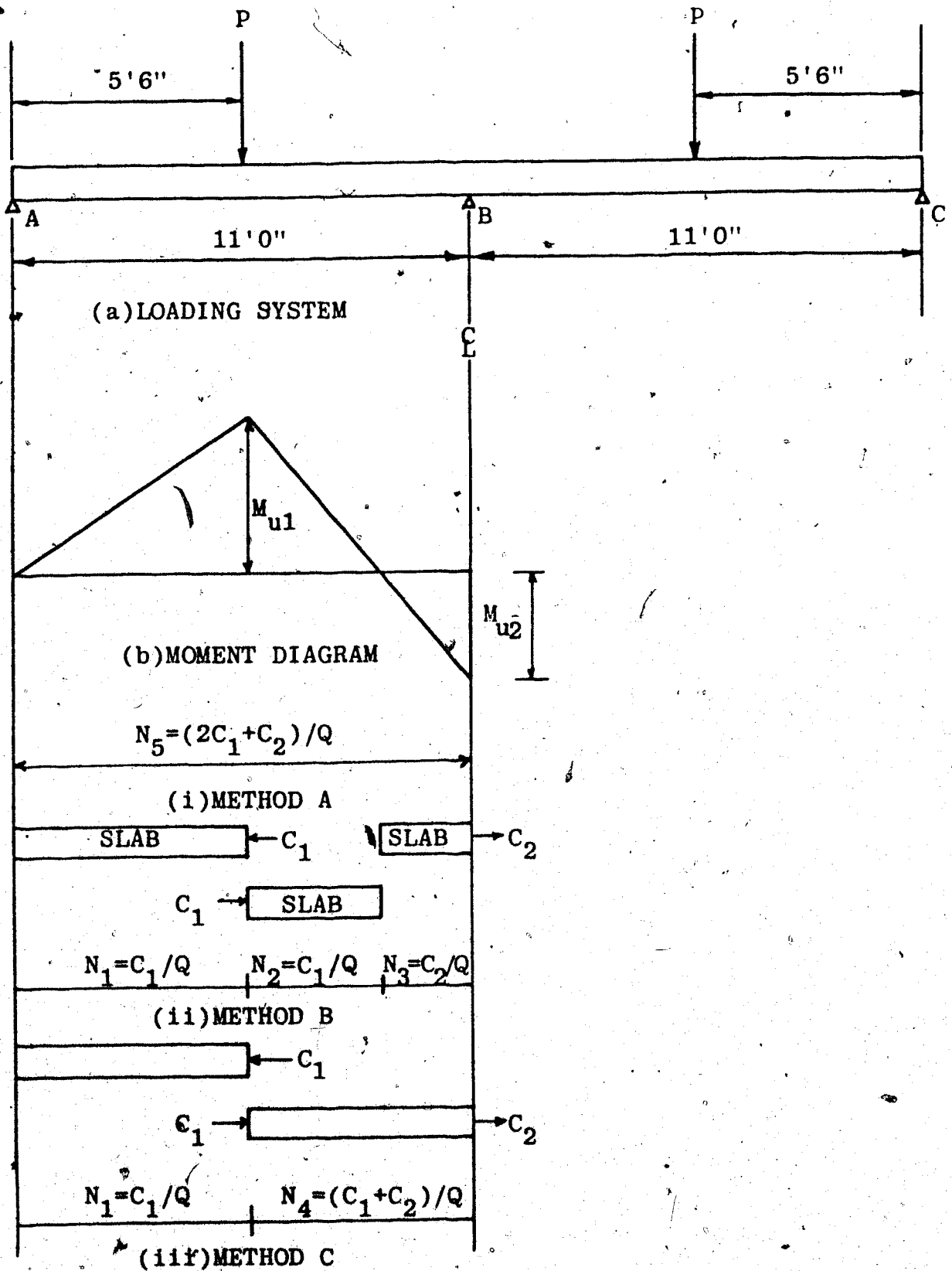


FIGURE 5.8 COMPARISON OF DEFLECTION VALUES (PLUM AND HORNE AND NUMERICAL SOLUTION)



(c) METHODS OF SHEAR CONNECTION DESIGN

FIGURE 5.9 YAM AND CHAPMAN'S TEST BEAM

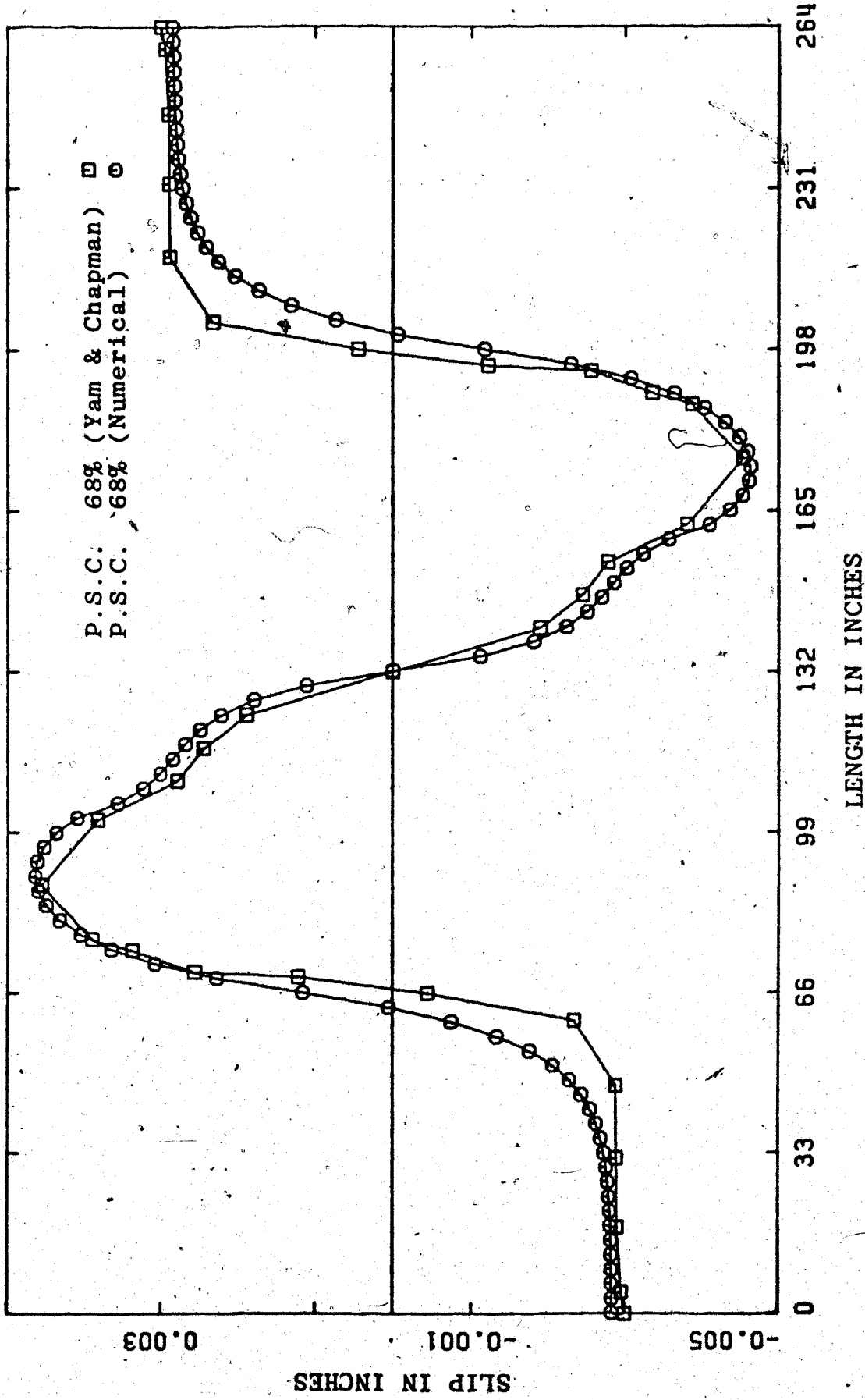


FIGURE 5.10 COMPARISON OF SLIP VALUES (YAM AND CHAPMAN AND NUMERICAL SOLUTION)

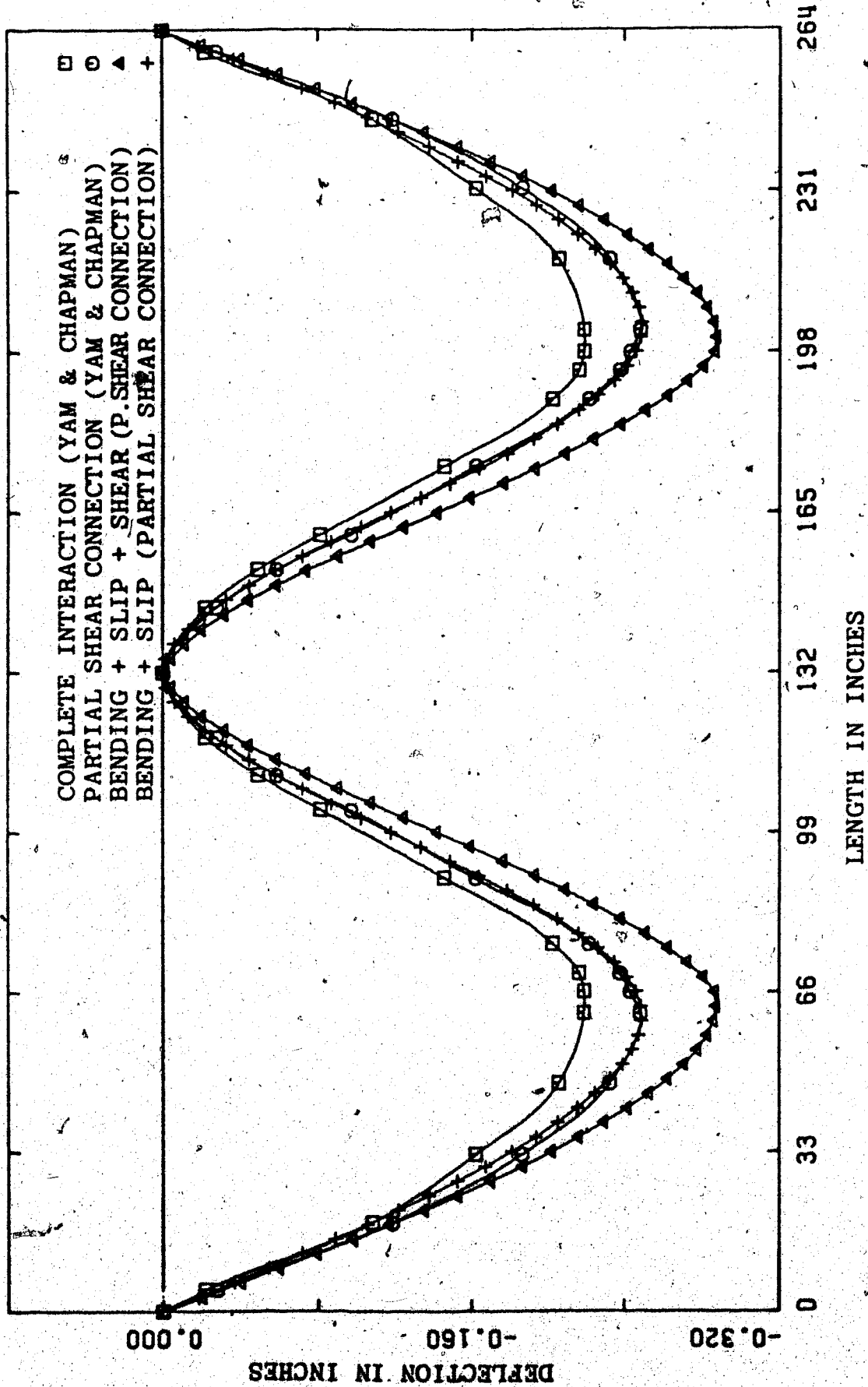


FIGURE 5.11 COMPARISON OF DEFLECTION VALUES (YAM AND CHAPMAN AND NUMERICAL SOLUTION)

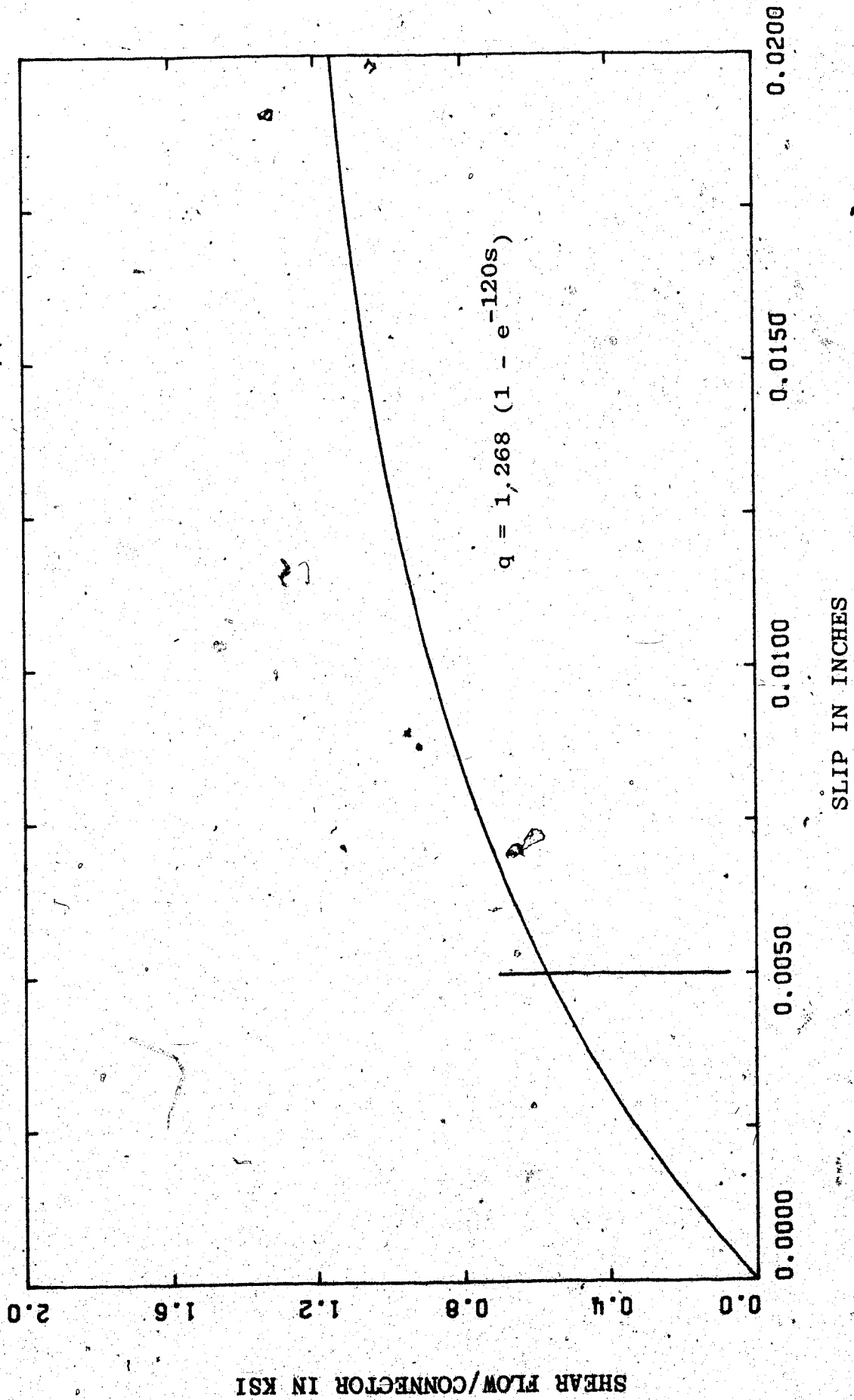


FIGURE 5.12 NON-LINEAR SHEAR FLOW AND SLIP RELATIONSHIP (YAM AND CHAPMAN)

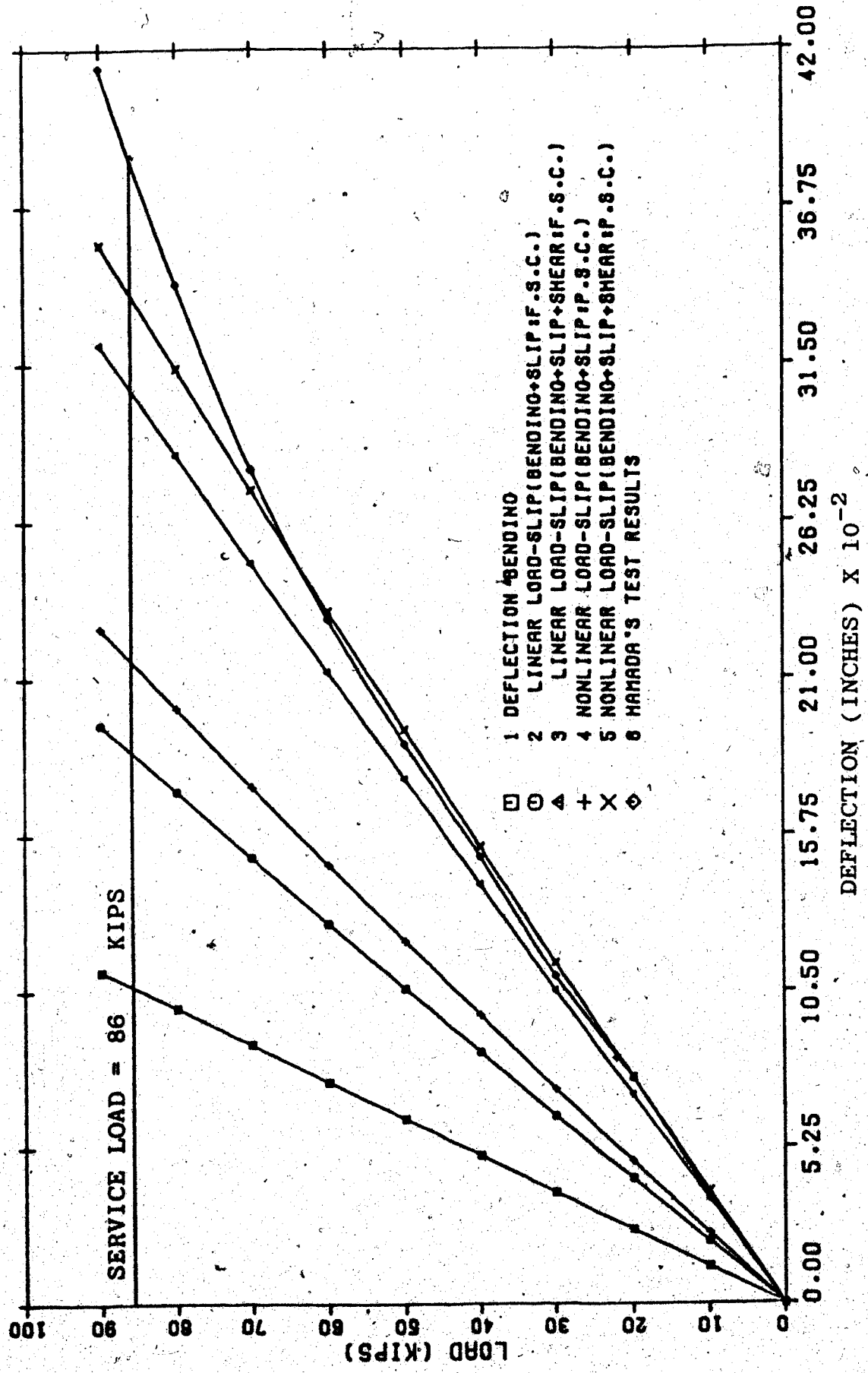


FIGURE 5.13 COMPARISON OF DEFLECTION VALUES (HAMADA AND LONGWORTH AND NUMERICAL SOLUTION)

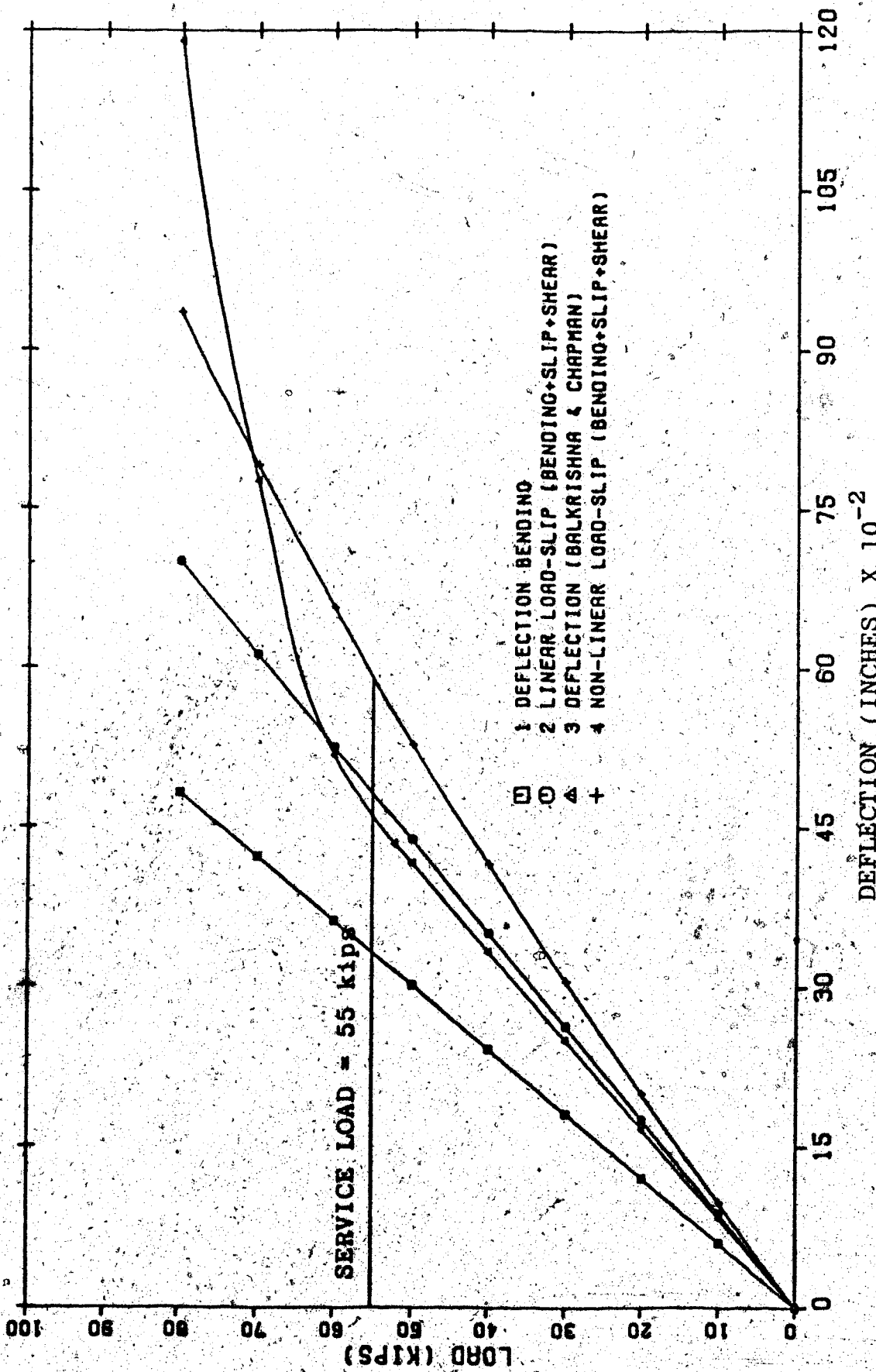


FIGURE 5.14 COMPARISON OF DEFLECTION VALUES (CHAPMAN AND BALAKRISHNAN AND NUMERICAL SOLUTION)

CHAPTER VI

APPLICATIONS

6.1 Introduction

In Chapter V the capabilities of the numerical solution developed in Chapter IV were compared with closed form solutions and published results. It was concluded that the program developed herein is adequate to reliably predict deflections of simply supported and continuous composite beams for a variety of loading conditions, and that the nonlinearities included in the program capture the essential aspects of behavior at service loads. It is necessary to attempt to draw some general conclusions with respect to the effect of shear connector flexibility and nonlinear behavior on service load deflections.

In this Chapter an evaluation of the effect of various parameters on service load deflections is attempted. For simply supported beams which respond in the linear elastic range at service loads, nondimensional parameters are derived from the closed form solution. This permits a quantitative evaluation of increments in deflections relative to those which would occur in a beam with complete interaction. Assuming the same nondimensional parameters

control the behavior of continuous beams, the numerical technique developed herein is used for the evaluation of deflection in continuous beams. However, for nonlinear response no valid method of nondimensionalizing the results has been found. Therefore, it has only been possible to examine the effects of the parameters on particular example problems, with the inference that the same qualitative type of result occurs in other beams of similar type.

6.2 Deflections of a Linear Elastic Simply Supported Composite Beam Subjected to Uniform Load

The solution of the differential equation for a simply supported beam subjected to uniform load was determined in Sect. 3.4. Evaluating Equation 3.51 at $x = L/2$ yields the maximum deflection in the span as

$$v_{L/2} = -\frac{5}{384} \frac{wL^4}{EI_t} + \frac{A_c Y_c \beta w}{I_t \alpha^4} \left(\cosh \frac{\alpha L}{2} + \frac{(1 - \cosh \alpha L)}{\sinh \alpha L} \sinh \frac{\alpha L}{2} + \frac{\alpha^2 L^2}{8} - 1 \right) \quad (6.1)$$

Considering downward deflection as positive, and recognizing that the first term is the deflection of a beam with complete interaction, Equation 6.1 may be written as

$$\frac{\delta_f}{\delta_0} = 1 + \frac{384}{5} \frac{EA_c Y_c \beta}{\alpha^4 L^4} \left(1 - \frac{\alpha^2 L^2}{8} - \frac{(1 - \cosh \alpha L)}{\sinh \alpha L} \sinh \frac{\alpha L}{2} - \cosh \frac{\alpha L}{2} \right) \quad (6.2)$$

in which δ_f is the midspan deflection (excluding shear deformation) of the composite beam and δ_0 is the midspan deflection of the same beam (due to bending only) assuming full interaction.

Recalling the definitions of α and β from Equations 3.21 and 3.22, Equation 6.2 may be written in terms of two nondimensional ratios as

$$\frac{\delta_f}{\delta_0} = 1 + \frac{384}{5\xi\eta^2} \left(1 - \frac{\xi\eta}{8} - \cosh \frac{\sqrt{\xi\eta}}{2} - \frac{(1 - \cosh \frac{\sqrt{\xi\eta}}{2}) \sinh \frac{\sqrt{\xi\eta}}{2}}{\sinh \sqrt{\xi\eta}} \right) \quad (6.3)$$

in which the following definitions apply.

$$\xi = \frac{A_t Y_s Y_c}{I_t + A_t Y_s Y_c} \quad (6.4)$$

and

$$\eta = \frac{KI_t L^2}{EA_s Y_s Y_c} \quad (6.5)$$

Note that ξ and η are always positive. It can be seen that the ratio ξ is dependent only on the geometry of the cross-section, whereas the ratio η depends on the geometry of the cross-section, the span, the shear connector stiffness factor (K), and the elastic moduli of steel and concrete.

The right hand side of Equation 6.3 represents a factor by which δ_0 can be multiplied in order to determine the maximum deflection of a composite beams with any shear connector. It is universally applicable to the type of span considered and can form the basis for a simple design aid. To determine the range of the nondimensional parameters

within which most composite beams would fall, and were computed for a number of typical sections. By arbitrarily varying these factors over this range, the plot of Fig. 6.1 was produced. This figure indicates that shear connector flexibility may have a considerable effect on composite beam deflection. With reduction in shear connector stiffness, that is, with partial shear connection, the shear connector modulus K is reduced. Due to this reduction in Equation 6.5, η decreases and hence the deflection due to slip increases. (See Fig. 6.1.)

Depending on the properties of the cross section, the geometry of the beam and the shear connector modulus, this deflection due to slip can be as high as 45% of the deflection due to flexure.

6.3 Evaluation of Shear Deflection for a Simply Supported Composite Beam Subjected to Uniform Load

The shear strain in a beam may be expressed

as (23)

$$\gamma = v'_s(x) = \frac{K_{sh} V}{GA_t} \quad (6.6)$$

in which v_s is the shear deflection and

$$K_{sh} = \frac{A_t}{I_t} \int_A \frac{Q^2}{b^2} dA \quad (6.7)$$

is a property of the cross-section. For a simply

supported beam, symmetrically loaded,

$$\delta_s = \int_0^{L/2} v'_s(x) dx = \frac{K_{sh}}{GA_t} \int_0^{L/2} V dx \quad (6.8)$$

Shear deflection is therefore simple to evaluate provided K_{sh} is known.

Recognizing that the integral on the right hand side of Equation 6.8 is the moment at midspan, the ratio of shear deflection to δ_0 can be written for uniform load as

$$\frac{\delta_s}{\delta_0} = \frac{K_{sh}}{GA_t} \frac{wL^2}{8} \frac{384EI_t}{5wL^4} \quad (6.9a)$$

or

$$\frac{\delta_s}{\delta_0} = \frac{48}{5} \frac{EK_{sh}I_t}{GA_t L^2} \quad (6.9b)$$

Unfortunately this ratio cannot be expressed directly in terms of ξ and η and, therefore, it is probably best to compute $\frac{\delta_s}{\delta_0}$ separately and add it to $\frac{\delta_f}{\delta_0}$ if shear deflections are to be combined with flexural deflections.

However, since the evaluation of K_{sh} by Equation 6.7 is not simple, its value has been computed for a number of cross-sections and is plotted against the width of the concrete slab in Fig. 6.2. K_{sh} for various wide flange steel sections with different concrete slab widths and for thickness $t = 6''$ and $4''$ are tabulated in Table 6.1. It is observed that K_{sh} values for the beams lie between 3.317 and 10.229. K_{sh} for the beams not included in the table may be derived from the upper and

lower bound values of the beam of the same designated rolled section using the linear variation in depth. Using these shear form factors, shear deflection for simply supported beams can be computed with ease for practical design purposes.

The magnitude of shear deflection for a specific simply supported uniformly loaded beam has been shown in Fig. 5.3 which indicates that it is not negligible.

6.4 Influence of Type of Loading, Shear Connection and Load-Slip Characteristics of the Shear Connectors and Shear Deformation on Deflections

6.4.1 Simply Supported Beam Subjected to Uniformly Distributed Load and a Concentrated Load

Beam U-6 tested by Chapman and Balakrishnan (5.) was modeled with the same parameters, and the load-deflection curve up to 80 kips (service load) was obtained using the numerical technique discussed in Chapter IV.

Fig. 6.3 shows the comparison of deflections for full shear connection and partial shear connection (50% of full shear connection) considering

(a) the linear and nonlinear load-slip characteristics for the shear connector

(b) the effect of shear deformations.

It can be seen that each effect, namely slip, nonlinear load-slip characteristics and the effect of shear deformation progressively increase deflection and slip and that deflection and slip for beams with partial shear connection are somewhat larger than for those with full shear connection. The total deflection of the composite beam considering the effects of nonlinear load-slip characteristics, shear and partial shear connection is approximately twice that of the bending deflection of the beam neglecting the above effects. A similar trend is observed in the case of beams subjected to concentrated load and the deflections are significantly greater than those for uniform load. The percentage increase in deflection as well as end slip from full shear connection to partial shear connection is given in Table 6.2 and Table 6.3 respectively. Referring to Table 6.2, it can be seen that the maximum percentage increase in deflection is found when both nonlinear load-slip characteristics for the connectors as well as shear deformations are included. The properties of the beams are given in Columns 1 and 2 of Table 6.5.

Fig. 6.4 shows the comparison of load deflection, load-slip curves for full and partial shear connection considering a) linear and nonlinear load-slip characteristics of the shear connectors and b) the effect of shear deformation for simply supported beam subjected to uniformly distributed load. Similar load deflection and load slip curves are

drawn in Fig. 6.5 and 6.6, when the beam is subjected to concentrated load. From the above figures, it can be observed that the deflections and slip of the beam are increased due to nonlinear load-slip characteristic of the shear connectors and the shear deformations. The effect of partial shear connection on deflection and slip is larger than that of full shear connection.

6.5 Deflection of a Continuous Beam Subjected to Uniform Load

Since a closed form solution for the deflection of a continuous beam considering nonlinear load-slip characteristics of shear connector is not available, it is not possible to derive an expression of the form of Equation 6.3 to determine the effect of flexible shear connectors on continuous beam deflections. However, it is reasonable to assume that the same nondimensional factors which control the deflection of simply supported beams also control the deflection of continuous beams. A universally applicable plot similar to that of Fig. 6.1 can then be constructed from the results of numerical solutions.

Fig. 6.7 is such a plot for a continuous beam with two equal spans subjected to uniform load. Two sets of results are shown, namely, those with zero stiffness

of the concrete in the negative moment region (variable I), and those with constant moment of inertia.

Fig. 6.8 is identical to Fig. 6.7 except that it includes the effect of shear deformation. Recalling the discussion from Sect. 6.3, it was pointed out that shear deflection is not directly a function of ξ and η . Nevertheless, the smooth variation of the curves indicates that, in the absence of better information, Fig. 6.8 could give a reasonable indication of the deflection of continuous beams including the shear effect. For a more accurate computation, shear deflections can be superimposed on the results from Fig. 6.7, as indicated in Sect. 6.3.

A comparison between Fig. 6.8 and 6.7 indicates the very significant increase in deflection due to the effect of shear deformations in continuous beams. This fact has previously been pointed out by Hamada and Longworth (9). Since the shear deflection of a continuous beam subjected to a concentrated load is approximately the same as that of a simple beam, the increase in deflection ratio results primarily from the fact that the flexural deflection in a continuous beam is approximately one-quarter of that for a simple beam and, hence, the shear deflection is a higher fraction of the flexural deflection.

6.6 Deflection of a Two-Span Continuous Beam Subjected to Concentrated Load

The properties of the beam are given in Column 3 of Table 6.5. Figs. 6.9 and 6.10 show the comparison of load-deflection and load-slip curves for full and partial shear connection considering a) linear and nonlinear load-slip characteristics for the shear connector and b) the effect of shear deformations. The figures are based on constant moment of inertia. Similar curves are drawn in Figs. 6.11 and 6.12 for a beam with variable moment of inertia. In continuous beams it may also be observed that each effect, namely slip, nonlinear load-slip behavior of the shear connectors and the effect of shear deformation increases deflection and slip. Partial shear connection causes larger deflection than that obtained for full shear connection. The deflection comparison of continuous beams at service load for partial and full shear connection is given in Table 6.4.

6.7 Influence of Negative Moment Cracking in Continuous Beams

While the figures in Sect. 6.5 give the influence of negative moment cracking on deflections, they give no insight into the effect of this cracking on the distribution of slip and slip-strain along the length of the beam.

The effect of cracking on these distributions is examined for a typical beam in this Section.

The example beam has the properties listed in Column 4 of Table 6.5. The distribution of deflection, slip, slip-strain and force in the slab are shown in Figs. 6.13 to 6.16, respectively, for the beam with and without cracking. It can be seen that the effect of cracking is to increase the deflections (Fig. 6.13), increase slip in the positive moment region (Fig. 6.14), introduce discontinuities in the slip-strain relationship (Fig. 6.15), and increase the slab force in the positive moment region (Fig. 6.16).

6.8 Analyses of a Three-Span Beam for Shored and Unshored Construction

The example problem is a beam with three equal spans subjected to uniform load with properties listed in Column 5 of Table 6.5. The live load to dead load ratio is 2.25. In the analysis of unshored construction all the dead load is assumed to be carried by the steel beam and the live load by the composite action. Full shear connection and linear load-slip behavior is assumed. Deflection, slip, slip strain and force distribution in Fig. 6.17 to 6.20. The effect of unshored construction is to increase the deflection, decrease slip in both positive and negative moment regions and decrease slip

strain as well as introduce discontinuities in the slip-strain relationship and decrease the slab force in both positive and negative moment regions.

6.9 Conclusions

In this Chapter an evaluation of the effect of various parameters such as

- (a) partial and full shear connection
- (b) linear and nonlinear load slip behavior
- (c) shear deformation
- (d) constant and variable moment of inertia, and
- (e) shored and unshored construction

on service load deflections have been studied. The computer program reliably predicts deflection and slip for simply supported and continuous beams under service loads. The shear form factors for various sections with different widths and thicknesses of concrete slab are tabulated for practical design. Shear, slip and partial shear connection significantly affect deflection values and should therefore be considered for an accurate evaluation of deflection.

TABLE 6.1 SHEAR FORM FACTORS (K_{sh}) FOR COMPOSITE BEAMS

Steel Beam	Slab Thickness = $t_c = 4.0"$			Slab Thickness = $t_c = 6.0"$		
	36.00	48.00	60.00	72.00	84.00	96.00
Section	36.00	48.00	60.00	72.00	84.00	96.00
W24x120	3.460	3.798	4.141	4.488	4.835	5.184
W24x 68	3.317	3.801	4.286	4.771	5.254	5.736
W21x 73	3.445	3.913	4.384	4.855	5.325	5.793
W21x 55	3.661	4.250	4.839	5.424	6.006	6.584
W18x 60	3.784	4.346	4.909	5.468	6.025	6.577
W18x 40	4.398	5.202	5.996	6.780	7.553	8.315
W16x 50	4.070	4.723	5.374	6.018	6.654	7.283
W16x 26	4.863	5.875	6.781	7.277	7.735	8.161
W14x 53	4.752	5.475	6.194	6.904	7.604	8.294
W14x 22	5.388	6.300	6.850	7.349	7.809	8.239
W12x190	3.771	3.933	4.114	4.307	4.507	4.712
W12x 27	6.029	7.092	7.666	8.188	8.671	9.122
W10x112	4.079	4.379	4.697	5.024	5.355	5.688
W10x 21	5.535	6.079	6.565	7.010	7.421	7.806
W 8x 67	4.263	4.721	5.185	5.645	6.099	6.353
W 8x 17	5.048	5.531	5.966	6.365	6.734	7.081
	36.00	48.00	60.00	72.00	84.00	96.00
	3.671	4.716	4.564	5.014	5.462	5.909
	3.667	4.287	4.901	5.507	6.104	6.691
	3.723	4.312	4.897	5.473	6.040	6.598
	4.030	4.756	5.467	6.161	6.575	6.860
	4.043	4.716	5.376	5.952	6.277	6.581
	4.785	5.581	6.029	6.438	6.816	7.171
	4.298	5.042	5.509	5.854	6.175	6.475
	4.713	5.206	5.640	6.047	6.419	6.765
	4.854	5.599	5.983	6.338	6.668	6.978
	4.640	5.120	5.550	5.951	6.316	6.658
	3.557	3.753	3.970	4.198	4.433	4.670
	5.139	5.623	6.060	6.460	6.831	7.178
	3.770	4.097	4.434	4.773	5.054	5.209
	4.204	4.599	4.956	5.785	5.590	5.877
	3.805	4.014	4.182	4.342	4.509	4.665
	3.625	3.962	4.269	4.552	4.815	5.062

TABLE 6.2 DEFLECTION COMPARISON OF SIMPLY SUPPORTED COMPOSITE BEAM AT SERVICE LOAD

Uniformly Distributed Load = 80 kips		Concentrated Load = 55 kips	
Load-Slip Characteristics		Load-Slip Characteristics	
Linear	Nonlinear	Linear	Nonlinear
Without Shear Deformation	With Shear Deformation	Without Shear Deformation	With Shear Deformation
15.13%	20.00%	19.62%	22.67%
15.90%	18.30%	20.78%	21.83%

Percentage Increase in Deflection From Full Shear Connection to Partial Shear Connection

TABLE 6.3 SLIP COMPARISON OF SIMPLY SUPPORTED COMPOSITE BEAMS AT SERVICE LOAD

Load-Slip Behavior and Degrees of Shear. Connection	Uniformly Distributed Load = 80-kips	Concentrated Load = 55 kips
Linear vs. Nonlinear at Full Shear Connection	26.00%	27.27%
Linear vs. Nonlinear at Partial Shear Connection	44.45%	52.42%
Full Shear Connection vs. Partial Shear Connection at Linear	75.60%	84.62%
Full Shear Connection vs. partial Shear Connection at Nonlinear	100.00%	121.10%

TABLE 6.4 DEFLECTION COMPARISON OF CONTINUOUS COMPOSITE BEAM AT SERVICE LOAD

		Concentrated Load = 80 kips			
		Uniform Moment of Inertia		Variable Moment of Inertia	
		Load-Slip Characteristics		Load-Slip Characteristics	
		Linear		Nonlinear	
		Without Shear Deformation	With Shear Deformation	Without Shear Deformation	With Shear Deformation
Percentage Increase in Deflection From Full Shear Connection to Partial Shear Connection	68.07%	64.20%	58.03%	52.00%	68.33%
	60.78%	65.95%	60.78%	56.36%	

TABLE 6.5 PROPERTIES OF COMPOSITE BEAMS USED FOR APPLICATION

Beam Designation	BSS12 x 6L	BSS12 x 6L	W12 x 31	W12 x 31	W12 x 31	W12 x 31
Total Depth	18.000	18.000	16.090	16.090	18.090	16.090
Concrete Slab						
bc (in.)	48.000	48.000	48.000	48.000	60.000	48.000
te (in.)	6.000	6.000	4.000	4.000	6.000	4.000
Ec (ksi)	3.500x10 ³	3.600x10 ³	4.100x10 ³	4.100x10 ³	3.830x10 ³	3.830x10 ³
f'c (psi)	3500.0	3500.0	4500.0	4500.0	4000.0	4000.0
Reinforcement						
A _{sr} (sq. in.)	-	-	1.570	1.570	1.960	1.960
d _{sr} (in.)	-	-	2.000	2.000	3.000	2.500
F _{yr} (ksi)	-	-	50.000	50.000	50.000	50.000
E _{sr} (ksi)	-	-	30.000x10 ³	30.000x10 ³	30.000x10 ³	30.100x10 ³
Steel Section						
f _y (ksi)	36.400	36.400	44.000	44.000	44.000	44.000
E _s (ksi)	30.200x10 ³	30.200x10 ³	30.000x10 ³	30.000x10 ³	30.000x10 ³	30.000x10 ³
G (ksi)	11.880x10 ³	11.880x10 ³	12.660x10 ³	12.660x10 ³	12.660x10 ³	12.660x10 ³
Shear Connector Type						
Paired Headed Stud Size	3/4"x4"	3/4"x4"	3/4"x4"	3/4"x4"	3/4"x4"	3/4"x4"
K (psi)	15.500x10 ⁴	15.500x10 ⁴	20.200x10 ⁴	20.200x10 ⁴	20.000x10 ⁴	20.000x10 ⁴
a (psi)	19.620x10 ²	19.620x10 ²	20.200x10 ²	20.200x10 ²	20.000x10 ²	20.000x10 ²
b	79.000	79.000	100.000	100.000	100.000	100.000
Q _u (kips)	28.000	28.000	28.000	28.000	28.000	28.000

Simply Supported Beam with U.D.L.

Simply Supported Beam with Conc. Load at Center Span

2 Equal Span Cont. Beam with Conc. Load at Center Span

Beam for Comparison of Shored and Unshored Construction

Beam for Comparison of Constant and Variable 'I' Construction

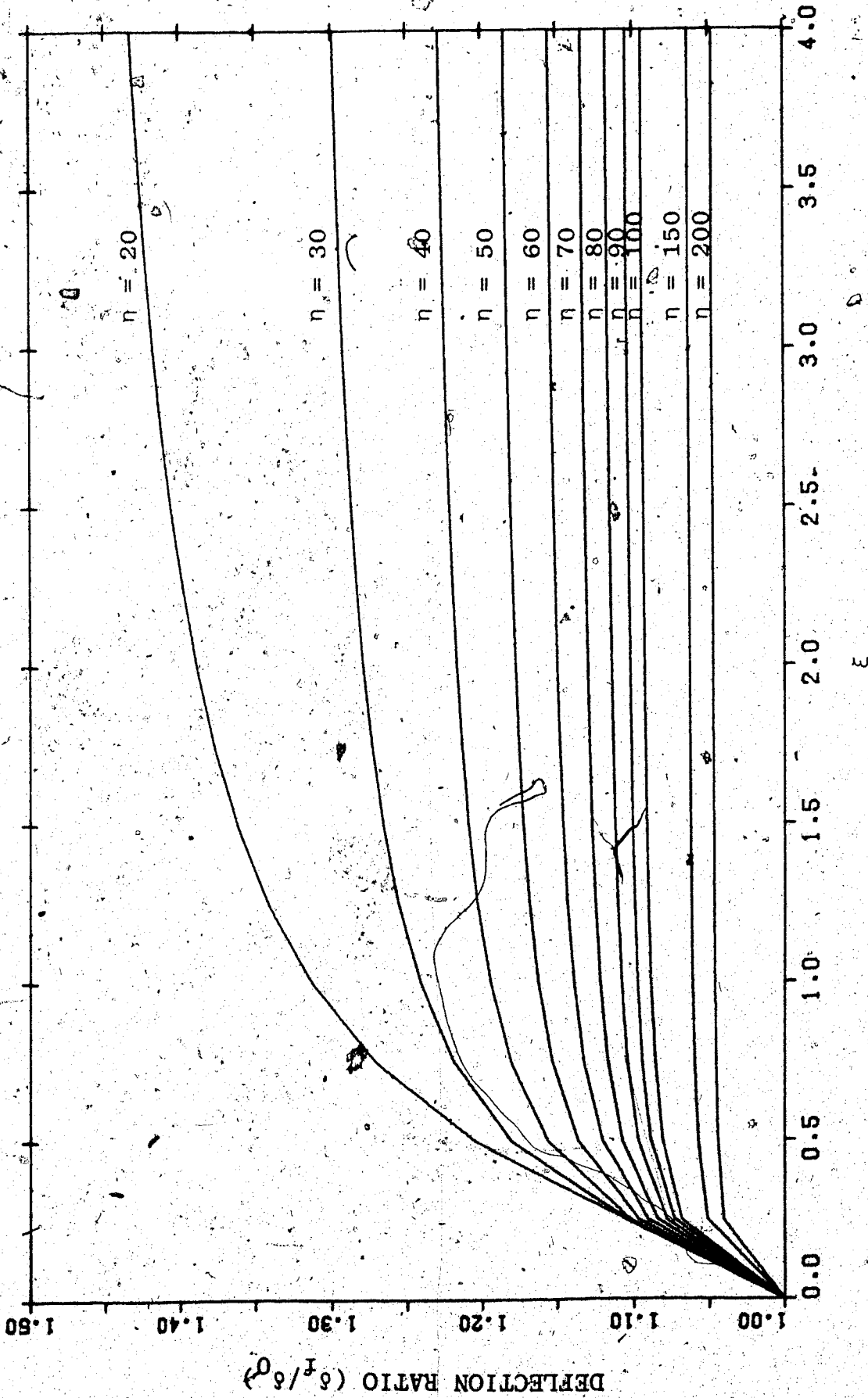


FIGURE 6.1 DEFLECTION RATIO (δ_f/δ_0) VS ξ FOR A SIMPLY SUPPORTED BEAM WITH UNIFORMLY DISTRIBUTED LOAD

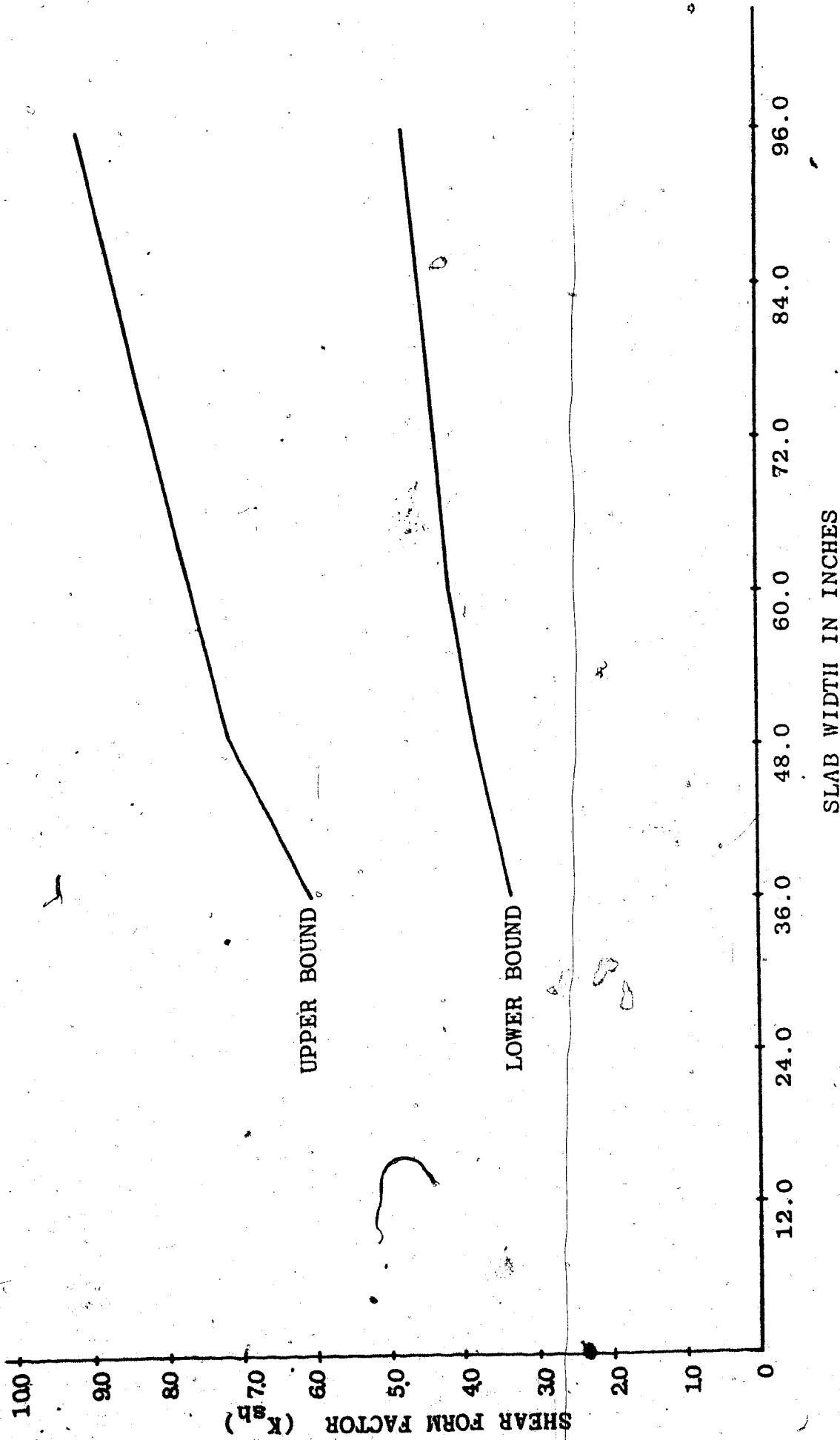


FIGURE 6.2 SHEAR FORM FACTOR (K_{sh}) VS SLAB WIDTH (bc) FOR COMPOSITE BEAMS

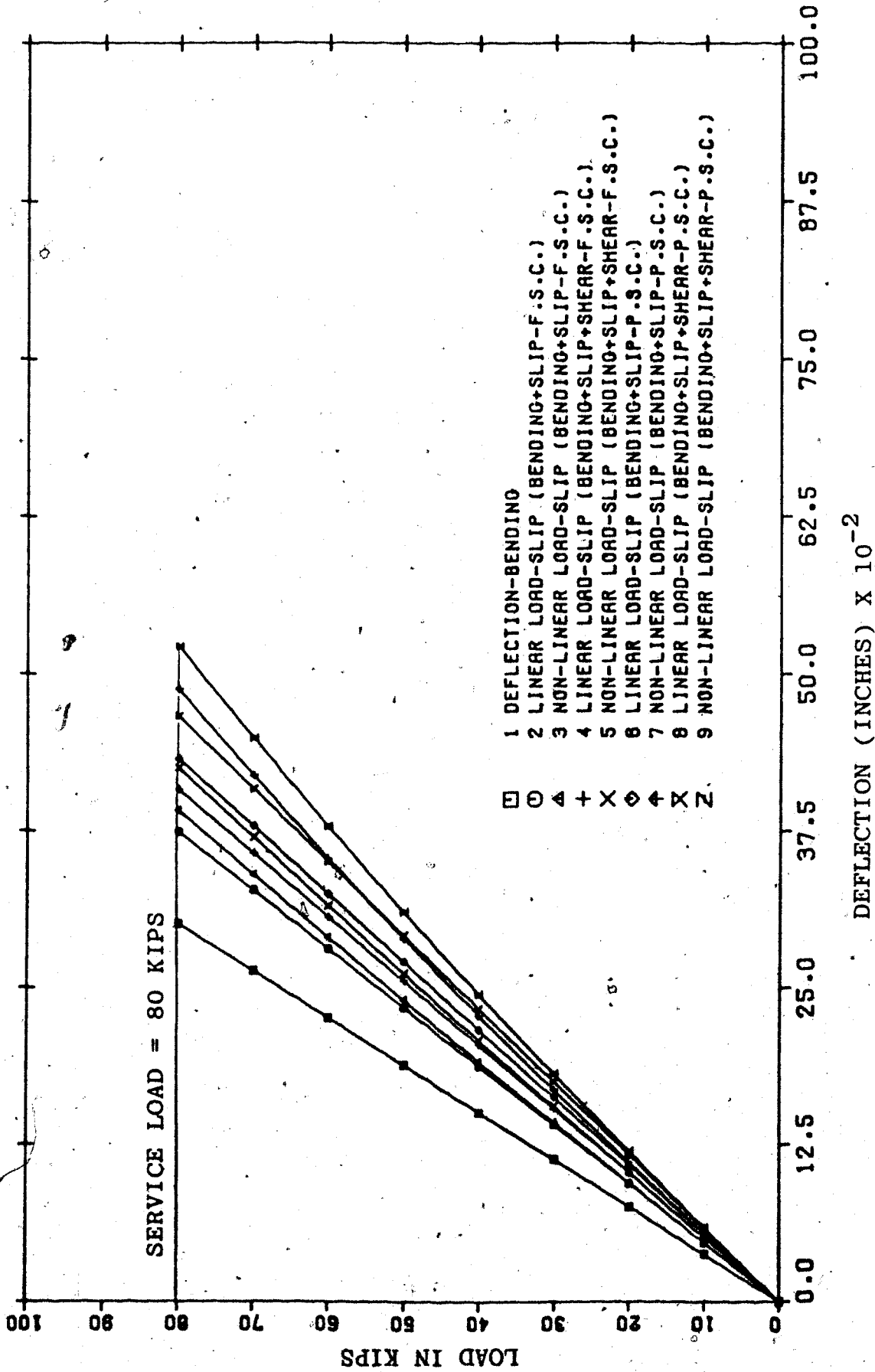


FIGURE 6.3 LOAD-DEFLECTION RELATIONSHIP (SIMPLY SUPPORTED BEAM, FULL AND PARTIAL SHEAR CONNECTION, UNIFORMLY DISTRIBUTED LOAD)

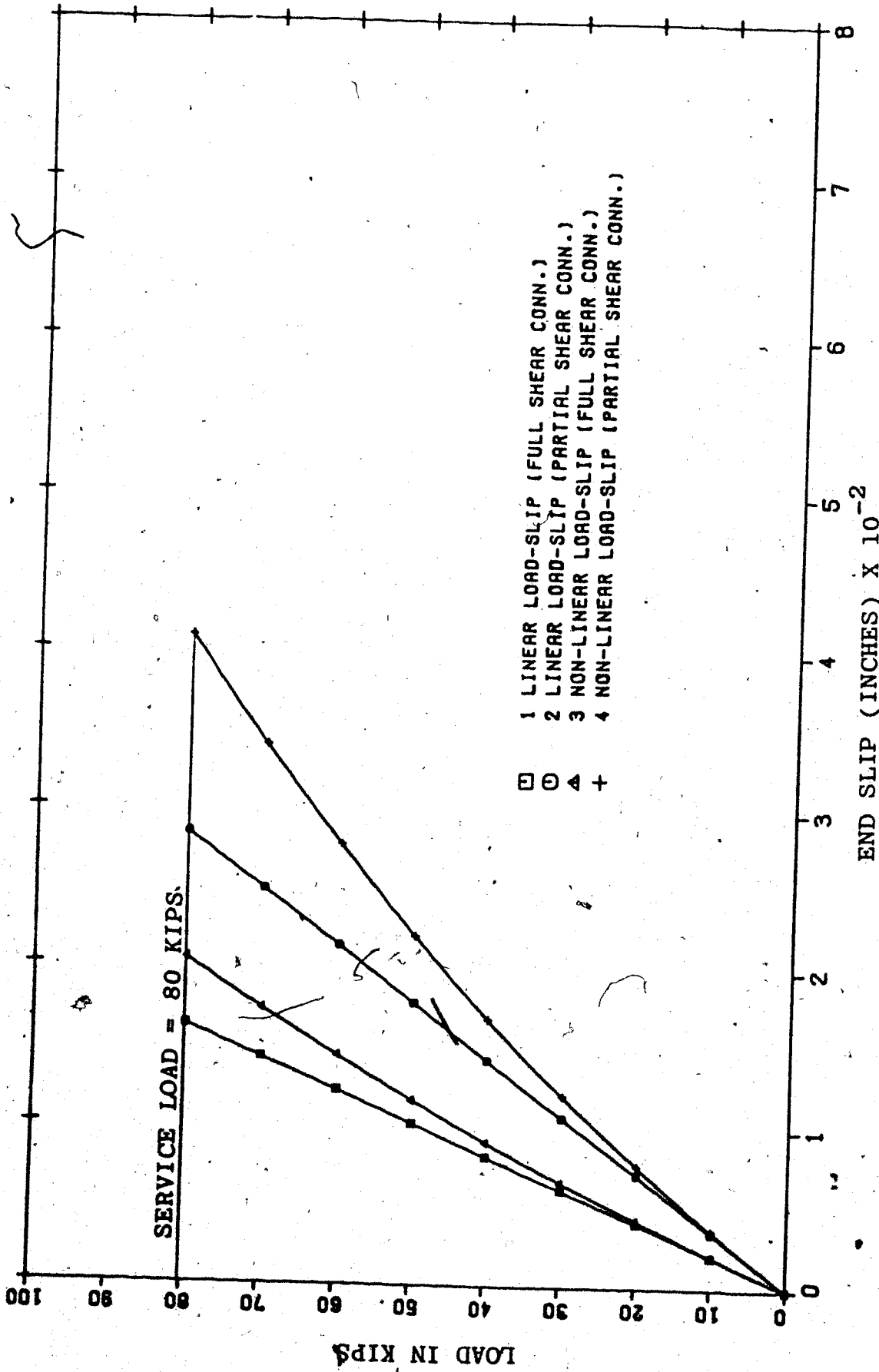
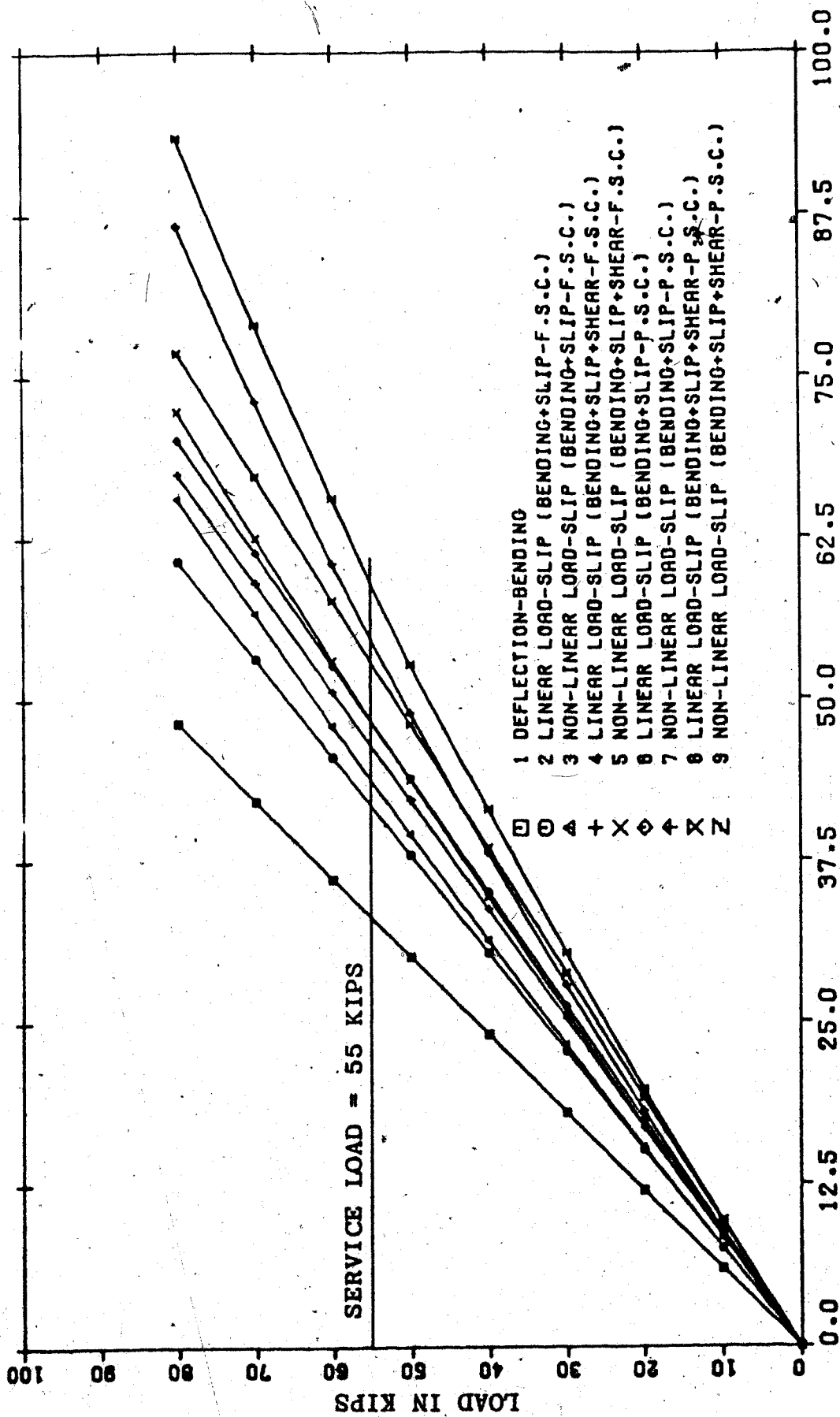


FIGURE 6.4 LOAD SLIP RELATIONSHIP (SIMPLY SUPPORTED BEAM, UNIFORMLY DISTRIBUTED LOAD)



DEFLECTION (INCHES) X 10⁻²

FIGURE 6.5 LOAD DEFLECTION RELATIONSHIP (SIMPLY SUPPORTED BEAM,
FULL AND PARTIAL SHEAR CONNECTION, CONCENTRATED LOAD AT CENTER)

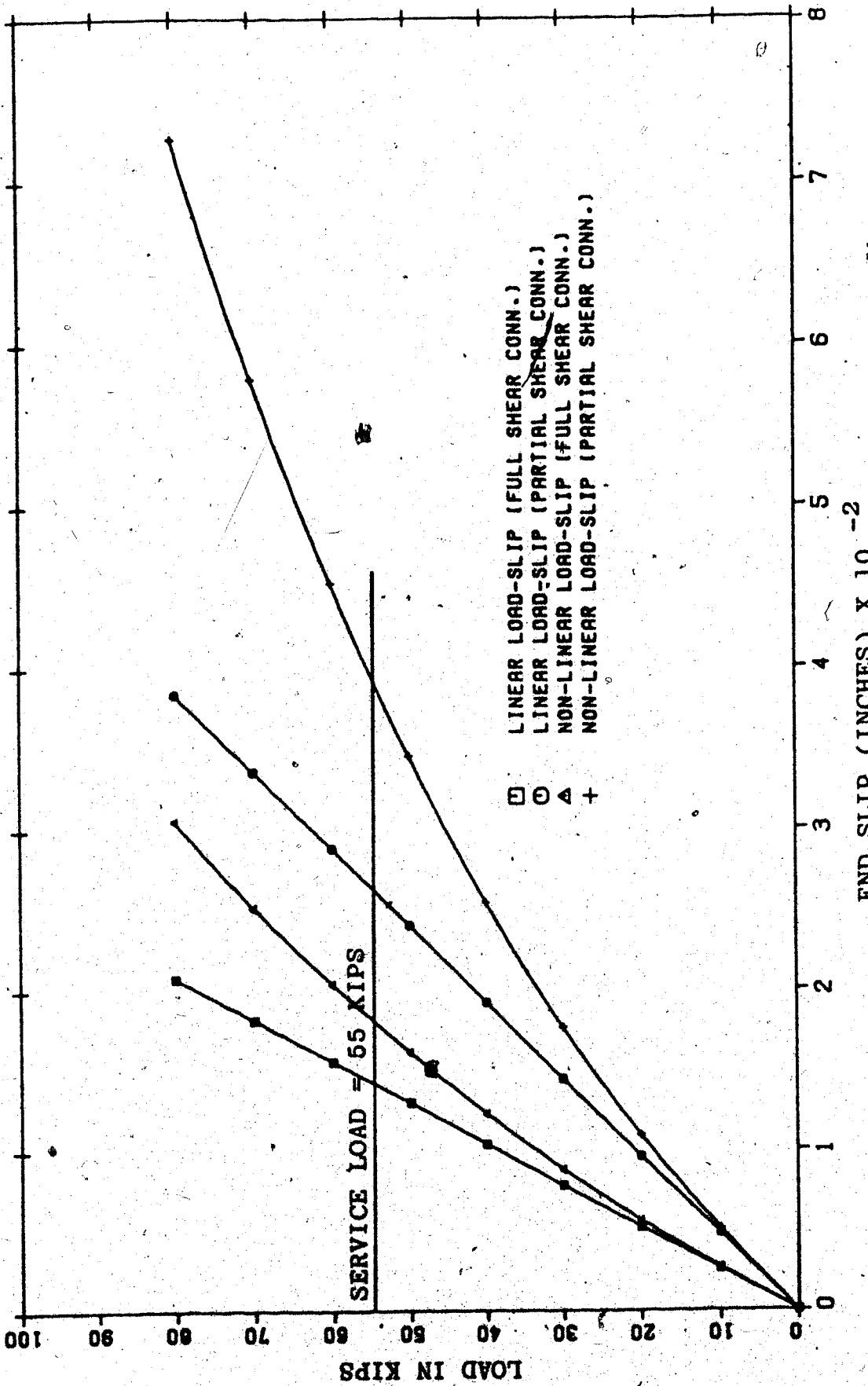


FIGURE 6.6. LOAD SLIP RELATIONSHIP (SIMPLY SUPPORTED BEAM, CONCENTRATED LOAD AT CENTER)

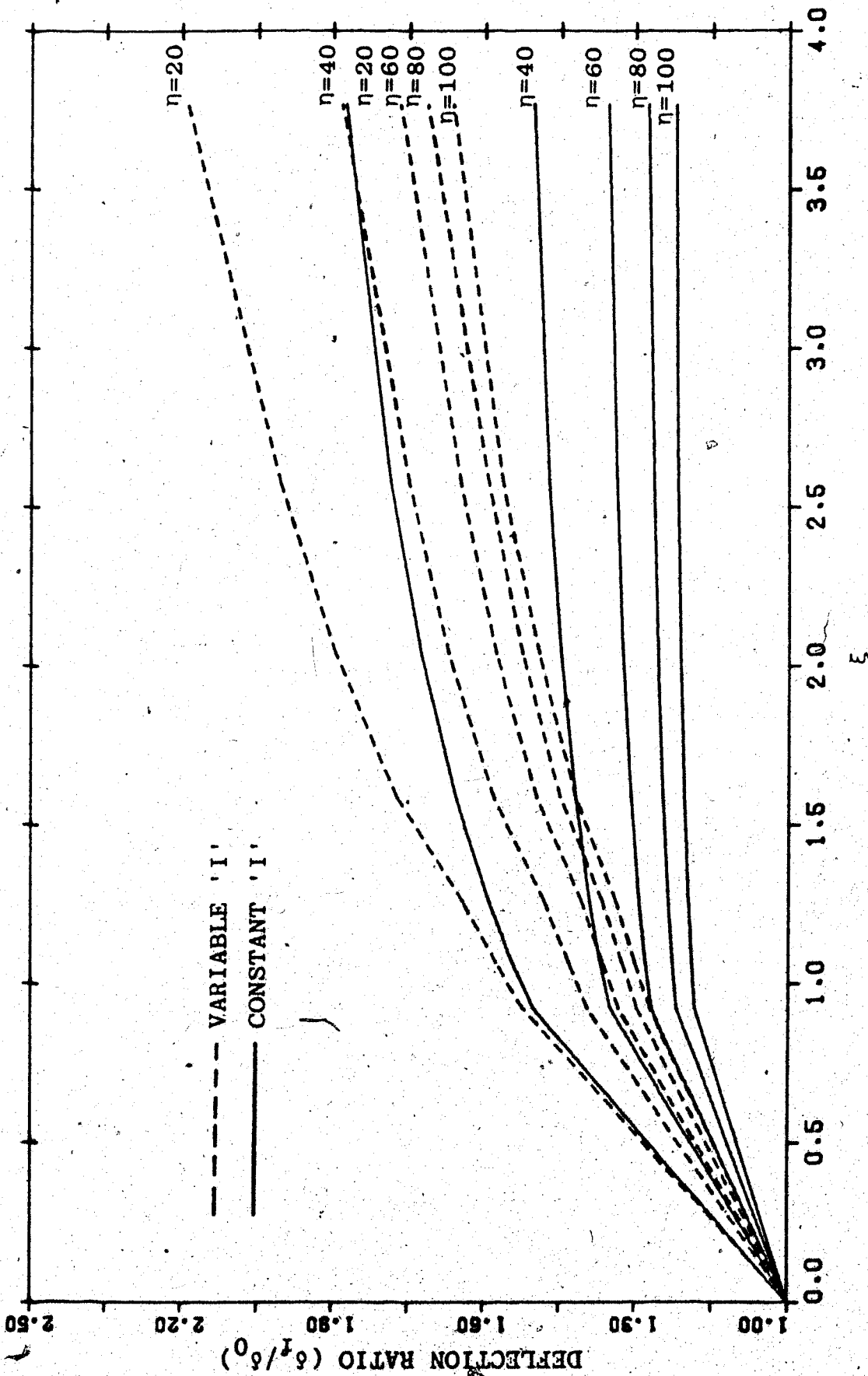


FIGURE 6.7 DEFLECTION RATIO (δ_f/δ_0) VS ξ FOR A TWO-SPAN CONTINUOUS BEAM WITH UNIFORMLY DISTRIBUTED LOAD

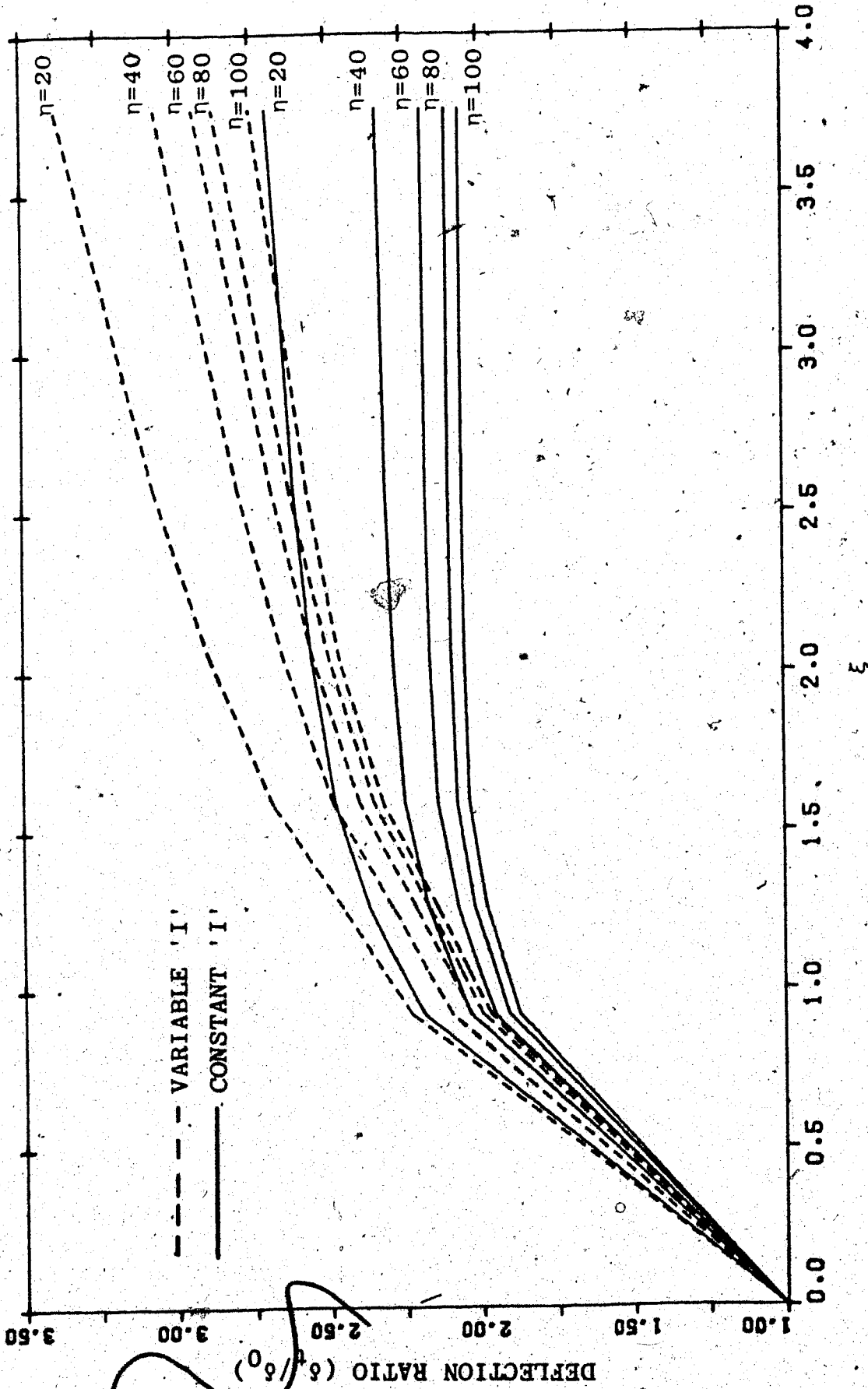


FIGURE 6.8 DEFLECTION RATIO (δ_t/δ_0) VS ξ FOR A TWO-SPAN CONTINUOUS BEAM WITH UNIFORMLY DISTRIBUTED LOAD

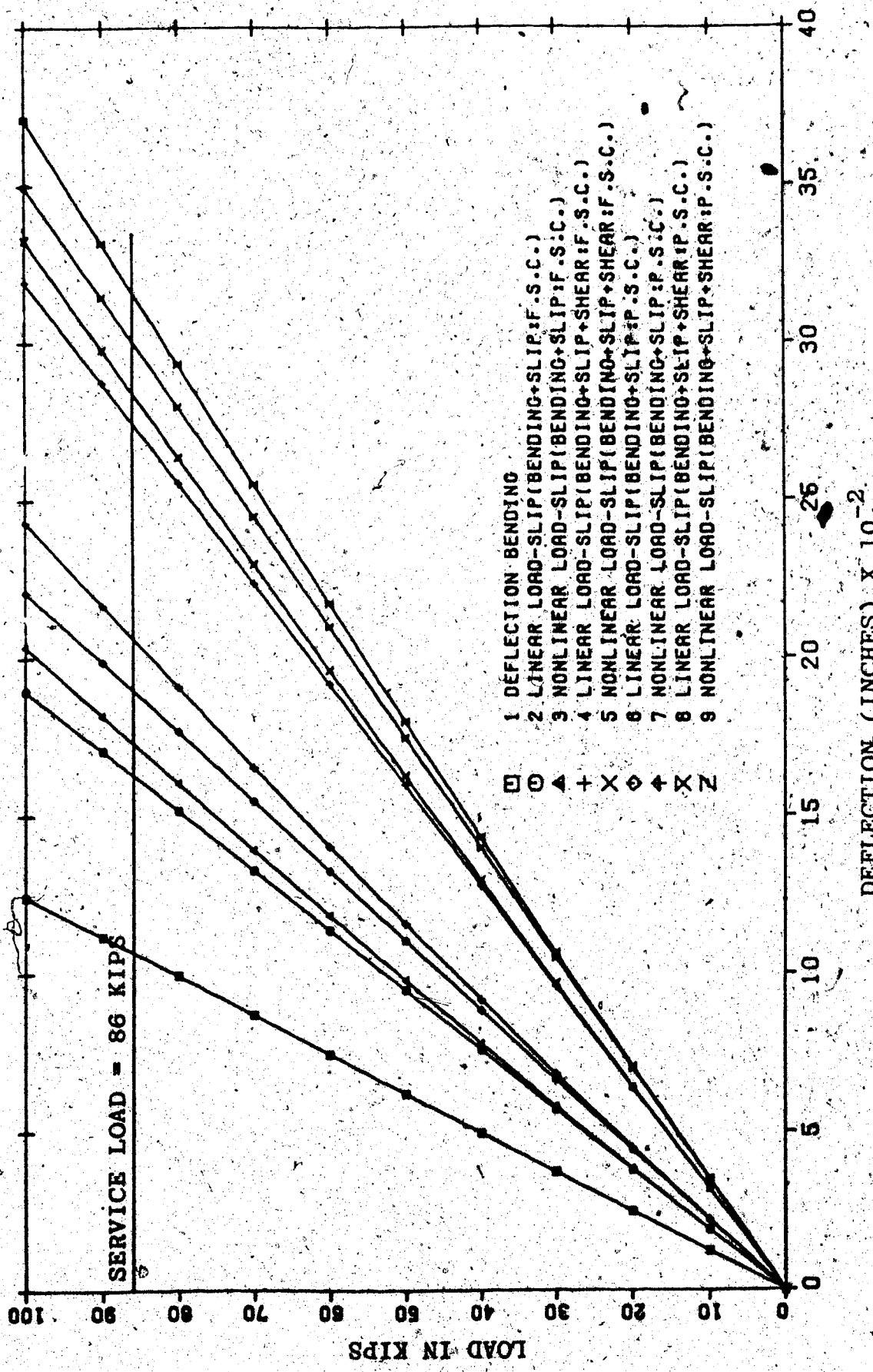
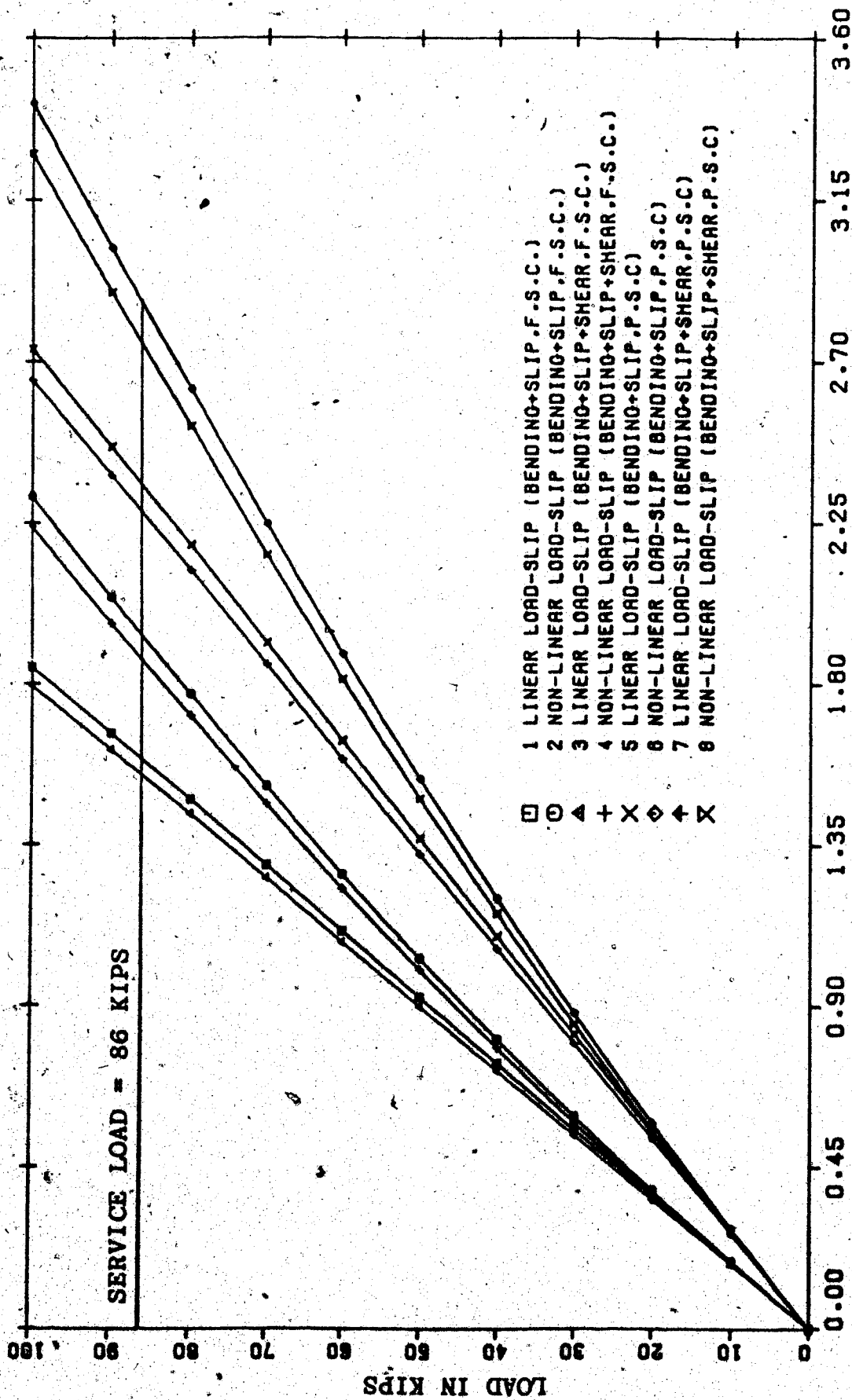


FIGURE 6.9 LOAD DEFLECTION RELATIONSHIP (CONTINUOUS BEAM, CONSTANT 'I', FULL AND PARTIAL SHEAR CONNECTION)



MAX. SLIP (INCHES) X 10⁻²

FIGURE 6.10 LOAD SLIP RELATIONSHIP (CONTINUOUS BEAM,
CONSTANT 'I', FULL AND PARTIAL SHEAR CONNECTION)

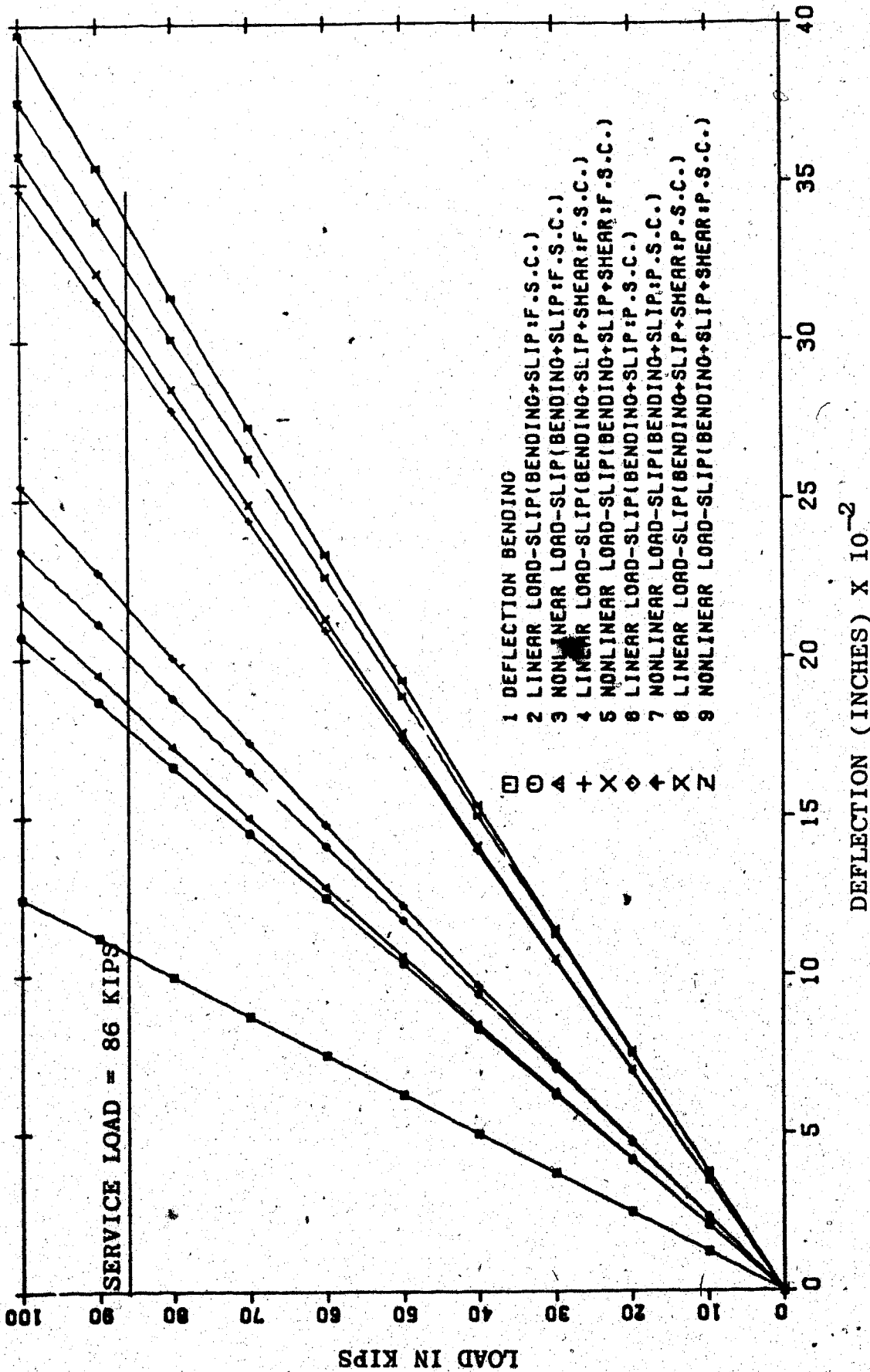


FIGURE 6.11 LOAD DEFLECTION RELATIONSHIP (CONTINUOUS BEAM, VARIABLE 'I', FULL AND PARTIAL SHEAR CONNECTION)

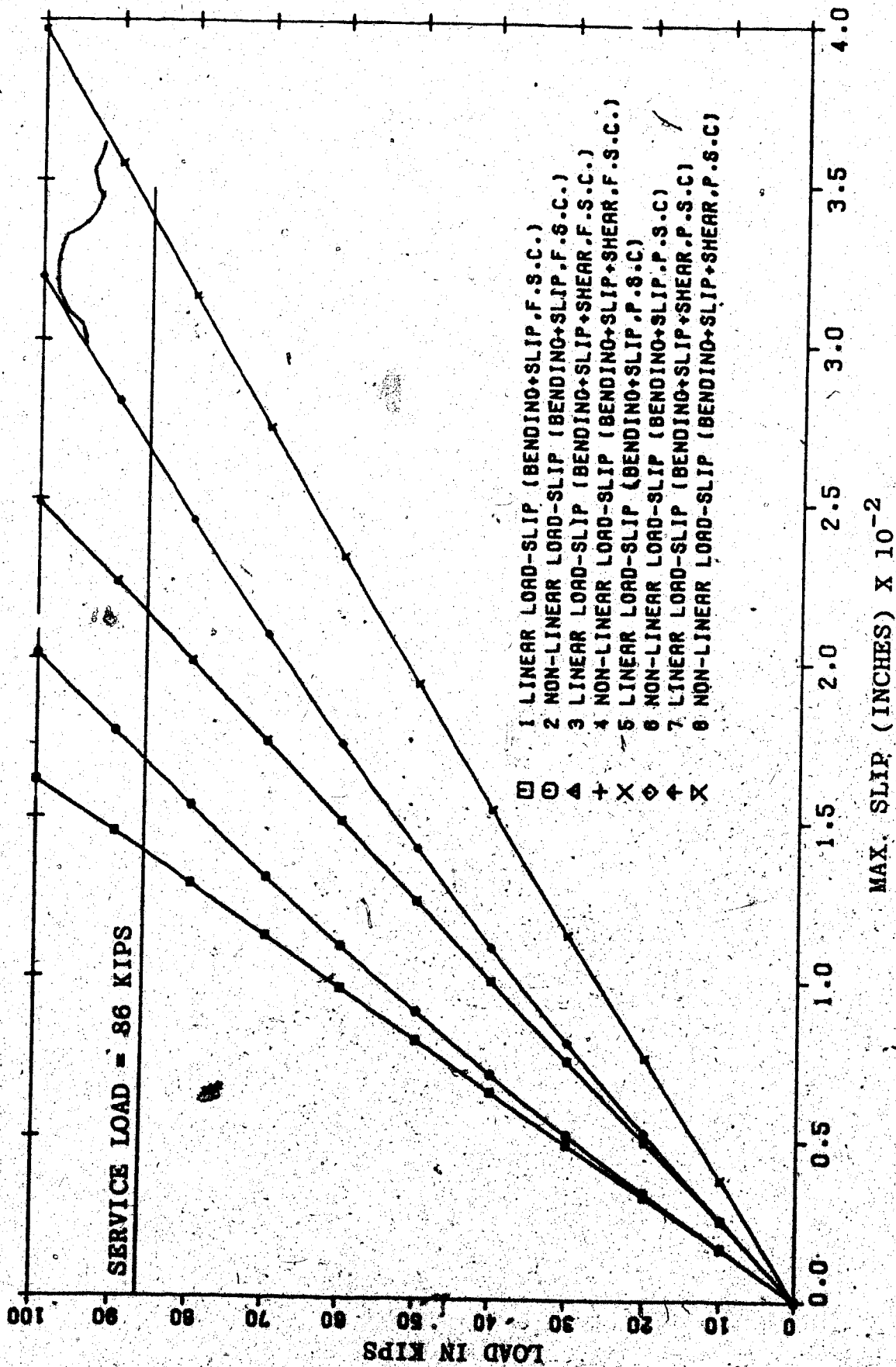


FIGURE 6.12 LOAD SLIP RELATIONSHIP (CONTINUOUS BEAM, VARIABLE 'I', FULL AND PARTIAL SHEAR CONNECTION)

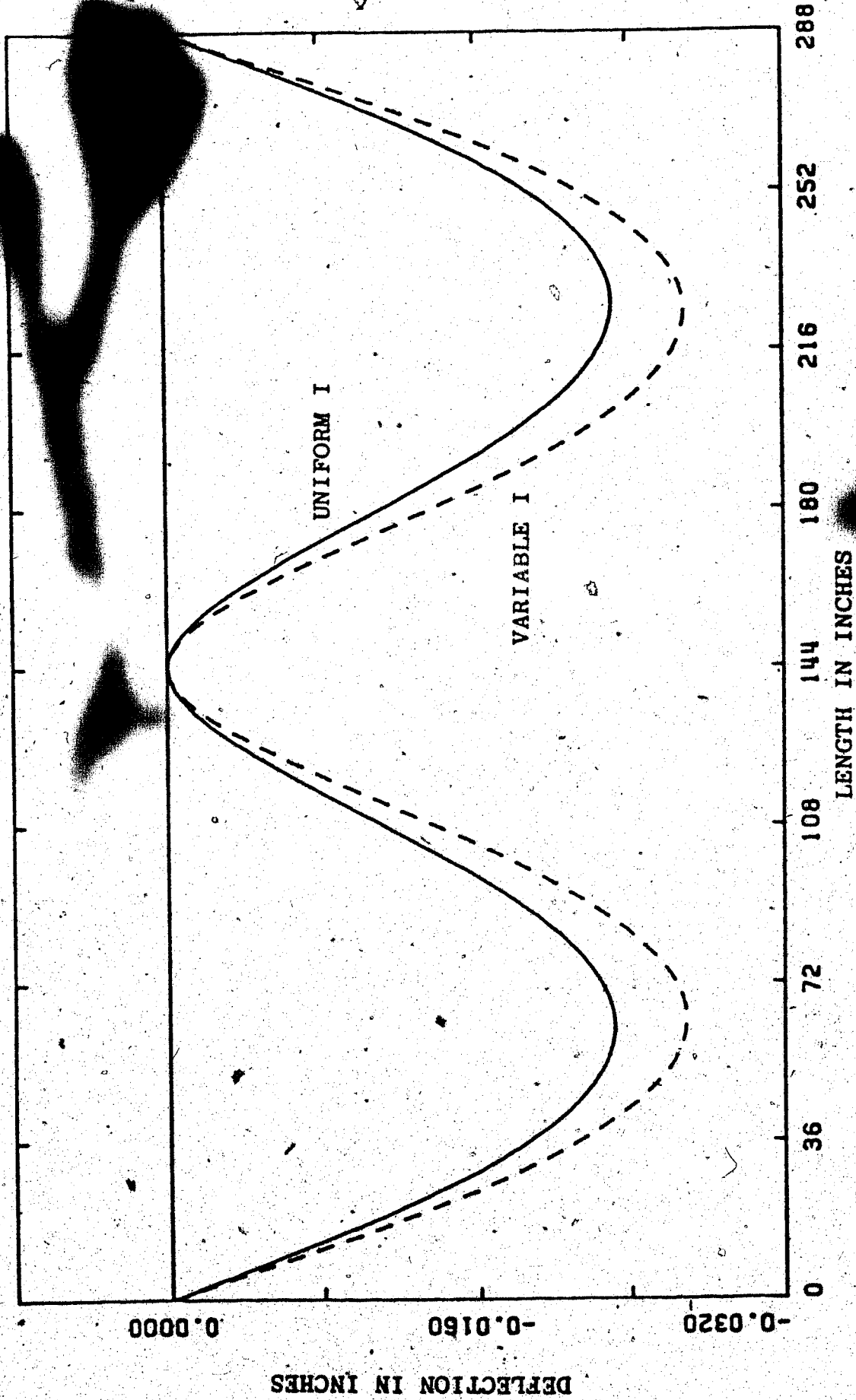


FIGURE 6.13 COMPARISON OF DEFLECTION VALUES CONSTANT AND VARIABLE 'I'

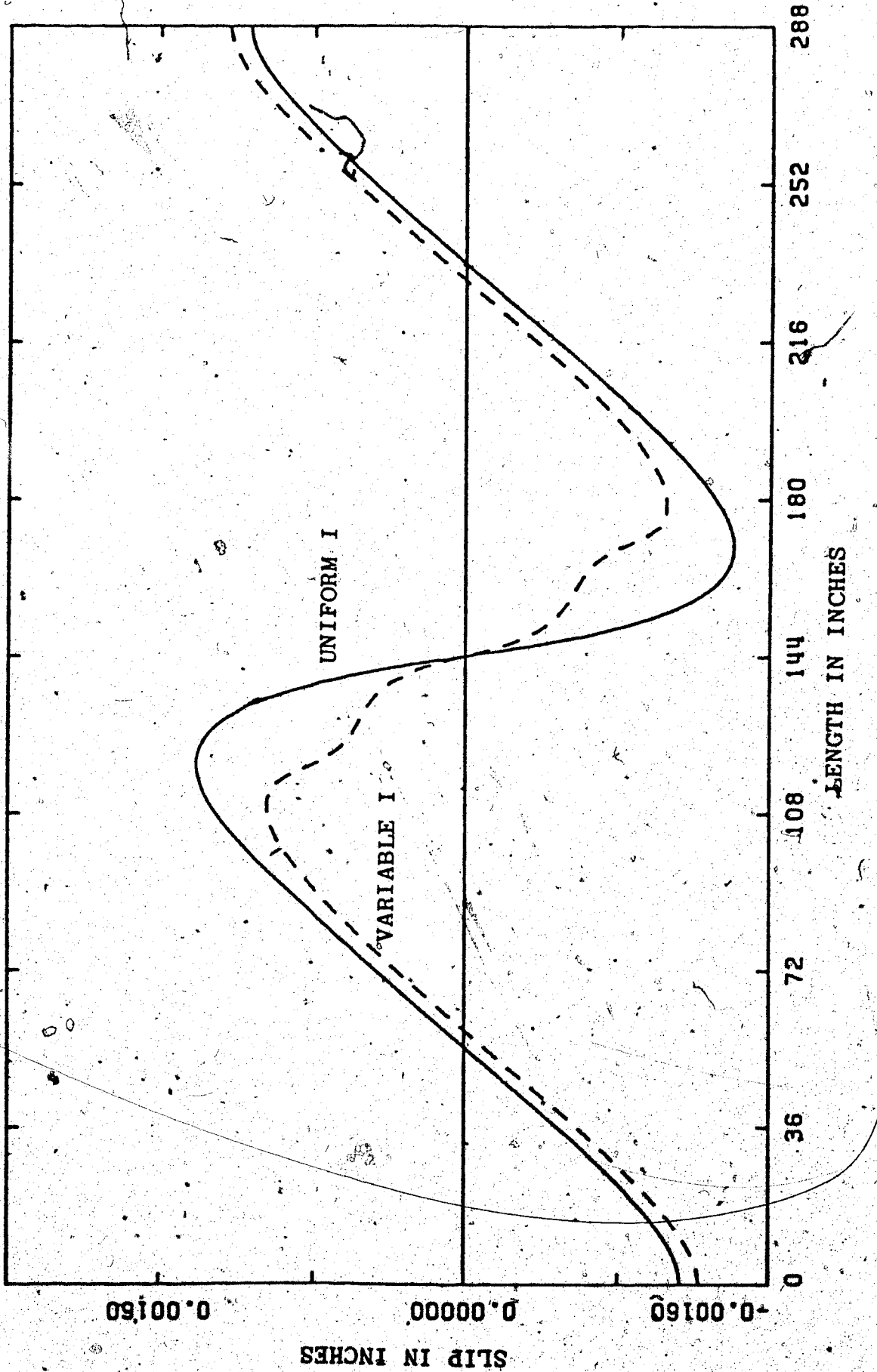


FIGURE 6.14 COMPARISON OF SLIP VALUES (CONSTANT AND VARIABLE 'I')

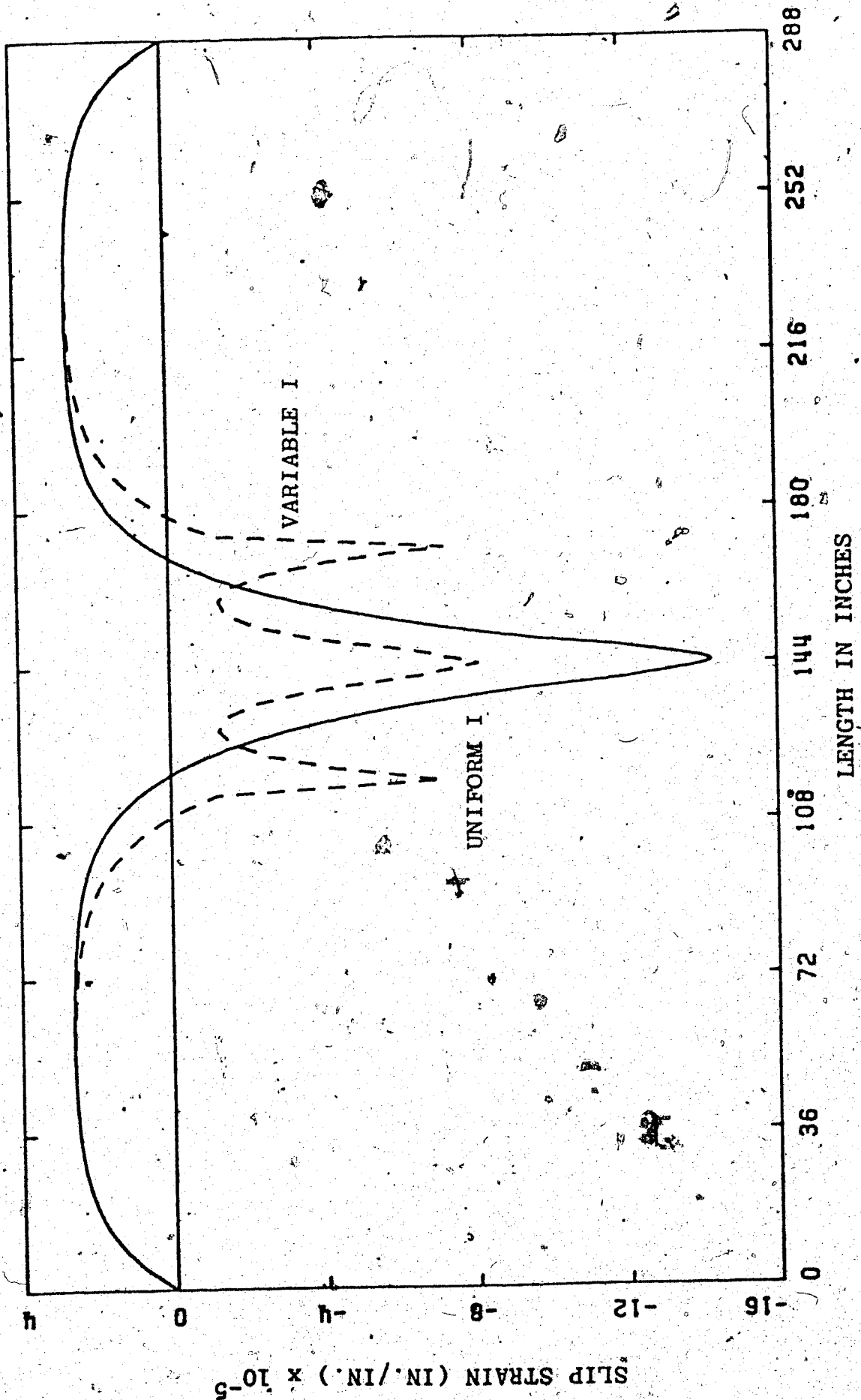


FIGURE 6.15 COMPARISON OF SLIP STRAIN VALUES (CONSTANT AND VARIABLE 'I')

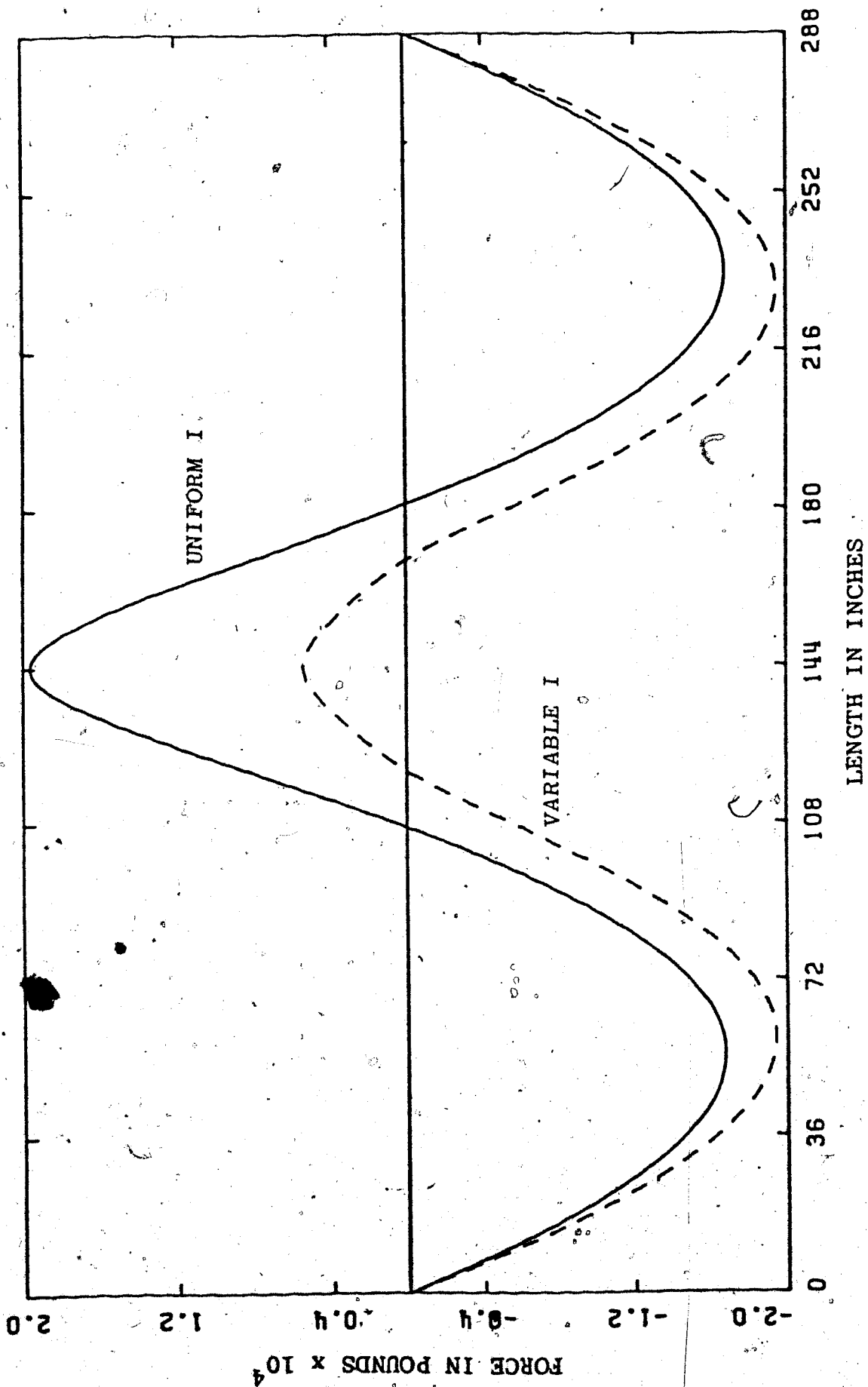


FIGURE 6.16 COMPARISON OF FORCE VALUES (CONSTANT AND VARIABLE 'I')

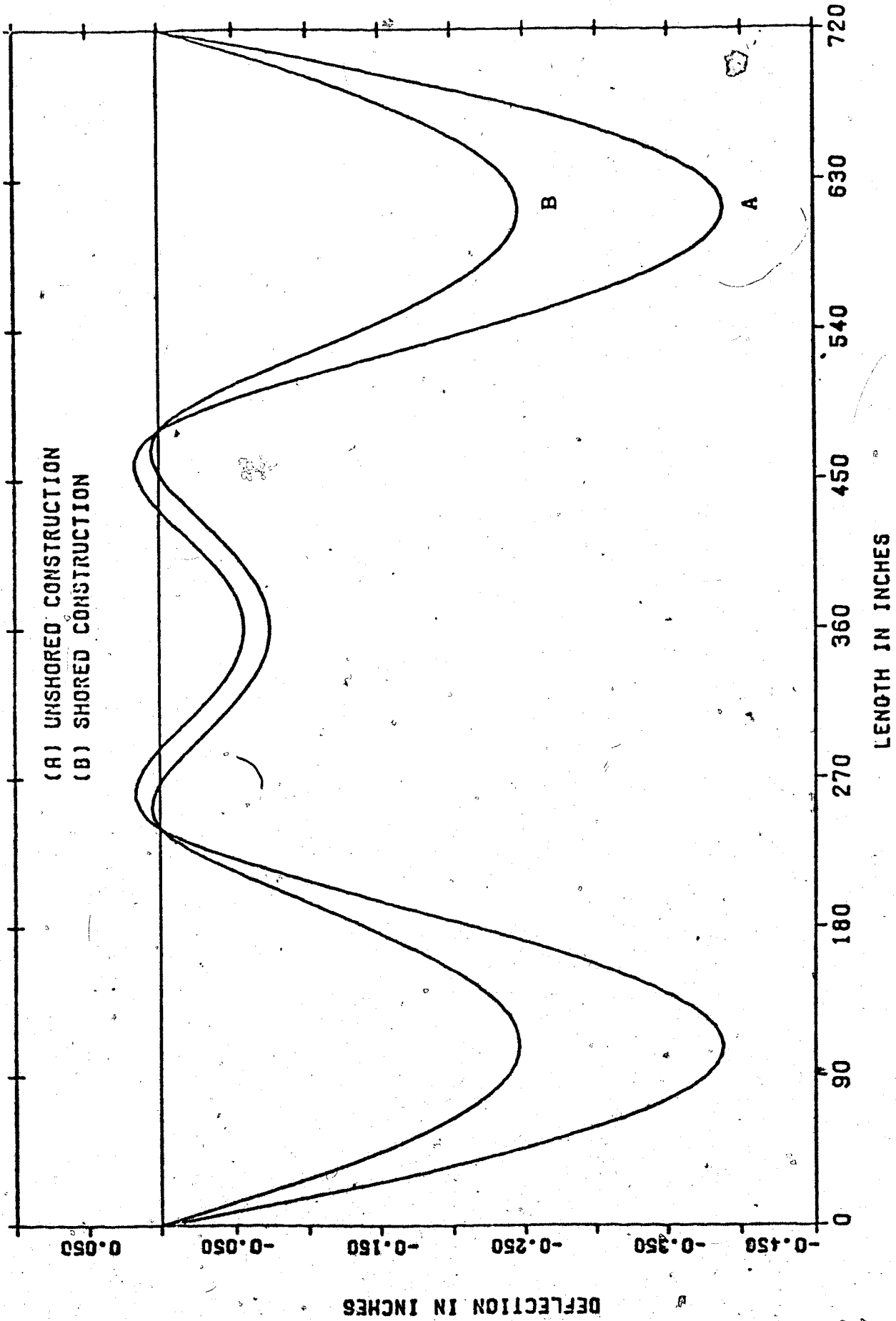
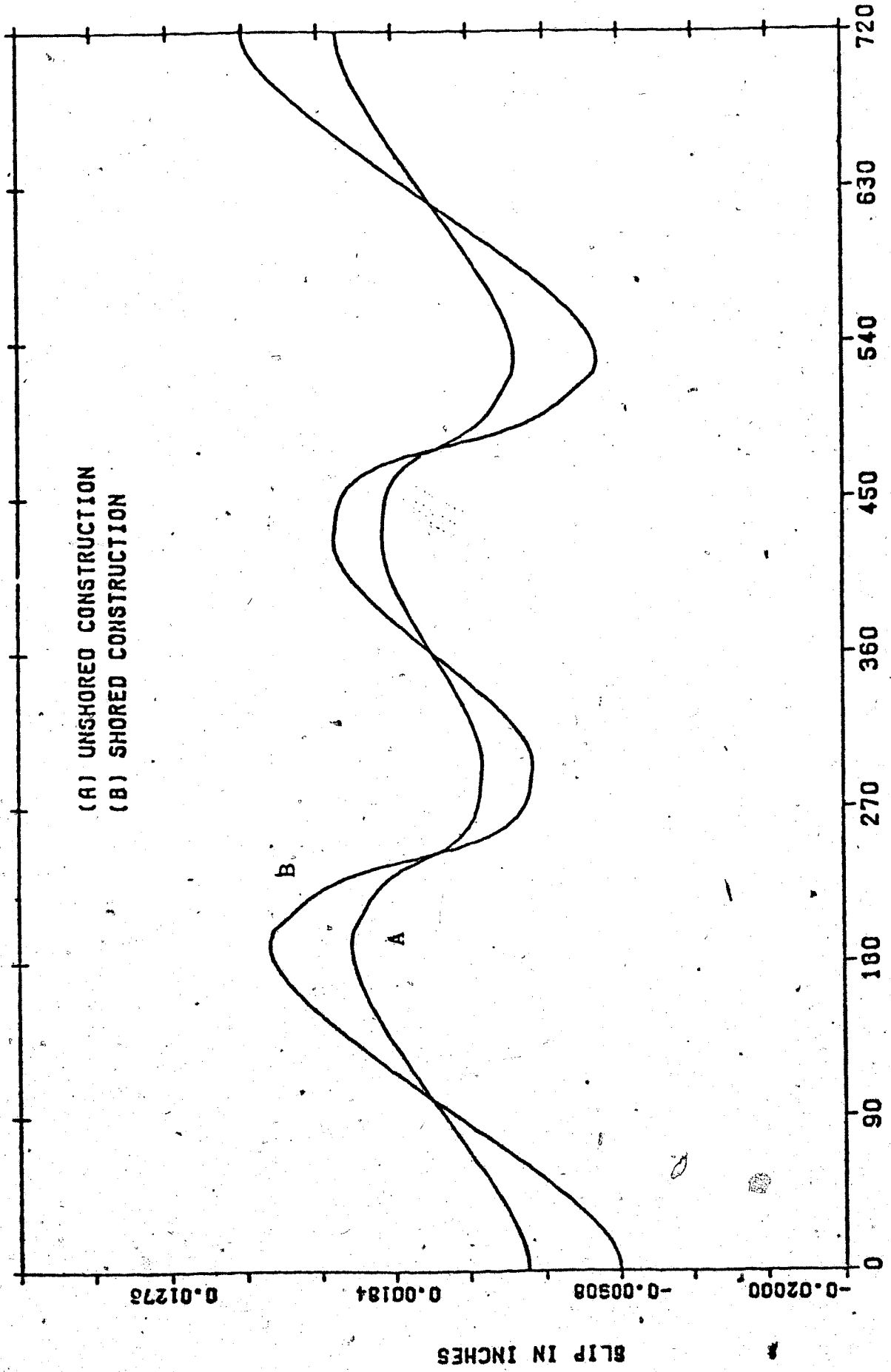


FIGURE 6.17 COMPARISON OF DEFLECTION VALUES (SHORED AND UNSHORED CONSTRUCTION)



(A) UNSHORED CONSTRUCTION
(B) SHORED CONSTRUCTION

LENGTH IN INCHES

SLIP IN INCHES

FIGURE 2-10 COMPARISON OF CITY WALLS / SHORED AND UNSHORED CONSTRUCTION

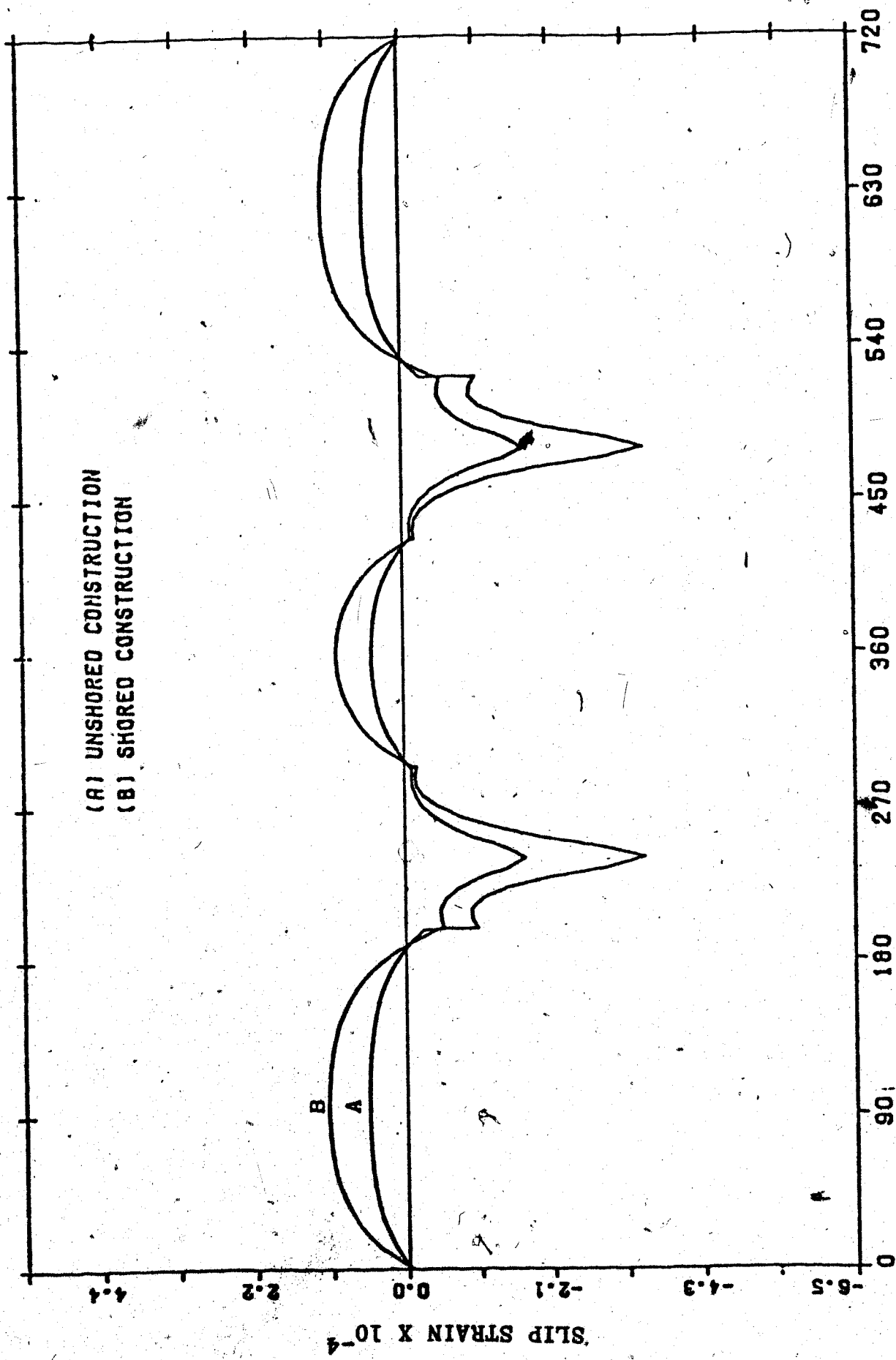


FIGURE 6.19 COMPARISON OF SLIP STRAIN VALUES (SHORED AND UNSHORED CONSTRUCTION)

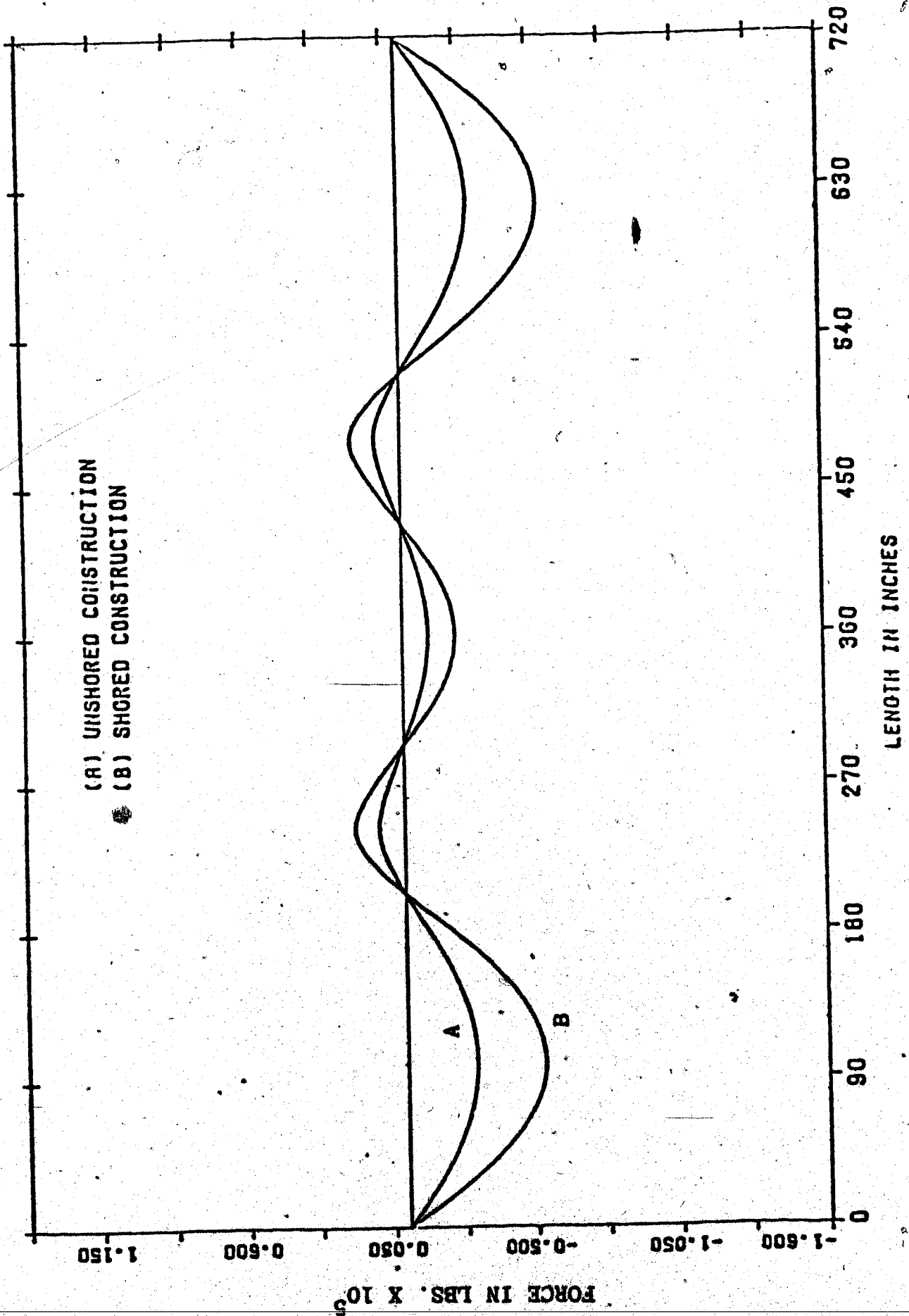


FIGURE 6.20 COMPARISON OF FORCE VALUES (SHORED AND UNSHORED CONSTRUCTION)

CHAPTER VII

SUMMARY AND CONCLUSIONS

7.1 Summary

This study has examined the formulation of governing equations for composite beams. Solutions of these equations have emphasized the effects of such factors as partial and full shear connection, shear deformation and linear or nonlinear load-slip characteristics of the shear connectors.

1. Classical solution techniques were examined in order to provide a standard comparison against which numerical solutions can be measured.
2. Programs were written for the evaluation of classical solutions for a simply supported beam and a continuous beam of two unequal spans, subjected to concentrated loads.
3. Results obtained from numerical technique developed herein were compared with published numerical results of Yam and Chapman (31), test results of Chapman and Balakrishnan (5) and Hamada and Longworth (9).

4. The solution for the deflection of a simply supported composite beam with uniform load was recast in terms of two dimensionless parameters, ξ and η . This permitted a plot to be developed to determine the effect of slip which is applicable to sections of any simply supported composite beam.
5. Shear form factors were computed for various rolled steel shapes with different concrete slab widths and thicknesses. These factors can be used to compute shear deflection.
6. The effects of parameters such as partial and full shear connection, shear deformation, linear and nonlinear load-slip characteristics on deflection and slip for a simply supported beam have been examined for two loading cases, viz. uniformly distributed load and concentrated load.
7. A numerical solution technique which permits the solution for slip and deflection of continuous beams under arbitrary loading was developed and programmed. This program is capable of treating the effects of slab cracking in negative moment regions and nonlinearities in the shear connector load-slip relationship. The numerical solution technique was checked against closed form solutions and other

numerical solutions and results were compared with selected experimental results. The program was used to prepare a simple design chart to determine deflections of two-span uniformly loaded continuous beams.

8. The solution for deflection due to shear and slip of a two span continuous composite beam with uniform load was recast in terms of the same two dimensionless parameters ξ and η . Plots were developed for beams with uniform and variable moment of inertia.
9. The effects of various design parameters on deflections were examined for particular example problems.
10. The effect of shored and unshored construction on the behavior of three span continuous beams was examined.

7.2 Conclusions

On the basis of this investigation, the following conclusions are drawn:

1. There is good agreement between the results of the numerical solution and the classical solution for deflection and slip for simply supported and continuous composite beams. However, there is a significant difference in the slip strain at the concentrated load locations in the case of continuous beams.

2. The results for deflection and maximum slip using the technique developed herein are in good agreement with Yam and Chapman's results, except for the distribution of slip along the length of the beam, which may be due to the error in the assumed data.
3. The results of the numerical solution are in good agreement with the test results of Chapman and Balakrishnan in the study of linear load-slip behavior. However, the numerical solution results in higher deflection values than test results for nonlinear load-slip behavior. On the basis of the end slip characteristics, the load-slip behavior is linear. The results obtained with the conditions of full shear connection and non-linear load slip behavior underestimates the deflection, whereas the condition of partial shear connection overestimates the deflections obtained by Hamada and Longworth (9) at maximum service load, even though Hamada and Longworth's beam was designed for full shear connection. The discrepancy in the deflection may be due to the assumed connector stiffness.
4. Deflection due to slip, in the case of simply supported beams subjected to uniformly distributed load, may be as high as 45% of the bending deflection, depending on the stiffness of the connector and geometry of the beam. Deflections due to shear and

slip can be computed for practical design purposes using the table of shear form factors as well as the plot developed in terms of dimensionless parameters ξ and η . Partial shear connection increases the slip and reduces the effective stiffness of the beam, thus increasing the deflection. Therefore the effect of shear, slip, and partial shear connection on deflections should not be neglected in design.

5. Using the plot in Fig. 6.8, the total deflection due to shear and slip can be computed for a two span continuous beam with uniform load. Total deflection can be as high as three times the bending deflection, depending on stiffness of shear connector and beam geometry. The effects of the various parameters on deflection and slip of continuous beams are similar to those for simply supported beams. However, increases in deflection and slip tend to be much higher.
6. Concrete cracking in negative moment regions produces increased deflection and slip in positive moment regions. The increase in deflection may be as high as 15% of the deflection of composite beams with uniform moment of inertia. Cracking also creates discontinuities in the slip-strain relationship.

7. Unshored construction results in increase in deflection, decrease in slip in both positive and negative moment regions, decrease in slip strain as well as in introducing discontinuities in the slip-strain relationship and decrease of slab force in both positive and negative moment region.

BIBLIOGRAPHY

- (1) British Standard Institution, "CP117: Part 1: British Standard Code of Practice, Composite Construction in Structural Steel and Concrete Part 1: Simply Supported Beams in Buildings", London, 1965.
- (2) Canadian Standard Association, "CSA Standard S16-1969 Steel Structures for Buildings", Ontario, Canada, 1969.
- (3) Canadian Standard Association, "CSA Standard S16.1 1974 Steel Structures for Buildings - Limit State Design", Ontario, Canada, 1974.
- (4) Chapman, J. C., "Composite Construction in Steel and Concrete - The Behaviour of Composite Beams", *The Structural Engineer*, Vol. 42, No. 4, April, 1964.
- (5) Chapman, J. C., and Balakrishnan, S., "Experiment on Composite Beams", *The Structural Engineer*, Vol. 42, No. 11, November, 1964.
- (6) Davison, J. H., "Ultimate Strength in Negative Bending", Masters Thesis, Department of Civil Engineering, University of Alberta, Edmonton, February, 1970.
- (7) Gerald, C. F., "Applied Numerical Analysis", Addison Wesley Publishing Company, 1978.
- (8) Ghali, A., and Neville, A. M., "Structural Analysis - A Unified Classical and Matrix Approach", Second Edition, Chapman and Hall, London, 1978.
- (9) Hamada, S., and Longworth, J., "Ultimate Strength of Continuous Composite Beams", *Structural Engineering Report No. 45*, Department of Civil Engineering, University of Alberta, Edmonton, August, 1973.
- (10) Hawkins, N. M., "Strength of Shear Connectors", *Proceedings of Institution of Civil Engineers*, Vol. 15, No. 1-2, August, 1973.

- (11) Johnson, R. P., and May, I.M., "Partial Interaction Design of Composite Beams", The Structural Engineer, Vol. 53, No. 8, August, 1975.
- (12) Johnson, R. P., Van Dalen, K., and Kemp, A. R., "Ultimate Strength of Continuous Composite Beams", Technical Report No. 3/7, Cambridge University Engineering Department, May, 1966.
- (13) Ketter, R. L., and Prawel, S. P., "Modern Methods of Engineering Computation", McGraw-Hill Book Company, Inc., New York, 1969.
- (14) Lever, G. V., "Ultimate Strength of Composite Beams in Negative Bending", Masters Thesis, Department of Civil Engineering, University of Alberta, Edmonton, February, 1970.
- (15) Mainstone, R. J., and Menzies, J. B., "Shear Connectors in Composite Beams for Bridges", Concrete, September, 1967.
- (16) Mallick, S. K., and Chattopadhyay, S. K., "Behavior of Continuous Steel - Concrete Composite Beams", Indian Concrete Journal, Vol. 49, No. 6, June, 1975.
- (17) Newmark, N. M., Siess, C.P., and Viest, I.M., "Test and Analysis of Composite Beams with Incomplete Interaction," Proceedings of Societ of Experimental Stress Analysis, Vol. 9, No. 1, 1951.
- (18) Park, R., and Pauley, T., "Reinforced Concrete Structures", John Wiley & Sons, Toronto, 1975.
- (19) Plum, D. R., and Horne, M. R., "The Analysis of Continuous Composite Beams with Partial Interaction", Proceedings of the Institution of Civil Engineers, London, Vol. 59, Part 2, December 1975.
- (20) Piegrass, E. G., "Behaviour of Composite Beams in Negative Bending", Masters Thesis, Department of Civil Engineering, University of Alberta, June, 1968.
- (21) Siess, C. P., "Composite construction for I Beam Bridges", Transaction of American Society of Civil Engineers, Vol. 114, 1949.

- (22) Slutter, R. G., and Driscoll, G. J. Jr., "Flexural Strength of Steel Concrete Composite Beams", Journal of the Structural Division, ASCE, Vol. 81, ST2, April, 1965.
- (23) Timoshenko, S., and Gere, J. M. "Mechanics of Materials", Van Nostarand Reinhold, Toronto, 1972.
- (24) Van Dalen, K., "Composite Action at the Support of Continuous Beams", Ph. D. Thesis, University of Cambridge, June, 1967.
- (25) Viest, I. M., "Review of Research on Composite Steel - Concrete Beams", Proceedings of American Society of Civil Engineers, Structural Division, Vol. 86, ST6, June, 1960.
- (26) Viest, I. M., "Investigation of Stud Shear Connectors for Composite Concrete and Steel Beams", Proceedings of American Concrete Institute, Vol. 52, 1956.
- (27) Viest, I. M., Fountain, R. S., and Singleton, R. C., "Composite Construction in Steel and Concrete for Bridges and Buildings", McGraw-Hill Book Company, Inc., Toronto, 1958.
- (28) Wang, Chu-Kia, and Salmon, C. G., "Reinforced Concrete Design", 2nd Edition, Intex Educational Publisher, New York, 1973.
- (29) Wastlund, G. and Ostlund, L., "Studies of Composite Beams", International Association of Bridge and Structural Engineers, 4th Congress, London, 1952.
- (30) Yam, L.C.P., and Chapman, J. C., "The Inelastic Behavior of Simply Supported Composite Beams of Steel and Concrete", Proceedings of Institution of Civil Engineers, London, Vol. 42, December, 1968.
- (31) Yam, L.C.P. and Chapman, J. C., "The Inelastic Behavior of Continuous Composite Beams of Steel and Concrete", Proceedings of Institution of Civil Engineers, London, Vol. 53, December, 1972.

APPENDIX A

CLOSED FORM SOLUTION (TWO-SPAN CONTINUOUS BEAM)

A.1 Classical Solution

Figure A1 illustrates a continuous beam with two unequal spans and with equal concentrated loads at the center of each span. The deflection equation may be expressed as

$$\frac{d^4 u}{dx^4} - k \frac{d^2 u}{dx^2} = -\frac{w}{\Sigma EI} - \frac{M}{EA \Sigma EI} \quad (A1)$$

where u = deflection

$$k = \frac{(\Sigma EI + EAz^2)}{EA \Sigma EI}$$

$\mu = K$ = shear connector modulus

M = bending moment

w = uniform load

W = concentrated load

$$\Sigma EI = E_1 I_1 + E_2 I_2$$

$$\frac{1}{EA} = \frac{E_1 A_1 + E_2 A_2}{E_1 A_1 E_2 A_2}$$

where E_1 and E_2 are moduli of elasticity of concrete and steel, respectively; A_1 and A_2 are areas of concrete slab and steel section, respectively; and I_1 and I_2 are moments of inertia of concrete slab and steel section, respectively.

The geometry of the beam is as shown in Fig. A1. The equations for moment for the four segments of the beam are as follows:

$$M_1(x) = \left(\frac{W}{2} - \frac{M_0}{L_1} \right) x \quad 0 < x < \frac{L_1}{2} \quad (A2)$$

$$M_2(x) = \frac{WL_1}{2} - \left(\frac{W}{2} + \frac{M_0}{L_1} \right) x \quad \frac{L_1}{2} < x < L_1 \quad (A3)$$

$$M_3(y) = \frac{WL_2}{2} - \left(\frac{W}{2} - \frac{M_0}{L_2} \right) y \quad 0 < y < \frac{L_2}{2} \quad (A4)$$

$$M_4(y) = \frac{WL_2}{2} - \left(\frac{W}{2} + \frac{M_0}{L_2} \right) y \quad \frac{L_2}{2} < y < L_2 \quad (A5)$$

where M_0 is the redundant moment at the interior support.

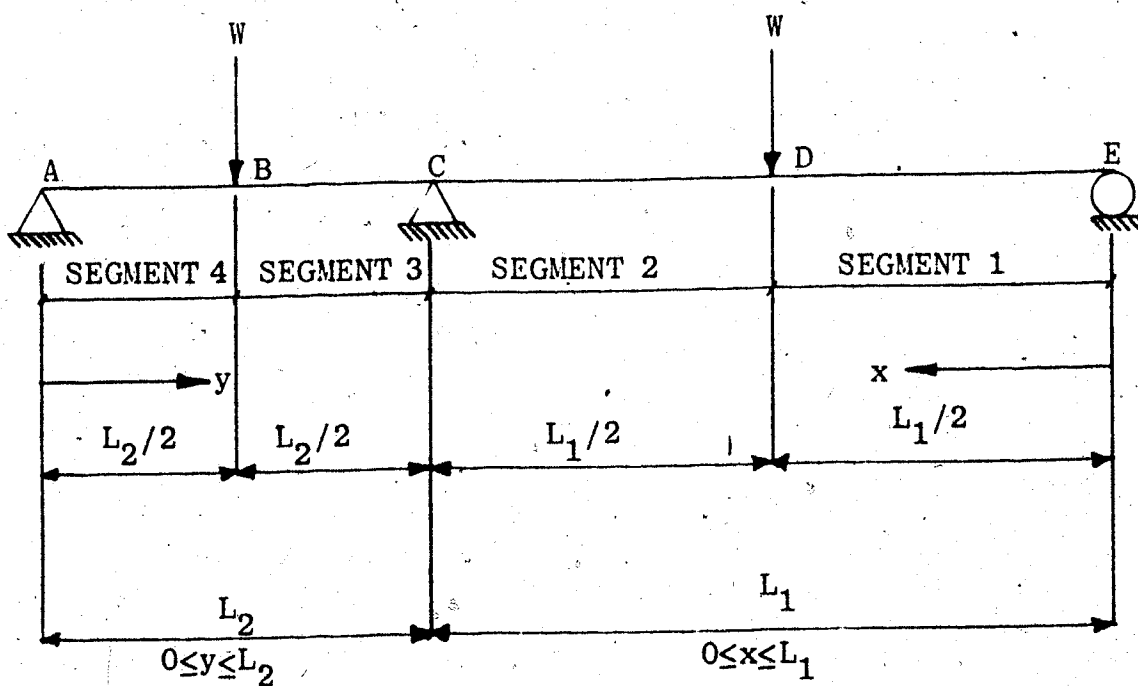


FIGURE A1. TWO-SPAN CONTINUOUS COMPOSITE BEAM

Equation A1 may be solved in each of the four segments of the beam as follows:

SEGMENT 1 $0 < x < \frac{L_1}{2}$

Homogeneous Solution:

$$u_h = C_1 + C_2 x + C_3 \sinh \sqrt{kx} + C_4 \cosh \sqrt{kx} \quad (A6)$$

Particular Solution:

$$u_p = \frac{x^3}{6EI} \frac{W}{2} - \frac{Mo}{L_1} \quad (A7)$$

Complete Solution:

$$u(x) = C_1 + C_2 x + C_3 \sinh \sqrt{kx} + C_4 \cosh \sqrt{kx} + \frac{x^3}{6EI} \frac{W}{2} - \frac{Mo}{L_1} \quad (A8)$$

SEGMENT 2 $\frac{L_1}{2} < x < L_1$

Homogeneous Solution:

$$u_h = C_5 + C_6 x + C_7 \sinh \sqrt{kx} + C_8 \cosh \sqrt{kx} \quad (A9)$$

Particular Solution:

$$u_p = \frac{WL_1 x^2}{4EI} - \frac{x^3}{6EI} \left(\frac{W}{2} - \frac{Mo}{L_1} \right) \quad (A10)$$

Complete Solution:

$$u(x) = C_5 + C_6 x + C_7 \sinh \sqrt{kx} + C_8 \cosh \sqrt{kx} + \frac{WL_1 x^2}{4EI} - \frac{x^3}{6EI} \left(\frac{W}{2} + \frac{Mo}{L_1} \right) \quad (A11)$$

Similarly by symmetry:

SEGMENT 3 $0 < y < \frac{L_2}{2}$

$$u(y) = C_9 + C_{10} y + C_{11} \sinh \sqrt{ky} + C_{12} \cosh \sqrt{ky} + \frac{y^3}{6EI} \left(\frac{W}{2} - \frac{Mo}{L_2} \right) \quad (A12)$$

SEGMENT 4

$$u(y) = C_{13} + C_{14}y + C_{15} \sinh \sqrt{ky} + C_{16} \cosh \sqrt{ky} \\ + \frac{WL_2 y^2}{4EI} - \frac{y^3}{6EI} \left(\frac{W}{2} + \frac{M_0}{L_2} \right) \quad (A13)$$

where C_i $i = 1, 2, \dots, 16$ are constants of integration for a particular beam, loading condition and geometry.

For any segment of the beam, the equations for force, slip, and slip strain are given by:

$$\text{Force:} \quad p = \frac{\Sigma EI}{z} \frac{d^2 u}{dx^2} - \frac{M}{z} \quad (A14)$$

$$\text{Slip:} \quad s = \frac{1}{\mu} \frac{dP}{dx} \quad (A15)$$

$$\text{Slip strain:} \quad s' = \frac{ds}{dx} \quad (A16)$$

The slope at any point is defined as

$$\theta = \frac{du}{dx} \quad (A17)$$

In order to solve for the 17 unknowns (16 constants of integration and 1 redundant moment), it is necessary to utilize 17 boundary conditions: six related to deflection, five related to force, three related to slip and three related to rotation. These boundary conditions are illustrated in Figure A2. A 17 x 17 matrix was formulated using the above conditions applied to the equations for deflection, force, slip, and rotation. The matrix was

coded in Fortran and solved using the subroutine LINV3F in the subroutine library IMSL.

After the constants of integration and redundant moment were solved, values for moment, deflection, force, slip, and slip strain were computed at 3-inch intervals along the length of the beam.

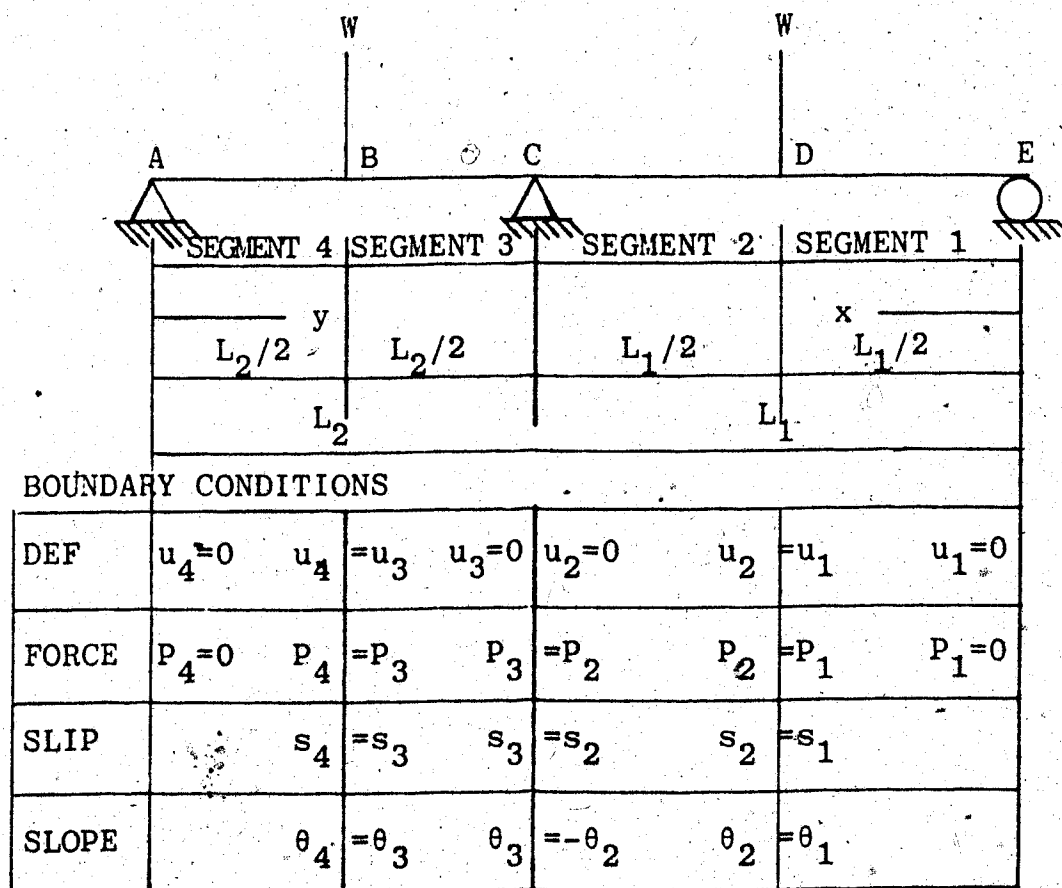


FIGURE A2. BOUNDARY CONDITIONS FOR CONTINUOUS COMPOSITE BEAM

A.2 Summary of Equations

Deflection

In segment 1

$$u_1 = C_1 + C_2x + C_3 \sinh \sqrt{kx} + C_4 \cosh \sqrt{kx} + \frac{x^3}{6EI} \left(\frac{W}{2} - \frac{Mo}{L_1} \right)$$

In segment 2

$$u_2 = C_5 + C_6x + C_7 \sinh \sqrt{kx} + C_8 \cosh \sqrt{kx} + \frac{WL_1x^2}{4EI} \tag{A18}$$

$$- \frac{x^3}{6EI} \left(\frac{W}{2} + \frac{Mo}{L_1} \right) \tag{A19}$$

In segment 3

$$u_3 = C_9 + C_{10}y + C_{11} \sinh \sqrt{ky} + C_{16} \cosh \sqrt{ky} + \frac{y^3}{6EI} \left(\frac{W}{2} - \frac{Mo}{L_2} \right) \tag{A20}$$

In segment 4

$$u_4 = C_{13} + C_{14}y + C_{15} \sinh \sqrt{ky} + C_{16} \cosh \sqrt{ky} + \frac{WL_2y^2}{4EI} - \frac{y^3}{6EI} \left(\frac{W}{2} + \frac{Mo}{L_2} \right) \tag{A21}$$

Slope

In segment 1

$$\theta = C^2 + \sqrt{k}C_3 \cosh \sqrt{kx} + \sqrt{k}C^4 \sinh \sqrt{kx} + \frac{x^2}{2EI} \left(\frac{W}{2} - \frac{Mo}{L_1} \right) \tag{A22}$$

In segment 2

$$\theta_2 = C_6 + \sqrt{k}C_7 \cosh \sqrt{kx} + \sqrt{k}C_8 \sinh \sqrt{kx} + \frac{WL_1 x}{2EI} - \frac{x^2}{2EI} \left(\frac{W}{2} + \frac{Mo}{L_1} \right) \quad (A23)$$

In segment 3

$$\theta_3 = C_{10} + \sqrt{k}C_{11} \cosh \sqrt{ky} + \sqrt{k}C_{12} \sinh \sqrt{ky} + \frac{y^2}{2EI} \left(\frac{W}{2} + \frac{Mo}{L_2} \right) \quad (A24)$$

In segment 4

$$\theta_4 = C_{14} + \sqrt{k}C_{15} \cosh \sqrt{ky} + \sqrt{k}C_{16} \sinh \sqrt{ky} + \frac{WL_2 y}{2EI} - \frac{y^2}{2EI} \left(\frac{W}{2} + \frac{Mo}{L_2} \right) \quad (A25)$$

Force

In segment 1

$$P_1 = \frac{\Sigma EI}{z} \left\{ kC_3 \sinh \sqrt{kx} + \frac{x}{2EI} \left(\frac{W}{2} - \frac{Mo}{L_1} \right) \right\} - \frac{x}{z} \left(\frac{W}{2} - \frac{Mo}{L_1} \right) \quad (A26)$$

In segment 2

$$P_2 = \frac{\Sigma EI}{z} \left\{ kC_7 \sinh \sqrt{kx} + kC_8 \cosh \sqrt{kx} + \frac{WL_1}{2EI} - \frac{x}{EI} \left(\frac{W}{2} + \frac{Mo}{L_1} \right) \right\} - \frac{1}{z} \left(\frac{WL_1}{2} - \left(\frac{W}{2} + \frac{Mo}{L_1} \right) x \right) \quad (A27)$$

In segment 3

$$P_3 = \frac{\Sigma EI}{z} \left\{ kC_{11} \sinh \sqrt{ky} + \frac{y}{EI} \left(\frac{W}{2} + \frac{Mo}{L_2} \right) \right\} - \frac{y}{z} \left(\frac{W}{2} - \frac{Mo}{L_2} \right) \quad (A28)$$

In segment 4

$$P_4 = \frac{\Sigma EI}{z} \left\{ kC_{15} \sinh \sqrt{ky} + kC_{16} \cosh \sqrt{ky} + \frac{WL_2}{2EI} - \frac{y}{EI} \left(\frac{W}{2} + \frac{Mo}{L_2} \right) \right\} - \frac{1}{z} \left\{ \frac{WL_2}{2} - \left(\frac{W}{2} + \frac{Mo}{L_2} \right) y \right\} \quad (A29)$$

Slip

In segment 1

$$s_1 = \frac{\Sigma EI}{z} k^{3/2} C_7 \cosh \sqrt{ky} + k^{3/2} C_4 \sinh \sqrt{kx} + \frac{1}{EI} \frac{W}{2} - \frac{Mo}{L_1} - \frac{1}{\mu z} \left(\frac{W}{2} - \frac{Mo}{L_1} \right) \quad (A30)$$

In segment 2

$$s_2 = \frac{\Sigma EI}{z} \left\{ k^{3/2} C_7 \cosh \sqrt{ky} + k^{3/2} C_8 \sinh \sqrt{kx} - \frac{1}{EI} \frac{W}{2} + \frac{Mo}{L_1} + \frac{1}{\mu z} \left(\frac{W}{2} + \frac{Mo}{L_1} \right) \right\} \quad (A31)$$

In segment 3

$$s_3 = \frac{\Sigma EI}{\mu z} \left\{ k^{3/2} C_{11} \cosh \sqrt{ky} + \frac{1}{EI} \frac{W}{2} - \frac{Mo}{L_2} + k^{3/2} C_{12} \sinh \sqrt{ky} \right\} - \frac{1}{z} \left(\frac{W}{2} + \frac{Mo}{L_2} \right) \quad (A32)$$

In segment 4

$$s_4 = \frac{\Sigma EI}{\mu z} \left\{ k^{3/2} \cosh \sqrt{ky} + k^{3/2} C_{16} \sinh \sqrt{ky} - \frac{1}{EI} \left(\frac{W}{2} + \frac{Mo}{L_2} \right) \right\} + \frac{1}{z} \left(\frac{W}{2} + \frac{Mo}{L_2} \right) \quad (A33)$$

Slip Strain

In segment 1

$$s'_1 = \frac{\Sigma EI}{\mu z} \left\{ k^2 C_3 \sinh \sqrt{kx} + k^2 C_4 \cosh \sqrt{kx} \right\} \quad (A34)$$

In segment 2

$$s'_2 = \frac{\Sigma EI}{\mu z} \left\{ k^2 C_7 \sinh \sqrt{kx} + k^2 C_8 \cosh \sqrt{kx} \right\} \quad (A35)$$

In segment 3

$$s'_3 = \frac{\Sigma EI}{\mu z} \left\{ k^2 C_{11} \sinh \sqrt{ky} + k^2 C_{12} \cosh \sqrt{ky} \right\} \quad (A36)$$

In segment 4

$$s'_4 = \frac{\Sigma EI}{\mu Z} \left\{ k^2 C_{15} \sinh \sqrt{ky} + k^2 C_{16} \cosh \sqrt{ky} \right\} \quad (A37)$$

A.3 Equations Used in Solution of Constants of
Integration and Redundant Moment

$$(1) \quad C_1 + C_4 = 0$$

$$(2) \quad C_9 + C_{12} = 0$$

$$(3) \quad C_1 + \frac{L_1}{2} C_2 + \sinh \frac{\sqrt{KL_1}}{2} C_3 + \cosh \frac{\sqrt{KL_1}}{2} C_4 \\ - L_1/2 C_6 - \sinh \frac{\sqrt{KL_1}}{2} C_7 - \cosh \frac{\sqrt{KL_1}}{2} C_8 \\ = \frac{WL_1^3}{24 EI}$$

$$(4) \quad C_9 + \frac{L_2}{2} C_{10} + \sinh \frac{\sqrt{KL_2}}{2} C_{11} + \cosh \frac{\sqrt{KL_2}}{2} C_{12} \\ - C_{13} - \sinh \frac{\sqrt{KL_2}}{2} C_{15} - \cosh \frac{\sqrt{KL_2}}{2} C_{16} \\ = \frac{WL_1^3}{6EI}$$

$$(5) \quad C_5 + L_1 C_6 + \sinh \sqrt{KL_1} C_7 + \cosh \sqrt{KL_1} C_8 - \frac{L_1^2 M_0}{6EI} \\ = - \frac{WL_1^3}{6EI}$$

$$(6) \quad \Sigma EI k \sinh \frac{\sqrt{KL_1}}{2} C_3 + \cosh \frac{\sqrt{KL_1}}{2} C_4 - \sinh \frac{\sqrt{KL_1}}{2} C_7 \\ - \cosh \frac{\sqrt{KL_2}}{2} C_8 = 0$$

$$(7) \quad \Sigma EI k \sinh \frac{\sqrt{kL_2}}{2} C_{11} + \cosh \frac{\sqrt{kL_2}}{2} C_{12} - \sinh \frac{\sqrt{kL_2}}{2} C_{15} \\ - \cosh \frac{\sqrt{kL_2}}{2} C_{16} = 0$$

$$(8) \quad kC_4 = 0$$

$$(9) \quad kC_{12} = 0$$

$$(10) \quad \Sigma EI k (\sinh \sqrt{kL_1} C_7 + \cosh \sqrt{kL_1} C_8 - \sinh \sqrt{kL_2} C_{15} \\ - \cosh \sqrt{kL_2} C_{16}) = 0$$

$$(11) \quad C_2 + \sqrt{k} \cosh \frac{\sqrt{kL_1}}{2} C_3 + \sqrt{k} \sinh \frac{\sqrt{kL_1}}{2} C_4 \\ - \sqrt{k} \cosh \frac{\sqrt{kL_1}}{2} C_7 - \sqrt{k} C_8 \sinh \frac{\sqrt{kL_1}}{2} = \frac{WL_1^2}{8EI}$$

$$(12) \quad C_{10} + \sqrt{k} C_{11} \cosh \frac{\sqrt{kL_2}}{2} + \sqrt{k} C_{12} \sinh \frac{\sqrt{kL_2}}{2} - C_{14} \\ - \sqrt{k} C_{15} \cosh \frac{\sqrt{kL_2}}{2} - \sqrt{k} C_{16} \sinh \frac{\sqrt{kL_2}}{2} = \frac{WL_2^2}{8EI}$$

$$(13) \quad C_6 + \sqrt{k} C_7 \cosh \sqrt{kL_1} + \sqrt{k} C_8 \sinh \sqrt{kL_1} C_{14} \\ + \sqrt{k} C_{15} \cosh \sqrt{kL_2} + \sqrt{k} C_{16} \sinh \sqrt{kL_2} - \frac{Mo}{2EI} (L_2 + L_1) \\ = \frac{E}{4EI} (L_2^2 + L_1^2)$$

$$(14) \quad \Sigma EI k^{3/2} \left(C_3 \cosh \frac{\sqrt{kL_1}}{2} + C_4 \sinh \frac{\sqrt{kL_1}}{2} - C_7 \cosh \frac{\sqrt{kL_1}}{2} \right. \\ \left. - C_8 \sinh \frac{\sqrt{kL_1}}{2} \right) = \left(1 - \frac{EI}{EI} \right) W$$

$$(15) \quad \Sigma EI k^{3/2} \left(C_{11} \cosh \frac{\sqrt{kL_2}}{2} + C_{12} \sinh \frac{\sqrt{kL_2}}{2} - C_{15} \cosh \frac{\sqrt{kL_2}}{2} - C_{16} \sinh \frac{\sqrt{kL_2}}{2} \right) = w \left(1 - \frac{EI}{EI} \right)$$

$$(16) \quad \Sigma EI k^{3/2} \left(C_7 \cosh \sqrt{kL_1} + C_8 \sinh \sqrt{kL_1} + C_{15} \cosh \sqrt{kL_2} + C_{16} \sinh \sqrt{kL_2} \right) + M_0 \frac{1}{L_1} + \frac{1}{L_2} \left(1 - \frac{EI}{EI} \right) = w \left(\frac{EI}{EI} - 1 \right)$$

$$(17) \quad C_{13} + C_{14} L_2 + C_{15} \sinh \sqrt{kL_2} + C_{16} \cosh \sqrt{kL_2}$$

$$- M_0 \frac{L_2^2}{6EI} = - \frac{w L_2^3}{6EI}$$

A.4 Constants Used in Closed Form Solution

Loading: $V = 22.5$ kips

$w = 0.0$ kips/in.

Lengths: $L_1 = 180$ in.

$L_2 = 120$ in.

Shear Connector Modulus: $\mu = K = 150$ kips/in.²

Beam Section Properties:

$E_1 = 3000.0$ ksi (transformed)

$E_2 = 30,000.0$ ksi

$I_1 = 32.0$ in.⁴

$I_2 = 278.28$ in.⁴

$A_1 = 24.0$ in.²

$A_2 = 10.499$ in.²

$z = 8.12$ in.

Therefore $\Sigma EI = 9312870.0$ kips-in.²

$\overline{EI} = 23760159.0$ kips-in.²

$\overline{EA} = 219115.9$ kips

$k = 0.0017465$

Appendix B

LINEAR CLOSED FORM SOLUTION FOR A SIMPLY
SUPPORTED BEAM WITH CONCENTRATED LOAD AT CENTER

B.1 Classical Solution

Figure B1 illustrates beam geometry, loading pattern and boundary conditions. The governing equation for slip is Equation 3.23,

$$s'' - \alpha^2 s = -\beta V \quad (\text{Ba})$$

The homogeneous solution for this equation is

$$S_h = A \sinh \alpha x + B \cosh \alpha x \quad (\text{B2})$$

and the particular solution for the concentrated load at the center

$$S_p = -\frac{\beta}{\alpha^2} V(x) \quad (\text{B3})$$

As the load is at the center of the span

$$V(x) = \frac{P}{2} \quad (\text{B4})$$

Therefore the general equation for slip can be expressed as

$$s = A \sinh \alpha x + B \cosh \alpha x + \frac{\beta P}{2\alpha^2} \quad (\text{B5})$$

The boundary conditions relating to slip and slip strain are

$$\text{at } x = 0 \quad \frac{ds}{dx} = 0 \quad (\text{B6})$$

$$\text{at } x = L/2 \quad s = 0 \quad (\text{B7})$$

Differentiating Equation B5 results in slip strain as

$$\frac{ds}{dx} = A\alpha \cosh \alpha x + B\alpha \sinh \alpha x \quad (\text{B8})$$

By substituting boundary condition Equation B6 into Equation B8,

$$A = 0 \quad (\text{B9})$$

Substituting boundary condition Equation B7 into Equation B5 gives

$$s_{L/2} = 0 = 0 + B \cosh \alpha L/2 + \frac{\beta P}{2\alpha^2} \quad (\text{B10})$$

Therefore

$$B = -\frac{\beta P}{2\alpha^2} \operatorname{sech} \alpha \frac{L}{2} \quad (\text{B11})$$

By substituting constants into Equation B5

$$s = -\frac{\beta P}{2\alpha^2} \operatorname{sech} \alpha \frac{L}{2} \cosh \alpha x + \frac{\beta P}{2\alpha^2} \quad (\text{B12})$$

or

$$s = \frac{\beta P}{2\alpha^2} (1 - \operatorname{sech} \alpha \frac{L}{2} \cosh \alpha x) \quad (\text{B13})$$

and

$$s' = \frac{\beta P}{2\alpha^2} (-\alpha \operatorname{sech} \alpha \frac{L}{2} \sinh \alpha x) \quad (\text{B14})$$

The deflection may now be determined by integration of Equation B14 and using Equation 3.19(a). Combining these two equations yields

$$-v'' = \frac{A_c Y_c s'}{I_t} + \frac{M}{EI_t} \quad (\text{B15})$$

$$-v'' = \frac{A_c Y_c}{I_t} \frac{\beta P}{2\alpha^2} (-\operatorname{sech} \alpha \frac{L}{2} \sinh \alpha x) + \frac{Px}{2EI_t} \quad (\text{B16})$$

Integrating Equation B16 yields

$$-v' = -\frac{P\beta A_c Y_c}{2I_t \alpha^2} \alpha \frac{\operatorname{sech} \alpha L/2 \cosh \alpha x}{\alpha} + \frac{Px^2}{4EI_t} + C_1 \quad (\text{B17})$$

$$-v = -\frac{P\beta A_c Y_c}{2I_t \alpha^2} \frac{\operatorname{sech} \alpha L/2 \sinh \alpha x}{\alpha} + \frac{Px^3}{12EI_t} + C_1 x + C_2 \quad (\text{B18})$$

The boundary conditions relating the deflection and slope are

$$\text{at } x = 0 \quad v = 0 \quad (\text{B19})$$

$$\text{at } x = L/2 \quad v' = 0 \quad (\text{B20})$$

By substituting Equation B20 into Equation B17 yields

$$0 = -\frac{P\beta A_c Y_c}{2I_t \alpha^2} \operatorname{sech} \alpha \frac{L}{2} \cosh \alpha \frac{L}{2} + \frac{PL^2}{16EI_t} + C_1 \quad (\text{B21})$$

Therefore

$$C_1 = \frac{P\beta A_c Y_c}{2I_t \alpha^2} - \frac{PL^2}{16EI_t} \quad (\text{B22})$$

Substituting Equation B19 into Equation B18 yields

$$C_2 = 0 \quad (\text{B23})$$

Substituting Equation B18 yields

$$-v = -\frac{P\beta A_c Y_c}{2I_t \alpha^3} \left(\operatorname{sech} \alpha \frac{L}{2} \sinh \alpha x \right) + \frac{Px^3}{12EI_t} + \frac{P\beta A_c Y_c}{2I_t \alpha^2} x - \frac{PL^2}{16EI_t} x \quad (\text{B24})$$

Equations B13, B14 and B24 give the solution for slip, slip strain and deflection of a simply supported beam subjected to a concentrated load at midspan. At $x = L/2$ Equation B24

yields the maximum deflection in the span as

$$v_{L/2} = \frac{PL^3}{48EI_t} + \frac{P\beta A_c Y_c}{2I_t \alpha^3} \tanh \alpha \frac{L}{2} - \frac{P\beta A_c Y_c}{4I_t \alpha^2} \quad (B25)$$

or

$$v_{L/2} = \frac{PL^3}{48EI_t} + \frac{P\beta A_c Y_c}{2I_t \alpha^3} \left(\tanh \alpha \frac{L}{2} - \alpha \frac{L}{2} \right) \quad (B26)$$

Recognizing that the first term is the deflection of a beam with complete interaction Equation B26 may be written

as

$$\frac{\delta_f}{\delta_o} = 1 + \frac{24\beta EA_c Y_c}{L^3 \alpha^3} \left(\tanh \alpha \frac{L}{2} - \frac{\alpha L}{2} \right) \quad (B27)$$

Recalling the definition of α and β from Equations 3.21 and 3.22, Equation B27 may be written in terms of two nondimensional ratios as

$$\frac{\delta_f}{\delta_o} = 1 + \frac{24\xi}{(\xi\eta)^{3/2}} \left(\tanh \frac{\sqrt{\xi\eta}}{2} - \frac{\sqrt{\xi\eta}}{2} \right) \quad (B28)$$

or

$$\frac{\delta_f}{\delta_o} = 1 + \frac{24}{\xi^{1/2} \eta^{3/2}} \left(\tanh \frac{\sqrt{\xi\eta}}{2} - \frac{\sqrt{\xi\eta}}{2} \right) \quad (B29)$$

The definition of ξ and η are given in Equations 6.4 and 6.5, respectively.

B.2 Evaluation of Shear Deflections for a Simply Supported Composite Beam Subjected to a Concentrated Load at the Center

The shear strain in a beam may be expressed as

$$\gamma = v'_s(x) = \frac{K_{sh} V}{GA_t} \quad (B30)$$

in which v_s is the shear deflection and

$$K_{sh} = \frac{A}{I_t} \int_A \frac{Q^2}{b^2} dA \quad (B31)$$

is a property of the cross section. For a simply supported beam subjected to concentrated load at midspan,

$$\delta_s = \int_0^{L/2} v'_s(x) dx = \frac{K_{sh}}{GA_t} \int_0^{L/2} V dx \quad (B32)$$

Shear deflection can therefore be evaluated provided K_{sh} is known.

The integral on the right hand side of the equation is the moment at midspan. The ratio of shear deflection to bending deflection can be expressed as

$$\frac{\delta_s}{\delta_o} = \frac{K_{sh}}{GA_t} \frac{PL}{4} \times \frac{48EI_t}{PL^3} \quad (B33)$$

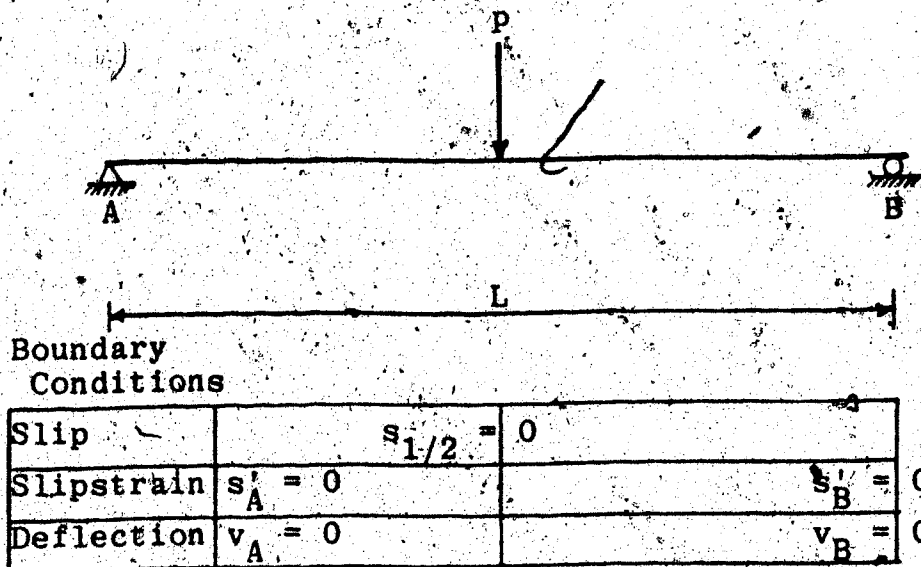
or

$$\frac{\delta_s}{\delta_o} = 12 K_{sh} \frac{E}{G} \frac{I_t}{A_t L^2}$$

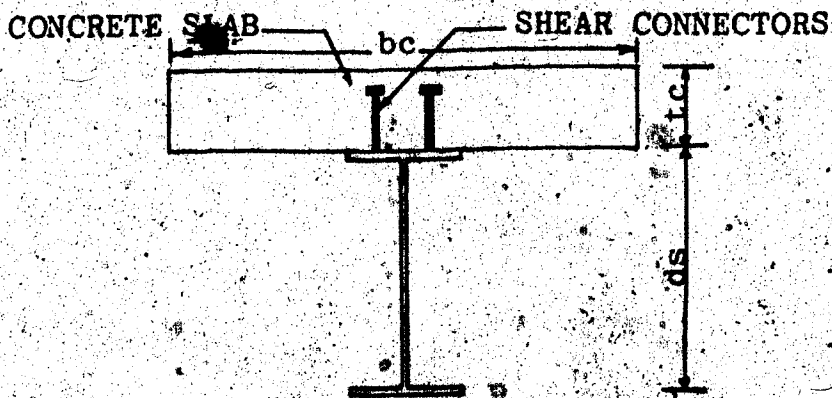
By adding Equations B30 and B34,

$$\frac{\delta}{L} + \frac{\delta_s}{L} = \frac{\delta_o + \delta_{sl} + \delta_s}{L} \quad (B35)$$

Equation B35 is the ratio of total deflection to bending deflection of a simply supported composite beam subjected to concentrated load at midspan.



(a) BOUNDARY CONDITIONS



(b) SECTION

FIGURE B.1 BEAM GEOMETRY AND BOUNDARY CONDITIONS

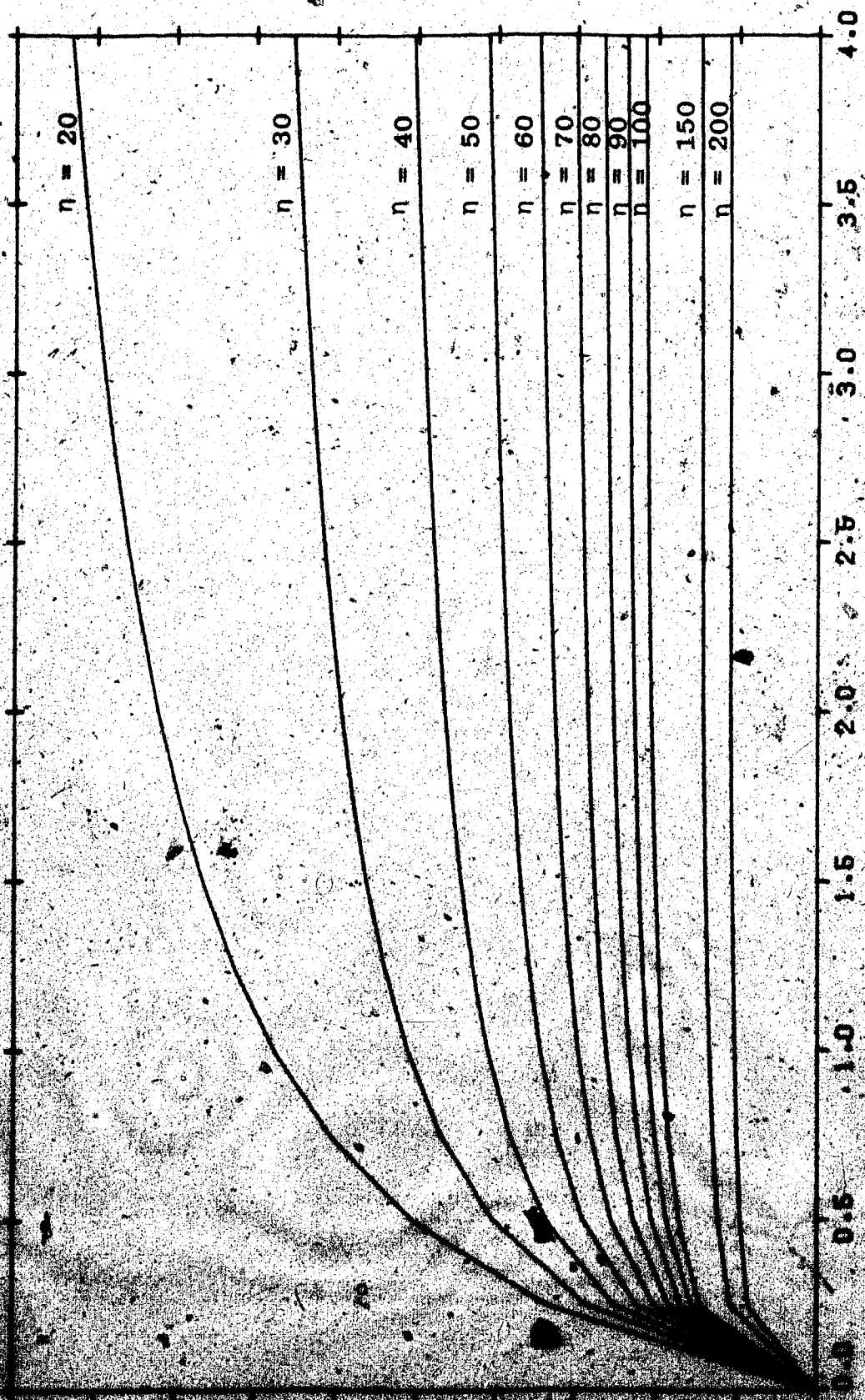


FIGURE B.2 DEFLECTION RATIO (δ_f/δ_0) VS ϵ FOR A SIMPLY SUPPORTED BEAM WITH A CONCENTRATED LOAD AT CENTER

APPENDIX C

EVALUATION OF SERVICE LOADS OF COMPOSITE BEAMS FOR TEST PROBLEMS

C.1 Introduction

Most experimental research in the behavior of composite beams is concerned with ultimate loading conditions. However, this present study is concerned with behavior under service load conditions. The following procedure is followed to evaluate service loads for experimental beams so that results from this analysis can be compared with test results reported by other researchers.

Under service load conditions the behavior of composite beams is governed by the geometry of the composite section and stiffness. Under ultimate load, however, the behavior is a function of geometry of composite section and material strength, that is, yield strength of steel and ultimate strength of concrete and shear connectors.

In Chapter V the experimental results obtained by Chapman and Balakrishnan, and Hamada and Longworth are compared with analytical results obtained from this study under service load. The properties of these beams used in the numerical analysis are computed in this Appendix.

C.2 Simply Supported Beam with Concentrated Load
at Center (Chapman & Balakrishnan)

Figure C1 illustrates the beam and its cross section.

Beam Geometry:

Length = $L = 18.0$ ft.

Width of slab = $b_c = 48.0$ in.

Thickness of slab = $t_c = 6.00$ in.

Steel section BSB12 x 6 x 44#

Depth of steel beam = $d_s = 12.0$ in.

Area of steel beam = $A_s = 13.0$ sq. in.

Area of web = $A_w = 4226$ sq. in.

Thickness of flange = $t_f = 0.717$ in.

Shear Connectors:

Size of shear connector = $3/4" \times 4"$

Spacing of shear connector = 14.88 in.

Total number of shear connectors = $N = 32$

Material Properties:

Yield strength of flange = $f_{yr} = 34.832$ ksi

Yield strength of web = $f_{yw} = 38.8192$ ksi

Elastic modulus of steel = $E_c = 31.6 \times 10^5$ ksi

Concrete strength (28 day cylinder) = $f'_c = 3440$ psi

Ultimate load capacity of connector = $q_r = 28$ kips

Ultimate capacity of concrete slab = $C = 0.85 f'_c b c$

$$= 0.85 \times 3.44 \times 48.0 \times 6.0 = 842.11 \text{ kips}$$

Total capacity of shear connector = $Q_u = Nqr/2$

$$= 28.0 \times 16.0 = 448.0 \text{ kips}$$

Ultimate capacity of steel section = $T = A_s f_y$

$$= A_s f_y + A_w f_w = 469.67 \text{ kips}$$

Therefore $T > Q_u$

$$T < C$$

$$C > Q_u$$

As the connector capacity is less than ultimate force that can be developed by the steel section or the concrete slab, and concrete slab strength is greater than the force that can be developed by steel section, the governing criteria in determining the location of the neutral axis at load is Q_u . Therefore it can be concluded that there is partial shear connection in this case. To achieve full shear connection the connectors must be designed to transfer the ultimate force that can be developed by the steel section. The degree of shear connection for this beam is

Partial shear connection (P.S.C.) = $\frac{Q_u}{T}$

$$= \frac{448.00}{469.67} \times 100 = 95.38$$

Due to this partial shear connection, the force Q_u can be developed in the steel section and tensile force must be equal to compressive force.

Force that can be developed by bottom flange

$$F_1 = A_f \times f_{yf} = 4.34832 \times 34.832 = 151.46 \text{ kips}$$

Force that can be developed by web

$$F_2 = A_w \times f_{yw} = 4.2264 \times 38.8192 = 164.06 \text{ kips}$$

The amount of force that should be developed in top flange to utilize the capacity of shear connection

$$F_3 = Q_u - F_1 - F_2 = 448.0 - 151.46 - 164.06 = 132.48 \text{ kips}$$

Depth of top flange below ultimate strength neutral axis

$$d_1 = 132.48 / 6.1183 \times 34.832 = 0.62164 \text{ in.}$$

Depth of top flange above ultimate strength neutral axis under compression

$$d_2 = 0.717 - 0.62164 = 0.9536 \text{ in.}$$

Compressive force that can be developed in this portion of top flange

$$F_4 = 0.09536 \times 6.1183 \times 34.832 = 20.322 \text{ kips}$$

The magnitude of compressive force that must be developed in the concrete slab for equilibrium

$$F_5 = Q_u - F_4 = 448.0 - 20.322 = 427.678 \text{ kips}$$

The depth of stress block in the concrete slab under compression

$$a = 427.678 / 0.85 f'_c b_c = 3.0472 \text{ in.}$$

Therefore location of ultimate strength neutral axis

$$CG = (t_f + d_w + d_1) = 11.905 \text{ in.}$$

The moment (neglecting strain hardening) that can be developed in the composite section before the failure of the shear connection

$$\begin{aligned} M_p &= F_1(CG - t_f/2) + F_2(CG - t_f - d_w/2) + F_3 d_1/2 \\ &\quad + F_4 d_2/3 + F_5(t + d_2 - a/2) \\ &= 4715 \text{ in. kips} = 393 \text{ ft. kips} \end{aligned}$$

M_p = Moment due to self wt + Moment due to applied load

$$\text{Self wt} = 44 + \frac{6 \times 48 \times 150}{144} = 344 \text{ lbs.}$$

Load factor for dead load = 1.25

Load factor for applied load = 1.5

$$M_p = \frac{1.25 \times 0.344 \times (118)^2}{8} + \frac{1.5P \times 18}{4}$$

$$P_u = (393.0 - 17.415) \times \frac{4}{18} = 83.463 \text{ kips}$$

$$P_{(\text{service})} = \frac{83.463}{1.5} = 55.65 \text{ kips}$$

The ultimate load given by Chapman and Balakrishnan

$$P_u = 96.95 \text{ kips and the load factor} = 1.75$$

$$P_{(\text{service})} = \frac{96.95}{1.75} = 55.4 \text{ kips}$$

Therefore it is evident that service load obtained by the above procedure is accurate to the degree required.

Figures E1 to E3 illustrate the beam geometry and the loading condition.

C.3. Two-Span Continuous Composite Beam Subjected to Equal Concentrated Loads at the Center of Each Span (Hamada & Longworth)

Figures C2 and C3 illustrate the section and beam geometry of the test specimen and Figure C4 illustrates the idealized stress condition at ultimate moment in positive moment region. Figures C5 and C8 illustrate the stress condition in the negative moment region.

Beam Geometry:

Length = $L = 12.0$ ft.

Width of slab = $bc = 48.0$ in.

Thickness of slab = $tc = 4.00$ in.

Steel section = W12 x 31

Depth of steel section = $ds = 12.09$ in.

Depth of web = $d_w = 11.16$ in.

Width of web = $w_w = 0.265$ in.

Area of web = $A_w = 2.9574$ sq. in.

Area of flange = $A_f = 3.0863$ sq. in.

Thickness of flange = $t_f = 0.465$ in.

Width of flange = $b_f = 6.6372$ in.

Total area of steel section = $A_s = 9.13$ sq. in.

Area of reinforcement in negative moment region

= $A_{sr} = 1.6$ sq. in.

Shear Connectors:

Size of connector $3/4'' \times 3''$

Number of connectors between zero and maximum
moment = $N = 16$

Capacity of a connector = $q_r = 28.716$ kips

Material Property:

Yield strength of flange = $F_{yt} = 40.5$ ksi

Yield strength of web = $F_{yf} = 46.9$ ksi

Elastic modulus of steel = $E_s = 30.550 \times 10^3$ ksi

Ultimate strength of concrete = $f'_c = 5577$ psi

Elastic modulus of concrete = $E_c = 4.527 \times 10^3$ ksi

Yield strength of reinforcing steel = $F_{ys} = 50.3$ ksi

In positive moment region:

Ultimate strength of slab is

$$C = 0.85 f'_c b c t c = 910.1664 \text{ kips}$$

The ultimate strength of steel section is

$$T = A_s f_y = A_{sf} f_{yf} + A_{sw} f_{yw} = 387.51 \text{ kips}$$

The ultimate capacity of shear connectors

$$Q_u = N \cdot q_r = 16 \times 28.716 = 459.456 \text{ kips}$$

Therefore $Q_u > T$

$$T < C$$

$$C > Q_u$$

As Q_u T and C T full shear connection can be achieved. As the concrete slab ultimate strength is greater than ultimate capacity of the steel section, the ultimate strength neutral axis will be in the concrete slab. The depth of the stress block in the concrete slab under compression is

$$a = \frac{T}{0.85 f'_c bc} = 2.0192 \text{ in.}$$

Therefore

$$CG = ds + t_c - a = 14.0708 \text{ in. from the bottom flange}$$

The ultimate moment that can be developed by the composite section in the positive moment region is

$$\begin{aligned} M_{u1} &= T (CG - ds/2 + a/2) = 3501.3078 \text{ in. kips} \\ &= 291.775 \text{ ft. kips} \end{aligned}$$

In negative moment region:

In the negative moment region as illustrated in Figure C4, the concrete slab is not effective as it is subjected to tension, therefore the moment has to be resisted by the steel section and the reinforcement. From Figure C6 the equilibrium equation can be expressed as

$$CS + T_r = TS$$

but

$$CS + TS = A_s f_y$$

$$T_r = 1.6 \times 50.3 = 80.48 \text{ kips}$$

$$CS + TS = 387.51 \text{ kips}$$

Therefore CS = $(387.51 - 80.48)/2 = 153.26$ kips

$$TS = 387.51 - 153.26 = 234.25 \text{ kips}$$

The bottom flange can develop

$$F_1 = A_f \times f_{yf} = 3.0863 \times 40.5 = 125 \text{ kips}$$

The web below the ultimate strength neutral axis must resist

$$F_2 = 234.25 - 125.0 = 109.25 \text{ kips}$$

The depth of web below ultimate strength neutral axis is

$$d_{w1} = 109.25/46.9 \times .265 = 8.7902 \text{ in.}$$

Therefore

$$CG = 8.7902 + .465 = 9.2552 \text{ in.}$$

The depth of web above the ultimate strength neutral axis is

$$d_{w2} = (11.16 - 8.7902) = 2.3698 \text{ in.}$$

$$\begin{aligned} \text{Area of web above neutral axis} &= 2.3698 \times .265 \\ &= 0.628 \text{ sq. i.n.} \end{aligned}$$

The force that can develop in web is

$$F_3 = 0.628 \times 46.9 = 29.453 \text{ kips}$$

Force that will develop in top flange

$$F_4 = 3.0863 \times 40.5 = 125 \text{ kips}$$

The center of reinforcement is 3 in. from the bottom of the slab, and the force in the reinforcement is

$$F_5 = 80.48 \text{ kips}$$

Therefore the moment that can be resisted by the section in the negative moment region is

$$\begin{aligned} M_{u2} &= F_1 (CG - tf/2) + F_2 (CG - tf - d_w/2) \\ &+ F_3 (D_{w2}/2) + F_4 (d_{w2} + tf/2) \\ &+ F_5 (ds + tc - CG - 1.0) \\ &= 2437.773 \text{ in. kips} = 203.147 \text{ ft. kips} \end{aligned}$$

$$\text{Total } M_p = M_{u1} + \frac{M_{u2}}{2} = 291.766 + \frac{203.147}{2} = 393.35 \text{ ft. kips}$$

$$\text{Moment due to self wt} = \frac{WL^2}{8} = 5.1975 \text{ ft. kips}$$

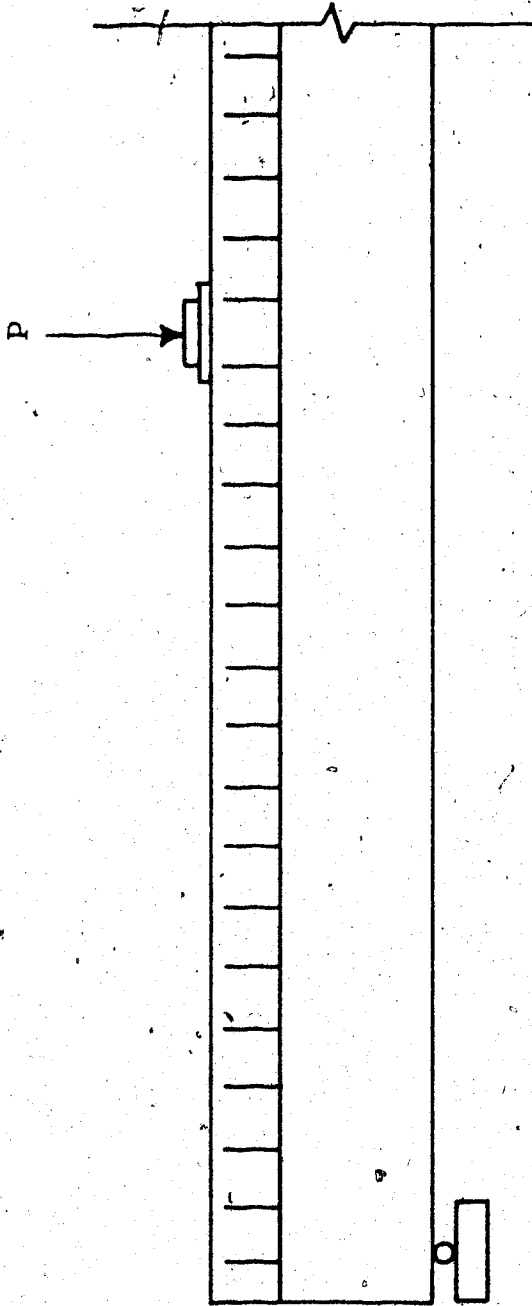
$$\begin{aligned} M_p &= M(\text{due self wt}) + M(\text{due to applied load}) \\ &= \frac{WL^2}{8} + \frac{P_u L}{4} \end{aligned}$$

$$\frac{P_u L}{4} = 393.35 - 5.1975 = 388.1525 \text{ ft. kips}$$

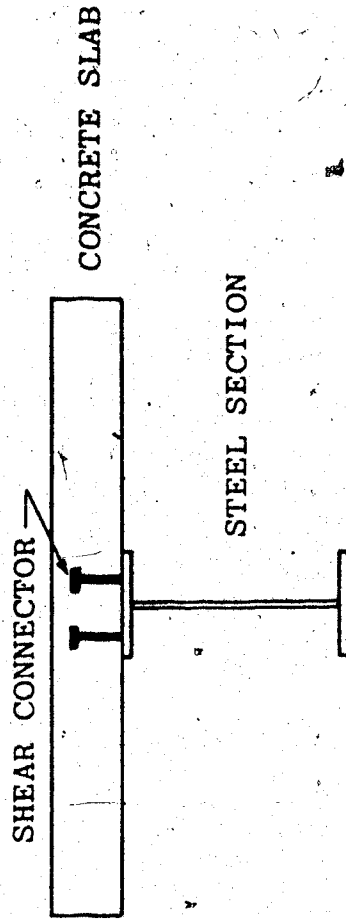
$$P_u = 129.384 \text{ kips}$$

$$\text{Load factor} = 1.5$$

$$\text{Service load } P(\text{service}) = \frac{129.384}{1.5} = 86.256 \text{ kips}$$

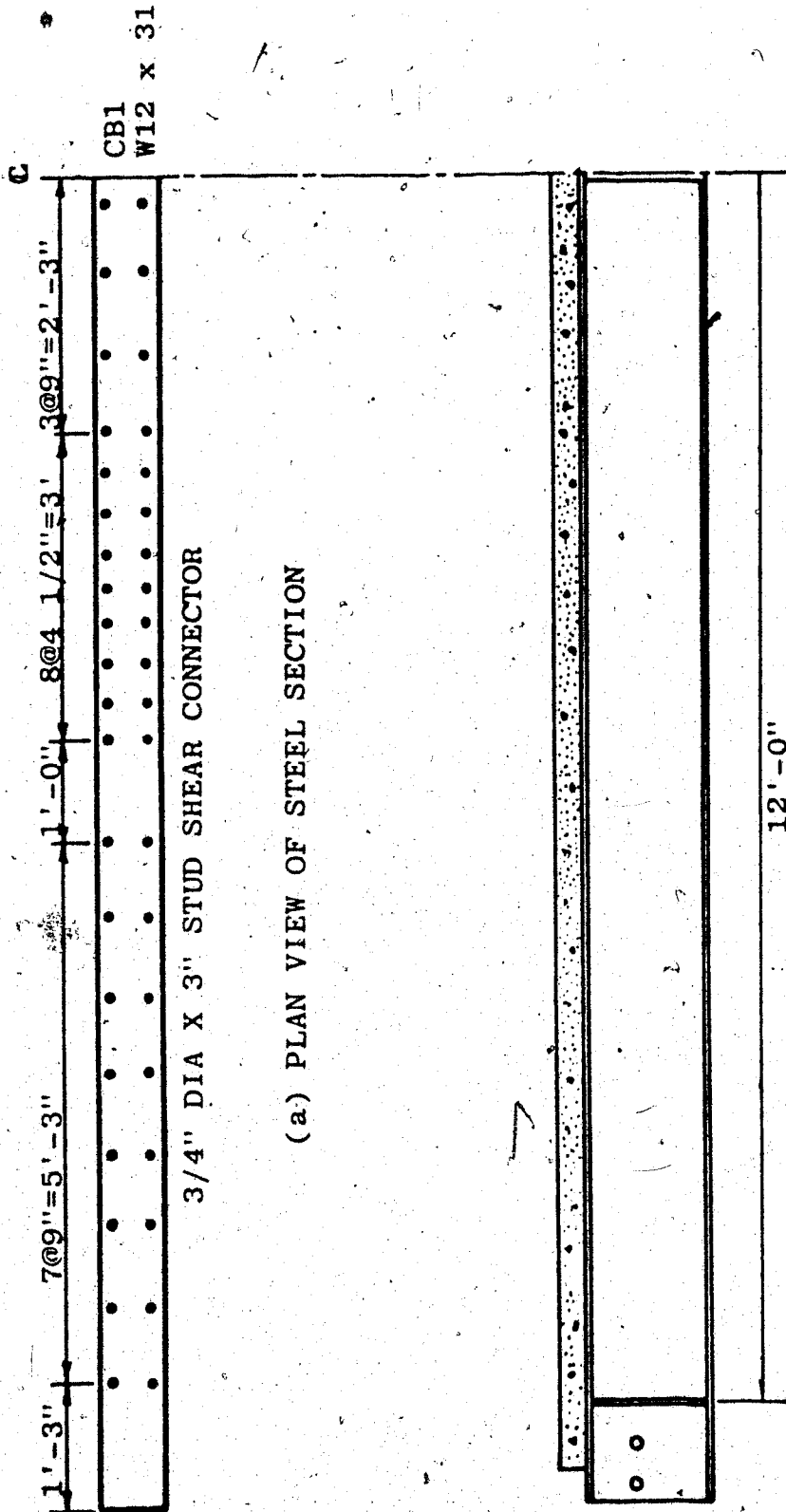


(a) SIDE VIEW



(b) SECTION

FIGURE C1. SIMPLY SUPPORTED COMPOSITE BEAM
SUBJECTED TO CONCENTRATED LOAD AT MIDSPAN
(CHAPMAN & BALAKRISHNAN)



CB1
W12 x 31

3/4" DIA X 3" STUD SHEAR CONNECTOR

(a) PLAN VIEW OF STEEL SECTION

(b) SIDE ELEVATION

FIGURE C2. DETAILS OF TEST SPECIMEN
(HAMADA & LONGWORTH)

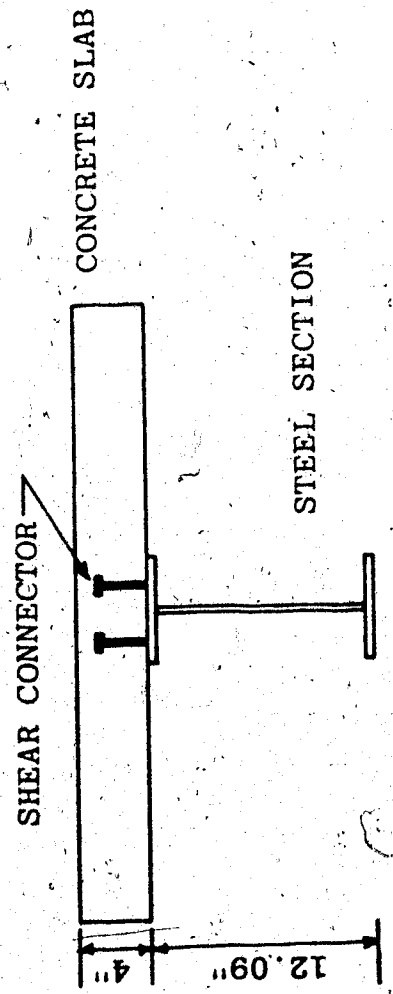
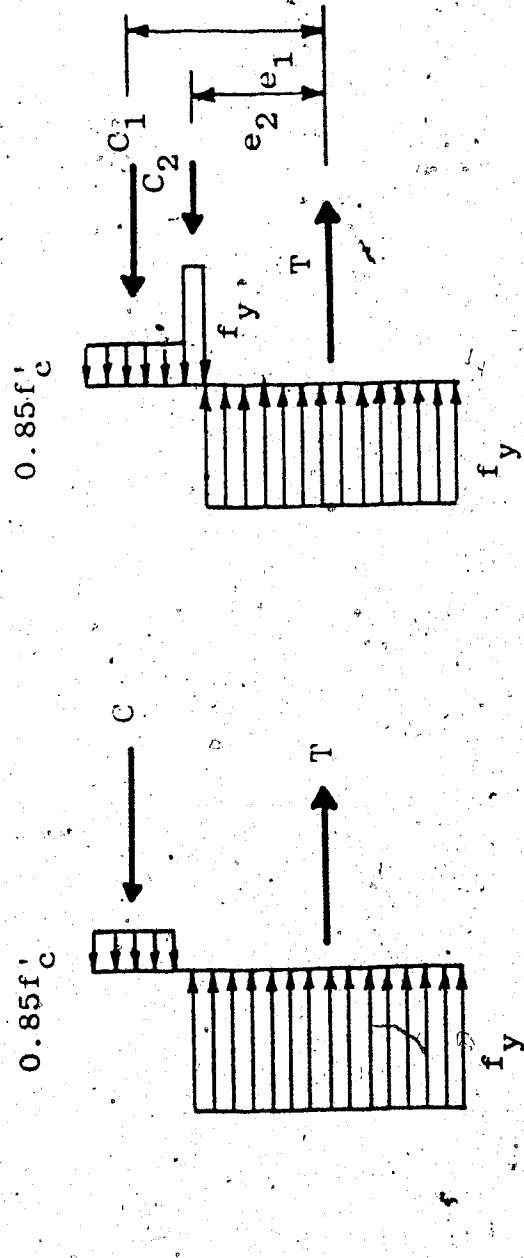
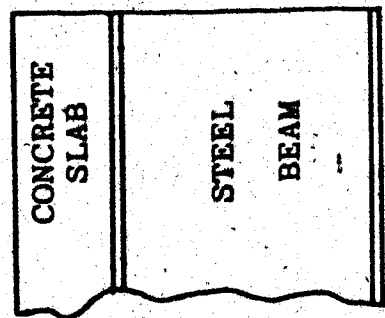


FIGURE C3. SECTION THROUGH TEST BEAM (HAMADA AND LONGWORTH)



(a) NEUTRAL AXIS IN SLAB (b) NEUTRAL AXIS BELOW SLAB

FIGURE C4. IDEALIZED STRESS CONDITIONS AT ULTIMATE MOMENT IN POSITIVE BENDING



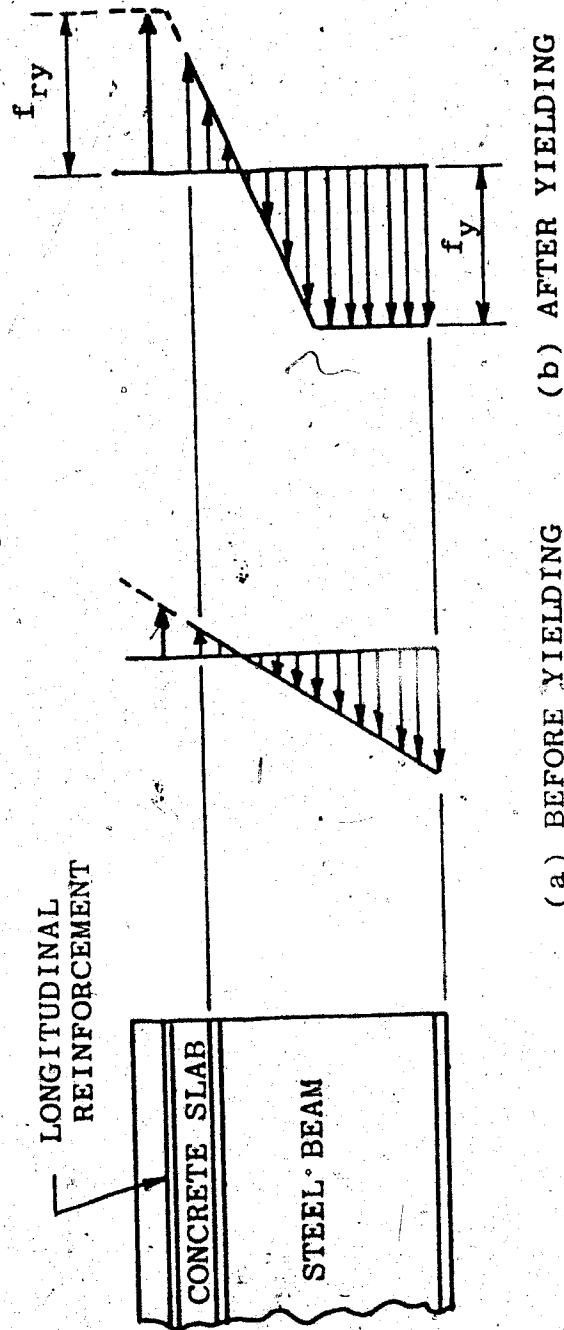


FIGURE C5. STRESS DISTRIBUTION IN A NEGATIVE MOMENT REGION

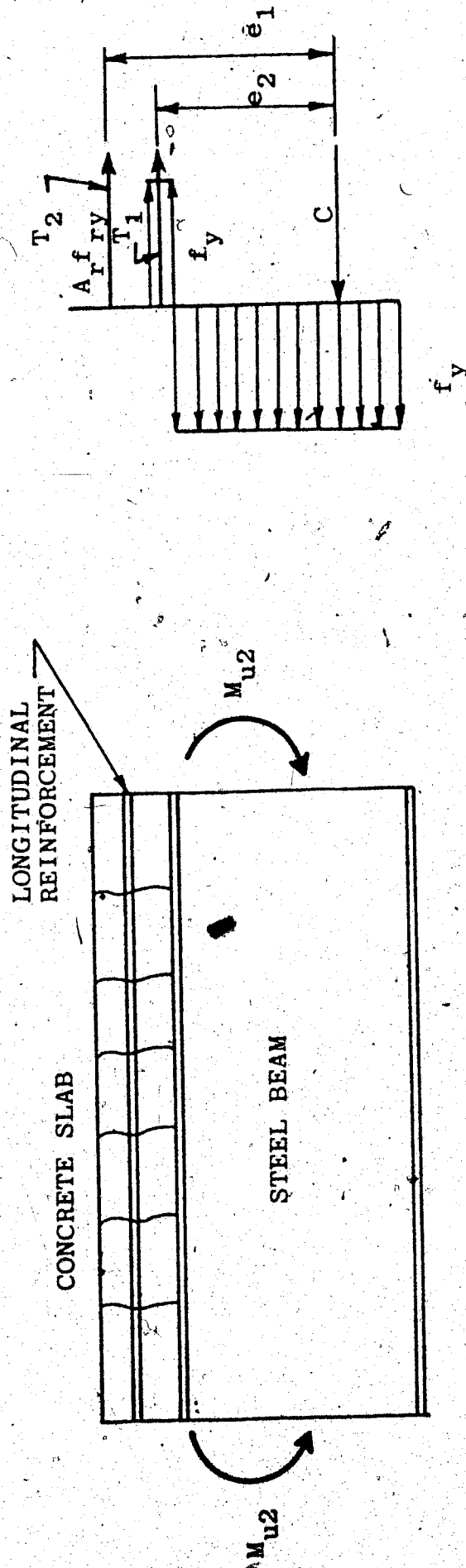


FIGURE C6. IDEALIZED STRESS DISTRIBUTION AT ULTIMATE MOMENT IN NEGATIVE BENDING

APPENDIX D

EVALUATION OF SHEAR CONNECTOR STIFFNESS FOR VARIOUS TYPES OF SHEAR CONNECTORS

D.1 Evaluation of Shear Connector Stiffness

In Chapter III the shear connector stiffness K used in analysis has been defined as load per connector per unit slip. In the numerical solution shear connection stiffness has been divided by the connector spacing as the computer program is based on the numerical technique.

For linear load slip behavior

$$Q = Ks \quad (D1)$$

$$\frac{dQ}{ds} = K \quad (D2)$$

For nonlinear load slip behavior

$$Q = a(1 - e^{-bs}) \quad (D3)$$

$$\frac{dQ}{ds} = ab = K \quad (D4)$$

Figures D1 to D5 illustrate load slip characteristics for various types of shear connectors (Chapman and Balakrishnan). For linear behavior the shear connector stiffness has been evaluated as the slope of the load-slip curve. For nonlinear behavior the value of a and b has been evaluated using the procedure as described in Section 2.1.3 (Yam and Chapman).

In most of the examples used for verification of the numerical analysis, difficulty was encountered in obtaining a shear connector stiffness. The example problems, which are compared with the closed form

solution, are designed for full shear connection and 3/4" x 4" stud shear connectors are used to achieve this. The load-slip relationship for this connector is available from push-out test results (Chapman & Balakrishnan).

In the example based on Chapman & Balakrishnan's beam, the shear connector stiffness was obtained from their load-slip data. As the ultimate strength of the concrete in the push-out test and the test beam are different, a linear interpolation was used to obtain the shear connector stiffness. The difference in results may be attributed to this interpolation.

In the case of Hamada and Longworth's beam, CBI, no push-out test results were available. To obtain a shear connector stiffness for this example, several examples were selected with various shear connector stiffnesses. After analysing these examples, the end slip from analysis was plotted against shear connector stiffness. With the end slip for Hamada and Longworth's beam, a shear connector stiffness was interpolated from this plot. Figure D6 illustrates the relationship between end slip and shear connector stiffness.

Push-out test results for various stud shear connectors are illustrated in Fig. D1 to D5. The ultimate load for these connectors are also obtained from test results. Two slip values are selected as $\gamma_1 = 0.01$ and $\gamma_2 = 0.02$. Expressing them in terms of ratio of Q/Q_u ()

$$a = \frac{Q_u \left(\frac{Q_1}{Q_u}\right)^2}{\frac{2Q_1}{Q_u} \frac{Q_2}{Q_u}} \quad (D5)$$

$$b = \frac{1}{\gamma_1} \ln \frac{\frac{Q_1}{Q_u}}{\frac{Q_2}{Q_u} - \frac{Q_1}{Q_u}} \quad (D6)$$

For 3/4" x 4" stud connector

$$Q_u = 12.5 \text{ tons}$$

$$\text{For } \gamma_1, \quad \frac{Q_1}{Q_u} = 0.35555$$

$$\text{For } \gamma_2, \quad \frac{Q_2}{Q_u} = 0.51666$$

Therefore $a = 8.126$ tons/in. or 18.20 kips/in.

$$b = 79.1578$$

$$K = 1440.67 \text{ kips/in.}$$

For other stud shear connectors, the values of a , b , and K are computed as per the above procedure and are tabulated in Table D1.

In the analysis the shear connector stiffness was divided by the connector spacing in a particular beam to obtain the shear connector stiffness per unit length of beam.

TABLE D1.. STIFFNESS OF HEADED STUD SHEAR CONNECTORS

Sl. No.	DIA Inches	LENGTH Inches	Qu kips	^a Kips/Inch	b	K Kips/Inch
1	3/4	4	28.000	18.200	79.1578	1440.676
2	3/4	3	23.072	21.296	81.3610	1732.663
3	3/4	2	24.864	19.152	84.5167	1618.670
4	1/2	4	13.440	12.017	114.0600	1370.640
5	1/2	2	14.560	10.822	100.8670	1091.583

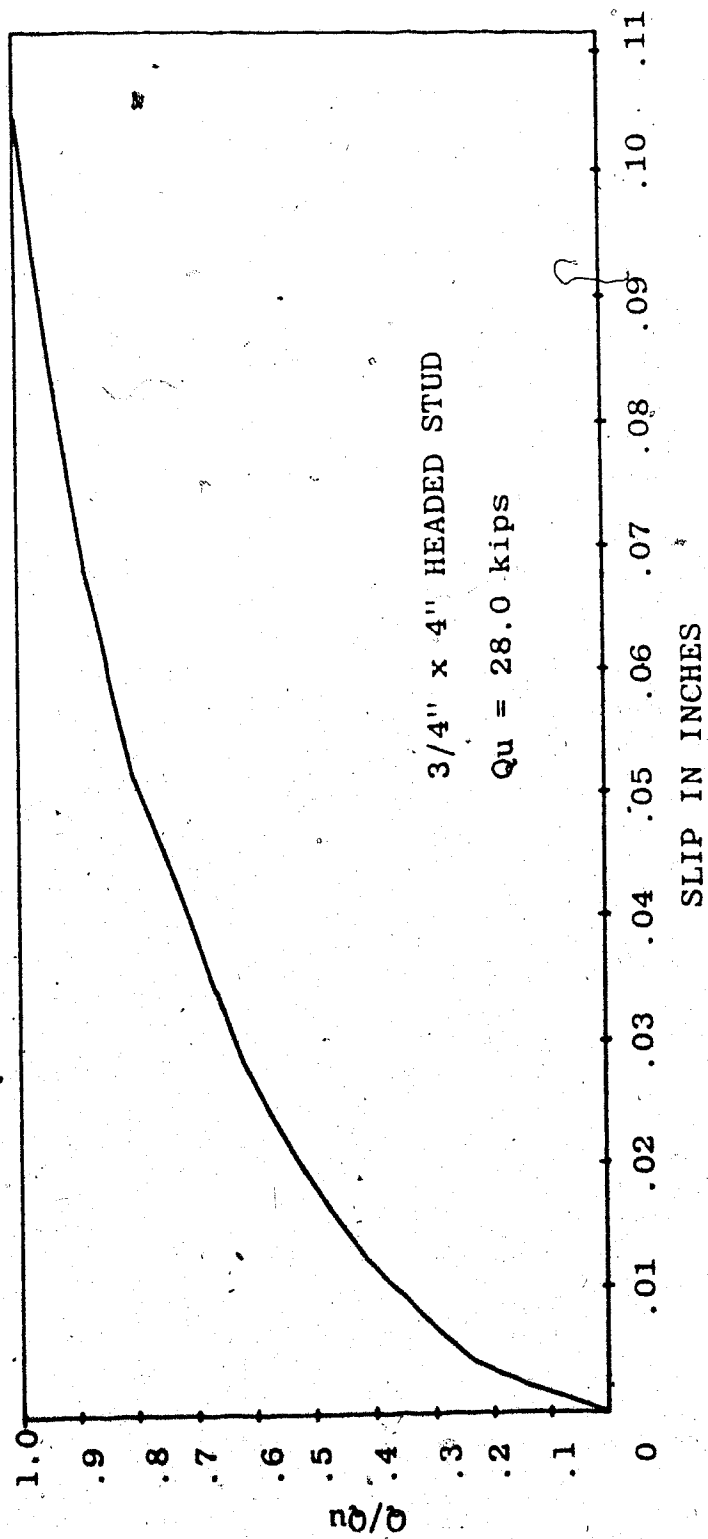


FIGURE D1. LOAD-SLIP RELATIONSHIP FOR PUSH-OUT SPECIMEN.

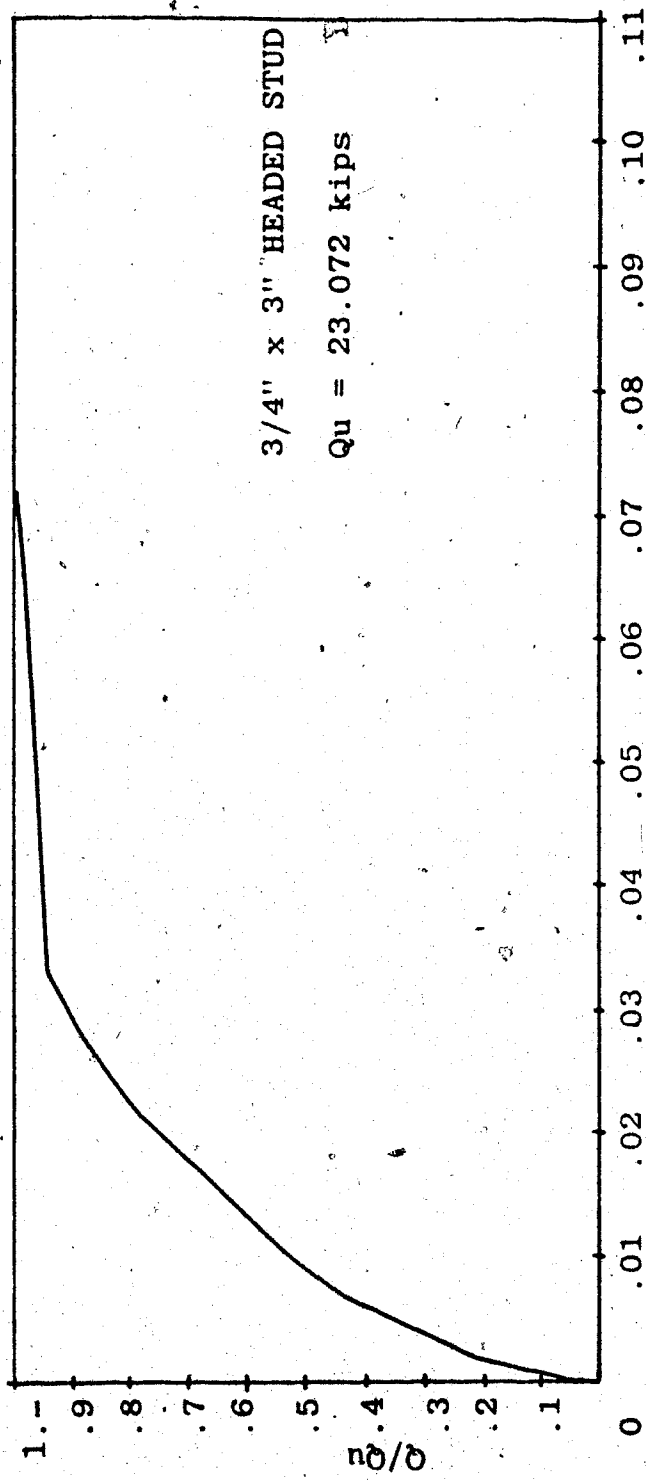


FIGURE D2. LOAD-SLIP RELATIONSHIP FOR PUSH-OUT SPECIMEN

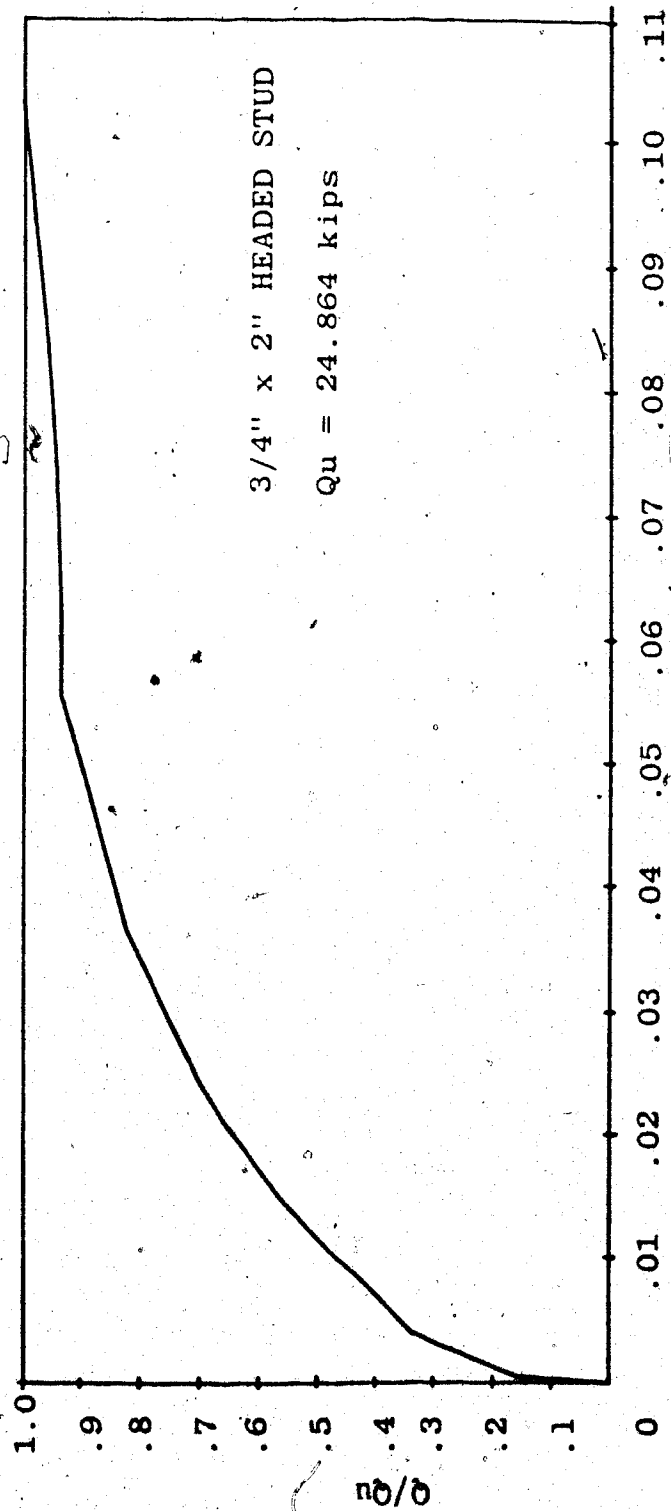


FIGURE D3. LOAD-SLIP RELATIONSHIP FOR PUSH-OUT SPECIMEN

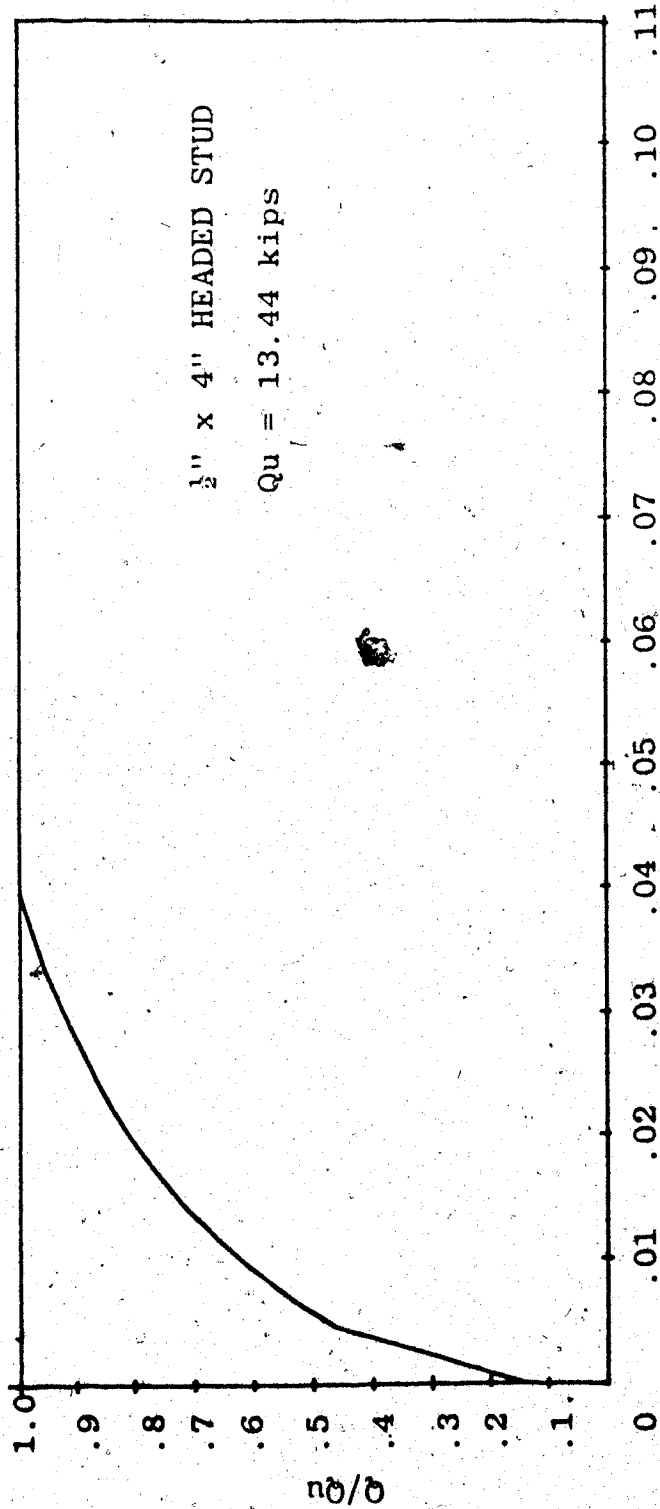


FIGURE D4. LOAD-SLIP RELATIONSHIP FOR PUSH-OUT SPECIMEN

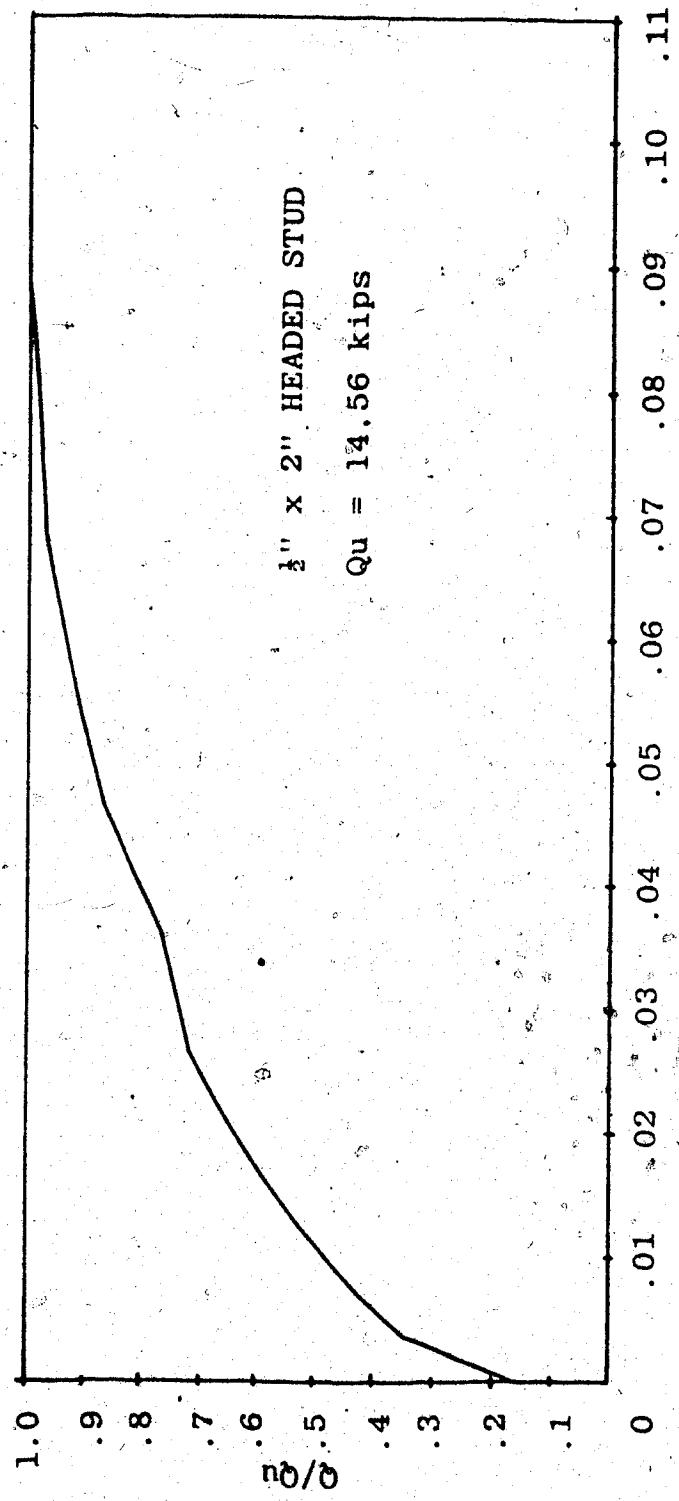


FIGURE D5. LOAD-SLIP RELATIONSHIP FOR PUSH-OUT SPECIMEN

APPENDIX E

SHEAR STRESS DISTRIBUTION IN COMPOSITE BEAM SECTIONS

E.1 Evaluation of Shear Stress

In a composite beam the neutral axis may be either in the concrete slab, in the top flange of steel section, or in the web of steel section. For these three locations, the variation in statical moment of area and the shear stress distribution are illustrated in Figs. E1 to E3. The shear deflection factor for three common steel sections used in composite beams for different slab widths and slab thicknesses are shown in Fig. E4 to E6.

The shear stress distribution is based on the following assumptions:

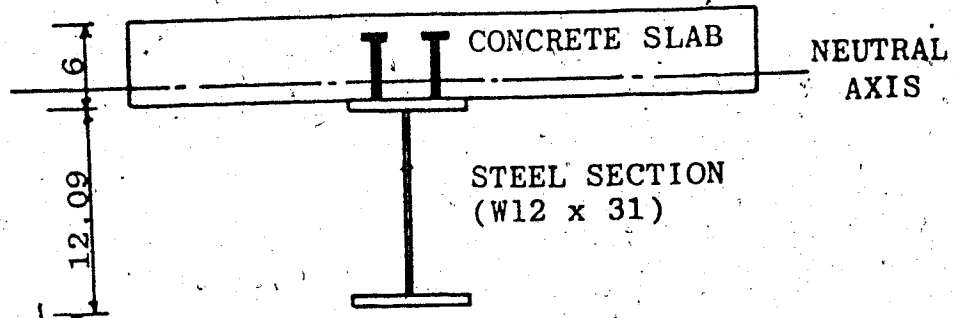
- (1) There is linear stress-strain behavior under service load conditions.
- (2) Concrete in tension is neglected.

It can be observed from Fig. E2 that the maximum shear stress occurs at the neutral axis when the neutral axis is in the web, whereas in the other two cases (Fig. E1 and Fig. E3), where the neutral axis is in the slab or in the top flange, the maximum shear stress occurs at the junction of top flange and web. Therefore it may be concluded that the major portion of the shear force in composite beam is resisted by the web of steel section.

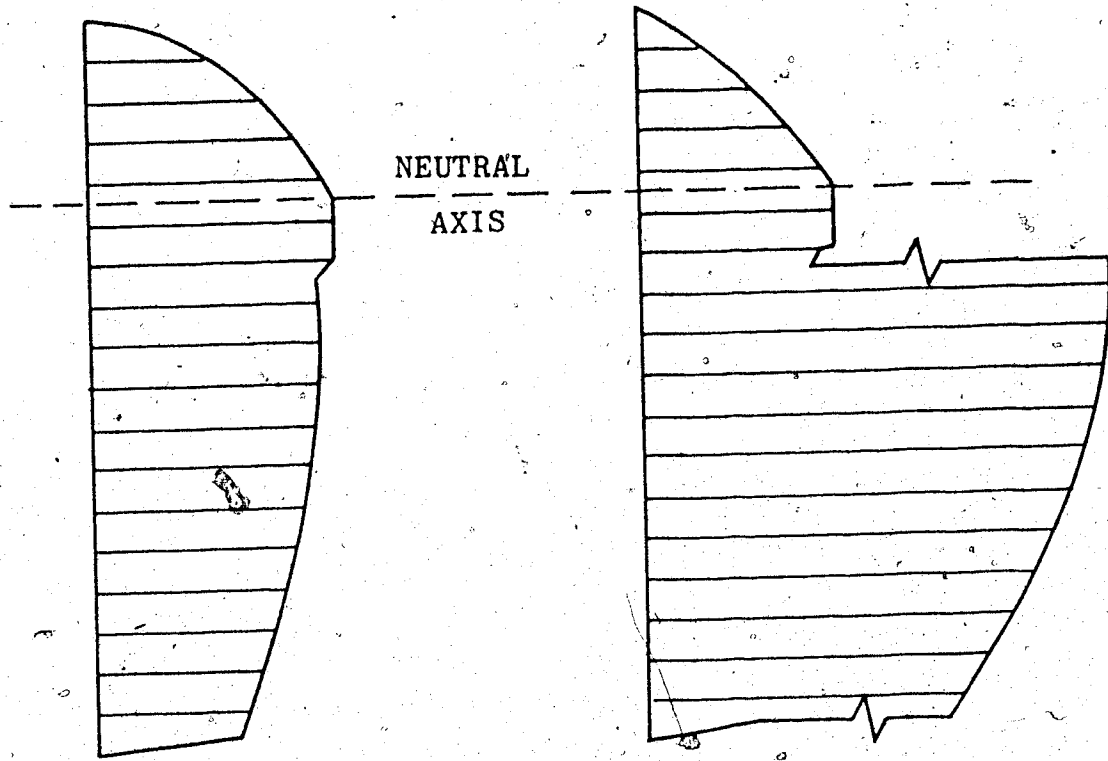
In case of composite beams due to the presence of concrete slab on the top of steel section, the shear stress at the top of the top flange of steel section is now zero, therefore the shear form factors for composite beams are much higher than that of wide flange beams.

Shear form factors for composite beams with steel sections (W16 x 50, W16 x 26, W14 x 53, W14 x 22, W12 x 190, W12 x 14) for various slab widths are illustrated in Fig. E4, E5, E6, respectively, for concrete slab thickness 6" and 4".

SHEAR CONNECTORS



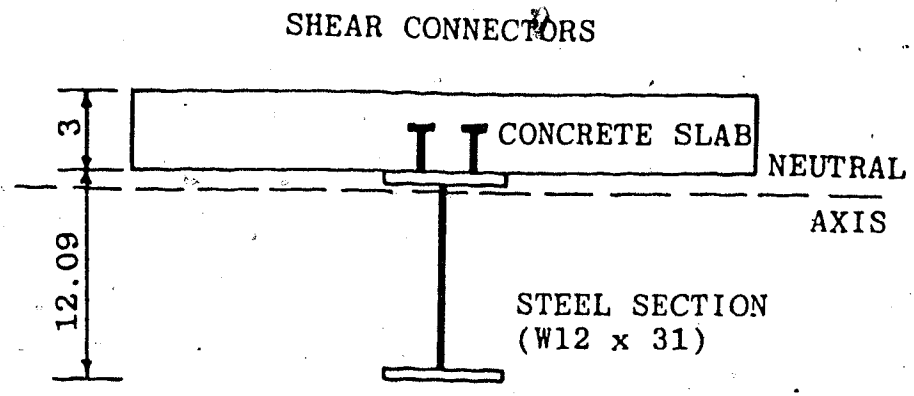
(a) SECTION OF COMPOSITE BEAM



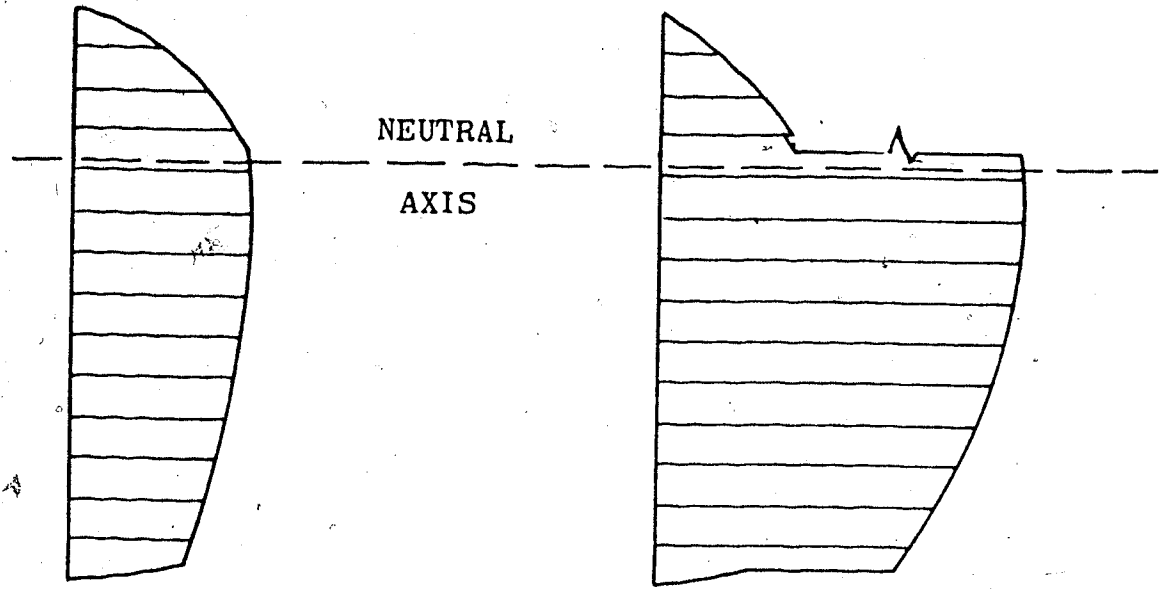
(b) STATICAL MOMENT VARIATION

(c) SHEAR STRESS DISTRIBUTION

FIGURE E1. STATICAL MOMENT AND SHEAR STRESS DISTRIBUTION IN COMPOSITE SECTION (NEUTRAL AXIS IN SLAB)



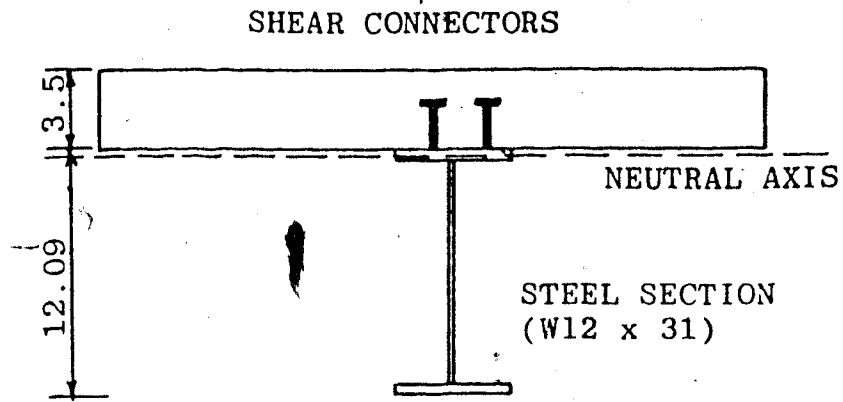
(a) SECTION OF COMPOSITE BEAM



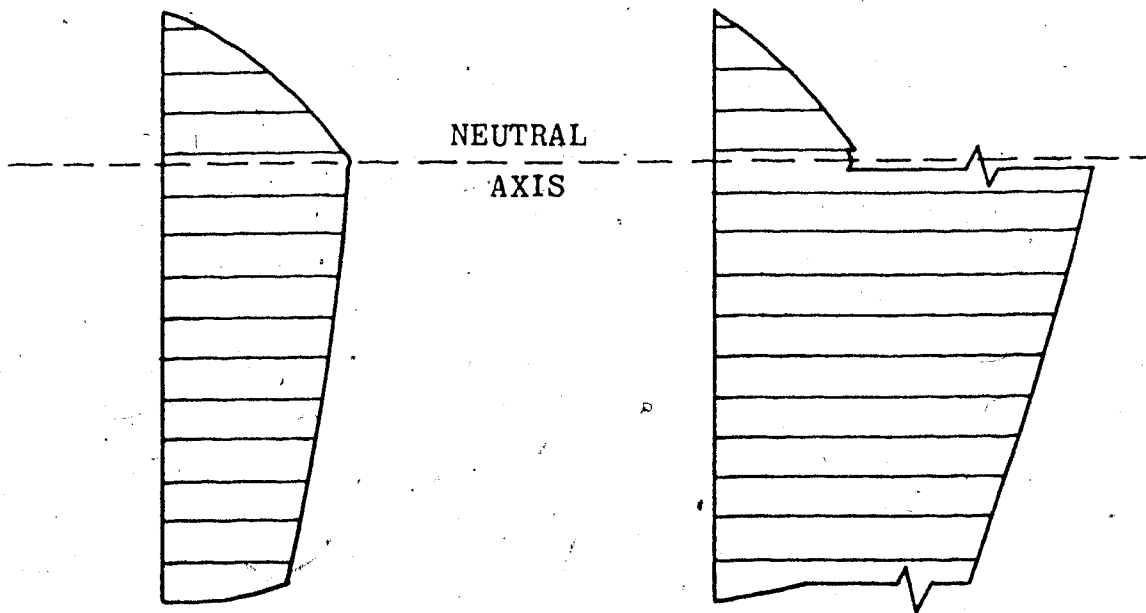
(b) STATICAL MOMENT VARIATION

(c) SHEAR STRESS DISTRIBUTION

FIGURE E2. STATICAL MOMENT AND SHEAR STRESS DISTRIBUTION IN COMPOSITE SECTION (NEUTRAL AXIS IN WEB)



(a) SECTION OF COMPOSITE BEAM



(b) STATICAL MOMENT
VARIATION

(c) SHEAR STRESS
DISTRIBUTION

FIGURE E3. STATICAL MOMENT AND SHEAR STRESS
DISTRIBUTION IN COMPOSITE SECTION
(NEUTRAL AXIS IN TOP FLANGE)

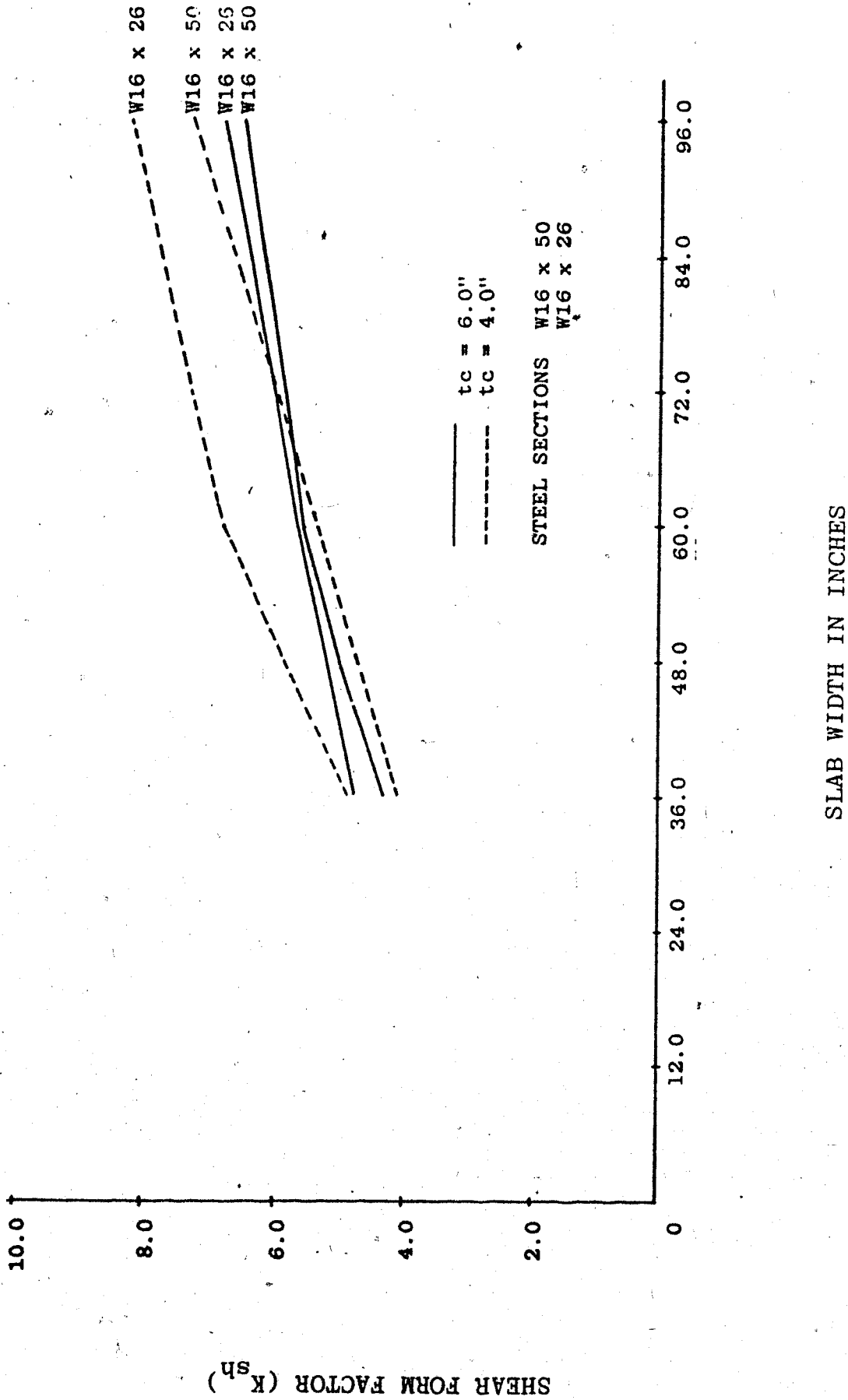
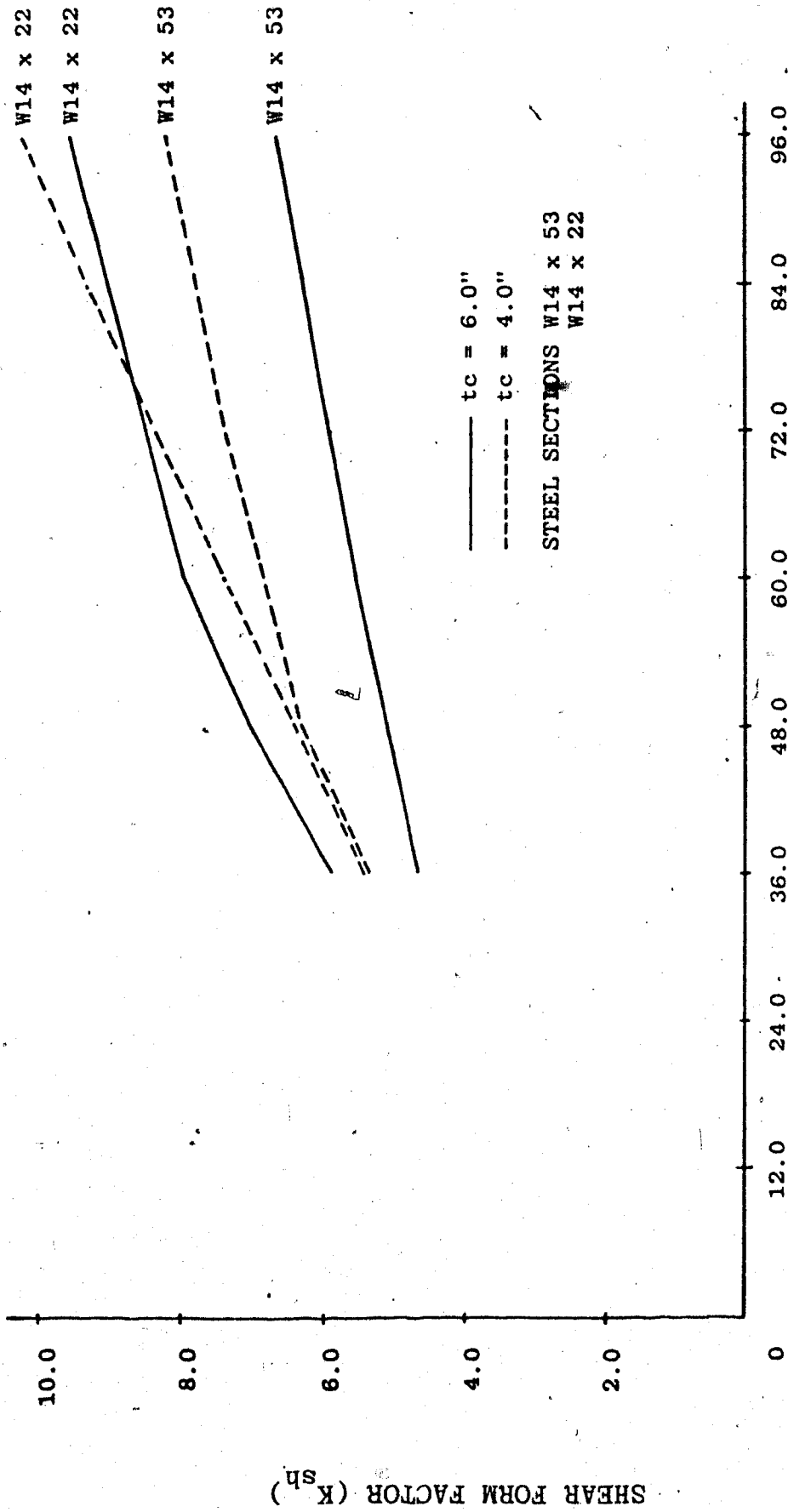
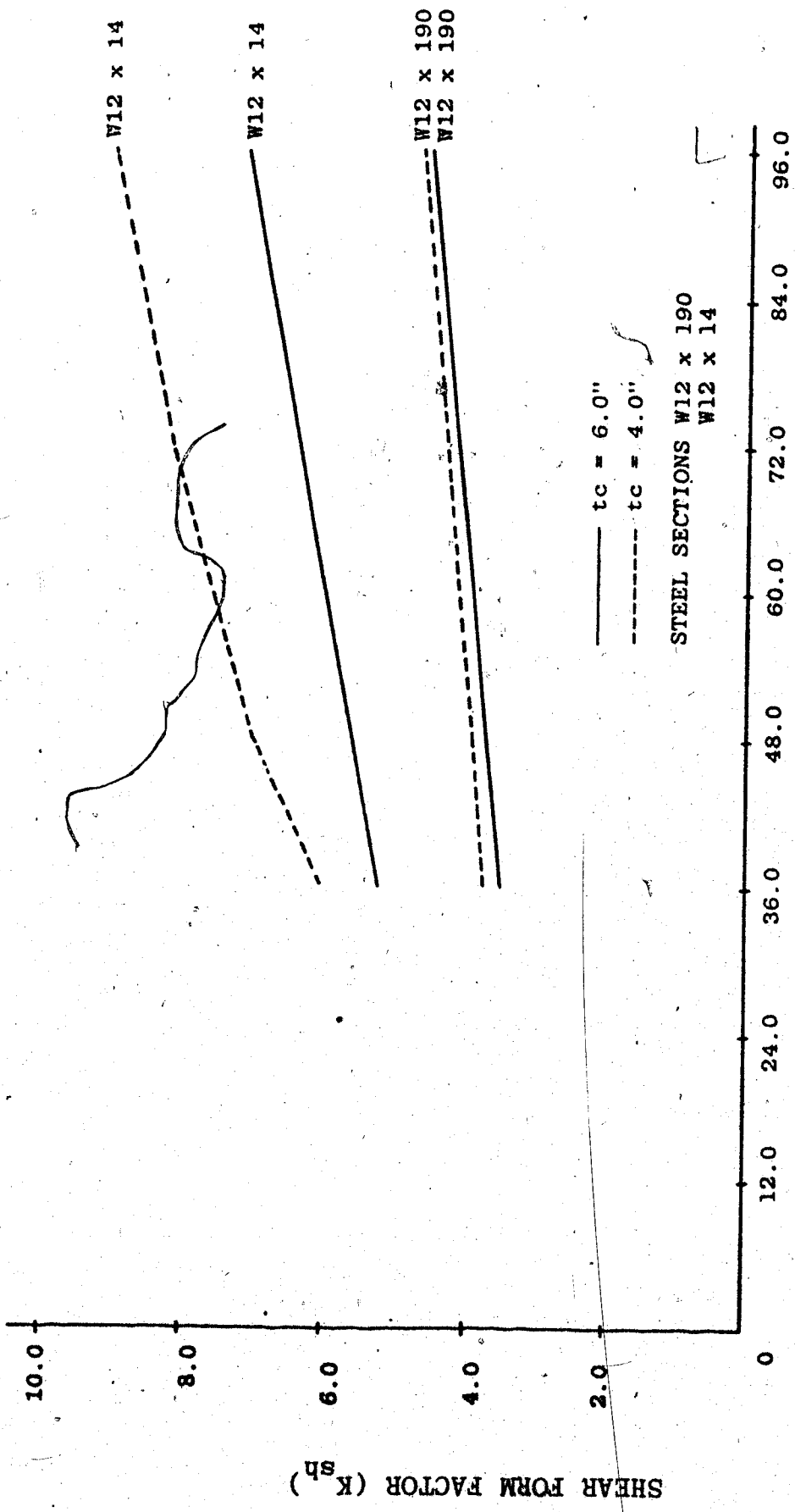


FIGURE E4. SHEAR FORM FACTOR (K_{sh}) VS SLAB WIDTH FOR COMPOSITE BEAMS



SLAB WIDTH IN INCHES

FIGURE E5. SHEAR FORM FACTOR (K_{sh}) VS SLAB WIDTH FOR COMPOSITE BEAMS



SLAB WIDTH IN INCHES

FIGURE E6. SHEAR FORM FACTOR (K_{sh}) VS SLAB WIDTH FOR COMPOSITE BEAMS

APPENDIX F

COMPUTER PROGRAM

F.1 Introduction

The following assumptions are made in the computation of slip, shear flow, force, slip strain and deflection:

1. The composite beam is divided into a number of elements of constant length, thus establishing a number of equally spaced nodal points.
2. Discontinuity of strain is assumed at the interface of the elements due to the presence of slip strain.
3. Concrete resists no tension in the negative moment regions.
4. Reinforcement exists at only one level in the slab.
5. In the analysis which accounts for different section properties in positive and negative moment regions, properties are constant throughout each region and equal to those associated with the transformed section (determined for full interaction) in the respective regions.

6. Due to the abrupt change in section properties at the junction between the positive and negative regions, the slip strain is discontinuous at the inflection points.

The following steps are required in the computations for slip, slip strain and deformation of a continuous beam for a given load:

1. Initialization
 - a. Determine the neutral axis and section properties.
 - b. Compute the stress resultants for unit reactions at the interior supports.
 - c. Compute the stress resultant for the external load.
2. Determine the flexibility influence coefficients and lack of compatibility displacements.

For each of the unit reactions in 1(b), and for each of the stress resultants obtained by combining the reactions and the external loads:

 - a. Compute the slip at each nodal point using the Runge-Kutta method of numerical integration.
 - b. Iterate the slip computation until the correct slip has been determined.

- c. Compute slip strain, curvature and deflection.
 - d. Enter the appropriate deflections in the equations of consistent deformation.
3. Solve for corrections to reactions.
 - a. Determine corrections to redundant reactions at the interior supports.
 - b. Determine the location of the inflection points and alter the length of beam with negative section properties.
 - c. Check the deflection at the supports computed in step 2(d).

The computer program was written in Fortran IV and computations were carried out on the AMDHAL 470/v at the University of Alberta computing services. The flow chart in Fig. B1 outlines the sequence of computation required for the analysis of a continuous beam. The program consists of eight subroutines and one function.

F.2 Description of Program

MAIN PROGRAM: The main program reads and writes the beam dimensions, material properties and loading conditions. It calls the following subroutines in sequence to compute stress resultants, slip and deflection.

PROP.: This subroutine computes the position of the neutral axis and the section properties. When necessary this subroutine calls subroutine "REGULA" to compute an average width so that average section properties are computed on this basis.

REGULA: This subroutine computes average width of concrete slab by using the section properties of the positive and negative moment regions by using the REGULA-FALSI method.

CONC.: This subroutine computes stress resultants due to all concentrated loads. The shears computed for each element are stored in two vectors, identified as the left shear and right shear of the element, and bending moment at the nodal point.

BMSU: Computes stress resultants due to uniform load and adds the stress resultants to those computed by "CONC" for external concentrated loads.

MASTER: This subroutine calls two subroutines and one function. First it calls "RUNGA" to compute slip, shear flow and axial force. A correction for slip is used if the axial force computed at the last nodal point is not zero. For variation in section properties, this subroutine selects the section properties depending upon the sign of the bending moment at the nodal point. The subroutine also computes slip strain and curvature. At the inflection points the

discontinuous slip strains are computed at the left and right side of the point. The subroutine calls "DEFLEX" to compute deflection at each nodal point assuming an initial slope of zero and then applies a linear correction to the deflections to arrive at the correct deflection at each nodal point.

RUNGA: This subroutine is based on a fourth order Runge-Kutta method of integration for a second order differential equation. The subroutine calls function "QF" to compute shear flow. The change in axial force is computed between every pair of nodal points by integrating the shear flow.

QF: This function defines the load-slip relationship for the shear connector.

DEFLEX: This subroutine computes deflection at every nodal point by using a second order Runge-Kutta method of integration for a second order differential equation.

SYMSOL: This subroutine is an equation solver. It solves the flexibility matrix to compute changes in reactions at the interior supports.

All notations for main vectors, geometric properties and indices are defined in the listing.

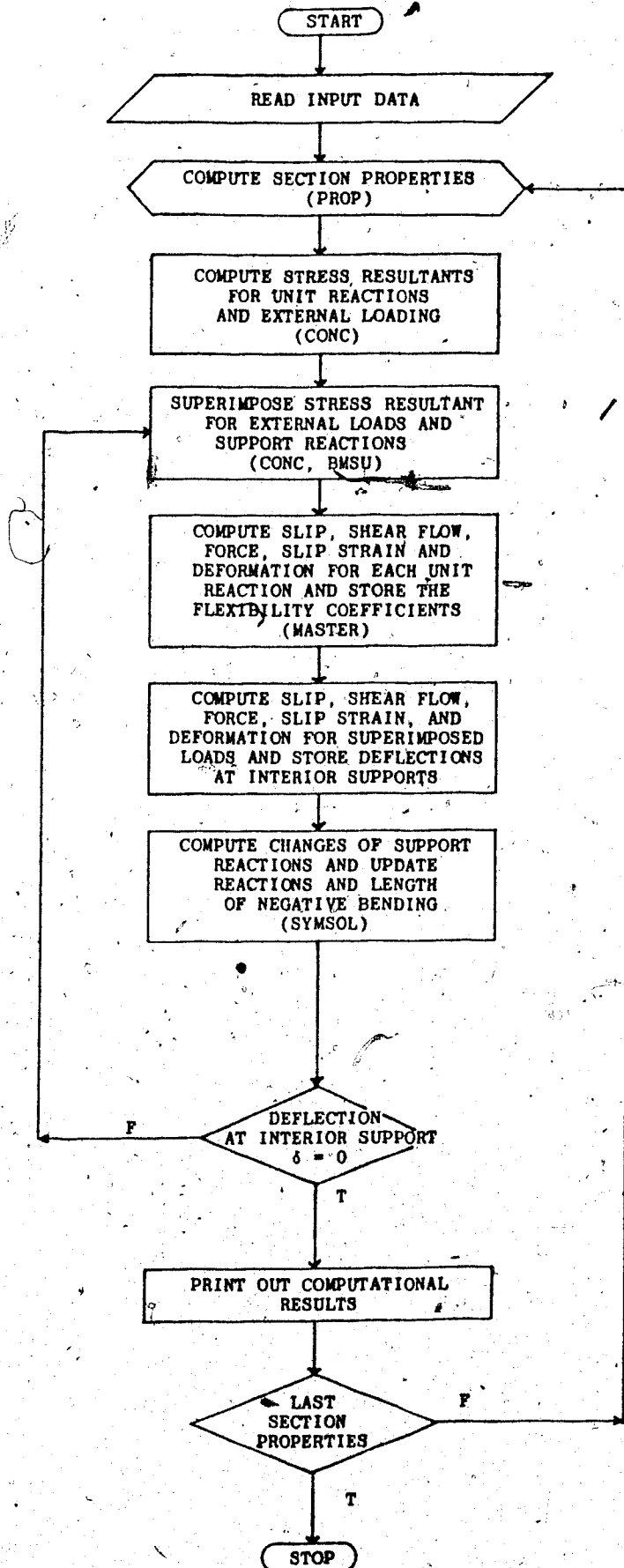


FIGURE F.1 FLOW CHART FOR COMPUTER PROGRAM

XL, BC, TC, DS, AS, SSI, DX, WF, TF, WW, NNP	10F10.0, I4
EC, ES, GS, SLIPK, TOLLER, MAXIT	5E14.4, I2
DIA, NO, DRTS	F10.4, I4, F10.4
ZZ, XCORDB, XCORDE, SOT, SETDS	5F20.10, E15.6
NSUP, NECL, IPRINT	3I4
CA, CB	2F15.5
NODES(I), DSL(I), SUP(I), SOS(I), I = 1, NSUP	I4, 2F10.0, E15.6
NODECL(I); DCL(I), ECL(I), I = 1 NECL	I4, 2F15.0

FIGURE F.2 INPUT DATA

F.3 List of Computer Programs

C THIS PROGRAM IS CALLED ***** COMPOSITE *****

C THIS PROGRAM EVALUATES DEFLECTION DUE TO :

C FLEXURE

C SLIP

C SHEAR

C AT SERVICE LOAD RANGE

C THIS PROGRAM IS DESIGNED TO ACCEPT MAXIMUM FIVE(5) INTERIOR SUPPORT AND SIX(6) SPANS

THIS PROGRAM HAS BEEN REDUCED TO OUT-PUT FINAL RESULTS ONLY

THIS IS GUIDE LINE FOR FUTURE USE

DESCRIPTION OF INPUT DATA

XL=TOTAL LENGTH OF BEAM IN INCHES

BC=WIDTH OF CONCRETE SLAB IN INCHES

TC=THICKNESS OF CONCRETE SLAB IN INCHES

DS=TOTAL DEPTH OF STEEL SECTION IN INCHES

AS=AREA OF STEEL SECTION SQUARE INCH

SSI=MOMENT OF INERTIA OF STEEL SECTION IN INCH**4

C C DX=LENGTH OF ELEMENT IN INCHES
 C C WF=WIDTH OF FLANGE IN INCHES
 C C WW=WIDTH OF WEB IN INCHES
 C C NMP=TOTAL NUMBER OF NODAL POINTS
 C C EC=ELASTIC MODULUS OF CONCRETE PSI
 C C ES=ELASTIC MODULUS OF STEEL IN PSI
 C C GS=SHEAR MODULUS OF STEEL IN PSI
 C C SLIPK=SHEAR CONNECTOR STIFFNESS IN PSI, SLIPK=K/SPACING OF SHEAR CONNECTORS
 C C TOLER=TOLERANCE LIMIT ON FORCE IN POUNDS FOR CONVERGENCE
 C C MAXIT=MAXIMUM NUMBER OF ITERATION
 C C DIA=DIAMETER OF REINFORCING STEEL
 C C NO=NUMBER OF REINFORCING BAR
 C C DRYS=CENTER DISTANCE OF REINFORCING STEEL FROM TOP OF TOP FLANGE
 C C ZZ=UNIFORMLY DISTRIBUTED LOAD IN POUNDS PER FOOT
 C C XCORD8=BEGINING CORDINATE OF UNIFORM LOAD
 C C XCORDE=ENDING CORDINATE OF UNIFORM LOAD
 C C SOT=INITIAL SLIP ASSUMPTION IN INCHES
 C C SETDS=MULTIPLIER FOR PREDICTION OF FORCE FOR NEXT ITERATION 0.1
 C C NSUP=NUMBER OF INTERIOR SUPPORT
 C C NECL=NUMBER OF EXTERNAL CONCENTRATED LOADS
 C C IPRINT=FLAG
 C C CA=SHEAR CONNECTOR STIFFNESS COEFFICIENT IN PSI
 C C CB=SHEAR CONNECTOR COEFFICIENT
 C C NODES(I)=NODAL NUMBER AT SUPPORT LOCATION
 C C DSL(I)=DISTANCE OF SUPPORT FROM LEFT END IN INCHES


```

READ(5, 1040)NSUP,NECL,IPRINT
WRITE(6,1240)NECL,NSUP,IPRINT
READ(5, 1241)CA,CB
1241 FORMAT(2F15.5)
WRITE(6,1242)CA,CB
1242 FORMAT(3X/,'*** CA=',E15.5,3X/,'*** CB=',E15.5)
WRITE(6,1550)
IF(NSUP.EQ.0) GOTO 33
DO 20 I=1,NSUP
READ(5,1161)(NODES(I),DSL(I),SUP(I),SOS(I))
WRITE(6,1291)(NODES(I),DSL(I),SUP(I),SOS(I))
20 CONTINUE
33 IF(NECL.EQ.0)GOTO 134
WRITE(6,1560)
DO 35 I=1,NECL
READ(5,1060)(NODECL(I),DCL(I),ECL(I))
WRITE(6,1280)(NODECL(I),DCL(I),ECL(I))
35 CONTINUE
990 FORMAT(3X/,'***** ECHO CHECK *****',3X/)
1550 FORMAT(3X/,'*** SUPPORT CONDITION ***',3X//)
1560 FORMAT(3X/,'*** CONCENTRATED LOADS ***',3X//)
1000 FORMAT(10F10.4,14)
1010 FORMAT(5E14.4,12)
1020 FORMAT(F10.4,14,F10.4)
1040 FORMAT(3I4)
1060 FORMAT(I4,F15.0,F15.0)
1161 FORMAT(I4,F10.0,F10.0,E15.6)
1100 FORMAT(5F20.10)
1210 FORMAT(3X/,'CONCRETE MODULUS=',E14.4/
*'STEEL MODULUS=',E14.4/
*'SHEAR MODULUS=',E14.4/
*'SHEAR CONNECTOR MODULUS=',E14.4/
*'TOLERANCE=',E14.4/
*'MAXIT=',I5,3X//)
1220 FORMAT(3X/,'DIA OF REBARS=',F10.4/
*'NUMBER OF REBARS=',I2/
*'CENTRID OF REBARS FROM TOP FLANGE=',F10.4/)
1240 FORMAT(3X/,'NO.OF CONCENTRATED LOAD=',I2/
*'NO.OF INTERIOR SUPPORT=',I2/
*'IPRINT=',I2,3X/)
1280 FORMAT(3X/,'NODE NO.=',I4,3X/,'LENGTH FROM LEFT END=',F15.4,
*'3X',LOAD=',F15.4)
1290 FORMAT(3X/,'NODE NO.=',I4,3X/,'LENGTH FROM LEFT END=',
*'F10.4,3X',LOAD=',F10.4)
1291 FORMAT(3X/,'NODE NO.=',I4,3X/,'LENGTH FROM LEFT END=',
*'F10.4,3X',LOAD=',F15.5,3X/,'INITIAL SLIP=',E15.6)
1300 FORMAT(3X/,'UNIFORM LOAD LBS PER FOOT=',F15.4/
*'STARTING COORDINATE=',F10.4/
*'ENDING COORDINATE=',F10.4,3X.

```

```

**INITIAL SLIP=.F12.6.3X,SETDS=.E14.6.3X/**
1200 FORMAT(3X,LENGTH OF BEAM=.F10.4/
**WIDTH OF CON.SLAB=.F10.4/
**DEPTH OF CON.SLAB=.F10.4/
**DEPTH OF ST.BEAM=.F10.4,3X/
**AREA OF ST.BEAM=.F10.4/
**MOMENT OF INERTIA OF ST.BEAM=.F10.4/
**ELEMENT LENGTH=.F10.4/
**WIDTH OF FLANGE=.F10.4/
**THICKNESS OF FLANGE=.F10.4/
**WIDTH OF WEB=.F10.4/
**NUMBER OF NODAL POINTS=.I4)

C 134 IF(NSUP.GT.5)CALL EXIT
IF(ZZ.EQ.0.0)GOTO 37
Z=ZZ/12.0

C 37 NSEG=1
NNP1=NNP-1
RNNP1=DFLOAT(NNP1),

C INITIALIZATION
DO 1 J=1,NNP
VLC(J)=0.000
VRC(J)=0.000
BMC(J)=0.000
DO 89 I=1,NSUP
VLS(J,I)=0.000
VRS(J,I)=0.000
BMS(J,I)=0.000
89 CONTINUE
1 CONTINUE

C COMPUTE INITIAL STRESS RESULTANT
C
IFLAG=0
DO 93 J=1,NNP
XLENG(J)=DFLOAT(J-1)*DX
93 CONTINUE
IF(NECL.EQ.0)GOTO 39
DO 5 I=1,NECL
X=XO
5 CALL CONC(VLC,VRC,BMC,NODECL(I),ECL(I),DCL(I))
39 CALL BMSU(Z,VLC,VRC,BMC)
36 CONTINUE
C 36 WRITE(6,7000)
C WRITE(6,4000)

```

```

C WRITE(6,4100)(I,VLC(I),VRC(I),BMC(I),I=1,NNP1)
DO 2 I=1,NSUP
X=XO
CALL CONC(VLS(1,I),VRS(1,I),BMS(1,I),NODES(I),-1,DSL(I))
C WRITE(6,7002)I
C WRITE(6,4000)
C WRITE(6,4100)(J,VLS(J,I),VRS(J,I),BMS(J,I),J=1,NNP1)
2 CONTINUE
C MAIN LOOP FOR DIFFERENT SECTION PROPERTIES BEGINS HERE
C
INT=1
IND=0
INC=0
TCC=0.5*TC
AREAR=NO*PI*DIA**2/4.
RMI=NO*PI*DIA**4/64.
XN=EC/ES
IND=IND+1
INC=INC+1
AR=AREAR
RM=RMI
DR=DRTS
AREAC=XN*BC*TC
CMI=XN*BC*TC**3/12.
WRITE(6,110)INT,IND
FORMAT(3X/,15.5X,15)
IF(IND.GT.1) GOTO 42
RM=CMI
AR=AREAC
DR=TCC
42 CALL PROP(CMI,AREAC,TCC,SEC(1,1))
CALL PROP(RM,AR,DR,SEC(1,2))
IF(NSUP.EQ.0) GOTO 73
43 IF(IND.NE.3) GOTO 73
AVEI=(SEC(3,1)+SEC(3,2))/2.
CALL REGULA(1.0,BC,1.0E-03,50,B)
BC=B
IND=1
GOTO 41
73 WRITE(6,1570)
WRITE(6,1580)
1570 FORMAT('1',***** NEW SECTION PROPERTIES ****'.5X//)
1580 FORMAT(5X//,*** OUT-PUT OF SECTION PROPERTIES ****')
C WRITE(6,5000)((SEC(I,J),J=1,2),I=1,11)
C
IMT=1
C LOOP FOR ITERATION OF REACTION BEGINS HERE

```



```

C COMPUTE TOTAL STRESS RESULTANTS
339 DO 25 J=1,NMP 1
    TBM=O.OOO
    TVL=O.OOO
    TVR=O.OOO
    DO 30 I=1,NSUP
        TBM=TBM+SUP(I)*BMS(J,I)
        TVL=TVL+SUP(I)*VLS(J,I)
        TVR=TVR+SUP(I)*VRS(J,I)
    30 CONTINUE
        BMT(J)=TBM+BMC(J)
        VLT(J)=TVL+VLC(J)
        VRT(J)=TVR+VRC(J)
    25 CONTINUE
        BMT(NMP)=O.OOO

C COMPUTE DEFLECTION,SLIP,SLIPSTRAIN,CURVATURE FOR
C TOTAL LOAD STRESS RESULTANT
    S1=SOT
    CALL MASTER(VLT,VRT,BMT,SEC(1,1))
    IF(NSUP.EQ.O) GOTO 7
    SUM=O.OOO

C STORE SUPPORT DEFLECTION
    DO 47 KK=1,NSUP
        FLEX(KK,6)=-DEF(NODES(KK))
        SUM=SUM+DABS(FLEX(KK,6))
    47 CONTINUE
    IF(SUM.LE.1.OE-06)GOTO 7
    IF(IMT.EQ.10) GOTO 7
    DO 51 I=1,NSUP
        S1=SOS(I)

C CALLS MASTER SUBROUTINE FOR UNIT REACTIONS
    CALL MASTER(VLS(1,I),VRS(1,I),BMS(1,I),SEC(1,1))
    SOS(1)=S1

C STORE UNIT REDUDANT DEFLECTION IN FLEX
    DO 51 II=1,NSUP
        FLEX(II,I)=DEF(NODES(II))
    51 CONTINUE
    WRITE(6,671)
C 671 FORMAT(3X//, 'FLEXIBILITY MATRIX FOR SUPPORT REACTION',3X//)
C DO 52 J=1,NSUP
C2 WRITE(6,672)(FLEX(J,I),I=1,NSUP)
C 672 FORMAT(6X,E15.6,6X,E15.6,4X)
    IF(NSUP.NE.#) GOTO 14

```

```

C
DELTA=FLEX(NSUP,6)/DEF(NODES(NSUP))
WRITE(6,7001)DELTA
SUP(NSUP)=SUP(NSUP)+DELTA
WRITE(6,196)SUP(NSUP)
GOTO 21

C SOLVE FOR CORRECTION TO SUPPORT REACTION
14 CALL SYMSOL(FLEX,FLEX(I,6),5,NSUP)
C WRITE(6,7001)(FLEX(I,6),I=1,NSUP)
C7001 FORMAT(3X//,'INCREMENT IN REACTION IS',E13.5,X,E13.5,X//)
DO 49 I=1,NSUP
SUP(I)=SUP(I)+FLEX(I,6)
49 CONTINUE
WRITE(6,196)(SUP(I),I=1,NSUP)
196 FORMAT(3X//,'SUPPORT REACTION=',5X,E14.6,5X,E14.6,4X//)
21 INT=INT+1
GOTO 339
7 DO 165 J=1,NMP
CM=CMI
IF(BMT(J).LT.O.O.AND.INT.EQ.2) CM=O.OOO
BMSC(J)=(SSI+CM)*ES*PHI(J)
CMC(J)=CM*ES*PHI(J)
165 CONTINUE
IF(NSUP.EQ.O) GOTO 38
38 WRITE(6,7300)
7400 FORMAT(3X,14,5X,E13.5,X,E13.5,7%,E13.5,7X,E13.5,3X)
7300 FORMAT(3X/,'NODE NO.',5X,'SHEAR FLOW',9X,'FORCE',14X,
*'SLIP',15X,'SLIP STRAIN',7X/)
IF(KSUM.EQ.O) GOTO 17
WRITE(6,4750)KSUM
WRITE(6,4710)
4710 FORMAT(3X/4X,'INPT',5X,'LENGTH',5X,'SLIP',5X,'LEFT STRAIN',
*'RIGHT STRAIN',6X,'LEFT CURVE',5X,'RIGHT CURVE',5X,
*'DEFLECTION')
4750 FORMAT(3X/,'NUMBER OF INFLECTION POINTS',I4)
WRITE(6,4900)(K,XI(K),SI(K),SPIL(K),SPIR(K),PHIL(K),PHIR(K),
*DEFI(K),K=1,KSUM)
17 WRITE(6,5500)
WRITE(6,4800)
4900 FORMAT(3X,14,3X,F10.4,3X,E13.5,3X,
*'E13.5,3X,E13.5,3X,E13.5,3X,E13.5,3X,E13.5,3X,E13.5,3X)
5300 FORMAT(3X/,'INFLECTION POINT OUT-PUT',5X/)
5400 FORMAT(//,'IN NO.',5X,'LENGTH',3X,'SLIP',5X,'LEFT STRAIN',5X,
*'RIGHT STRAIN',5X,'LEFT CURV',5X,'RIGHT CURV',5X,'DEFLECTION')
5500 FORMAT(3X/,'FINAL OUT-PUT FOR SLIP STRAIN,CURV,DEF',5X/)
4800 FORMAT(8X/,'NODAL NO',2X,'NODE LENGTH',6X,'SLIP',8X,
*'SLIP STRAIN',8X,'CURVATURE',5X,'DEFLECTION',8X/)

```



```

COMMON /PROPT/ ES,GS,AS,DS,SSI,XN,BC,TC,AVEI,WF,TF,WV
COMMON /NODE/ NNP,NMP1,RNMP1,IPRINT,KSUM,MAKIT
COMMON /DIST/ XL,XO,X,DX
COMMON /SLIP/ SLIPK,TOLER,SETDS
COMMON /MTOT/ BMT(500)
COMMON /BLOCK/ S(500),FORCE(500),Q(500),SP(500),PHI(500),
*DEF(500),XI(10),SI(10),SPIL(10),SPIR(10),PHIL(10),PHIR(10),
*DEFI(5),SOS(5),SOT,S1,SOC
IT=0
ITT=0
KSUM=0
S(1)=S1
SL1=0.000
SL2=0.000
FL1=0.000
FL2=0.000
DDS=0.000
DF=0.000
SP(1)=0.000
SP(NNP)=0.000
Q(1)=-QF(S(1))
WRITE(6,4200)
46 FORCE(1)=0.000
IT=IT+1
ITT=ITT+1
V1=0.000
K=0
I1=1
I2=2
IFLAG=0
DO 100 J=1,NMP1
IF((J.EQ.1).OR.(J.EQ.NMP1))GOTO 131
IF(BMT(J)=BMT(J+1).LT.-1.00-06) GOTO 200
CALL RUNGA(S(J),VL(J),VR(J),V1,SS,SFORCE,SQ,SEC(1,I1),DX)
IF(J.EQ.1) GOTO 800
IF(IFLAG.NE.0) GOTO 800
SP(J)=(S(J)+SS-S(J-1))/(2.*DX)
GOTO 800
200 K=K+1
FRACT=DABS(BMT(J))/(DABS(BMT(J))+DABS(BMT(J+1)))
VLT=VL(J)+(VR(J)-VL(J))*FRACT
VRT=VLT
DX1=DX*FRACT
CALL RUNGA(S(J),VL(J),VRT,V1,SS,SFORCE,SQ,SEC(1,I1),DX1)
A=DX
B=DX1
IF(DABS(B).LT.1.00-03) GOTO 999
XI(K)=DFLOAT(J-1)*DX+DX1
SI(K)=S(J)+SS

```

```

TFORCE=FORCE(J)+SFORCE
ST=S(J)+SS
SP(J)=-B*S(J-1)/(A*(A+B))-(A-B)*S(J)/(A*B)+A*ST/(B*(A+B))
SPIL(K)=B*S(J-1)/(A*(A+B))-(A+B)*S(J)/(A*B)+(2.*B+A)*ST/
*(B*(A+B))
PHIN=SEC(4, I1)*SEC(5, I1)*SPIL(K)/SEC(3, I1)
EO=-SEC(4, I1)*SPIL(K)/SEC(6, I1)
CONST=1./((SEC(4, I2)/SEC(6, I2))+SEC(4, I2)*SEC(5, I2)*
*SEC(7, I2)/SEC(3, I2))
V1=(PHIN*SEC(7, I1)-EO)*CONST
DX2=DX-DX1
CALL RUNGA(ST, VLT, VR(J), V1, SS, SFORCE, SQ, SEC(J, I2), DX2)
JT=I1
I1=I2
I2=JT
S(J+1)=ST+SS
FORCE(J+1)=TFORCE+SFORCE
Q(J+1)=SQ
IFLAG=1
GOTO 100
800 S(J+1)=SS+S(J)
FORCE(J+1)=SFORCE+FORCE(J)
Q(J+1)=SQ
IF(IFLAG.EQ.O) GOTO 100
A=DX2
IF(DABS(A).LT.1.O0-03) GOTO 999
B=DX
SPIR(K)=-((2.*A+B)*ST/(A*(A+B)))+(A+B)*S(J)/(A*B)-A*S(J+1)/
*(B*(A+B))
SP(J)=-B*ST/(A*(A+B))-(A-B)*S(J)/(A*B)+A*S(J+1)/(B*(A+B))
IFLAG=0
C KSUM=NUMBER OF INFECTION POINTS.
100 CONTINUE
C
C KSUM=K
IF(DABS(FORCE(NNP)).LT.TOLER.OR.ITT.GT.MAXIT)GOTO 53
IF(IT.NE.1) GOTO 40
PROD=(SEC(5, 1)-SEC(7, 1))*(SEC(5, 1)-SEC(7, 1))
CNUM=SEC(3, 1)*SEC(6, 1)+(PROD*SEC(9, 1)*SEC(4, 1))
DENOM=SEC(3, 1)-(SEC(5, 1)-SEC(7, 1))*SEC(4, 1)*SEC(5, 1)
CDENO=SEC(8, 1)*SEC(9, 1)*SEC(10, 1)*DSINH(SEC(10, 1)*XL)
SL1=S(1)
FL1=FORCE(NNP)
DSR=FORCE(NNP)*CNUM/(DENOM*CDENO)
IF(S(1).EQ.O.O00) GOTO 39
DSR=SETDS*DABS(S(1))*FL1/DABS(FL1)
39 S(1)=S(1)-DSR
GOTO 45

```

```

C 40 IF(IT.NE.2) GOTO 43
C 41 SL2=S(1)
FL2=FORCE(NNP)
IF(FL1*FL2.LT.O.000) GOTO 42
SL1=SL2
FL1=FL2
S(1)=S(1)-DSR
IT=IT-1
GOTO 45
C 42 DF=FL2-FL1
IF(DABS(DF).LT.1.00-06)GOTO 999
DDS=SL2-SL1
TEMP=S(1)
S(1)=SL2-FL2*(DDS/DF)
SRATIO=S(1)/TEMP
IF(DABS(SRATIO-1.000).GT.1.00-12) GOTO 45
C 43 WRITE(6,1232) SRATIO
C1232 FORMAT(' CONVERGENCE OF SRATIO ',E20.6)
C 44 GOTO 53
C 45 GOTO 45
C 46 FOR1=FORCE(NNP)*FL1
FOR2=FORCE(NNP)*FL2
IF(FOR1*FOR2.LT.O.000) GOTO 44
KL=2
IF(DABS(FORCE(NNP)-FL1).GT.DABS(FORCE(NNP)-FL2)) KL=1
GOTO(47,48),KL
C 47 FL2=FORCE(NNP)
SL2=S(1)
GOTO 42
C 48 FL1=FORCE(NNP)
SL1=S(1)
GOTO 42
C 49 IF(FOR1.LT.O.O) GOTO 41
FL1=FORCE(NNP)
SL1=S(1)
GOTO 42
C 50 Q(1)=-QF(S(1))
C 51 WRITE(6,124)IT,SL1,FL1,SL2,FL2,DDS,DF,S(1)
C124 FORMAT(/5X,14.7E15.6,3X//)
C 52 GO TO 46
C 53 WRITE(6,323)ITT,S(1),FORCE(NNP)
C 323 FORMAT('O',ITT=',14.10X','S(1)=' ,E15.6,10X,'FORCE(NNP)=' ,E15.6)
C 54 S1=S(1)
C

```

```

K=O
I1=1
I2=2
PHI(NNP)=O.ODO
DO 170 J=1,NNP1
IF((J.EQ.1).OR.(J.EQ.NNP1)) GOTO 132
IF(BMT(J)*BMT(J+1).LT.-1.0D-06) GOTO 150
132 PHI(J)=BM(J)/(ES*SEC(3,I1))+SEC(4,I1)*SEC(5,I1)*SP(J)/
*SEC(3,I1)
GOTO 170
150 K=K+1
PHI(J)=BM(J)/(ES*SEC(3,I1))+SEC(4,I1)*SEC(5,I1)*SP(J)/
*SEC(3,I1)
PHIL(K)=SEC(4,I1)*SEC(5,I1)*SPIL(K)/SEC(3,I1)
PHIR(K)=SEC(4,I2)*SEC(5,I2)*SPIR(K)/SEC(3,I2)
JT=I1
I1=I2
I2=JT
170 CONTINUE
C THIS PART OF MAIN PROGRAM COMPUTES DEFLECTION
C THIS PART ALSO HANDLES TRANSITION ELEMENTS
RV=O.ODO
IT=O
175 IT=IT+1
I1=1
I2=2
K=O
V1=RV
DEF(1)=O.ODO
DO 900 J=1,NNP1
IF((J.EQ.1).OR.(J.EQ.NNP1))GOTO 133
IF(BMT(J)*BMT(J+1).LT.-1.0D-06) GOTO 600
133 SDEFL=VL(J)*SEC(11,I1)
SDEFR=VR(J)*SEC(11,I1)
CALL DEFLEX(V1,PHI(J),PHI(J+1),DX,DW,SDEFL,SDEFR)
DEF(J+1)=DEF(J)+DW
GOTO 900
600 K=K+1
DX1=XI(K)-DFLOAT(J-1)*DX
SDEFL=VL(J)*SEC(11,I1)
VT=(VL(J)+(VR(J)-VL(J))*DX1/DX)
SDEFR=VT*SEC(11,I1)
CALL DEFLEX(V1,PHI(J),PHI(K),DX1,DW1,SDEFL,SDEFR)
DEFI(K)=DEF(J)+DW1
DX2=DX-DX1
SDEFL=VT*SEC(11,I2)
SDEFR=VR(J)*SEC(11,I2)
CALL DEFLEX(V1,PHIR(K),PHI(J+1),DX2,DW2,SDEFL,SDEFR)

```

```

DEF(J+1)=DEF(J)+DW1+DW2
JT=I1
I1=I2
I2=JT
900 CONTINUE
COR=DEF(NNP)/XL
DO 732 J=2,NNP
732 DEF(J)=DEF(J)-(COR*DFLOAT(J-1)*DX)
DO 733 KK=1,KSUM
DEFI(KK)=DEFI(KK)-(COR*XI(KK))
733 CONTINUE
IF(IT GE 2) GOTO 735
RV=(DEF(2)-DEF(1))/DX
GOTO 175
735 RETURN
999 WRITE(6,1001)A,B
1001 FORMAT('O',***** STOP FOR UNACCEPTED VALUES OF A OR B//A =',
          *E12.5,' STOP FOR UNACCEPTED VALUE OF A OR B//A =',E12.5)
STOP
END
C V
C C
C THIS SUBROUTINE CALLED PROP
C C
SUBROUTINE PROP(C,A,T,SEC)
IMPLICIT REAL*8(A-H,O-Z)
DIMENSION SEC(4)
COMMON /PROPT/ ES,GS,AS,DS,SSI,XN,BC,TC,AVEI,WF,TF,WW
COMMON /SLIP/ SLIPK,TOLER,SETDS
BBC=BC*XN
EAC=ES*A
YS=O.5*DS
YC=DS+T
AT=A+AS
CG=(A*YC+AS*YS)/AT
WRITE(6,113)EAC,YS,YC,AT,CG
113, FORMAT(3X/,'VALUES ARE',E13.5)
IF(CG.GT.DS) GOTO 50
GOTO 60
50 TX=-AS/BBC+DSORT((AS/BBC)**2-(2.0*AS*(DS/2.-(DS+TC))/BBC))
CG=DS+TC-TX
YC=TX/2.
YS=YS-CG
AC=BBC*TX
C=BBC*TX**3/12.
A=AC
AT=AS+AC
EAC=ES*AC

```



```

60 TT=TC-TX/2.
   GOTO 70
   YS=YS-CG
   YC=YC-CG
70 TT=T.
   TI=SSI+C+AYC**2+AS*YS**2
   FACT=1./(AS/AT+AS*YS*YC/TI)
   ALPHA2=FACT/EAC
   ALPHA=DSQRT(SLIPK*ALPHA2)
   BETA=AS*YS*FACT/(EAC*TI)
   SEC(1)=ALPHA2
   SEC(2)=BETA
   SEC(3)=TI
   SEC(4)=A
   SEC(5)=YC
   SEC(6)=AT
   SEC(7)=YS
   SEC(8)=EAC
   SEC(9)=AS
   SEC(10)=ALPHA
   CALL QS(SEC,BBC,A,TT,CG)
   SEC(11)=SEC(11)/GS
   WRITE(6,101)CG
101 FORMAT(3X,'CENTROID OF COMPOSITE SECTION =',E15.5)
   RETURN
   END

```

C THIS SUBROUTINE IS CALLED QS
C
C
C

```

SUBROUTINE QS(SEC,BBC,A,T,CG)
  IMPLICIT REAL*8(A-H,O-Z)
  DIMENSION NSUB(4),WIDTH(4),ZR(4),DEPTH(4),SEC(1)
  COMMON /PROPT/ ES,GS,AS,DS,SSI,XN,BC,TC,AVEI,WF,TF,WW
  DATA NSUB/10,5,10,5/
  WIDTH(1)=BBC
  WIDTH(2)=WF
  WIDTH(3)=WW
  WIDTH(4)=WF
  DEPTH(1)=A/BBC
  DEPTH(2)=TF
  DEPTH(3)=DS-2.*TF
  DEPTH(4)=TF
  AW=WW*DEPTH(3)
  ZR(1)=DS+(T+DEPTH(1))/2.-CG
  ZR(2)=DS-CG
  ZR(3)=ZR(2)-TF

```

```

ZR(4)=ZR(3)-DEPTH(3)
Q1=0.0
FAC=0.0
DO 531 J=1,4
W=WIDTH(U)
Z=ZR(J)
DY=DEPTH(J)/DFLOAT(NSUB(J))
N=NSUB(J)
DO 532 I=1,N
YT=Z-OY*DFLOAT(I-1)
YB=YT-DY
Q2=Q1+W*(YT+YB)*(YT-YB)/2.
FAC=FAC+(Q1**2+Q2**2)*DY/W
Q1=Q2
532 CONTINUE
531 SEC(11)=FAC/((SEC(3))**2)
RETURN
END

```

FORM A SUBROUTINE FOR SLIP COMPUTATION

THIS SUB ROUTINE USES FOURTH ORDER DIFFERENTIAL EQ.

SOLUTION IS RUNGA-KUTTA METHOD

THIS SUBROUTINE IS CALLED RUNGA

```

SUBROUTINE RUNGA(S1,VL,VR,V1,SS,SFORCE,SO,SEC,DX)
IMPLICIT REAL*8(A-H,O-Z)
DIMENSION SEC(1)
DX=DX/2.
VC=(VR-VL)/2.+VL
C1S=V1
C1V=SEC(1)*OF(S1)-SEC(2)*VL
C2S=V1+C1V*DX
C2V=SEC(1)*OF(S1+C1S*DX)-SEC(2)*VC
C3S=V1+C2V*DX
C3V=SEC(1)*OF(S1+C2S*DX)-SEC(2)*VC
C4S=V1+C3V*DX
C4V=SEC(1)*OF(S1+C3S*DX)-SEC(2)*VR
SS=(C1S+2.*(C2S+C3S)+C4S)*DX/6.
V1=V1+(C1V+2.*(C2V+C3V)+C4V)*DX/6.
SQ=-OF(S1+SS)
SFORCE=0.5*(OF(S1)-SQ)*DX
RETURN

```

```

END
C
C
C
C THIS IS A SUBROUTINE TO COMPUTE DEFLECTION FOR NODAL POINTS
C THIS SUBROUTINE IS BASED ON A SECOND ORDER DIFFERENTIAL EQUATION
C SOLUTION THIS EQUATION IS BASED ON RUNGA-KUTTA METHOD
C THIS SUBROUTINE IS CALLED ***** DEFLEX *****
C
C

```

```

SUBROUTINE DEFLEX(V1,PHIL,PHIR,DX,DW,SDEFL,SDEFR)
IMPLICIT REAL*8(A-H,O-Z)
DV=0.5*(PHIL+PHIR)*DX
VR=V1+DV
DW=0.5*(V1-SDEFL-SDEFR+VR)*DX
V1=VR
RETURN
END

```

```

C
C
C
C FORM ASUBROUTINE FOR B.M. & SHEAR FOR UNIFORM LOAD
SUBROUTINE BMSU(Z,VL,VR,BM)
IMPLICIT REAL*8(A-H,O-Z)
COMMON /NODE/ NNP,NNP1,NNP2,IPRINT,KSUM,MAXIT
COMMON /DIST/ XL,XO,X,DX
DIMENSION VL(1),VR(1),BM(1)
X=0.000
DO 150 J=1,NNP1
VL(J)=(Z*XL/2.-Z*X)+VL(J)
VR(J)=(Z*XL/2.-Z*(X+DX))+VR(J)
BM(J)=(Z*XL*X/2.-Z*X*X/2.)+BM(J)
X=X+DX
CONTINUE
BM(NNP)=0.000
RETURN
END
150
C
C

```

```

SUBROUTINE CONC(VL,VR,BML,NODE,P,DP)
IMPLICIT REAL*8(A-H,O-Z)
COMMON /NODE/ NNP,NNP1,NNP2,IPRINT,KSUM,MAXIT
COMMON /DIST/ XL,XO,X,DX
DIMENSION VL(500),VR(500),BML(500)
NI=NODE-1

```

```

RR=-P*DP/XL
RL=P+RR
BML(1)=O.OOO
DO 200 J=1,NNP1
IF(J.GT.NI) GOTO 16
VL(J)=RL+VL(J)
VR(J)=RL+VR(J)
X=X+DX
BML(J+1)=RL*X+BML(J+1)
GOTO 200
16 VL(J)=RR+VL(J)
VR(J)=RR+VR(J)
X=X+DX
BML(J+1)=-RR*(XL-X)+BML(J+1)
200 CONTINUE
RETURN
END

```

C C C C C C C C C C

C THIS SUBROUTINE SOLVES THE SIMULTANEOUS EQ OF DEFLECTION

```

SUBROUTINE SYMSOL(A,B,MN,NEQ)
IMPLICIT REAL*8(A-H,O-Z)
DIMENSION A(MN,MN),B(MN)
M=NEQ-1
DO 67 N=1,NL
IF(A(N,N).LE.O.) GO TO 549
N1=N+1
DO 68 J=N1,NEQ
A(N,J)=A(N,J)/A(N,N)
DO 79 I=N1,NEQ
IF(A(N,I).EQ.O.) GO TO 73
DO 74 J=I,NEQ
A(I,J)=A(I,J)-A(I,N)*A(N,J)
A(J,I)=A(I,J)
B(I)=B(I)-A(N,I)*B(N)
74 B(N)=B(N)/A(N,N)
BACK SUBSTITUTION
M=NEQ
B(M)=B(M)/A(M,M)
DO 91 N=1,NL
M1=M

```

68 74 73 67 C

```

M=M-1
DO 91 J=M1,NEQ
  B(M)=B(M)-B(J)*A(M,J)
  GO TO 97
549 WRITE(6,1001)
  CALL EXIT
1001 FORMAT('ZERO OR NEGATIVE ELEMENT ON MAIN DAIGONAL OF
  *TRIANGULARIZED STIFFNESS MATRIX')
97 RETURN
  END
C
C SUBROUTINE TO COMPUTE THE ROOT OF AN EQUATION BY THE
C REGULA-FALSI METHOD
C
C
C SUBROUTINE REGULA(XLOW,XHIGH,EPS,MAX,X3)
  IMPLICIT REAL*8(A-H,D-Z)
  X1=XLOW
  X2=XHIGH
  Y1=F(X1)
  Y2=F(X2)
  M=0
  P=-1000.0
  IF(Y1*Y2.GT.O.O) RETURN
  WRITE(6,2001)X1,X2
  IF(DABS(Y1-Y2).LT.1.0E-06) GO TO 300
  X3=(Y1*X2-Y2*X1)/(Y1-Y2)
  TEST=DABS(X3-P)
  IF(TEST.LT.EPS) GO TO 300
  Y3=F(X3)
  P=X3
  IF(Y1*Y3.GT.O.O) GO TO 150
  X2=X3
  Y2=Y3
  GO TO 200
150 X1=X3
  Y1=Y3
200 M=M+1
  IF(M.LE.MAX) GO TO 100
  WRITE(6,2201)M
  STOP
300 WRITE(6,2202)X3,TEST,M
  RETURN
C
C 2001 FORMAT('O','A ROOT HAS BEEN LOCATED BETWEEN',F13.5,'AND',

```

```
*F13.5)
2201 FORMAT('*** POGRAM HAS EXCEEDED',I3,'ITERATE')
2202 FORMAT(' THE ROOT IS ',F13.5,' WITHIN AN INTERVAL OF ',
           F12.9,' IT TOOK ',I3,'ITERATE')
END
```

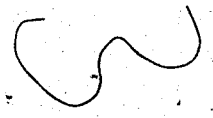
```
DOUBLE PRECISION FUNCTION F(Z)
IMPLICIT REAL*8(A-H,O-Z)
COMMON /PROPT/ ES,GS,AS,DS,SSI,XN,BC,TC,AVEI,WF,TF,WV
CAG=Z*TC*XN*(DS/2.+TC/2.)/(Z*TC*XN+AS)
CMAI=Z*XN*TC**3/12.
TCI=Z*XN*TC*((DS/2.+TC/2.)**2)
TTA=AS+(Z*XN*TC)
F=CMAI+TCI+SSI-(TTA*CAG**2)-AVEI
RETURN
END
```

```
C FORM A FUNCTION FOR COMPUTATION OF QF
C THIS FILE IS CALLED *** QFL ****
C THIS IS BASED ON LINEAR LOAD-SLIP BEHAVIOUR OF SHEAR CONNECTORS
C
```

```
DOUBLE PRECISION FUNCTION QF(DUMMY)
IMPLICIT REAL*8(A-H,O-Z)
COMMON /STUD/ CA,CB
COMMON /SLIP/ SLIPK,TOLER
GOTO 100
CONTINUE
IF(DUMMY.EQ.0.000.OR.SLIPK.EQ.0.000) GO TO 125
IF(DLOG(DABS(DUMMY))+DLOG(DABS(SLIPK)).GE.7400) GO TO 150
QF=SLIPK*DUMMY
RETURN
QF=DSIGN(1.0D74,SLIPK)*DSIGN(1.0D0,DUMMY)
RETURN
END
```

```
C FORM A FUNCTION FOR COMPUTATION OF QF
C THIS FILE IS CALLED *** QF ****
C THIS FILE IS BASED ON NON-LINEAR LOAD-SLIP BEHAVIOUR OF SHEAR CONNECTORS
C
```

```
DOUBLE PRECISION FUNCTION QF(DUMMY)
IMPLICIT REAL*8(A-H,O-Z)
COMMON /STUD/ CA,CB
COMMON /SLIP/ SLIPK,TOLER
D=DABS(DUMMY)
IF(DABS(D).LT.1.0D-10)GOTO 100
DD=DUMMY/DABS(DUMMY)
QF=DD*CA*(1.-DEXP(-CB*D))
```



100 RETURN
OF-SLIPK+DUMMAY
RETURN
END

F.4 List of Data and Outputs

C THIS DATA FILE IS FOR LINEAR LOAD-SLIP BEHAVIOUR

C

288.48.4.12.09.9.13.239.3.6.53.465.265.97,

3834250.0.29600000.0.1.0030.350000.0.001.30,

.5.4.3.0.

2000.0.0.0.288.0.-.000719.1.

1.0.0.

350.0.100.0.

49.144.0.28773.0.10E-06.

C THIS OUT-PUT IS BASED ON LINEAR LOAD-SLIP BEHAVIOUR OF SHEAR CONNECTORS

C

***** ECHO CHECK *****

LENGTH OF BEAM= 288.0000
 WIDTH OF CON. SLAB= 48.0000
 DEPTH OF CON. SLAB= 4.0000
 DEPTH OF ST. BEAM= 12.0800
 AREA OF ST. BEAM= 9.1300
 MOMENT OF INERTIA OF ST. BEAM= 239.0000
 ELEMENT LENGTH= 3.0000
 WIDTH OF FLANGE= 6.5300
 THICKNESS OF FLANGE= 0.4650
 WIDTH OF WEB= 0.2650
 NUMBER OF NODAL POINTS= 97

CONCRETE MODULUS= 0.3834E+07
 STEEL MODULUS= 0.2960E+08
 SHEAR MODULUS= 0.1000E+31
 SHEAR CONNECTOR MODULUS= 0.3500E+06
 TOLERANCE = 0.1000E-02
 MAXIT= 30

DIA OF REBARS= 0.5000
NUMBER OF REBARS= 4
CENTRID OF REBARS FROM TOP FLANGE= 3.0000

UNIFORM LOAD LBS PER FOOT= 2000.0000
STARTING COORDINATE= 0.0
ENDING COORDINATE= 288.0000 INITIAL SLIP= -0.000719 SETDS= 0.100000E+00

NO. OF CONCENTRATED LOAD= 0
NO. OF INTERIOR SUPPORT= 1
IPRINT= 0

*** CA= 0.35000E+03 *** CB= 0.10000E+03

*** SUPPORT CONDITION ***

NODE NO.= 49 LENGTH FROM LEFT END= 144.0000 LOAD= 29773.00000 INITIAL SLIP= 0.100000E-06

CENTROID OF COMPOSITE SECTION = 0.11930E+02

CENTROID OF COMPOSITE SECTION = 0.11930E+02

1*** NEW SECTION PROPERTIES ***

*** OUT-PUT OF SECTION PROPERTIES ***

ALPHA	=	0.13093E-07	0.13093E-07
BETA	=	-0.99864E-09	-0.99864E-09
TOTAL MOMENT OF INERTIA	=	0.70440E+03	0.70440E+03
AREA OF SLAB	=	0.24871E+02	0.24871E+02
CENTROIDAL DISTANCE OF CONCRETE	=	0.21603E+01	0.21603E+01

TOTAL AREA = 0.34001E+02 0.34001E+02
 CENTROIDAL DISTANCE OF STEEL = -0.58847E+01 -0.58847E+01
 PRODUCT OF ES AND CONC. AREA = 0.73618E+09 0.73618E+09
 AREA OF STEEL SECTION = 0.91300E+01 0.91300E+01
 ALPHA = 0.67694E-01 0.67694E-01
 SHEAR DEFLECTION FACTOR = 0.39295E-30 0.39295E-30
 OITT= 13 S(1)= 0.14499E-02 FORCE(NNP)= 0.34783E-04
 OITT= 3 S(1)= 0.108951E-06 FORCE(NNP)= -0.907666E-09
 SUPPORT REACTION= 0.298366E+05
 OITT= 3 S(1)= -0.144297E-02 FORCE(NNP)= -0.116396E-04
 OITT= 3 S(1)= 0.108951E-06 FORCE(NNP)= -0.436151E-08
 SUPPORT REACTION= 0.298355E+05
 OITT= 3 S(1)= -0.144310E-02 FORCE(NNP)= -0.317949E-04

NODE NO.	SHEAR FLOW	FORCE	SLIP	SLIP STRAIN
1	0.50508E+03	0.0	-0.14431E-02	0.0
2	0.50146E+03	-0.15098E+04	-0.14328E-02	0.64663E-05
3	0.49150E+03	-0.29993E+04	-0.14043E-02	0.11947E-04
4	0.47638E+03	-0.44511E+04	-0.13611E-02	0.16418E-04
5	0.45703E+03	-0.58512E+04	-0.13058E-02	0.20066E-04
6	0.43424E+03	-0.71881E+04	-0.12407E-02	0.23042E-04
7	0.40864E+03	-0.84524E+04	-0.11675E-02	0.25468E-04
8	0.38075E+03	-0.96365E+04	-0.10879E-02	0.27445E-04
9	0.35100E+03	-0.10734E+05	-0.10029E-02	0.29054E-04
10	0.31974E+03	-0.11740E+05	-0.91354E-03	0.30363E-04
11	0.28724E+03	-0.12651E+05	-0.82069E-03	0.31425E-04
12	0.25375E+03	-0.13462E+05	-0.72499E-03	0.32284E-04
13	0.21945E+03	-0.14172E+05	-0.62699E-03	0.32977E-04
14	0.18450E+03	-0.14778E+05	-0.52713E-03	0.33531E-04
15	0.14903E+03	-0.15278E+05	-0.42581E-03	0.33969E-04
16	0.11316E+03	-0.15671E+05	-0.32332E-03	0.34310E-04
17	0.76980E+02	-0.15957E+05	-0.21994E-03	0.34568E-04
18	0.40568E+02	-0.16133E+05	-0.11591E-03	0.34754E-04
19	0.39966E+01	-0.16200E+05	-0.11419E-04	0.34875E-04
20	-0.32669E+02	-0.16157E+05	0.93339E-04	0.34935E-04
21	-0.69368E+02	-0.16004E+05	0.19819E-03	0.34939E-04
22	-0.10604E+03	-0.15741E+05	0.30297E-03	0.34885E-04
23	-0.14263E+03	-0.15368E+05	0.40750E-03	0.34772E-04
24	-0.17906E+03	-0.14885E+05	0.51160E-03	0.34594E-04

25	-0.21527E+03	0.61507E-03	0.34346E-04
26	-0.25119E+03	0.71768E-03	0.34015E-04
27	-0.28671E+03	0.81916E-03	0.33589E-04
28	-0.32172E+03	0.91921E-03	0.33050E-04
29	-0.35611E+03	0.10175E-02	0.32376E-04
30	-0.38971E+03	0.11135E-02	0.31538E-04
31	-0.42234E+03	0.12067E-02	0.30502E-04
32	-0.45377E+03	0.12965E-02	0.29226E-04
33	-0.48372E+03	0.13820E-02	0.27656E-04
34	-0.51185E+03	0.14624E-02	0.25727E-04
35	-0.53774E+03	0.15364E-02	0.23360E-04
36	-0.56090E+03	0.16026E-02	0.20457E-04
37	-0.58070E+03	0.16591E-02	0.16988E-04
38	-0.59643E+03	0.17041E-02	0.12640E-04
39	-0.60712E+03	0.17346E-02	0.72445E-05
40	-0.61164E+03	0.17475E-02	0.69587E-06
41	-0.60858E+03	0.17388E-02	-0.73271E-05
42	-0.59625E+03	0.17036E-02	-0.17156E-04
43	-0.57356E+03	0.16359E-02	-0.29199E-04
44	-0.53493E+03	0.15284E-02	-0.43952E-04
45	-0.48026E+03	0.13722E-02	-0.62028E-04
46	-0.40468E+03	0.11562E-02	-0.84173E-04
47	-0.30349E+03	0.86712E-03	-0.11131E-03
48	-0.17093E+03	0.48838E-03	-0.14455E-03
49	0.57325E-01	-0.16350E-06	-0.16285E-03
50	0.17105E+03	-0.48872E-03	-0.14455E-03
51	0.30361E+03	-0.86747E-03	-0.11131E-03
52	0.40481E+03	-0.1566E-02	-0.84188E-04
53	0.48041E+03	-0.13725E-02	-0.62048E-04
54	0.53511E+03	-0.15289E-02	-0.43979E-04
55	0.57276E+03	-0.16365E-02	-0.29233E-04
56	0.59650E+03	-0.17043E-02	-0.17200E-04
57	0.60886E+03	-0.17397E-02	-0.73816E-05
58	0.61200E+03	-0.17486E-02	0.62821E-06
59	0.60756E+03	-0.17359E-02	0.71609E-05
60	0.59695E+03	-0.17056E-02	0.12538E-04
61	0.58128E+03	-0.16608E-02	0.17101E-04
62	0.56137E+03	-0.16039E-02	0.20549E-04
63	0.53813E+03	-0.15375E-02	0.23436E-04
64	0.51216E+03	-0.14633E-02	0.25789E-04
65	0.48397E+03	-0.13828E-02	0.27706E-04
66	0.45397E+03	-0.12971E-02	0.29267E-04
67	0.42251E+03	-0.12072E-02	0.30536E-04
68	0.38985E+03	-0.11139E-02	0.31566E-04
69	0.35622E+03	-0.10178E-02	0.32399E-04
70	0.32181E+03	-0.91946E-03	0.33069E-04
71	0.28678E+03	-0.81936E-03	0.33605E-04
72	0.25124E+03	-0.71783E-03	0.34029E-04
73	0.21532E+03	-0.61519E-03	0.34357E-04

INPT	LENGTH	SLIP	LEFT STRAIN	RIGHT STRAIN	LEFT CURVE	RIGHT CURVE	DEFLECTION
74	0.17909E+03	-0.14902E+05	-0.51169E-03	-0.34605E-04	0.12037E-05	0.12175E-05	-0.11352E-01
75	0.14265E+03	-0.15385E+05	-0.40756E-03	-0.34781E-04	0.12085E-05	0.12128E-05	-0.11354E-01
76	0.10605E+03	-0.15758E+05	-0.30300E-03	-0.34894E-04	0.12085E-05	0.12128E-05	-0.11354E-01
77	0.69369E+02	-0.16021E+05	-0.19820E-03	-0.34947E-04	0.12085E-05	0.12128E-05	-0.11354E-01
78	0.32661E+02	-0.16174E+05	-0.93318E-04	-0.34944E-04	0.12085E-05	0.12128E-05	-0.11354E-01
79	-0.40134E+01	-0.16217E+05	0.11467E-04	-0.34884E-04	0.12085E-05	0.12128E-05	-0.11354E-01
80	-0.40594E+02	-0.16150E+05	0.11598E-03	-0.34764E-04	0.12085E-05	0.12128E-05	-0.11354E-01
81	-0.77017E+02	-0.15974E+05	0.22005E-03	-0.34580E-04	0.12085E-05	0.12128E-05	-0.11354E-01
82	-0.11321E+03	-0.15689E+05	0.32346E-03	-0.34323E-04	0.12085E-05	0.12128E-05	-0.11354E-01
83	-0.14910E+03	-0.15295E+05	0.42599E-03	-0.33984E-04	0.12085E-05	0.12128E-05	-0.11354E-01
84	-0.18458E+03	-0.14795E+05	0.52737E-03	-0.33549E-04	0.12085E-05	0.12128E-05	-0.11354E-01
85	-0.21955E+03	-0.14188E+05	0.62728E-03	-0.32998E-04	0.12085E-05	0.12128E-05	-0.11354E-01
86	-0.25388E+03	-0.13478E+05	0.72536E-03	-0.32310E-04	0.12085E-05	0.12128E-05	-0.11354E-01
87	-0.28740E+03	-0.12666E+05	0.82114E-03	-0.31457E-04	0.12085E-05	0.12128E-05	-0.11354E-01
88	-0.31893E+03	-0.11755E+05	0.91410E-03	-0.30401E-04	0.12085E-05	0.12128E-05	-0.11354E-01
89	-0.35124E+03	-0.10749E+05	0.10036E-02	-0.29101E-04	0.12085E-05	0.12128E-05	-0.11354E-01
90	-0.38105E+03	-0.96502E+04	0.10887E-02	-0.27502E-04	0.12085E-05	0.12128E-05	-0.11354E-01
91	-0.40900E+03	-0.84651E+04	0.11686E-02	-0.25538E-04	0.12085E-05	0.12128E-05	-0.11354E-01
92	-0.43468E+03	-0.71995E+04	0.12419E-02	-0.23128E-04	0.12085E-05	0.12128E-05	-0.11354E-01
93	-0.45757E+03	-0.58613E+04	0.13073E-02	-0.20172E-04	0.12085E-05	0.12128E-05	-0.11354E-01
94	-0.47704E+03	-0.44593E+04	0.13630E-02	-0.16548E-04	0.12085E-05	0.12128E-05	-0.11354E-01
95	-0.49232E+03	-0.30053E+04	0.14066E-02	-0.12105E-04	0.12085E-05	0.12128E-05	-0.11354E-01
96	-0.50246E+03	-0.15131E+04	0.14356E-02	-0.66603E-05	0.12085E-05	0.12128E-05	-0.11354E-01
97	-0.50630E+03	-0.31795E+04	0.14466E-02	0.0	0.12085E-05	0.12128E-05	-0.11354E-01

NUMBER OF INFLECTION POINT= 2

INPT	LENGTH	SLIP	LEFT STRAIN	RIGHT STRAIN	LEFT CURVE	RIGHT CURVE	DEFLECTION
1	108.9691	0.16750E-02	0.15781E-04	0.15962E-04	0.12037E-05	0.12175E-05	-0.11352E-01
2	179.0309	-0.16768E-02	0.15845E-04	0.15900E-04	0.12085E-05	0.12128E-05	-0.11354E-01

FINAL OUT-PUT FOR SLIP,SLIP STRAIN,CURV,DEF.

NODAL NO	NODE LENGTH	SLIP	SLIP STRAIN	CURVATURE	DEFLECTION
1	0.0	-0.14431E-02	0.0	0.0	0.0
2	3.0000	-0.14328E-02	0.64663E-05	0.17640E-05	-0.19372E-02
3	6.0000	-0.14043E-02	0.11947E-04	0.33809E-05	-0.38588E-02
4	9.0000	-0.13611E-02	0.16418E-04	0.48489E-05	-0.57503E-02
5	12.0000	-0.13058E-02	0.20066E-04	0.61822E-05	-0.75985E-02
6	15.0000	-0.12407E-02	0.23042E-04	0.73922E-05	-0.93913E-02
7	18.0000	-0.11675E-02	0.25468E-04	0.84883E-05	-0.11118E-01
8	21.0000	-0.10879E-02	0.27445E-04	0.94782E-05	-0.12768E-01
9	24.0000	-0.10029E-02	0.29054E-04	0.10368E-04	-0.14334E-01
10	27.0000	-0.91354E-03	0.30363E-04	0.11163E-04	-0.15806E-01
11	30.0000	-0.82069E-03	0.31425E-04	0.11868E-04	-0.17178E-01
12	33.0000	-0.72499E-03	0.32284E-04	0.12485E-04	-0.18443E-01
13	36.0000	-0.62699E-03	0.32977E-04	0.13017E-04	-0.19596E-01

19	39.0000	-0.52713E-03	0.33531E-04	0.13467E-04	-0.20633E-01
20	42.0000	-0.42581E-03	0.33969E-04	0.13836E-04	-0.21548E-01
21	45.0000	-0.32332E-03	0.34310E-04	0.14125E-04	-0.22339E-01
22	48.0000	-0.21994E-03	0.34568E-04	0.14337E-04	-0.23002E-01
23	51.0000	-0.11591E-03	0.34754E-04	0.14471E-04	-0.23537E-01
24	54.0000	-0.11419E-04	0.34875E-04	0.14528E-04	-0.23942E-01
25	57.0000	0.93339E-04	0.34935E-04	0.14508E-04	-0.24217E-01
26	60.0000	0.19819E-03	0.34939E-04	0.14412E-04	-0.24361E-01
27	63.0000	0.30297E-03	0.34885E-04	0.14240E-04	-0.24375E-01
28	66.0000	0.40750E-03	0.34772E-04	0.13992E-04	-0.24262E-01
29	69.0000	0.51160E-03	0.34594E-04	0.13666E-04	-0.24022E-01
30	72.0000	0.61507E-03	0.34346E-04	0.13263E-04	-0.23660E-01
31	75.0000	0.71768E-03	0.34015E-04	0.12782E-04	-0.23179E-01
32	78.0000	0.81916E-03	0.33589E-04	0.12222E-04	-0.22583E-01
33	81.0000	0.91921E-03	0.33050E-04	0.11581E-04	-0.21877E-01
34	84.0000	0.10175E-02	0.32376E-04	0.10858E-04	-0.21067E-01
35	87.0000	0.11355E-02	0.31538E-04	0.10051E-04	-0.20159E-01
36	90.0000	0.12067E-02	0.30502E-04	0.91564E-05	-0.19162E-01
37	93.0000	0.12965E-02	0.29226E-04	0.81716E-05	-0.18081E-01
38	96.0000	0.13820E-02	0.27656E-04	0.70925E-05	-0.16928E-01
39	99.0000	0.14624E-02	0.25727E-04	0.59140E-05	-0.15711E-01
40	102.0000	0.15364E-02	0.23360E-04	0.46302E-05	-0.14441E-01
41	105.0000	0.16026E-02	0.20457E-04	0.32336E-05	-0.13130E-01
42	108.0000	0.16591E-02	0.16988E-04	0.17219E-05	-0.11790E-01
43	111.0000	0.17041E-02	0.12640E-04	0.71153E-07	-0.10433E-01
44	114.0000	0.17346E-02	0.72445E-05	-0.17314E-05	-0.90775E-02
45	117.0000	0.17475E-02	0.69587E-06	-0.36939E-05	-0.77377E-02
46	120.0000	0.17388E-02	-0.73271E-05	-0.58408E-05	-0.64315E-02
47	123.0000	0.17036E-02	-0.17156E-04	-0.81973E-05	-0.51783E-02
48	126.0000	0.16359E-02	-0.29199E-04	-0.10795E-04	-0.39994E-02
49	129.0000	0.15284E-02	-0.43952E-04	-0.13671E-04	-0.29184E-02
50	132.0000	0.13722E-02	-0.62028E-04	-0.16872E-04	-0.19611E-02
51	135.0000	0.11562E-02	-0.84173E-04	-0.20456E-04	-0.11565E-02
52	138.0000	0.86712E-03	-0.11131E-03	-0.24492E-04	-0.53698E-03
53	141.0000	0.48838E-03	-0.14455E-03	-0.29066E-04	-0.13914E-03
54	144.0000	-0.16350E-06	-0.16285E-03	-0.32572E-04	-0.49221E-06
55	147.0000	-0.48872E-03	-0.14455E-03	-0.29066E-04	-0.13922E-03
56	150.0000	-0.86747E-03	-0.11131E-03	-0.24493E-04	-0.53713E-03
57	153.0000	-0.11566E-02	-0.84188E-04	-0.20457E-04	-0.11567E-02
58	156.0000	-0.13726E-02	-0.62048E-04	-0.16874E-04	-0.19614E-02
59	159.0000	-0.15289E-02	-0.43979E-04	-0.13673E-04	-0.29188E-02
60	162.0000	-0.16365E-02	-0.29233E-04	-0.10797E-04	-0.40000E-02
61	165.0000	-0.17043E-02	-0.17200E-04	-0.82007E-05	-0.51790E-02
62	168.0000	-0.17397E-02	-0.73816E-05	-0.58449E-05	-0.64324E-02
63	171.0000	-0.17486E-02	0.62821E-06	-0.36991E-05	-0.77388E-02
64	174.0000	-0.17359E-02	0.71609E-05	-0.17378E-09	-0.90789E-02
65	177.0000	-0.17056E-02	0.12538E-04	0.63311E-07	-0.10435E-01
66	180.0000	-0.16608E-02	0.17101E-04	0.17304E-05	-0.11792E-01
67	183.0000	-0.16039E-02	0.20549E-04	0.32406E-05	-0.13132E-01

63	186.0000	-0.15375E-02	0.23436E-04	0.46360E-05	-0.14444E-01
64	189.0000	-0.14633E-02	0.25789E-04	0.59187E-05	-0.15714E-01
65	192.0000	-0.13828E-02	0.27706E-04	0.70963E-05	-0.16931E-01
66	195.0000	-0.12971E-02	0.29267E-04	0.81747E-05	-0.18085E-01
67	198.0000	-0.12072E-02	0.30536E-04	0.91590E-05	-0.19165E-01
68	201.0000	-0.11139E-02	0.31566E-04	0.10053E-04	-0.20163E-01
69	204.0000	-0.10178E-02	0.32399E-04	0.10860E-04	-0.21071E-01
70	207.0000	-0.91946E-03	0.33069E-04	0.11583E-04	-0.21881E-01
71	210.0000	-0.81936E-03	0.33605E-04	0.12223E-04	-0.22587E-01
72	213.0000	-0.71783E-03	0.34029E-04	0.12783E-04	-0.23183E-01
73	216.0000	-0.61519E-03	0.34357E-04	0.13264E-04	-0.23664E-01
74	219.0000	-0.51169E-03	0.34605E-04	0.13667E-04	-0.24026E-01
75	222.0000	-0.40756E-03	0.34781E-04	0.13992E-04	-0.24266E-01
76	225.0000	-0.30300E-03	0.34894E-04	0.14241E-04	-0.24379E-01
77	228.0000	-0.19820E-03	0.34947E-04	0.14413E-04	-0.24365E-01
78	231.0000	-0.93318E-04	0.34944E-04	0.14509E-04	-0.24221E-01
79	234.0000	0.11467E-04	0.34884E-04	0.14528E-04	-0.23946E-01
80	237.0000	0.11598E-03	0.34764E-04	0.14471E-04	-0.23541E-01
81	240.0000	0.22005E-03	0.34580E-04	0.14338E-04	-0.23006E-01
82	243.0000	0.32346E-03	0.34323E-04	0.14126E-04	-0.22342E-01
83	246.0000	0.42598E-03	0.33984E-04	0.13837E-04	-0.21551E-01
84	249.0000	0.52737E-03	0.33549E-04	0.13468E-04	-0.20636E-01
85	252.0000	0.62728E-03	0.32988E-04	0.13019E-04	-0.19600E-01
86	255.0000	0.72536E-03	0.32310E-04	0.12487E-04	-0.18447E-01
87	258.0000	0.82114E-03	0.31457E-04	0.11870E-04	-0.17181E-01
88	261.0000	0.91410E-03	0.30401E-04	0.11166E-04	-0.15809E-01
89	264.0000	0.10036E-02	0.29101E-04	0.10372E-04	-0.14337E-01
90	267.0000	0.10887E-02	0.27502E-04	0.94826E-05	-0.12771E-01
91	270.0000	0.11686E-02	0.25538E-04	0.84937E-05	-0.11121E-01
92	273.0000	0.12419E-02	0.23128E-04	0.73987E-05	-0.93938E-02
93	276.0000	0.13073E-02	0.20172E-04	0.61902E-05	-0.76007E-02
94	279.0000	0.13630E-02	0.16548E-04	0.48588E-05	-0.57521E-02
95	282.0000	0.14066E-02	0.12105E-04	0.33930E-05	-0.38601E-02
96	285.0000	0.14356E-02	0.66603E-05	0.17788E-05	-0.19379E-02
97	288.0000	0.14466E-02	0.0	0.0	0.54210E-19

2 2
 CENTROID OF COMPOSITE SECTION = 0.11930E+02
 CENTROID OF COMPOSITE SECTION = 0.67615E+01

1*** NEW SECTION PROPERTIES ***

*** OUT-PUT OF SECTION PROPERTIES ***

ALPHA = 0.13093E-07 0.58279E-07

BETA = -0.99864E-09 -0.12785E-08

TOTAL MOMENT OF INERTIA = 0.70440E+03 0.29818E+03

AREA OF SLAB = 0.24871E+02 0.78540E+00

CENTROIDAL DISTANCE OF CONCRETE = 0.21603E+01 0.83285E+01

TOTAL AREA = 0.34004E+02 0.99154E+01

CENTROIDAL DISTANCE OF STEEL = -0.58847E+01 -0.71645E+00

PRODUCT OF ES AND CONC. AREA = 0.73618E+09 0.23248E+08

AREA OF STEEL SECTION = 0.91300E+01 0.91300E+01

ALPHA = 0.67694E-01 0.14282E+00

SHEAR DEFLECTION FACTOR = 0.39295E-30 0.53367E-30

OITT= 31 S(1)= -0.144372E-02 FORCE(NNP)= 0.41379E-02

OITT= 3 S(1)= 0.108932E-06 FORCE(NNP)= -0.321175E-05

SUPPORT REACTION= 0.286861E+05

OITT= 31 S(1)= -0.156861E-02 FORCE(NNP)= 0.103718E-02

OITT= 3 S(1)= 0.108943E-06 FORCE(NNP)= -0.764985E-06

SUPPORT REACTION= 0.286858E+05

OITT= 3 S(1)= -0.156865E-02 FORCE(NNP)= 0.552407E-03

NODE NO.	SHEAR FLOW	FORCE	SLIP	SLIP STRAIN
1	0.54903E+03	0.0	-0.15686E-02	0.0
2	0.54541E+03	-0.16417E+04	-0.15683E-02	0.64625E-05
3	0.53546E+03	-0.32629E+04	-0.15299E-02	0.11939E-04
4	0.52034E+03	-0.48466E+04	-0.14867E-02	0.16406E-04
5	0.50100E+03	-0.63786E+04	-0.14314E-02	0.20049E-04
6	0.47823E+03	-0.78475E+04	-0.13664E-02	0.23019E-04
7	0.45266E+03	-0.92438E+04	-0.12933E-02	0.25439E-04
8	0.42481E+03	-0.10560E+05	-0.12137E-02	0.27408E-04
9	0.39511E+03	-0.11790E+05	-0.11289E-02	0.29008E-04
10	0.36389E+03	-0.12928E+05	-0.10397E-02	0.30306E-04
11	0.33146E+03	-0.13971E+05	-0.94704E-03	0.31354E-04
12	0.29805E+03	-0.14916E+05	-0.85157E-03	0.32197E-04
13	0.26385E+03	-0.15759E+05	-0.75385E-03	0.32870E-04
14	0.22902E+03	-0.16498E+05	-0.65435E-03	0.33400E-04
15	0.19371E+03	-0.17132E+05	-0.55346E-03	0.33808E-04

16	0.15803E+03	-0.17660E+05	-0.45150E-03	0.34113E-04
17	0.12207E+03	-0.18080E+05	-0.34878E-03	0.34326E-04
18	0.85940E+02	-0.18392E+05	-0.24554E-03	0.34457E-04
19	0.49712E+02	-0.18595E+05	-0.14203E-03	0.34511E-04
20	0.13467E+02	-0.18690E+05	-0.38477E-04	0.34490E-04
21	-0.22717E+02	-0.18676E+05	0.64905E-04	0.34393E-04
22	-0.58758E+02	-0.18554E+05	0.16788E-03	0.34216E-04
23	-0.94571E+02	-0.18324E+05	0.27020E-03	0.33952E-04
24	-0.13006E+03	-0.17987E+05	0.37159E-03	0.33590E-04
25	-0.16511E+03	-0.17544E+05	0.47174E-03	0.33115E-04
26	-0.19960E+03	-0.16997E+05	0.57029E-03	0.32508E-04
27	-0.23338E+03	-0.16348E+05	0.66679E-03	0.31742E-04
28	-0.2626E+03	-0.15598E+05	0.76074E-03	0.30788E-04
29	-0.29803E+03	-0.14752E+05	0.85152E-03	0.29604E-04
30	-0.32843E+03	-0.13812E+05	0.93836E-03	0.28142E-04
31	-0.35713E+03	-0.12784E+05	0.10204E-02	0.26341E-04
32	-0.38374E+03	-0.11672E+05	0.10964E-02	0.24128E-04
33	-0.40780E+03	-0.10485E+05	0.11651E-02	0.21410E-04
34	-0.42871E+03	-0.92304E+04	0.12249E-02	0.18075E-04
35	-0.44576E+03	-0.79187E+04	0.12736E-02	0.13985E-04
36	-0.45807E+03	-0.65630E+04	0.13088E-02	0.89708E-05
37	-0.46459E+03	-0.51790E+04	0.13274E-02	0.28247E-05
38	-0.46401E+03	-0.37861E+04	0.13257E-02	-0.47077E-05
39	-0.45471E+03	-0.24080E+04	0.12992E-02	-0.13804E-04
40	-0.41131E+03	-0.10850E+04	0.11752E-02	0.75713E-04
41	-0.34829E+03	-0.54329E+02	0.89499E-03	-0.49294E-04
42	-0.30779E+03	0.16384E+04	0.87940E-03	-0.32330E-04
43	-0.28035E+03	0.19206E+04	0.80101E-03	-0.23334E-04
44	-0.25879E+03	0.27293E+04	0.73839E-03	-0.20631E-04
45	-0.23703E+03	0.34730E+04	0.67723E-03	-0.23717E-04
46	-0.20898E+03	0.41421E+04	0.59709E-03	-0.33167E-04
47	-0.16738E+03	0.47066E+04	0.47822E-03	-0.50744E-04
48	-0.10243E+03	0.51113E+04	0.29263E-03	-0.79722E-04
49	0.37820E-01	0.52649E+04	-0.10806E-06	-0.97574E-04
50	0.10249E+03	0.51111E+04	-0.29282E-03	-0.79726E-04
51	0.16746E+03	0.47062E+04	-0.47846E-03	-0.50774E-04
52	0.20911E+03	0.41413E+04	-0.59746E-03	-0.33225E-04
53	0.23723E+03	0.34718E+04	-0.67781E-03	-0.23811E-04
54	0.25911E+03	0.27273E+04	-0.74033E-03	-0.20778E-04
55	0.28087E+03	0.19173E+04	-0.80248E-03	-0.23561E-04
56	0.30859E+03	0.10331E+04	-0.88169E-03	-0.32681E-04
57	0.34950E+03	0.45966E+02	-0.99857E-03	-0.49836E-04
58	0.41325E+03	-0.10982E+04	-0.11807E-02	-0.76521E-04
59	0.45672E+03	-0.24275E+04	-0.13049E-02	-0.13413E-04
60	0.46565E+03	-0.38111E+04	-0.13304E-02	-0.43870E-05
61	0.45593E+03	-0.52085E+04	-0.13312E-02	0.30866E-05
62	0.45917E+03	-0.65961E+04	-0.13119E-02	0.91848E-05
63	0.44665E+03	-0.79548E+04	-0.12761E-02	0.14160E-04
64	0.42943E+03	-0.92690E+04	-0.12269E-02	0.18218E-04

INPT	LENGTH	SLIP	LEFT STRAIN	RIGHT STRAIN	LEFT CURVE	RIGHT CURVE	DEFLECTION
65	0.40839E+03	-0.10526E+05	-0.11668E-02	-0.10978E-02	0.21527E-04	0.24224E-04	0.19204E-05
66	0.38422E+03	-0.11715E+05	-0.12827E+05	-0.10215E-02	0.26420E-04	0.28307E-04	-0.99908E-02
67	0.35752E+03	-0.13857E+05	-0.85224E-03	-0.93926E-03	0.29657E-04	0.30832E-04	-0.10000E-01
68	0.32874E+03	-0.14797E+05	-0.15644E+05	-0.76132E-03	0.31780E-04	0.32540E-04	
69	0.29828E+03	-0.16394E+05	-0.17044E+05	-0.57064E-03	0.33143E-04	0.33615E-04	
70	0.26646E+03	-0.17592E+05	-0.18335E+05	-0.47201E-03	0.33975E-04	0.34238E-04	
71	0.23354E+03	-0.18335E+05	-0.18602E+05	-0.27032E-03	0.34414E-04	0.34512E-04	
72	0.19972E+03	-0.18602E+05	-0.18774E+05	-0.16793E-03	0.34355E-04	0.34483E-04	
73	0.16520E+03	-0.18774E+05	-0.18938E+05	-0.64890E-04	0.34355E-04	0.34148E-04	
74	0.13012E+03	-0.18938E+05	-0.18643E+05	0.38556E-04	0.33849E-04	0.33448E-04	
75	0.94610E+02	-0.18643E+05	-0.14218E-03	0.14218E-03	0.32929E-04	0.32269E-04	
76	0.58775E+02	-0.18439E+05	0.24576E-03	0.24576E-03	0.31441E-04	0.30411E-04	
77	0.22711E+02	-0.18127E+05	0.34908E-03	0.34908E-03	0.29137E-04	0.27565E-04	
78	0.13495E+02	-0.17706E+05	0.45190E-03	0.45190E-03	0.25631E-04	0.23255E-04	
79	0.49763E+02	-0.17178E+05	0.55397E-03	0.55397E-03	0.20338E-04	0.16759E-04	
80	0.86017E+02	-0.16544E+05	0.65590E-03	0.65590E-03	0.12371E-04	0.69923E-05	
81	0.15817E+03	-0.15804E+05	0.75466E-03	0.75466E-03	0.0	0.0	
82	0.19389E+03	-0.15804E+05	0.85257E-03	0.85257E-03			
83	0.22925E+03	-0.14960E+05	0.94827E-03	0.94827E-03			
84	0.26413E+03	-0.14014E+05	0.10412E-02	0.10412E-02			
85	0.29840E+03	-0.12970E+05	0.11307E-02	0.11307E-02			
86	0.33189E+03	-0.11830E+05	0.12160E-02	0.12160E-02			
87	0.36442E+03	-0.10597E+05	0.12961E-02	0.12961E-02			
88	0.39576E+03	-0.92786E+04	0.13698E-02	0.13698E-02			
89	0.42561E+03	-0.78790E+04	0.14357E-02	0.14357E-02			
90	0.45364E+03	-0.64061E+04	0.14918E-02	0.14918E-02			
91	0.47944E+03	-0.50248E+03	0.15362E-02	0.15362E-02			
92	0.50248E+03	-0.52215E+03	0.15661E-02	0.15661E-02			
93	0.52215E+03	-0.53767E+03	0.15782E-02	0.15782E-02			
94	0.53767E+03	-0.54813E+03					
95	0.53767E+03	-0.54813E+03					
96	0.54813E+03	-0.55241E-03					
97	-0.55241E-03						

NUMBER OF INFLECTION POINT= 2

INPT	LENGTH	SLIP	LEFT STRAIN	RIGHT STRAIN	LEFT CURVE	RIGHT CURVE	DEFLECTION
1	115.8670	0.12676E-02	-0.19964E-04	-0.87539E-04	-0.15227E-05	-0.19204E-05	-0.99908E-02
2	172.1330	-0.12742E-02	-0.88459E-04	-0.19524E-04	-0.19406E-05	-0.14892E-05	-0.10000E-01

FINAL OUT-PUT FOR SLIP, SLIP STRAIN, CURV, DEF.

NODAL NO	MODE	LENGTH	SLIP	LEFT STRAIN	RIGHT STRAIN	CURVATURE	DEFLECTION
1	0.0	0.0	-0.15686E-02	0.0	0.0	0.0	0.0
2	3.0000	3.0000	-0.15583E-02	0.64625E-05	0.18464E-05	0.18464E-05	-0.21571E-02
3	6.0000	6.0000	-0.15299E-02	0.11939E-04	0.35457E-05	0.35457E-05	-0.42979E-02
4	9.0000	9.0000	-0.14867E-02	0.16406E-04	0.50961E-05	0.50961E-05	-0.64071E-02

5	12.0000	-0.14314E-02	0.20049E-04	0.65117E-05	-0.84707E-02
6	15.0000	-0.13664E-02	0.23019E-04	0.78040E-05	-0.10476E-01
7	18.0000	-0.12933E-02	0.25439E-04	0.89824E-05	-0.12411E-01
8	21.0000	-0.12137E-02	0.27408E-04	0.10054E-04	-0.14266E-01
9	24.0000	-0.11289E-02	0.29008E-04	0.11026E-04	-0.16031E-01
10	27.0000	-0.10397E-02	0.30306E-04	0.11903E-04	-0.17696E-01
11	30.0000	-0.94704E-03	0.31354E-04	0.12689E-04	-0.19255E-01
12	33.0000	-0.85157E-03	0.32197E-04	0.13388E-04	-0.20699E-01
13	36.0000	-0.75385E-03	0.32870E-04	0.14001E-04	-0.22023E-01
14	38.0000	-0.65435E-03	0.33400E-04	0.14532E-04	-0.23222E-01
15	42.0000	-0.55346E-03	0.33808E-04	0.14981E-04	-0.24289E-01
16	45.0000	-0.45150E-03	0.34113E-04	0.15351E-04	-0.25223E-01
17	48.0000	-0.34878E-03	0.34326E-04	0.15642E-04	-0.26018E-01
18	51.0000	-0.24554E-03	0.34457E-04	0.15854E-04	-0.26672E-01
19	54.0000	-0.14203E-03	0.34511E-04	0.15989E-04	-0.27184E-01
20	57.0000	-0.38477E-04	0.34490E-04	0.16046E-04	-0.27553E-01
21	60.0000	0.64905E-04	0.34393E-04	0.16025E-04	-0.27777E-01
22	63.0000	0.16788E-03	0.34216E-04	0.15926E-04	-0.27857E-01
23	66.0000	0.27020E-03	0.33952E-04	0.15749E-04	-0.27794E-01
24	69.0000	0.37159E-03	0.33590E-04	0.15492E-04	-0.27589E-01
25	72.0000	0.47174E-03	0.33115E-04	0.15155E-04	-0.27245E-01
26	75.0000	0.57028E-03	0.32508E-04	0.14735E-04	-0.26765E-01
27	78.0000	0.66679E-03	0.31742E-04	0.14232E-04	-0.26152E-01
28	81.0000	0.76074E-03	0.30788E-04	0.13642E-04	-0.25412E-01
29	84.0000	0.85152E-03	0.29604E-04	0.12963E-04	-0.24549E-01
30	87.0000	0.93836E-03	0.28142E-04	0.12190E-04	-0.23569E-01
31	90.0000	0.10204E-02	0.26341E-04	0.11320E-04	-0.22480E-01
32	93.0000	0.10964E-02	0.24128E-04	0.10347E-04	-0.21290E-01
33	96.0000	0.11651E-02	0.21410E-04	0.92628E-05	-0.20006E-01
34	99.0000	0.12249E-02	0.18075E-04	0.80598E-05	-0.18640E-01
35	102.0000	0.12736E-02	0.13985E-04	0.67273E-05	-0.17201E-01
36	105.0000	0.13088E-02	0.89708E-05	0.52524E-05	-0.15702E-01
37	108.0000	0.13274E-02	0.28247E-05	0.36191E-05	-0.14156E-01
38	111.0000	0.13257E-02	0.47077E-05	0.18082E-05	-0.12578E-01
39	114.0000	0.12992E-02	0.13804E-04	0.19393E-06	-0.10984E-01
40	117.0000	0.11752E-02	0.75713E-04	0.28924E-05	-0.93908E-02
41	120.0000	0.99499E-03	0.49294E-04	0.57434E-05	-0.78256E-02
42	123.0000	0.87940E-03	0.32330E-04	0.89718E-05	-0.63129E-02
43	126.0000	0.80101E-03	0.23334E-04	0.12545E-04	-0.48818E-02
44	129.0000	0.73939E-03	0.20631E-04	0.16426E-04	-0.35642E-02
45	132.0000	0.67723E-03	0.23717E-04	0.20604E-04	-0.23951E-02
46	135.0000	0.59709E-03	0.33167E-04	0.25092E-04	-0.14122E-02
47	138.0000	0.47822E-03	0.50744E-04	0.29928E-04	-0.65591E-03
48	141.0000	0.29263E-03	0.79722E-04	0.35184E-04	-0.16990E-03
49	144.0000	0.10806E-06	0.97574E-04	0.40366E-04	-0.37136E-06
50	147.0000	-0.29282E-03	0.79726E-04	0.35184E-04	-0.17082E-03
51	150.0000	-0.47846E-03	0.50774E-04	0.29928E-04	-0.65775E-03
52	153.0000	-0.59746E-03	0.33225E-04	0.25093E-04	-0.14150E-02
53	156.0000	-0.67781E-03	0.23811E-04	0.20606E-04	-0.23988E-02

54	159.0000	-0.74033E-03	-0.20778E-04	-0.16429E-04	-0.35689E-02
55	162.0000	-0.80248E-03	-0.23561E-04	0.12550E-04	-0.48874E-02
56	165.0000	-0.88169E-03	-0.32681E-04	0.89795E-05	-0.63196E-02
57	168.0000	-0.99857E-03	-0.49836E-04	-0.57553E-05	-0.78334E-02
58	171.0000	-0.11807E-02	-0.76524E-04	-0.29101E-05	-0.93998E-02
59	174.0000	-0.13049E-02	-0.13413E-04	-0.16405E-06	-0.10994E-01
60	177.0000	-0.13304E-02	-0.43870E-05	0.18327E-05	-0.12589E-01
61	180.0000	-0.13312E-02	0.30866E-05	0.36391E-05	-0.14168E-01
62	183.0000	-0.13119E-02	0.91848E-05	0.52687E-05	-0.15715E-01
63	186.0000	-0.12761E-02	0.14160E-04	0.67406E-05	-0.17214E-01
64	189.0000	-0.12269E-02	0.18218E-04	0.80707E-05	-0.18653E-01
65	192.0000	-0.11668E-02	0.21527E-04	0.92717E-05	-0.20020E-01
66	195.0000	-0.10978E-02	0.24224E-04	0.10354E-04	-0.21304E-01
67	198.0000	-0.10215E-02	0.26420E-04	0.11326E-04	-0.22495E-01
68	201.0000	-0.93926E-03	0.28207E-04	0.12195E-04	-0.23584E-01
69	204.0000	-0.85224E-03	0.29657E-04	0.12967E-04	-0.24563E-01
70	207.0000	-0.76132E-03	0.30832E-04	0.13645E-04	-0.25426E-01
71	210.0000	-0.65724E-03	0.31780E-04	0.14235E-04	-0.26167E-01
72	213.0000	-0.57064E-03	0.32540E-04	0.14738E-04	-0.26779E-01
73	216.0000	-0.47201E-03	0.33143E-04	0.15157E-04	-0.27259E-01
74	219.0000	-0.37178E-03	0.33615E-04	0.15494E-04	-0.27603E-01
75	222.0000	-0.27032E-03	0.33975E-04	0.15750E-04	-0.27808E-01
76	225.0000	-0.16793E-03	0.34238E-04	0.15928E-04	-0.27871E-01
77	228.0000	-0.64890E-04	0.34414E-04	0.16027E-04	-0.27790E-01
78	231.0000	0.38556E-04	0.34512E-04	0.16047E-04	-0.27566E-01
79	234.0000	0.14218E-03	0.34535E-04	0.15990E-04	-0.27198E-01
80	237.0000	0.24576E-03	0.34483E-04	0.15856E-04	-0.26685E-01
81	240.0000	0.34908E-03	0.34356E-04	0.15644E-04	-0.26031E-01
82	243.0000	0.45190E-03	0.34148E-04	0.15354E-04	-0.25235E-01
83	246.0000	0.55397E-03	0.33849E-04	0.14984E-04	-0.24302E-01
84	249.0000	0.65500E-03	0.33448E-04	0.14536E-04	-0.23234E-01
85	252.0000	0.75466E-03	0.32929E-04	0.14006E-04	-0.22035E-01
86	255.0000	0.85257E-03	0.32269E-04	0.13393E-04	-0.20710E-01
87	258.0000	0.94827E-03	0.31441E-04	0.12696E-04	-0.19265E-01
88	261.0000	0.10412E-02	0.30411E-04	0.11911E-04	-0.17706E-01
89	264.0000	0.11307E-02	0.29137E-04	0.11036E-04	-0.16040E-01
90	267.0000	0.12160E-02	0.27565E-04	0.10066E-04	-0.14275E-01
91	270.0000	0.12961E-02	0.25631E-04	0.89970E-05	-0.12420E-01
92	273.0000	0.13698E-02	0.23255E-04	0.78220E-05	-0.10484E-01
93	276.0000	0.14357E-02	0.20338E-04	0.65337E-05	-0.84773E-02
94	279.0000	0.14918E-02	0.16759E-04	0.51231E-05	-0.64124E-02
95	282.0000	0.15362E-02	0.12371E-04	0.35787E-05	-0.43017E-02
96	285.0000	0.15661E-02	0.69923E-05	0.18869E-05	-0.21591E-02
97	288.0000	0.15782E-02	0.0	0.0	0.54210E-19

3.

CENTROID OF COMPOSITE SECTION = 0.11930E+02

CENTROID OF COMPOSITE SECTION = 0.67615E+01
 OA ROOT HAS BEEN LOCATED BETWEEN 1.00000AND 48.00000
 THE ROOT IS 13.20813WITHIN AN INTERVAL OF 0.00050 IT TOOK 11ITERATE

3
 1

CENTROID OF COMPOSITE SECTION = 0.94918E+01

CENTROID OF COMPOSITE SECTION = 0.94918E+01
 1*** NEW SECTION PROPERTIES ***

*** OUT-PUT OF SECTION PROPERTIES ***

ALPHA = 0.17449E-07 0.17449E-07

BETA = -0.10954E-08 -0.10954E-08

TOTAL MOMENT OF INERTIA = 0.50129E+03 0.50129E+03

AREA OF SLAB = 0.68437E+01 0.68437E+01

CENTROIDAL DISTANCE OF CONCRETE = 0.45982E+01 0.45982E+01

TOTAL AREA = 0.15974E+02 0.15974E+02

CENTROIDAL DISTANCE OF STEEL = -0.34468E+01 -0.34468E+01

PRODUCT OF ES AND CONC.AREA = 0.20257E+09 0.20257E+09

AREA OF STEEL SECTION = 0.91300E+01 0.91300E+01

ALPHAK = 0.78149E-01 0.78149E-01

SHEAR DEFLECTION FACTOR = 0.45312E-30 0.45312E-30
 OITT= 4 S(1)= -0.134964E-02 FORCE(NNP)= 0.928647E-03
 OITT= 4 S(1)= 0.896770E-07 FORCE(NNP)= -0.244821E-06

SUPPORT REACTION= 0.299361E+05
 OITT= 3 S(1)= -0.123751E-02 FORCE(NNP)= 0.105841E-03
 OITT= 3 S(1)= 0.896771E-07 FORCE(NNP)= -0.562287E-07

SUPPORT REACTION= 0.299109E+05
 OITT= 3 S(1)= -0.123978E-02 FORCE(NNP)= 0.373346E-03
 OITT= 3 S(1)= 0.896771E-07 FORCE(NNP)= 0.693258E-07

SUPPORT REACTION= 0.299113E+05
 OIIT= 3 S(1)= -0.123974E-02

FORCE(MNP)= 0.460790E-04

NODE NO.	SHEAR FLOW	FORCE	SLIP	SLIP STRAIN
1	0.43391E+03	0.0	-0.12397E-02	0.0
2	0.43050E+03	-0.12966E+04	-0.12300E-02	0.60294E-05
3	0.42125E+03	-0.25742E+04	-0.12036E-02	0.11015E-04
4	0.40737E+03	-0.38171E+04	-0.11639E-02	0.14958E-04
5	0.38983E+03	-0.50130E+04	-0.11138E-02	0.18077E-04
6	0.36941E+03	-0.61518E+04	-0.10554E-02	0.20543E-04
7	0.34669E+03	-0.72260E+04	-0.99055E-03	0.22493E-04
8	0.32217E+03	-0.82293E+04	-0.92049E-03	0.24034E-04
9	0.29622E+03	-0.91569E+04	-0.84635E-03	0.25522E-04
10	0.26914E+03	-0.10005E+05	-0.76898E-03	0.26213E-04
11	0.24117E+03	-0.10770E+05	-0.68907E-03	0.26972E-04
12	0.21250E+03	-0.11451E+05	-0.60715E-03	0.27569E-04
13	0.18328E+03	-0.12045E+05	-0.52366E-03	0.28037E-04
14	0.15362E+03	-0.12550E+05	-0.43893E-03	0.28403E-04
15	0.12363E+03	-0.12966E+05	-0.35324E-03	0.28687E-04
16	0.93381E+02	-0.13291E+05	-0.26680E-03	0.28905E-04
17	0.62933E+02	-0.13525E+05	-0.17981E-03	0.29068E-04
18	0.32339E+02	-0.13669E+05	-0.92398E-04	0.29185E-04
19	0.16448E+01	-0.13720E+05	-0.46995E-05	0.29263E-04
20	-0.29113E+01	-0.13678E+05	0.83179E-04	0.29306E-04
21	-0.59898E+02	-0.13545E+05	0.17114E-03	0.29317E-04
22	-0.90679E+02	-0.13319E+05	0.25908E-03	0.29296E-04
23	-0.12142E+03	-0.13001E+05	0.34692E-03	0.29242E-04
24	-0.15209E+03	-0.12591E+05	0.43454E-03	0.29153E-04
25	-0.18264E+03	-0.12089E+05	0.52183E-03	0.29022E-04
26	-0.21303E+03	-0.11495E+05	0.60867E-03	0.28843E-04
27	-0.24321E+03	-0.10811E+05	0.69489E-03	0.28607E-04
28	-0.27311E+03	-0.10036E+05	0.78031E-03	0.28299E-04
29	-0.30264E+03	-0.91726E+04	0.86469E-03	0.27903E-04
30	-0.33170E+03	-0.82211E+04	0.94773E-03	0.27397E-04
31	-0.36017E+03	-0.71833E+04	0.10291E-02	0.26754E-04
32	-0.38789E+03	-0.60612E+04	0.11083E-02	0.25937E-04
33	-0.41464E+03	-0.48574E+04	0.11847E-02	0.24902E-04
34	-0.44018E+03	-0.35752E+04	0.12577E-02	0.23591E-04
35	-0.46418E+03	-0.22186E+04	0.13262E-02	0.21933E-04
36	-0.48624E+03	-0.79296E+03	0.13893E-02	0.19834E-04
37	-0.50584E+03	0.69516E+03	0.14452E-02	0.17277E-04
38	-0.52234E+03	0.22378E+04	0.14924E-02	0.13872E-04
39	-0.53491E+03	0.38237E+04	0.15283E-02	0.96074E-05
40	-0.54252E+03	0.54398E+04	0.15500E-02	0.42463E-05
41	-0.54383E+03	0.70693E+04	0.15538E-02	0.25309E-05
42	-0.53720E+03	0.86909E+04	0.15349E-02	-0.11098E-04

43	-0.52053E+03	0.10277E+05	0.14872E-02	-0.21929E-04
44	-0.49115E+03	0.11795E+05	0.14033E-02	-0.35621E-04
45	-0.44572E+03	0.13200E+05	0.12735E-02	-0.52931E-04
46	-0.38005E+03	0.14439E+05	0.10857E-02	-0.74813E-04
47	-0.28861E+03	0.15442E+05	0.82461E-03	-0.10248E-03
48	-0.16473E+03	0.16122E+05	0.47084E-03	-0.13745E-03
49	0.33060E-01	0.16369E+05	-0.94458E-07	-0.15698E-03
50	0.16485E+03	0.16122E+05	-0.47103E-03	-0.13745E-03
51	0.28868E+03	0.15441E+05	-0.82481E-03	-0.10248E-03
52	0.38007E+03	0.14438E+05	-0.10859E-02	-0.74824E-04
53	0.44581E+03	0.13189E+05	-0.12738E-02	-0.52947E-04
54	0.49126E+03	0.11794E+05	-0.14036E-02	-0.35643E-04
55	0.52066E+03	0.10276E+05	-0.14876E-02	-0.21958E-04
56	0.53738E+03	0.85888E+04	-0.15354E-02	-0.11136E-04
57	0.54405E+03	0.70667E+04	-0.15544E-02	-0.25786E-05
58	0.54279E+03	0.54364E+04	-0.15508E-02	0.41855E-05
59	0.53528E+03	0.38194E+04	-0.15293E-02	0.95302E-05
60	0.52278E+03	0.23233E+04	-0.14936E-02	0.13775E-04
61	0.50639E+03	0.68820E+03	-0.14467E-02	0.17391E-04
62	0.48664E+03	-0.80128E+03	-0.13904E-02	0.19925E-04
63	0.46450E+03	-0.22280E+04	-0.13271E-02	0.22004E-04
64	0.44043E+03	-0.35854E+04	-0.12584E-02	0.23648E-04
65	0.41484E+03	-0.48683E+04	-0.11853E-02	0.24947E-04
66	0.38604E+03	-0.60726E+04	-0.11087E-02	0.25973E-04
67	0.36030E+03	-0.71952E+04	-0.10294E-02	0.26782E-04
68	0.33180E+03	-0.82333E+04	-0.94801E-03	0.27420E-04
69	0.30272E+03	-0.91851E+04	-0.86490E-03	0.27921E-04
70	0.27317E+03	-0.10048E+05	-0.78048E-03	0.28313E-04
71	0.24326E+03	-0.10824E+05	-0.69502E-03	0.28618E-04
72	0.21307E+03	-0.11508E+05	-0.60877E-03	0.28853E-04
73	0.18267E+03	-0.12102E+05	-0.52181E-03	0.29030E-04
74	0.15211E+03	-0.12604E+05	-0.43459E-03	0.29159E-04
75	0.12143E+03	-0.13014E+05	-0.34695E-03	0.29248E-04
76	0.90686E+02	-0.13332E+05	-0.25910E-03	0.29301E-04
77	0.59901E+02	-0.13558E+05	-0.17114E-03	0.29322E-04
78	0.28110E+02	-0.13692E+05	-0.83171E-04	0.29311E-04
79	-0.16529E+01	-0.13733E+05	0.47225E-05	0.29268E-04
80	-0.32353E+02	-0.13682E+05	0.92438E-04	0.29181E-04
81	-0.62953E+02	-0.13539E+05	0.17987E-03	0.29074E-04
82	-0.93409E+02	-0.13304E+05	0.26588E-03	0.28913E-04
83	-0.12367E+03	-0.12879E+05	0.35334E-03	0.28697E-04
84	-0.15367E+03	-0.12563E+05	0.43906E-03	0.28415E-04
85	-0.18334E+03	-0.12057E+05	0.52383E-03	0.28052E-04
86	-0.21258E+03	-0.11463E+05	0.60738E-03	0.27587E-04
87	-0.24127E+03	-0.10783E+05	0.68935E-03	0.26995E-04
88	-0.26927E+03	-0.10017E+05	0.76934E-03	0.26242E-04
89	-0.29638E+03	-0.91683E+04	0.84681E-03	0.25288E-04
90	-0.32238E+03	-0.82401E+04	0.92107E-03	0.24080E-04
91	-0.34695E+03	-0.72361E+04	0.99129E-03	0.22551E-04

92	-0.36973E+03	-0.61611E+04	0.10564E-02	0.20616E-04
93	-0.39024E+03	-0.50211E+04	0.11150E-02	0.18169E-04
94	-0.40789E+03	-0.38240E+04	0.11654E-02	0.15075E-04
95	-0.42190E+03	-0.25793E+04	0.12054E-02	0.11163E-04
96	-0.43133E+03	-0.12994E+04	0.12324E-02	0.62160E-05
97	-0.43485E+03	0.46073E-04	0.12427E-02	0.0

NUMBER OF INFLECTION POINT= 2

INPT	LENGTH	SLIP	LEFT STRAIN	RIGHT STRAIN	LEFT CURVE	RIGHT CURVE	DEFLECTION
1	108.5203	0.14541E-02	0.16797E-04	0.17009E-04	0.10544E-05	0.10677E-05	-0.14016E-01
2	179.4797	-0.14556E-02	0.16892E-04	0.16915E-04	0.10604E-05	0.10618E-05	-0.14017E-01

FINAL OUT-PUT FOR SLIP,SLIP STRAIN,CURV,DEF.

NODAL.NO	NODE.LENGTH	SLIP	SLIP STRAIN	CURVATURE	DEFLECTION
1	0.0	-0.12397E-02	0.0	0.0	0.0
2	3.0000	-0.12300E-02	0.60294E-05	0.21565E-05	-0.24134E-02
3	6.0000	-0.12036E-02	0.11015E-04	0.41465E-05	-0.48077E-02
4	9.0000	-0.11639E-02	0.14958E-04	0.59698E-05	-0.71651E-02
5	12.0000	-0.11138E-02	0.18077E-04	0.76404E-05	-0.94691E-02
6	15.0000	-0.10544E-02	0.20543E-04	0.91689E-05	-0.11705E-01
7	18.0000	-0.99055E-03	0.22483E-04	0.10564E-04	-0.13858E-01
8	21.0000	-0.92049E-03	0.24034E-04	0.11832E-04	-0.15917E-01
9	24.0000	-0.84635E-03	0.25252E-04	0.12979E-04	-0.17869E-01
10	27.0000	-0.76898E-03	0.26213E-04	0.14009E-04	-0.19705E-01
11	30.0000	-0.68907E-03	0.26972E-04	0.14925E-04	-0.21415E-01
12	33.0000	-0.60715E-03	0.27569E-04	0.15729E-04	-0.22991E-01
13	36.0000	-0.52366E-03	0.28037E-04	0.16425E-04	-0.24425E-01
14	39.0000	-0.43893E-03	0.28403E-04	0.17013E-04	-0.25712E-01
15	42.0000	-0.35324E-03	0.28687E-04	0.17494E-04	-0.26846E-01
16	45.0000	-0.26680E-03	0.28905E-04	0.17871E-04	-0.27823E-01
17	48.0000	-0.17981E-03	0.29068E-04	0.18143E-04	-0.28640E-01
18	51.0000	-0.92398E-04	0.29185E-04	0.18311E-04	-0.29293E-01
19	54.0000	-0.46995E-05	0.29263E-04	0.18375E-04	-0.29782E-01
20	57.0000	0.83179E-04	0.29306E-04	0.18336E-04	-0.30105E-01
21	60.0000	0.17114E-03	0.29317E-04	0.18194E-04	-0.30264E-01
22	63.0000	0.25908E-03	0.29296E-04	0.17949E-04	-0.30259E-01
23	66.0000	0.34692E-03	0.29242E-04	0.17601E-04	-0.30093E-01
24	69.0000	0.43454E-03	0.29153E-04	0.17149E-04	-0.29769E-01
25	72.0000	0.52183E-03	0.29022E-04	0.16594E-04	-0.29291E-01
26	75.0000	0.60867E-03	0.28843E-04	0.15935E-04	-0.28663E-01
27	78.0000	0.69489E-03	0.28607E-04	0.15171E-04	-0.27892E-01
28	81.0000	0.78031E-03	0.28299E-04	0.14301E-04	-0.26986E-01
29	84.0000	0.86469E-03	0.27903E-04	0.13325E-04	-0.25950E-01
30	87.0000	0.94773E-03	0.27397E-04	0.12241E-04	-0.24795E-01
31	90.0000	0.10291E-02	0.26754E-04	0.11047E-04	-0.23530E-01

32	93.0000	0.11083E-02	0.25937E-04	0.97407E-05	-0.22166E-01
33	96.0000	0.11847E-02	0.24902E-04	0.83199E-05	-0.20714E-01
34	99.0000	0.12577E-02	0.23591E-04	0.67808E-05	-0.19188E-01
35	102.0000	0.13262E-02	0.21933E-04	0.51187E-05	-0.17601E-01
36	105.0000	0.13893E-02	0.19834E-04	0.33280E-05	-0.15968E-01
37	108.0000	0.14452E-02	0.17277E-04	0.14074E-05	-0.14306E-01
38	111.0000	0.14924E-02	0.13872E-04	-0.66757E-06	-0.12631E-01
39	114.0000	0.15283E-02	0.96074E-05	-0.28976E-05	-0.10962E-01
40	117.0000	0.15500E-02	0.42463E-05	-0.52975E-05	-0.93204E-02
41	120.0000	0.15538E-02	0.25309E-05	-0.78874E-05	-0.77265E-02
42	123.0000	0.15349E-02	-0.11098E-04	-0.10691E-04	-0.62041E-02
43	126.0000	0.14872E-02	-0.21829E-04	-0.13737E-04	-0.47785E-02
44	129.0000	0.14033E-02	-0.35621E-04	-0.17065E-04	-0.34772E-02
45	132.0000	0.12735E-02	-0.52931E-04	-0.20720E-04	-0.23302E-02
46	135.0000	0.10857E-02	-0.74813E-04	-0.24764E-04	-0.13705E-02
47	138.0000	0.82461E-03	-0.10248E-03	-0.29271E-04	-0.63474E-03
48	141.0000	0.47084E-03	-0.13745E-03	-0.34339E-04	-0.16369E-03
49	144.0000	-0.84458E-07	-0.15698E-03	-0.38538E-04	0.26788E-06
50	147.0000	-0.47103E-03	-0.13745E-03	-0.34339E-04	-0.16372E-03
51	150.0000	-0.82481E-03	-0.10248E-03	-0.29272E-04	-0.63481E-03
52	153.0000	-0.10859E-02	-0.74824E-04	-0.24764E-04	-0.13706E-02
53	156.0000	-0.12738E-02	-0.52947E-04	-0.20721E-04	-0.23303E-02
54	159.0000	-0.14036E-02	-0.35643E-04	-0.17066E-04	-0.34774E-02
55	162.0000	-0.14876E-02	-0.21958E-04	-0.13739E-04	-0.47788E-02
56	165.0000	-0.15354E-02	-0.11136E-04	-0.10693E-04	-0.62045E-02
57	168.0000	-0.15544E-02	0.41855E-05	-0.78904E-05	-0.77270E-02
58	171.0000	-0.15508E-02	0.95302E-05	-0.29025E-05	-0.93210E-02
59	174.0000	-0.14936E-02	0.13775E-04	-0.67371E-06	-0.10863E-01
60	177.0000	-0.14467E-02	0.17391E-04	0.14145E-05	-0.14307E-01
61	180.0000	-0.13904E-02	0.19925E-04	0.33337E-05	-0.15970E-01
62	183.0000	-0.13271E-02	0.23004E-04	0.51232E-05	-0.17603E-01
63	186.0000	-0.12584E-02	0.23648E-04	0.67844E-05	-0.19190E-01
64	189.0000	-0.11853E-02	0.24947E-04	0.83227E-05	-0.20716E-01
65	192.0000	-0.11087E-02	0.25973E-04	0.97429E-05	-0.22168E-01
66	195.0000	-0.10294E-02	0.26782E-04	0.11048E-04	-0.23532E-01
67	198.0000	-0.94801E-03	0.27420E-04	0.12242E-04	-0.24797E-01
68	201.0000	-0.86490E-03	0.27921E-04	0.13326E-04	-0.25952E-01
69	204.0000	-0.78048E-03	0.28313E-04	0.14302E-04	-0.26988E-01
70	207.0000	-0.69502E-03	0.28618E-04	0.15171E-04	-0.27895E-01
71	210.0000	-0.60877E-03	0.28853E-04	0.15935E-04	-0.28665E-01
72	213.0000	-0.52191E-03	0.29030E-04	0.16595E-04	-0.29293E-01
73	216.0000	-0.43459E-03	0.29159E-04	0.17150E-04	-0.29771E-01
74	219.0000	-0.34695E-03	0.29248E-04	0.17601E-04	-0.30095E-01
75	222.0000	-0.25910E-03	0.29301E-04	0.17949E-04	-0.30262E-01
76	225.0000	-0.17114E-03	0.29322E-04	0.18194E-04	-0.30266E-01
77	228.0000	-0.83171E-04	0.29311E-04	0.18336E-04	-0.30107E-01
78	231.0000	0.47225E-05	0.29268E-04	0.18375E-04	-0.29784E-01
79	234.0000	0.92438E-04	0.29191E-04	0.18311E-04	-0.29295E-01
80	237.0000				

81	240.0000	0.17987E-03	0.29074E-04	0.18143E-04	-0.28642E-01
82	243.0000	0.26688E-03	0.28913E-04	0.17871E-04	-0.27826E-01
83	246.0000	0.35334E-03	0.28697E-04	0.17495E-04	-0.26849E-01
84	249.0000	0.43906E-03	0.28415E-04	0.17013E-04	-0.25714E-01
85	252.0000	0.52383E-03	0.28052E-04	0.16426E-04	-0.24427E-01
86	255.0000	0.60738E-03	0.27587E-04	0.15730E-04	-0.22993E-01
87	258.0000	0.68935E-03	0.26995E-04	0.14926E-04	-0.21417E-01
88	261.0000	0.76934E-03	0.26242E-04	0.14011E-04	-0.19707E-01
89	264.0000	0.84681E-03	0.25288E-04	0.12981E-04	-0.17871E-01
90	267.0000	0.92107E-03	0.24080E-04	0.11835E-04	-0.15919E-01
91	270.0000	0.99129E-03	0.22551E-04	0.10568E-04	-0.13860E-01
92	273.0000	0.10564E-02	0.20616E-04	0.91735E-05	-0.11706E-01
93	276.0000	0.11150E-02	0.18169E-04	0.76462E-05	-0.94706E-02
94	279.0000	0.11654E-02	0.15075E-04	0.59772E-05	-0.71663E-02
95	282.0000	0.12054E-02	0.11163E-04	0.41557E-05	-0.48086E-02
96	285.0000	0.12324E-02	0.62160E-05	0.21683E-05	-0.24139E-02
97	288.0000	0.12427E-02	0.0	0.0	0.54210E-19

C THIS DATAFILE IS FOR NON-LINEAR LOAD-SLIP BEHAVIOUR

C C

288.0000	48.0000	4.0000	12.0900	9.1300	239.0000	3.0000	6.5300	0.4650	0.2650	97
0.3834E+07	0.2960E+08	0.1000E+31	0.3500E+06	0.1000E-0230						
0.5000	4	3.0000								
2000.0000000000	0.0			288.000000000000						0.100000000000
1	0									
150.0000	144.	29835.	0.108951E-06							

C THIS QU-PUT IS BASED ON NON-LINEAR LOAD-SLIP BEHAVIOUR OF SHEAR CONNECTORS

C C

***** ECHO CHECK *****

LENGTH OF BEAM= 288.0000
 WIDTH OF CON. SLAB= 48.0000
 DEPTH OF CON. SLAB= 4.0000
 DEPTH OF ST. BEAM= 12.0900
 AREA OF ST. BEAM= 9.1300
 MOMENT OF INERTIA OF ST. BEAM= 239.0000
 ELEMENT LENGTH= 3.0000
 WIDTH OF FLANGE= 6.5300
 THICKNESS OF FLANGE= 0.4650
 WIDTH OF WEB= 0.2650
 NUMBER OF NODAL POINTS= 97

CONCRETE MODULUS= 0.3834E+07
 STEEL MODULUS= 0.2960E+08
 SHEAR MODULUS= 0.1000E+31

SHEAR CONNECTOR MODULUS= 0.3500E+06
 TOLERANCE = 0.0000E-02
 MAXIT = 30

DIA OF REBARS= 0.5000
 NUMBER OF REBARS= 4
 CENTRID OF REBARS FROM TOP FLANGE= 3.0000

UNIFORM LOAD LBS PER FOOT= 2000.0000
 STARTING COORDINATE= 0.0
 ENDING COORDINATE= 288.0000 INITIAL SLIP= -0.001443 SETDS= 0.100000E+00

NO. OF CONCENTRATED LOAD= 0
 NO. OF INTERIOR SUPPORT= 1
 IPRINT= 0

*** CA= 0.35000E+03 *** CB= 0.10000E+03

*** SUPPORT CONDITION ***

1 1
 NODE NO. = 49 LENGTH FROM LEFT END= 144.0000 LOAD= 29835.00000 INITIAL SLIP= 0.108951E-06

CENTROID OF COMPOSITE SECTION = 0.11930E+02

CENTROID OF COMPOSITE SECTION = 0.11930E+02

1*** NEW SECTION PROPERTIES ***

*** OUT-PUT OF SECTION PROPERTIES ***

ALPHA	=	0.13093E-07	0.13093E-07
BETA	=	-0.99865E-09	-0.99865E-09
TOTAL MOMENT OF INERTIA	=	0.70439E+03	0.70439E+03

AREA OF SLAB = 0.24869E+02 0.24869E+02
 CENTROIDAL DISTANCE OF CONCRETE = 0.21604E+01 0.21604E+01
 TOTAL AREA = 0.33999E+02 0.33999E+02
 CENTROIDAL DISTANCE OF STEEL = -0.58846E+01 -0.58846E+01
 PRODUCT OF ES AND CONC.AREA = 0.73613E+09 0.73613E+09
 AREA OF STEEL SECTION = 0.91300E+01 0.91300E+01
 ALPHA = 0.67694E-01 0.67694E-01
 SHEAR DEFLECTION FACTOR = 0.39295E-30 0.39295E-30
 OITT= 31 S(1)= -0.577239E-02 FORCE(NNP)= 0.399512E+05
 OITT= 31 S(1)= 0.435804E-06 FORCE(NNP)= -0.214585E+03
 SUPPORT REACTION= 0.302048E+05 0.302048E+05
 OITT= 7 S(1)= -0.595070E-02 FORCE(NNP)= 0.748781E-03
 OITT= 15 S(1)= 0.989944E-06 FORCE(NNP)= -0.981741E-03
 SUPPORT REACTION= 0.296435E+05 0.296435E+05
 OITT= 8 S(1)= -0.671906E-02 FORCE(NNP)= 0.148803E-03
 OITT= 3 S(1)= 0.989939E-06 FORCE(NNP)= 0.246029E-03
 SUPPORT REACTION= 0.296958E+05 0.296958E+05
 OITT= 10 S(1)= -0.664613E-02 FORCE(NNP)= 0.228661E-03
 OITT= 3 S(1)= 0.989945E-06 FORCE(NNP)= 0.117494E-05
 SUPPORT REACTION= 0.296906E+05 0.296906E+05
 OITT= 6 S(1)= -0.665342E-02 FORCE(NNP)= 0.148781E-03
 OITT= 1 S(1)= 0.989945E-06 FORCE(NNP)= -0.148259E-04
 SUPPORT REACTION= 0.296911E+05 0.296911E+05
 OITT= 5 S(1)= -0.665270E-02 FORCE(NNP)= 0.516570E-04
 OITT= 1 S(1)= 0.989945E-06 FORCE(NNP)= 0.211173E-03
 SUPPORT REACTION= 0.296911E+05 0.296911E+05
 OITT= 4 S(1)= -0.665277E-02 FORCE(NNP)= 0.465523E-03

NODE NO. SHEAR FLOW FORCE SLIP SLIP STRAIN

1	0.17005E+03	0.0	-0.66528E-02	0.0
2	0.16951E+03	-0.50934E+03	-0.66224E-02	0.19762E-04
3	0.16791E+03	-0.10155E+04	-0.65342E-02	0.38318E-04
4	0.16531E+03	-0.15153E+04	-0.63925E-02	0.55459E-04
5	0.16175E+03	-0.20059E+04	-0.62014E-02	0.71222E-04
6	0.15725E+03	-0.24844E+04	-0.59651E-02	0.85648E-04
7	0.15182E+03	-0.29480E+04	-0.56876E-02	0.98766E-04
8	0.14548E+03	-0.33939E+04	-0.53726E-02	0.11062E-03
9	0.13822E+03	-0.38194E+04	-0.50238E-02	0.12124E-03
10	0.13004E+03	-0.42218E+04	-0.46451E-02	0.13067E-03
11	0.12095E+03	-0.45983E+04	-0.42398E-02	0.13894E-03
12	0.11092E+03	-0.49461E+04	-0.38115E-02	0.14609E-03
13	0.98964E+02	-0.52625E+04	-0.33633E-02	0.15215E-03
14	0.88070E+02	-0.55445E+04	-0.28986E-02	0.15716E-03
15	0.61478E+02	-0.57895E+04	-0.24203E-02	0.16116E-03
16	0.46795E+02	-0.59946E+04	-0.19316E-02	0.16418E-03
17	0.6795E+02	-0.61570E+04	-0.14352E-02	0.16627E-03
18	0.31210E+02	-0.62740E+04	-0.93401E-03	0.16745E-03
19	0.14750E+02	-0.63429E+04	-0.43056E-03	0.16776E-03
20	-0.25300E+01	-0.63612E+04	0.72548E-04	0.16723E-03
21	-0.19486E+02	-0.63282E+04	0.57284E-03	0.16367E-03
22	-0.35448E+02	-0.62458E+04	0.10678E-02	0.16588E-03
23	-0.50401E+02	-0.61171E+04	0.15549E-02	0.16058E-03
24	-0.64339E+02	-0.59449E+04	0.20313E-02	0.15655E-03
25	-0.77261E+02	-0.57325E+04	0.24942E-02	0.15155E-03
26	-0.89168E+02	-0.54829E+04	0.29406E-02	0.14554E-03
27	-0.10007E+03	-0.51990E+04	0.33674E-02	0.13848E-03
28	-0.10996E+03	-0.48840E+04	0.37715E-02	0.13033E-03
29	-0.11887E+03	-0.45407E+04	0.41494E-02	0.12106E-03
30	-0.12678E+03	-0.41723E+04	0.44978E-02	0.11061E-03
31	-0.13371E+03	-0.37815E+04	0.48131E-02	0.98960E-04
32	-0.13965E+03	-0.33715E+04	0.50916E-02	0.86064E-04
33	-0.14459E+03	-0.29451E+04	0.53295E-02	0.71883E-04
34	-0.14853E+03	-0.25055E+04	0.55229E-02	0.56379E-04
35	-0.15143E+03	-0.20555E+04	0.56677E-02	0.39510E-04
36	-0.15325E+03	-0.15985E+04	0.57599E-02	0.21237E-04
37	-0.15394E+03	-0.11377E+04	0.57952E-02	0.16112E-05
38	-0.15343E+03	-0.67645E+03	0.57693E-02	-0.19301E-04
39	-0.15163E+03	-0.21885E+03	0.56780E-02	-0.42218E-04
40	-0.14839E+03	0.23117E+03	0.55160E-02	-0.66577E-04
41	-0.14354E+03	0.66908E+03	0.52785E-02	-0.92592E-04
42	-0.13687E+03	0.10897E+04	0.49604E-02	-0.12033E-03
43	-0.12809E+03	0.14871E+04	0.45565E-02	-0.14988E-03
44	-0.11682E+03	0.18545E+04	0.40612E-02	-0.18131E-03
45	-0.10258E+03	0.21836E+04	0.34686E-02	-0.21495E-03
46	-0.84752E+02	0.24646E+04	0.27727E-02	-0.25032E-03
47	-0.62489E+02	0.26855E+04	0.19667E-02	-0.28817E-03
48	-0.34685E+02	0.28312E+04	0.10436E-02	-0.32852E-03
49	0.15326E+00	0.28830E+04	-0.43799E-05	-0.34934E-03

50	0.34962E+02	0.218304E+04	-0.10524E-02	-0.32853E-03
51	0.62742E+02	0.26838E+04	-0.19755E-02	-0.28820E-03
52	0.84988E+02	0.24622E+04	-0.27816E-02	-0.25035E-03
53	0.10281E+03	0.21805E+04	-0.34776E-02	-0.21479E-03
54	0.11703E+03	0.18508E+04	-0.40703E-02	-0.18136E-03
55	0.12829E+03	0.14828E+04	-0.45658E-02	-0.14993E-03
56	0.13707E+03	0.10847E+04	-0.49699E-02	-0.12040E-03
57	0.14374E+03	0.66348E+03	-0.52882E-02	-0.92666E-04
58	0.14859E+03	0.22498E+03	-0.55259E-02	-0.66658E-04
59	0.15183E+03	-0.22565E+03	-0.56881E-02	-0.42307E-04
60	0.15364E+03	-0.68386E+03	-0.57798E-02	-0.19398E-04
61	0.15414E+03	-0.11457E+04	-0.58052E-02	0.18911E-05
62	0.15343E+03	-0.16071E+04	-0.57692E-02	0.21509E-04
63	0.15158E+03	-0.20646E+04	-0.56762E-02	0.39776E-04
64	0.14868E+03	-0.25150E+04	-0.55305E-02	0.56638E-04
65	0.14474E+03	-0.29552E+04	-0.53363E-02	0.72136E-04
66	0.13978E+03	-0.33819E+04	-0.50977E-02	0.86312E-04
67	0.13833E+03	-0.37924E+04	-0.48185E-02	0.99204E-04
68	0.12689E+03	-0.41834E+04	-0.45025E-02	0.11085E-03
69	0.11896E+03	-0.45522E+04	-0.41534E-02	0.12129E-03
70	0.11004E+03	-0.48957E+04	-0.37747E-02	0.13057E-03
71	0.10013E+03	-0.52109E+04	-0.33700E-02	0.13871E-03
72	0.89217E+02	-0.54950E+04	-0.29424E-02	0.14577E-03
73	0.77293E+02	-0.57447E+04	-0.24954E-02	0.15177E-03
74	0.64354E+02	-0.59572E+04	-0.20318E-02	0.15677E-03
75	0.50396E+02	-0.61293E+04	-0.15547E-02	0.16080E-03
76	0.35422E+02	-0.62581E+04	-0.10670E-02	0.16390E-03
77	0.19436E+02	-0.63403E+04	-0.57134E-03	0.16611E-03
78	0.24540E+01	-0.63732E+04	-0.70362E-04	0.16746E-03
79	-0.14846E+02	-0.63546E+04	0.43344E-03	0.16799E-03
80	-0.31324E+02	-0.62853E+04	0.93759E-03	0.16768E-03
81	-0.46925E+02	-0.61680E+04	0.14395E-03	0.16651E-03
82	-0.61623E+02	-0.60051E+04	0.19366E-02	0.16443E-03
83	-0.75398E+02	-0.57996E+04	0.24261E-02	0.16141E-03
84	-0.88241E+02	-0.55541E+04	0.29051E-02	0.15742E-03
85	-0.10015E+03	-0.52716E+04	0.33706E-02	0.15241E-03
86	-0.12115E+03	-0.49547E+04	0.38196E-02	0.14636E-03
87	-0.12115E+03	-0.46063E+04	0.42488E-02	0.13922E-03
88	-0.13026E+03	-0.42291E+04	0.46549E-02	0.13096E-03
89	-0.13845E+03	-0.38261E+04	0.50346E-02	0.12154E-03
90	-0.14571E+03	-0.33998E+04	0.53842E-02	0.11093E-03
91	-0.15207E+03	-0.29532E+04	0.57001E-02	0.99083E-04
92	-0.15751E+03	-0.24888E+04	0.59787E-02	0.85973E-04
93	-0.16202E+03	-0.20095E+04	0.62160E-02	0.71559E-04
94	-0.16560E+03	-0.15181E+04	0.64080E-02	0.55807E-04
95	-0.16821E+03	-0.10174E+04	0.65508E-02	0.38678E-04
96	-0.16983E+03	-0.51033E+03	0.66401E-02	0.20134E-04
97	-0.17039E+03	0.46552E-03	0.66716E-02	0.0

NUMBER OF INFLECTION POINT= 2

INPT	LENGTH	SLIP	LEFT STRAIN	RIGHT STRAIN	LEFT STRAIN	RIGHT STRAIN	LEFT CURVE	RIGHT CURVE	DEFLECTION
1	108.8342	0.57867E-02	-0.10778E-04	-0.10778E-04	-0.10639E-04	-0.10639E-04	-0.82205E-06	-0.81145E-06	-0.17289E-01
2	178.1658	-0.57973E-02	-0.10739E-04	-0.10739E-04	-0.10493E-04	-0.10493E-04	-0.81908E-06	-0.80034E-06	-0.17314E-01

FINAL OUT-PUT FOR SLIP,SLIP STRAIN,CURV,DEF.

NODAL NO	NODE LENGTH	SLIP	SLIP STRAIN	CURVATURE	DEFLECTION
1	0.0	0.66528E-02	0.0	0.0	0.0
2	3.0000	-0.66224E-02	0.19762E-04	0.27886E-05	-0.32326E-02
3	8.0000	-0.65342E-02	0.38318E-04	0.54132E-05	-0.64404E-02
4	9.0000	-0.63925E-02	0.55459E-04	0.78579E-05	-0.95999E-02
5	12.0000	-0.62014E-02	0.71222E-04	0.10126E-04	-0.12689E-01
6	15.0000	-0.59651E-02	0.85646E-04	0.12219E-04	-0.15688E-01
7	18.0000	-0.56876E-02	0.98766E-04	0.14142E-04	-0.18576E-01
8	21.0000	-0.53726E-02	0.11062E-03	0.15895E-04	-0.21338E-01
9	24.0000	-0.50238E-02	0.12124E-03	0.17483E-04	-0.23958E-01
10	27.0000	-0.46451E-02	0.13067E-03	0.18908E-04	-0.26420E-01
11	30.0000	-0.42398E-02	0.13894E-03	0.20172E-04	-0.28713E-01
12	33.0000	-0.38115E-02	0.14609E-03	0.21279E-04	-0.30824E-01
13	36.0000	-0.33633E-02	0.15215E-03	0.22231E-04	-0.32744E-01
14	39.0000	-0.28986E-02	0.15716E-03	0.23032E-04	-0.34464E-01
15	42.0000	-0.24203E-02	0.16116E-03	0.23683E-04	-0.35978E-01
16	45.0000	-0.19316E-02	0.16418E-03	0.24187E-04	-0.37279E-01
17	48.0000	-0.14352E-02	0.16627E-03	0.24548E-04	-0.38362E-01
18	51.0000	-0.93401E-03	0.16745E-03	0.24768E-04	-0.39225E-01
19	54.0000	-0.43056E-03	0.16776E-03	0.24850E-04	-0.39865E-01
20	57.0000	0.72548E-04	0.16723E-03	0.24797E-04	-0.40281E-01
21	60.0000	0.57284E-03	0.16588E-03	0.24608E-04	-0.40475E-01
22	63.0000	0.10678E-02	0.16367E-03	0.24282E-04	-0.40448E-01
23	66.0000	0.15549E-02	0.16058E-03	0.23816E-04	-0.40202E-01
24	69.0000	0.20313E-02	0.15655E-03	0.23207E-04	-0.39743E-01
25	72.0000	0.24842E-02	0.15155E-03	0.22452E-04	-0.39075E-01
26	75.0000	0.29406E-02	0.14554E-03	0.21549E-04	-0.38205E-01
27	78.0000	0.33674E-02	0.13848E-03	0.20493E-04	-0.37141E-01
28	81.0000	0.37715E-02	0.13033E-03	0.19282E-04	-0.35894E-01
29	84.0000	0.41493E-02	0.12106E-03	0.17913E-04	-0.34473E-01
30	87.0000	0.44978E-02	0.11061E-03	0.16384E-04	-0.32892E-01
31	90.0000	0.48131E-02	0.98960E-04	0.14690E-04	-0.31163E-01
32	93.0000	0.50916E-02	0.86064E-04	0.12829E-04	-0.29302E-01
33	96.0000	0.53295E-02	0.71883E-04	0.10798E-04	-0.27327E-01
34	99.0000	0.55229E-02	0.56379E-04	0.85948E-05	-0.25255E-01
35	102.0000	0.56677E-02	0.39510E-04	0.62153E-05	-0.23105E-01
36	105.0000	0.57599E-02	0.21237E-04	0.36567E-05	-0.20900E-01
37	108.0000	0.57952E-02	0.16112E-05	0.92302E-06	-0.18663E-01
38	111.0000	0.57693E-02	-0.19301E-04	-0.19807E-05	-0.16416E-01

39	114.0000	0.56780E-02	-0.42218E-04	-0.51094E-05	-0.14180E-01
40	117.0000	0.55160E-02	-0.66577E-04	-0.84199E-05	-0.12008E-01
41	120.0000	0.52785E-02	-0.92592E-04	-0.11929E-04	-0.99039E-02
42	123.0000	0.49604E-02	-0.12033E-03	-0.15641E-04	-0.79072E-02
43	126.0000	0.45565E-02	-0.14988E-03	-0.19563E-04	-0.60518E-02
44	128.0000	0.40612E-02	-0.18131E-03	-0.23701E-04	-0.43730E-02
45	132.0000	0.34686E-02	-0.21475E-03	-0.28064E-04	-0.29079E-02
46	135.0000	0.27727E-02	-0.25032E-03	-0.32661E-04	-0.16959E-02
47	138.0000	0.19667E-02	-0.28817E-03	-0.37505E-04	-0.77850E-03
48	141.0000	0.10436E-02	-0.32852E-03	-0.42610E-04	-0.19918E-03
49	144.0000	-0.43789E-05	-0.34934E-03	-0.46298E-04	-0.16394E-06
50	147.0000	-0.10524E-02	-0.32853E-03	-0.42611E-04	-0.20123E-03
51	150.0000	-0.19755E-02	-0.28820E-03	-0.37506E-04	-0.78261E-03
52	153.0000	-0.27816E-02	-0.25035E-03	-0.32663E-04	-0.17021E-02
53	156.0000	-0.34776E-02	-0.21479E-03	-0.28067E-04	-0.29162E-02
54	159.0000	-0.40703E-02	-0.18136E-03	-0.23705E-04	-0.43834E-02
55	162.0000	-0.45658E-02	-0.14993E-03	-0.19567E-04	-0.60544E-02
56	165.0000	-0.49699E-02	-0.12040E-03	-0.15646E-04	-0.79220E-02
57	168.0000	-0.52882E-02	-0.92666E-04	-0.11934E-04	-0.99209E-02
58	171.0000	-0.55259E-02	-0.66658E-04	-0.84261E-05	-0.12028E-01
59	174.0000	-0.56881E-02	-0.42307E-04	-0.51162E-05	-0.14211E-01
60	177.0000	-0.57798E-02	-0.19398E-04	-0.19881E-05	-0.16440E-01
61	180.0000	-0.58052E-02	0.18911E-05	0.94437E-06	-0.18690E-01
62	183.0000	-0.57692E-02	0.21509E-04	0.36775E-05	-0.20929E-01
63	186.0000	-0.56762E-02	0.39776E-04	0.62356E-05	-0.23136E-01
64	188.0000	-0.55305E-02	0.56638E-04	0.86146E-05	-0.25287E-01
65	192.0000	-0.53363E-02	0.72136E-04	0.10818E-04	-0.27361E-01
66	195.0000	-0.50977E-02	0.86312E-04	0.12848E-04	-0.29338E-01
67	198.0000	-0.48185E-02	0.99204E-04	0.14708E-04	-0.31200E-01
68	201.0000	-0.45025E-02	0.11085E-03	0.16402E-04	-0.32930E-01
69	204.0000	-0.41534E-02	0.12129E-03	0.17931E-04	-0.34513E-01
70	207.0000	-0.37747E-02	0.13057E-03	0.19300E-04	-0.35934E-01
71	210.0000	-0.33700E-02	0.13871E-03	0.20510E-04	-0.37182E-01
72	213.0000	-0.29424E-02	0.14577E-03	0.21566E-04	-0.38246E-01
73	216.0000	-0.24954E-02	0.15177E-03	0.22470E-04	-0.39117E-01
74	219.0000	-0.20318E-02	0.15677E-03	0.23224E-04	-0.39785E-01
75	222.0000	-0.15547E-02	0.16080E-03	0.23833E-04	-0.40245E-01
76	225.0000	-0.10670E-02	0.16390E-03	0.24299E-04	-0.40490E-01
77	228.0000	-0.57134E-03	0.16611E-03	0.24625E-04	-0.40517E-01
78	231.0000	-0.70362E-04	0.16746E-03	0.24814E-04	-0.40323E-01
79	234.0000	0.43344E-03	0.16799E-03	0.24868E-04	-0.39906E-01
80	237.0000	0.93759E-03	0.16768E-03	0.24787E-04	-0.39265E-01
81	240.0000	0.14395E-02	0.16651E-03	0.24567E-04	-0.38401E-01
82	243.0000	0.19366E-02	0.16443E-03	0.24206E-04	-0.37317E-01
83	246.0000	0.24261E-02	0.16141E-03	0.23702E-04	-0.36015E-01
84	249.0000	0.29051E-02	0.15742E-03	0.23051E-04	-0.34500E-01
85	252.0000	0.33706E-02	0.15241E-03	0.22252E-04	-0.32778E-01
86	255.0000	0.38196E-02	0.14636E-03	0.21300E-04	-0.30857E-01
87	258.0000	0.42488E-02	0.13922E-03	0.20194E-04	-0.28743E-01

88	261.0000	0.46549E-02	0.13095E-03	0.18930E-04	-0.26449E-01
89	264.0000	0.50346E-02	0.12154E-03	0.17506E-04	-0.23984E-01
90	267.0000	0.53842E-02	0.11093E-03	0.15919E-04	-0.21362E-01
91	270.0000	0.57001E-02	0.99089E-04	0.14166E-04	-0.18596E-01
92	273.0000	0.59767E-02	0.85973E-04	0.12344E-04	-0.15706E-01
93	276.0000	0.62160E-02	0.71559E-04	0.10151E-04	-0.12704E-01
94	279.0000	0.64090E-02	0.55807E-04	0.78845E-05	-0.96115E-02
95	282.0000	0.65508E-02	0.38678E-04	0.54407E-05	-0.64484E-02
96	285.0000	0.66401E-02	0.20134E-04	0.28170E-05	-0.32366E-02
97	288.0000	0.66718E-02	0.0	0.0	0.54210E-19

2 2
 CENTROID OF COMPOSITE SECTION = 0.11930E+02
 CENTROID OF COMPOSITE SECTION = 0.67615E+01
 THESE NEW SECTION PROPERTIES

*** OUT-PUT OF SECTION PROPERTIES ***

ALPHA	=	0.13093E-07	0.58279E-07
BETA	=	-0.99865E-09	-0.12785E-08
TOTAL MOMENT OF INERTIA	=	0.70439E+03	0.29818E+03
AREA OF SLAB	=	0.24869E+02	0.78540E+00
CENTROIDAL DISTANCE OF CONCRETE	=	0.21604E+01	0.83285E+01
TOTAL AREA	=	0.33999E+02	0.99154E+01
CENTROIDAL DISTANCE OF STEEL	=	-0.58846E+01	-0.71645E+00
PRODUCT OF ES AND CONC AREA	=	0.73613E+09	0.23248E+08
AREA OF STEEL SECTION	=	0.91300E+01	0.91300E+01
ALPHA	=	0.67694E-01	0.14282E+00
SHEAR DEFLECTION FACTOR	=	0.39295E-30	0.53367E-30
Q1TT= 8	S(1)=	-0.66738E-02	0.582894E-04
Q1TT= 4	S(1)=	0.102058E-05	-0.604387E-03

SUPPORT REACTION= 0.293708E+05

OITT= 11 S(1)= -0.703054E-02 FORCE(NNP)= 0.546381E-03
 OITT= 4 S(1)= 0.103169E-05 FORCE(NNP)= -0.157498E-05

SUPPORT REACTION- 0.293953E+05
 OITT= 11 S(1)= -0.700227E-02 FORCE(NNP)= 0.593442E-03
 OITT= 3 S(1)= 0.103161E-05 FORCE(NNP)= -0.700219E-03

SUPPORT REACTION- 0.293931E+05
 OITT= 6 S(1)= -0.700482E-02 FORCE(NNP)= 0.265213E-03
 OITT= 3 S(1)= 0.103162E-05 FORCE(NNP)= 0.628305E-04

SUPPORT REACTION- 0.293933E+05
 OITT= 5 S(1)= -0.700458E-02 FORCE(NNP)= 0.471124E-03

NODE NO.	SHEAR FLOW	FORCE	SLIP	SLIP STRAIN
1	0.17627E+03	0.0	-0.70046E-02	0.0
2	0.17574E+03	0.0	-0.69739E-02	0.19964E-04
3	0.17418E+03	-0.10529E+04	-0.68848E-02	0.38720E-04
4	0.17165E+03	-0.15716E+04	-0.67416E-02	0.56059E-04
5	0.16817E+03	-0.20814E+04	-0.65485E-02	0.72017E-04
6	0.16377E+03	-0.25793E+04	-0.63095E-02	0.86633E-04
7	0.15847E+03	-0.30626E+04	-0.60287E-02	0.99941E-04
8	0.15226E+03	-0.35287E+04	-0.57098E-02	0.11198E-03
9	0.14518E+03	-0.39748E+04	-0.53568E-02	0.12278E-03
10	0.13714E+03	-0.43983E+04	-0.49732E-02	0.13237E-03
11	0.12822E+03	-0.47963E+04	-0.45626E-02	0.14081E-03
12	0.11838E+03	-0.51662E+04	-0.41283E-02	0.14811E-03
13	0.10761E+03	-0.55052E+04	-0.36739E-02	0.15432E-03
14	0.95909E+02	-0.58195E+04	-0.32024E-02	0.15947E-03
15	0.8322E+02	-0.60793E+04	-0.27170E-02	0.16361E-03
16	0.69701E+02	-0.63087E+04	-0.22208E-02	0.16676E-03
17	0.55204E+02	-0.64861E+04	-0.17165E-02	0.16896E-03
18	0.38795E+02	-0.66386E+04	-0.12070E-02	0.17026E-03
19	0.23498E+02	-0.67335E+04	-0.69496E-03	0.17067E-03
20	0.63453E+01	-0.67783E+04	-0.18296E-03	0.17025E-03
21	-0.11244E+02	-0.67710E+04	0.32654E-03	0.16901E-03
22	-0.27912E+02	-0.67122E+04	0.83108E-03	0.16694E-03
23	-0.43531E+02	-0.66051E+04	0.13282E-02	0.16400E-03
24	-0.59094E+02	-0.64526E+04	0.18151E-02	0.16016E-03
25	-0.71611E+02	-0.62531E+04	0.22891E-02	0.15538E-03
26	-0.84078E+02	-0.60245E+04	0.27474E-02	0.14960E-03
27	-0.95511E+02	-0.57551E+04	0.31867E-02	0.14280E-03
28	-0.10591E+03	-0.54530E+04	0.36042E-02	0.13493E-03
29	-0.11530E+03	-0.51212E+04	0.39963E-02	0.12595E-03
30	-0.12368E+03	-0.47627E+04	0.43598E-02	0.11582E-03

31	-0.13108E+03	-0.43806E+04	0.46912E-02	0.10450E-03
32	-0.13743E+03	-0.39779E+04	0.49868E-02	0.91954E-04
33	-0.14281E+03	-0.35575E+04	0.52430E-02	0.78141E-04
34	-0.14717E+03	-0.31225E+04	0.54557E-02	0.63021E-04
35	-0.15050E+03	-0.26760E+04	0.56211E-02	0.46553E-04
36	-0.15276E+03	-0.22211E+04	0.57350E-02	0.28698E-04
37	-0.15390E+03	-0.17611E+04	0.57933E-02	0.94110E-05
38	-0.15387E+03	-0.12995E+04	0.57915E-02	-0.11151E-04
39	-0.15027E+03	-0.84239E+03	0.56099E-02	-0.77422E-04
40	-0.14524E+03	-0.39912E+03	0.53609E-02	-0.89846E-04
41	-0.13921E+03	0.27552E+02	0.50707E-02	-0.10506E-03
42	-0.13191E+03	0.43424E+03	0.47305E-02	-0.12337E-03
43	-0.12302E+03	0.81663E+03	0.43305E-02	-0.14501E-03
44	-0.11209E+03	0.11693E+04	0.38604E-02	-0.17031E-03
45	-0.98993E+02	0.14853E+04	0.33086E-02	-0.19968E-03
46	-0.81809E+02	0.17659E+04	0.26629E-02	-0.23362E-03
47	-0.60764E+02	0.19698E+04	0.19069E-02	-0.27280E-03
48	-0.34114E+02	0.21121E+04	0.10255E-02	-0.31809E-03
49	0.57399E-01	0.21632E+04	-0.16527E-05	-0.34240E-03
50	0.34219E+02	0.21118E+04	-0.10289E-02	-0.31811E-03
51	0.60883E+02	0.19691E+04	-0.19103E-02	-0.27284E-03
52	0.81904E+02	0.17550E+04	-0.26659E-02	-0.23367E-03
53	0.98688E+02	0.14841E+04	-0.33124E-02	-0.19975E-03
54	0.11218E+03	0.11678E+04	-0.38644E-02	-0.17040E-03
55	0.12311E+03	0.81485E+03	-0.43348E-02	-0.14512E-03
56	0.13202E+03	0.43216E+03	-0.47351E-02	-0.12349E-03
57	0.13937E+03	0.25165E+02	-0.50757E-02	-0.10520E-03
58	0.14530E+03	-0.40183E+03	-0.53663E-02	-0.90004E-04
59	0.15039E+03	-0.84544E+03	-0.56157E-02	-0.77600E-04
60	0.15399E+03	-0.13029E+04	-0.57978E-02	-0.10988E-04
61	0.15402E+03	-0.17649E+04	-0.57991E-02	0.95693E-05
62	0.15286E+03	-0.22252E+04	-0.57403E-02	0.28852E-04
63	0.15098E+03	-0.26804E+04	-0.56259E-02	0.46703E-04
64	0.14726E+03	-0.31272E+04	-0.54601E-02	0.63167E-04
65	0.14289E+03	-0.35624E+04	-0.52469E-02	0.78284E-04
66	0.13751E+03	-0.39830E+04	-0.49904E-02	0.92094E-04
67	0.13113E+03	-0.43860E+04	-0.46944E-02	0.10464E-03
68	0.12374E+03	-0.47683E+04	-0.43626E-02	0.11595E-03
69	0.11536E+03	-0.51269E+04	-0.39987E-02	0.12608E-03
70	0.10596E+03	-0.54589E+04	-0.36061E-02	0.13506E-03
71	0.95551E+02	-0.57612E+04	-0.31883E-02	0.14293E-03
72	0.84111E+02	-0.60307E+04	-0.27485E-02	0.14973E-03
73	0.71623E+02	-0.62643E+04	-0.22899E-02	0.15550E-03
74	0.58109E+02	-0.64589E+04	-0.18155E-02	0.16029E-03
75	0.43532E+02	-0.66114E+04	-0.13282E-02	0.16413E-03
76	0.27902E+02	-0.67185E+04	-0.83077E-03	0.16706E-03
77	0.13221E+02	-0.67772E+04	-0.32584E-03	0.16913E-03
78	-0.69822E+01	-0.67845E+04	0.18403E-03	0.17038E-03
79	-0.23848E+02	-0.67396E+04	0.68642E-03	0.17080E-03

IMP1	LENGTH	SLIP	LEFT STRAIN	RIGHT STRAIN	CURVATURE	LEFT CURVE	RIGHT CURVE	DEFLECTION
80	-0.39852E+02	-0.66445E+04	0.1208E-02	0.17187E-02	0.0	0.17039E-03		
81	-0.85270E+02	-0.65018E+04	0.17187E-02	0.17187E-02	0.0	0.16910E-03		
82	-0.69775E+02	-0.63142E+04	0.22234E-02	0.22234E-02	0.0	0.16689E-03		
83	-0.83354E+02	-0.60845E+04	0.27201E-02	0.27201E-02	0.0	0.16375E-03		
84	-0.95996E+02	-0.58155E+04	0.32059E-02	0.32059E-02	0.0	0.15962E-03		
85	-0.10771E+03	-0.55100E+04	0.36778E-02	0.36778E-02	0.0	0.15447E-03		
86	-0.11848E+03	-0.51707E+04	0.41327E-02	0.41327E-02	0.0	0.14826E-03		
87	-0.12838E+03	-0.48005E+04	0.45674E-02	0.45674E-02	0.0	0.14096E-03		
88	-0.13726E+03	-0.44021E+04	0.49785E-02	0.49785E-02	0.0	0.13253E-03		
89	-0.14527E+03	-0.39783E+04	0.53626E-02	0.53626E-02	0.0	0.12294E-03		
90	-0.15238E+03	-0.35318E+04	0.57161E-02	0.57161E-02	0.0	0.11214E-03		
91	-0.15850E+03	-0.30583E+04	0.60354E-02	0.60354E-02	0.0	0.10011E-03		
92	-0.16391E+03	-0.25816E+04	0.63168E-02	0.63168E-02	0.0	0.86810E-04		
93	-0.16931E+03	-0.20833E+04	0.65563E-02	0.65563E-02	0.0	0.72200E-04		
94	-0.17179E+03	-0.15731E+04	0.67500E-02	0.67500E-02	0.0	0.56247E-04		
95	-0.17424E+03	-0.10539E+04	0.68938E-02	0.68938E-02	0.0	0.38115E-04		
96	-0.17591E+03	-0.52854E+03	0.69835E-02	0.69835E-02	0.0	0.20165E-04		
97	-0.17645E+03	0.47112E-03	0.70148E-02	0.70148E-02	0.0	0.0		

NUMBER OF INFLECTION POINT= 2

IMP2	LENGTH	SLIP	LEFT STRAIN	RIGHT STRAIN	CURVATURE	LEFT CURVE	RIGHT CURVE	DEFLECTION
1	111.6268	0.57831E-02	-0.15561E-04	-0.68528E-04	0.0	-0.11869E-05	-0.15055E-05	-0.17063E-01
2	176.3732	-0.57895E-02	-0.68822E-04	-0.15398E-04	0.0	-0.15098E-05	-0.11744E-05	-0.17077E-01

FINAL OUT-PUT FOR SLIP, SLIP STRAIN, CURV, DEF.

NODAL NO	NODE LENGTH	SLIP	SLIP STRAIN	CURVATURE	DEFLECTION
1	0.0	-0.70046E-02	0.0	0.0	0.0
2	3.0000	-0.69739E-02	0.19964E-04	0.28254E-05	-0.33347E-02
3	6.0000	-0.68848E-02	0.38720E-04	0.54867E-05	-0.66443E-02
4	9.0000	-0.67416E-02	0.56059E-04	0.79679E-05	-0.99050E-02
5	12.0000	-0.65485E-02	0.72017E-04	0.10272E-04	-0.13094E-01
6	15.0000	-0.63085E-02	0.86633E-04	0.12402E-04	-0.16192E-01
7	18.0000	-0.60287E-02	0.99941E-04	0.14360E-04	-0.19178E-01
8	21.0000	-0.57098E-02	0.11198E-03	0.16149E-04	-0.22035E-01
9	24.0000	-0.53568E-02	0.12278E-03	0.17771E-04	-0.24747E-01
10	27.0000	-0.49732E-02	0.13237E-03	0.19231E-04	-0.27300E-01
11	30.0000	-0.45626E-02	0.14081E-03	0.20529E-04	-0.29680E-01
12	33.0000	-0.41263E-02	0.4811E-03	0.21669E-04	-0.31875E-01
13	36.0000	-0.36739E-02	0.15432E-03	0.22654E-04	-0.33876E-01
14	39.0000	-0.32024E-02	0.15847E-03	0.23487E-04	-0.35673E-01
15	42.0000	-0.27170E-02	0.16361E-03	0.24169E-04	-0.37260E-01
16	45.0000	-0.22208E-02	0.16676E-03	0.24705E-04	-0.38629E-01
17	48.0000	-0.17165E-02	0.16896E-03	0.25097E-04	-0.39776E-01
18	51.0000	-0.12070E-02	0.17026E-03	0.25347E-04	-0.40687E-01
19	54.0000	-0.69496E-03	0.17067E-03	0.25458E-04	-0.41391E-01

20	17025E-03	0.17025E-03	0.18296E-03	57.0000	-0.41856E-01
21	0.16901E-03	0.16901E-03	0.32654E-03	60.0000	-0.42092E-01
22	0.16694E-03	0.16694E-03	0.83108E-03	62.0000	-0.42101E-01
23	0.16400E-03	0.16400E-03	0.13282E-02	66.0000	-0.41886E-01
24	0.16016E-03	0.16016E-03	0.18151E-02	68.0000	-0.41450E-01
25	0.15536E-03	0.15536E-03	0.22891E-02	72.0000	-0.40799E-01
26	0.14960E-03	0.14960E-03	0.27474E-02	75.0000	-0.39838E-01
27	0.14280E-03	0.14280E-03	0.31867E-02	78.0000	-0.38876E-01
28	0.13493E-03	0.13493E-03	0.36042E-02	81.0000	-0.37623E-01
29	0.12595E-03	0.12595E-03	0.39963E-02	84.0000	-0.36187E-01
30	0.11582E-03	0.11582E-03	0.43588E-02	87.0000	-0.34583E-01
31	0.10450E-03	0.10450E-03	0.46912E-02	90.0000	-0.32821E-01
32	0.91944E-04	0.91944E-04	0.49868E-02	92.0000	-0.30919E-01
33	0.78141E-04	0.78141E-04	0.52430E-02	96.0000	-0.28891E-01
34	0.63021E-04	0.63021E-04	0.54587E-02	98.0000	-0.26756E-01
35	0.46533E-04	0.46533E-04	0.56211E-02	102.0000	-0.24533E-01
36	0.28638E-04	0.28638E-04	0.57350E-02	106.0000	-0.22244E-01
37	0.94110E-05	0.94110E-05	0.57933E-02	108.0000	-0.19910E-01
38	-0.11151E-04	-0.11151E-04	0.57915E-02	111.0000	-0.17555E-01
39	-0.77422E-04	-0.77422E-04	0.56098E-02	114.0000	-0.15207E-01
40	-0.88846E-04	-0.88846E-04	0.53608E-02	117.0000	-0.12898E-01
41	-0.10506E-03	-0.10506E-03	0.50707E-02	120.0000	-0.10660E-01
42	-0.12337E-03	-0.12337E-03	0.47308E-02	123.0000	-0.85297E-02
43	-0.14501E-03	-0.14501E-03	0.43306E-02	126.0000	-0.65426E-02
44	-0.17031E-03	-0.17031E-03	0.38604E-02	128.0000	-0.47384E-02
45	-0.19968E-03	-0.19968E-03	0.33066E-02	132.0000	-0.31588E-02
46	-0.23362E-03	-0.23362E-03	0.26623E-02	135.0000	-0.18475E-02
47	-0.27280E-03	-0.27280E-03	0.19069E-02	138.0000	-0.85099E-03
48	-0.31809E-03	-0.31809E-03	0.10255E-02	141.0000	-0.21813E-03
49	-0.34240E-03	-0.34240E-03	-0.16527E-05	144.0000	0.79634E-06
50	-0.31811E-03	-0.31811E-03	-0.10289E-02	147.0000	-0.21935E-03
51	-0.27284E-03	-0.27284E-03	-0.19103E-02	150.0000	-0.85343E-03
52	-0.23367E-03	-0.23367E-03	-0.26559E-02	153.0000	-0.18512E-02
53	-0.19975E-03	-0.19975E-03	-0.33124E-02	156.0000	-0.31637E-02
54	-0.17040E-03	-0.17040E-03	-0.36644E-02	159.0000	-0.47446E-02
55	-0.14512E-03	-0.14512E-03	-0.43349E-02	162.0000	-0.65500E-02
56	-0.12349E-03	-0.12349E-03	-0.47351E-02	165.0000	-0.85384E-02
57	-0.10520E-03	-0.10520E-03	-0.50757E-02	168.0000	-0.10671E-01
58	-0.90004E-04	-0.90004E-04	-0.53663E-02	171.0000	-0.12909E-01
59	-0.77600E-04	-0.77600E-04	-0.56157E-02	174.0000	-0.15219E-01
60	-0.10888E-04	-0.10888E-04	-0.57978E-02	177.0000	-0.17569E-01
61	0.95693E-05	0.95693E-05	-0.57991E-02	180.0000	-0.18925E-01
62	0.28852E-04	0.28852E-04	-0.57403E-02	183.0000	-0.22260E-01
63	0.46703E-04	0.46703E-04	-0.56269E-02	186.0000	-0.24551E-01
64	0.83167E-04	0.83167E-04	-0.54601E-02	189.0000	-0.26775E-01
65	0.78284E-04	0.78284E-04	-0.52469E-02	192.0000	-0.28911E-01
66	0.92094E-04	0.92094E-04	-0.49804E-02	195.0000	-0.30939E-01
67	0.10464E-03	0.10464E-03	-0.46944E-02	198.0000	-0.32843E-01
68	0.11595E-03	0.11595E-03	-0.43626E-02	201.0000	-0.34605E-01

69	204.0000	-0.39987E-02	0.12508E-03	0.18996E-04	-0.36210E-01
70	207.0000	-0.36061E-02	0.13506E-03	0.20221E-04	-0.37646E-01
71	210.0000	-0.31883E-02	0.14293E-03	0.03890E-01	-0.38900E-01
72	213.0000	-0.27485E-02	0.14973E-03	0.22404E-04	-0.39962E-01
73	216.0000	-0.22899E-02	0.15550E-03	0.23288E-04	-0.40822E-01
74	219.0000	-0.18155E-02	0.16029E-03	0.23855E-04	-0.41474E-01
75	222.0000	-0.13282E-02	0.16413E-03	0.24558E-04	-0.41910E-01
76	225.0000	-0.83077E-03	0.16706E-03	0.24900E-04	-0.42125E-01
77	228.0000	-0.32584E-03	0.16913E-03	0.25284E-04	-0.42116E-01
78	231.0000	0.18403E-03	0.17038E-03	0.25443E-04	-0.41880E-01
79	234.0000	0.69642E-03	0.17080E-03	0.25468E-04	-0.41414E-01
80	237.0000	0.12088E-02	0.17039E-03	0.25357E-04	-0.40720E-01
81	240.0000	0.17187E-02	0.16910E-03	0.25107E-04	-0.39798E-01
82	243.0000	0.22234E-02	0.16689E-03	0.24715E-04	-0.38650E-01
83	246.0000	0.27201E-02	0.16375E-03	0.24180E-04	-0.37281E-01
84	249.0000	0.32059E-02	0.15962E-03	0.23497E-04	-0.35694E-01
85	252.0000	0.36778E-02	0.15447E-03	0.22665E-04	-0.33895E-01
86	255.0000	0.41327E-02	0.14826E-03	0.21681E-04	-0.31894E-01
87	258.0000	0.45674E-02	0.14096E-03	0.20541E-04	-0.29697E-01
88	261.0000	0.49785E-02	0.13253E-03	0.19243E-04	-0.27316E-01
89	264.0000	0.53626E-02	0.12294E-03	0.17784E-04	-0.24762E-01
90	267.0000	0.57161E-02	0.11214E-03	0.16161E-04	-0.22048E-01
91	270.0000	0.60354E-02	0.10011E-03	0.14373E-04	-0.19189E-01
92	273.0000	0.63168E-02	0.86810E-04	0.12415E-04	-0.16202E-01
93	276.0000	0.65563E-02	0.72200E-04	0.10286E-04	-0.13103E-01
94	279.0000	0.67500E-02	0.56247E-04	0.79823E-05	-0.99114E-02
95	282.0000	0.68938E-02	0.38915E-04	0.55015E-05	-0.66487E-02
96	285.0000	0.69835E-02	0.20165E-04	0.28407E-05	-0.33369E-02
97	288.0000	0.70148E-02	0.0	0.0	-0.0

3 3

CENTROID OF COMPOSITE SECTION = 0.11930E+02

CENTROID OF COMPOSITE SECTION = 0.67615E+01
OA ROOT HAS BEEN LOCATED BETWEEN 1.00000AND
THE ROOT IS 13.20857WITHIN AN INTERVAL OF 48.00000

0.00050 IT TOOK 11ITERATE

3 1

CENTROID OF COMPOSITE SECTION = 0.94917E+01

CENTROID OF COMPOSITE SECTION = 0.94917E+01
1**** NEW SECTION PROPERTIES ****

*** OUT-PUT OF SECTION PROPERTIES ***

ALPHA	=	0.17449E-07	0.17449E-07
BETA	=	-0.10954E-08	-0.10954E-08
TOTAL MOMENT OF INERTIA	=	0.50129E+03	0.50129E+03
AREA OF SLAB	=	0.68435E+01	0.68435E+01
CENTROIDAL DISTANCE OF CONCRETE	=	0.45983E+01	0.45983E+01
TOTAL AREA	=	0.15973E+02	0.15973E+02
CENTROIDAL DISTANCE OF STEEL	=	-0.34467E+01	-0.34467E+01
PRODUCT OF ES AND CONC. AREA	=	0.20257E+09	0.20257E+09
AREA OF STEEL SECTION	=	0.91300E+01	0.91300E+01
ALPHAX	=	0.78149E-01	0.78149E-01
SHEAR DEFLECTION FACTOR	=	0.45312E-30	0.45312E-30
OIT1= 11	S(1)=	0.69198E-02	FORCE(NNP)= 0.376809E-03
OIT1= 12	S(1)=	0.845771E-06	FORCE(NNP)= -0.599000E-05
OIT1= 3	S(1)=	0.297914E+05	FORCE(NNP)= 0.425074E-03
SUPPORT REACTION=	S(1)=	-0.643428E-02	FORCE(NNP)= -0.158278E-03
OIT1= 11	S(1)=	0.297644E+05	FORCE(NNP)= 0.188308E-03
OIT1= 3	S(1)=	-0.646692E-02	FORCE(NNP)= 0.141403E-03
SUPPORT REACTION=	S(1)=	0.297663E+05	FORCE(NNP)= 0.247487E-03
OIT1= 6	S(1)=	-0.646469E-02	FORCE(NNP)= 0.243416E-04
OIT1= 1	S(1)=	0.845765E-06	
SUPPORT REACTION=	S(1)=	0.297662E+05	FORCE(NNP)= 0.184343E-04
OIT1= 6	S(1)=	-0.646484E-02	

NODE NO.	SHEAR FLOW	FORCE	SLIP	SLIP STRAIN
1	0.18664E+03	0.0	-0.64648E-02	0.0
2	0.18607E+03	-0.49907E+03	-0.64338E-02	0.20161E-04
3	0.16141E+03	-0.99479E+03	-0.63439E-02	0.39010E-04

4	0.16171E+03	0.14840E+04	-0.61997E-02	0.56330E-04
5	0.15803E+03	-0.19636E+04	-0.60059E-02	0.72174E-04
6	0.15338E+03	-0.24307E+04	-0.57667E-02	0.86593E-04
7	0.14779E+03	-0.28825E+04	-0.54863E-02	0.99637E-04
8	0.14127E+03	-0.33161E+04	-0.51689E-02	0.11135E-03
9	0.13381E+03	-0.37287E+04	-0.48182E-02	0.12180E-03
10	0.12544E+03	-0.41176E+04	-0.44381E-02	0.13101E-03
11	0.11614E+03	-0.44800E+04	-0.40322E-02	0.13904E-03
12	0.10691E+03	-0.48130E+04	-0.36039E-02	0.14594E-03
13	0.94741E+02	-0.51140E+04	-0.31565E-02	0.15175E-03
14	0.82639E+02	-0.53801E+04	-0.26934E-02	0.15654E-03
15	0.69605E+02	-0.56084E+04	-0.22173E-02	0.16033E-03
16	0.55642E+02	-0.57963E+04	-0.17314E-02	0.16319E-03
17	0.40760E+02	-0.59409E+04	-0.12382E-02	0.16517E-03
18	0.24979E+02	-0.60395E+04	-0.74035E-03	0.16630E-03
19	0.93125E+01	-0.60895E+04	-0.24037E-03	0.16664E-03
20	-0.89648E+01	-0.60885E+04	0.25947E-03	0.16622E-03
21	-0.25515E+02	-0.60368E+04	0.75693E-03	0.16503E-03
22	-0.41118E+02	-0.59368E+04	0.12497E-02	0.16305E-03
23	-0.55758E+02	-0.57915E+04	0.17352E-02	0.16022E-03
24	-0.68427E+02	-0.56037E+04	0.22110E-02	0.15648E-03
25	-0.82125E+02	-0.53764E+04	0.26741E-02	0.15179E-03
26	-0.93850E+02	-0.51124E+04	0.31217E-02	0.14609E-03
27	-0.10461E+03	-0.48148E+04	0.35507E-02	0.13935E-03
28	-0.11440E+03	-0.44863E+04	0.39578E-02	0.13149E-03
29	-0.12322E+03	-0.41298E+04	0.43396E-02	0.12248E-03
30	-0.13109E+03	-0.37484E+04	0.46927E-02	0.11227E-03
31	-0.13799E+03	-0.33447E+04	0.50132E-02	0.10079E-03
32	-0.14394E+03	-0.29218E+04	0.52974E-02	0.88015E-04
33	-0.14890E+03	-0.24826E+04	0.55413E-02	0.73878E-04
34	-0.15287E+03	-0.20298E+04	0.57407E-02	0.58332E-04
35	-0.15582E+03	-0.15669E+04	0.58913E-02	0.41323E-04
36	-0.15770E+03	-0.10966E+04	0.59886E-02	0.23798E-04
37	-0.15845E+03	-0.62240E+03	0.60281E-02	0.28460E-05
38	-0.15901E+03	-0.14747E+03	0.60051E-02	-0.18723E-04
39	-0.15927E+03	0.32396E+03	0.59147E-02	-0.42289E-04
40	-0.15309E+03	0.78799E+03	0.57514E-02	-0.67497E-04
41	-0.14826E+03	0.12400E+04	0.55097E-02	-0.94559E-04
42	-0.14159E+03	0.16748E+04	0.51840E-02	-0.12357E-03
43	-0.13274E+03	0.20863E+04	0.47683E-02	-0.15462E-03
44	-0.12132E+03	0.24674E+04	0.42563E-02	-0.18786E-03
45	-0.10682E+03	0.28096E+04	0.36412E-02	-0.22342E-03
46	-0.88522E+02	0.31026E+04	0.29158E-02	-0.26148E-03
47	-0.65809E+02	0.33336E+04	0.20723E-02	-0.30227E-03
48	-0.36527E+02	0.34867E+04	0.11022E-02	-0.34607E-03
49	0.14342E+00	0.35413E+04	0.40987E-05	-0.36877E-03
50	0.36784E+02	0.34859E+04	-0.11104E-02	-0.34609E-03
51	0.65746E+02	0.33321E+04	-0.20806E-02	-0.30230E-03
52	0.88741E+02	0.31003E+04	-0.29242E-02	-0.26152E-03

INPT	LENGTH	SLIP	LEFT STRAIN	RIGHT STRAIN	LEFT CURVE	RIGHT CURVE	DEFLECTION
53	0.10702E+03		0.28067E+04		-0.36497E-02	-0.22347E-03	
54	0.12152E+03		0.24638E+04		-0.42650E-02	-0.18792E-03	
55	0.13293E+03		0.20822E+04		-0.47772E-02	-0.15469E-03	
56	0.14178E+03		0.16701E+04		-0.51932E-02	-0.12365E-03	
57	0.14845E+03		0.12348E+04		-0.55191E-02	-0.94650E-04	
58	0.15327E+03		0.7821E+03		-0.57611E-02	-0.67598E-04	
59	0.15646E+03		0.3176E+03		-0.59247E-02	-0.42399E-04	
60	0.15821E+03		-0.15441E+03		-0.60154E-02	-0.18844E-04	
61	0.15866E+03		-0.62994E+03		-0.60382E-02	0.31328E-05	
62	0.15788E+03		-0.11047E+04		-0.59979E-02	0.23075E-04	
63	0.15588E+03		-0.15755E+04		-0.58998E-02	0.41592E-04	
64	0.15202E+03		-0.20390E+04		-0.57484E-02	0.58592E-04	
65	0.14904E+03		-0.24921E+04		-0.55482E-02	0.74130E-04	
66	0.14406E+03		-0.29318E+04		-0.53036E-02	0.88260E-04	
67	0.13811E+03		-0.33550E+04		-0.50186E-02	0.10103E-03	
68	0.13119E+03		-0.37590E+04		-0.46974E-02	0.11250E-03	
69	0.12331E+03		-0.41407E+04		-0.43436E-02	0.12271E-03	
70	0.11447E+03		-0.44974E+04		-0.39611E-02	0.13172E-03	
71	0.10487E+03		-0.48261E+04		-0.35534E-02	0.13957E-03	
72	0.93902E+02		-0.51240E+04		-0.31237E-02	0.14631E-03	
73	0.82161E+02		-0.53881E+04		-0.26755E-02	0.15200E-03	
74	0.69447E+02		-0.56155E+04		-0.22117E-02	0.15669E-03	
75	0.55758E+02		-0.58033E+04		-0.17353E-02	0.16043E-03	
76	0.41100E+02		-0.59486E+04		-0.12491E-02	0.16326E-03	
77	0.25476E+02		-0.60485E+04		-0.75575E-03	0.16525E-03	
78	0.89024E+01		-0.61000E+04		-0.25765E-03	0.16643E-03	
79	0.83974E+01		-0.61008E+04		0.24285E-03	0.16686E-03	
80	-0.25078E+02		-0.60506E+04		0.74350E-03	0.16652E-03	
81	-0.40879E+02		-0.59516E+04		0.12420E-02	0.16540E-03	
82	-0.55775E+02		-0.59066E+04		0.17359E-02	0.16349E-03	
83	-0.69752E+02		-0.56184E+04		0.23226E-02	0.16058E-03	
84	-0.82800E+02		-0.53895E+04		0.26994E-02	0.15679E-03	
85	-0.94914E+02		-0.51230E+04		0.31633E-02	0.15202E-03	
86	-0.10608E+03		-0.48214E+04		0.36115E-02	0.14621E-03	
87	-0.11634E+03		-0.44878E+04		0.40406E-02	0.13932E-03	
88	-0.12665E+03		-0.41248E+04		0.44474E-02	0.13130E-03	
89	-0.13404E+03		-0.37353E+04		0.48284E-02	0.12210E-03	
90	-0.14150E+03		-0.33220E+04		0.51800E-02	0.11167E-03	
91	-0.14804E+03		-0.28877E+04		0.54984E-02	0.99965E-04	
92	-0.15264E+03		-0.24351E+04		0.57798E-02	0.86934E-04	
93	-0.15830E+03		-0.19672E+04		0.60200E-02	0.72529E-04	
94	-0.16200E+03		-0.14868E+04		0.62149E-02	0.56700E-04	
95	-0.16471E+03		-0.99672E+03		0.63602E-02	0.39395E-04	
96	-0.16638E+03		-0.50006E+03		0.64513E-02	0.20562E-04	
97	-0.16688E+03		-0.18434E-04		0.64836E-02	0.0	

NUMBER 57 INFLECTION POINT = 2

1 109.3826 0.60255E-02 0.66509E-05 -0.64161E-05 -0.41751E-06 -0.40277E-06 -0.19355E-01
 2 178.6174 -0.60860E-02 -0.65427E-05 -0.63595E-05 -0.41072E-06 -0.39922E-06 -0.19374E-01

FINAL OUT-PUT FOR SLIP, SLIP, STRAIN, CURV, DEF.

NODAL NO	NODE LENGTH	SLIP	SLIP STRAIN	CURVATURE	DEFLECTION
1	0.0	-0.64648E-02	0.0	0.0	0.0
2	3.0000	-0.64338E-02	0.20161E-04	0.30583E-05	-0.35457E-02
3	6.0000	-0.63439E-02	0.39010E-04	0.59332E-05	-0.70643E-02
4	9.0000	-0.61997E-02	0.56330E-04	0.86111E-05	-0.10530E-01
5	12.0000	-0.60059E-02	0.72174E-04	0.11095E-04	-0.13918E-01
6	15.0000	-0.57667E-02	0.86593E-04	0.13389E-04	-0.17208E-01
7	18.0000	-0.54863E-02	0.99637E-04	0.15495E-04	-0.20377E-01
8	21.0000	-0.51689E-02	0.11135E-03	0.17417E-04	-0.23407E-01
9	24.0000	-0.48182E-02	0.12180E-03	0.19157E-04	-0.26280E-01
10	27.0000	-0.44381E-02	0.13101E-03	0.20719E-04	-0.28982E-01
11	30.0000	-0.40322E-02	0.13904E-03	0.22106E-04	-0.31498E-01
12	33.0000	-0.36039E-02	0.14594E-03	0.23321E-04	-0.33815E-01
13	36.0000	-0.31565E-02	0.15175E-03	0.24367E-04	-0.35922E-01
14	39.0000	-0.26934E-02	0.15654E-03	0.25247E-04	-0.37811E-01
15	42.0000	-0.22173E-02	0.16033E-03	0.25964E-04	-0.39472E-01
16	45.0000	-0.17314E-02	0.16319E-03	0.26521E-04	-0.40901E-01
17	48.0000	-0.12382E-02	0.16517E-03	0.26921E-04	-0.42091E-01
18	51.0000	-0.74035E-03	0.16630E-03	0.27168E-04	-0.43039E-01
19	54.0000	-0.24037E-03	0.16664E-03	0.27263E-04	-0.43743E-01
20	57.0000	-0.25947E-03	0.16622E-03	0.27210E-04	-0.44202E-01
21	60.0000	0.75693E-03	0.16503E-03	0.27007E-04	-0.44416E-01
22	63.0000	0.12497E-02	0.16305E-03	0.26654E-04	-0.44388E-01
23	66.0000	0.17352E-02	0.16022E-03	0.26146E-04	-0.44120E-01
24	69.0000	0.22110E-02	0.15648E-03	0.25480E-04	-0.43617E-01
25	72.0000	0.26741E-02	0.15179E-03	0.24653E-04	-0.42885E-01
26	75.0000	0.31217E-02	0.14609E-03	0.23662E-04	-0.41932E-01
27	78.0000	0.35507E-02	0.13935E-03	0.22504E-04	-0.40766E-01
28	81.0000	0.39578E-02	0.13149E-03	0.21175E-04	-0.39398E-01
29	84.0000	0.43396E-02	0.12248E-03	0.19673E-04	-0.37840E-01
30	87.0000	0.46927E-02	0.11227E-03	0.17994E-04	-0.36105E-01
31	90.0000	0.50132E-02	0.10079E-03	0.16135E-04	-0.34208E-01
32	93.0000	0.52974E-02	0.88015E-04	0.14093E-04	-0.32167E-01
33	96.0000	0.55413E-02	0.73878E-04	0.11864E-04	-0.30000E-01
34	98.0000	0.57407E-02	0.58332E-04	0.94459E-05	-0.27726E-01
35	102.0000	0.58913E-02	0.41323E-04	0.68349E-05	-0.25367E-01
36	105.0000	0.59886E-02	0.22798E-04	0.40276E-05	-0.22947E-01
37	108.0000	0.60281E-02	0.28460E-05	0.10297E-05	-0.20492E-01
38	111.0000	0.60091E-02	-0.18723E-04	-0.21709E-05	-0.18026E-01
39	114.0000	0.59147E-02	-0.42289E-04	-0.55978E-05	-0.15581E-01
40	117.0000	0.57514E-02	-0.67497E-04	-0.92290E-05	-0.13188E-01
41	120.0000	0.55097E-02	-0.94559E-04	-0.13078E-04	-0.10878E-01

42	123.0000	0.51840E-02	-0.12357E-03	-0.17149E-04	-0.86859E-02
43	126.0000	0.47683E-02	-0.15462E-03	-0.21451E-04	-0.66490E-02
44	129.0000	0.42563E-02	-0.18786E-03	-0.25990E-04	-0.48056E-02
45	132.0000	0.36412E-02	-0.22342E-03	-0.30777E-04	-0.31968E-02
46	135.0000	0.28158E-02	-0.26148E-03	-0.35821E-04	-0.18655E-02
47	138.0000	0.20723E-02	-0.30227E-03	-0.41139E-04	-0.85717E-03
48	141.0000	0.14022E-02	-0.34607E-03	-0.46746E-04	-0.21977E-03
49	144.0000	-0.40867E-05	-0.36877E-03	-0.51129E-04	-0.33165E-06
50	147.0000	-0.11104E-02	-0.34609E-03	-0.46747E-04	-0.22133E-03
51	150.0000	-0.20906E-02	-0.30230E-03	-0.41140E-04	-0.86029E-03
52	153.0000	-0.28242E-02	-0.26152E-03	-0.35824E-04	-0.18702E-02
53	156.0000	-0.36497E-02	-0.22347E-03	-0.30780E-04	-0.32031E-02
54	159.0000	-0.42650E-02	-0.18792E-03	-0.25994E-04	-0.48136E-02
55	162.0000	-0.47772E-02	-0.15469E-03	-0.21456E-04	-0.66586E-02
56	165.0000	-0.51832E-02	-0.12365E-03	-0.17155E-04	-0.86972E-02
57	168.0000	-0.55191E-02	-0.94650E-04	-0.13083E-04	-0.10891E-01
58	171.0000	-0.57611E-02	-0.67598E-04	-0.82353E-05	-0.13203E-01
59	174.0000	-0.59247E-02	-0.42399E-04	-0.56048E-05	-0.15598E-01
60	177.0000	-0.60154E-02	-0.18844E-04	-0.21785E-05	-0.18044E-01
61	180.0000	-0.60382E-02	0.31328E-05	0.10477E-05	-0.20512E-01
62	183.0000	-0.59979E-02	0.23075E-04	0.40450E-05	-0.22970E-01
63	186.0000	-0.58998E-02	0.41594E-04	0.68517E-05	-0.25391E-01
64	189.0000	-0.57484E-02	0.58592E-04	0.94622E-05	-0.27751E-01
65	192.0000	-0.55482E-02	0.74130E-04	0.11880E-04	-0.30027E-01
66	195.0000	-0.53036E-02	0.88260E-04	0.14108E-04	-0.32195E-01
67	198.0000	-0.50186E-02	0.10109E-03	0.16150E-04	-0.34238E-01
68	201.0000	-0.46974E-02	0.11250E-03	0.18008E-04	-0.36135E-01
69	204.0000	-0.43436E-02	0.12271E-03	0.19687E-04	-0.37871E-01
70	207.0000	-0.39611E-02	0.13172E-03	0.21189E-04	-0.39430E-01
71	210.0000	-0.35534E-02	0.13957E-03	0.22518E-04	-0.40798E-01
72	213.0000	-0.31237E-02	0.14631E-03	0.23676E-04	-0.41965E-01
73	216.0000	-0.26755E-02	0.15200E-03	0.24666E-04	-0.42918E-01
74	219.0000	-0.22117E-02	0.15669E-03	0.25493E-04	-0.43651E-01
75	222.0000	-0.17353E-02	0.16043E-03	0.26159E-04	-0.44153E-01
76	225.0000	-0.12491E-02	0.16326E-03	0.26667E-04	-0.44421E-01
77	228.0000	-0.75675E-03	0.16525E-03	0.27021E-04	-0.44450E-01
78	231.0000	-0.25765E-03	0.16643E-03	0.27223E-04	-0.44235E-01
79	234.0000	0.24285E-03	0.16686E-03	0.27277E-04	-0.43776E-01
80	237.0000	0.74350E-03	0.16552E-03	0.27182E-04	-0.43071E-01
81	240.0000	0.12420E-02	0.16540E-03	0.26936E-04	-0.42122E-01
82	243.0000	0.17359E-02	0.16243E-03	0.26536E-04	-0.40932E-01
83	246.0000	0.22226E-02	0.16058E-03	0.25979E-04	-0.39602E-01
84	249.0000	0.26994E-02	0.15679E-03	0.25263E-04	-0.37839E-01
85	252.0000	0.31633E-02	0.15202E-03	0.24384E-04	-0.35950E-01
86	255.0000	0.36115E-02	0.14621E-03	0.23338E-04	-0.33841E-01
87	258.0000	0.40406E-02	0.13932E-03	0.22124E-04	-0.31522E-01
88	261.0000	0.44474E-02	0.13130E-03	0.20738E-04	-0.29009E-01
89	264.0000	0.48284E-02	0.12210E-03	0.19176E-04	-0.26302E-01
90	267.0000	0.51800E-02	0.11167E-03	0.17436E-04	-0.23426E-01

91	270.0000	0.54984E-02	0.99965E-04	0.15515E-04	-0.20394E-01
92	273.0000	0.57798E-02	0.86934E-04	0.13410E-04	-0.17222E-01
93	276.0000	0.60200E-02	0.72529E-04	0.11177E-04	-0.19931E-01
94	279.0000	0.62149E-02	0.56700E-04	0.86943E-05	-0.10539E-01
95	282.0000	0.63602E-02	0.39385E-04	0.59574E-05	-0.70708E-02
96	285.0000	0.64513E-02	0.20562E-04	0.30835E-05	-0.35490E-02
97	288.0000	0.64836E-02	0.0	0.0	0.54210E-19